The role of integrins in flavivirus infection

I n a u g u r a l d i s s e r t a t i o n

zur

Erlangung des akademischen Grades eines

Doktors der Naturwissenschaften (Dr. rer. nat.)

der

Mathematisch-Naturwissenschaftlichen Fakultät

der

Ernst-Moritz-Arndt-Universität Greifswald

vorgelegt von

Vinícius Pinho dos Reis

geboren am 21.12.1984

in São Paulo, Brasilien

Greifswald, 29.03.2018

Dekan: Prof. Dr. rer. nat. Werner Weitschies

1. Gutachter: PD Dr. rer. nat. Rainer G. Ulrich

2. Gutachter: Prof. Dr. Stefanie Becker

Tag der Promotion: 09.10.2018

Table of Contents

List of abbreviations

+ssRNA	Single-stranded RNA of positive polarity
ADE	Antibody-dependent enhancement
BHK-21	Baby hamster kidney cell strain 21
BHQ-1	Black Hole Quencher 1
BSA	Bovine serum albumin
C protein	Capsid protein
Ca	Calcium
CAR	Coxsackie and adenovirus receptor
CHO	Chinese hamster ovary cells
CRISPR	Clustered Regularly Interspaced Short Palindromic Repeats
DAPI	4',6-diamidino-2-phenylindole
DC-SIGN	Dendritic cell-specific intercellular adhesion molecule-3 grabbing non-integrin
DMEM	Dulbecco's modified minimum essential medium
DMSO	Dimethylsulfoxide
DNA	Deoxyribonucleic acid
dNTPs	Deoxynucleotide triphosphates
dsRNA	Double-stranded RNA
DTT	Ditiotreitol
E protein	Envelope protein
ECM	Extracellular matrix
EDTA	Ethylenediaminetetraacetic acid
EGF	Epidermal growth factor
E-MEM	Eagle's minimum essential medium
ER	Endoplasmatic reticulum
ERAD	Endoplasmatic reticulum associated protein degradation
FAK	Focal adhesion kinase
FAM	6-carboxyfluorescein
FBS	Fetal bovine serum
FRC	Flavivirus RNA replication complex
GAG	Glycosaminoglycans
GFP	Green fluorescent protein
HEX	Hexachlorofluorescein
HF	High-Fidelity (in reference to restriction enzymes)
HUVEC	Human endothelial vascular cell
ICAM	Intracellular cell adhesion molecule
ICTV	International committee on taxonomy of viruses
IgG	Immunoglobulin G
IL	Interleukin
ISF	Insect-specific flavivirus
ITG	Integrin
JAM	Junctional cell adhesion molecule
LB medium	Luria Bertani medium
M protein	Membrane protein
MAP	Mitogen activated protein
MBFV	Mosquito-borne flavivirus
MEF	Mouse embryonic fibroblast
MFI	Mean fluorescence intensity
Mg	Magnesium

MHC	Major Histocompatibility complex
MKF	Mouse kidney fibroblast
Mn	Manganes
MOI	Multiplicity of infection
mRNA	Messenger ribonucleic acid
NCAM	neural cell adhesion molecule
NCR	Non-coding region
NKVF	No known vector flavivirus
NS1	Nonstructural flavivirus protein 1
NS2a	Nonstructural flavivirus protein 2a
NS2b	Nonstructural flavivirus protein 2b
NS3	Nonstructural flavivirus protein 3
NS4a	Nonstructural flavivirus protein 4a
NS4b	Nonstructural flavivirus protein 4b
NS5	Nonstructural flavivirus protein 5
OD	Optical density
ORF	Open reading frame
OST	Oligosaccharyltransferase protein complex
PBS	Phospate buffered saline
PCR	Polymerase chain reaction
PEG	Polyethylene glycol
PFU	Plaque forming unit
Poly A	Polyadenylation
Poly-L-Lsy	Poly-L-Lysine
prM protein	Precursor-membrane protein
RdRp	RNA-dependent RNA polymerase
RGD	Arginine-Glycine-Aspartic motif
RNA	Ribonucleic acid
RPM	Revolution per minute/Rotation per minute
RSB	RNA safe buffer
RT	Reverse transcription
RT-PCR	Reverse transcription-polymerase chain reaction
RT-qPCR	Quantitative reverse transcription-polymerase chain reaction
siRNA	Small interfering RNA
TAE	Tris-acetate-EDTA buffer
TAMRA	Tetramethylrhodamine
Taq	*Thermus aquaticus*
TBFV	Tick-borne flavivirus
TCID	Tissue culture infectious dose
TE	Tris-EDTA buffer
TNE	Tris-Natrium EDTA buffer
UV	Ultra-violet
VCAM	Vascular cell adhesion molecule
VTN	Vitronectin
WHO	World Health Organization
α	Alpha (integrin subunit)
β	Beta (integrin subunit)

List of abbreviations for units of measurements

Volume

l	liter
ml	milliliter
μl	microliter

Mass and Weight

g	gram
mg	milligram
μg	microgram
ng	nanogram
kDa	Kilodalton

Concentration

mM	milimolar
μM	micromolar

Length

mm	milimeter
μm	micrometer
nm	nanometer

Acid-base measurement

pH	potential of hydrogen

List of virus abbreviations according to the International Committee on Taxonomy of Viruses (ICTV)

BVDV	Bovine viral diarrhea virus
CSFV	Classical swine fever virus
DENV	Dengue virus
EBOV	Ebola virus
FMDV	Foot and mouth disease virus
HCMV	Human cytomegalovirus
HCV	Hepatitis C virus
HHV-1	Human herpesvirus 1
JEV	Japanese encephalitis virus
KFDV	Kyasanur forest disease virus
KSHV	Kaposi's sarcoma associated virus
KUJV	Kunjin virus
LGTV	Langat virus
LIV	Louping-ill virus
MVEV	Murray Valley Encephalitis virus
NYV-1	New York virus 1
OHFV	Omsk hemorrhagic fever virus
PHV	Prospect Hill virus
POWV	Powassan virus
RRV	Ross-river virus
SLEV	St. Louis encephalitis virus
SNV	Sin nombre virus
TBEV	Tick-borne encephalitis virus
USUV	Usutu virus
WNV	West Nile virus
YFV	Yellow fever virus
YFV-17D	Yellow fever virus strain 17 D
ZIKV	Zika virus

List of figures

List of tables

Summary

The role of integrins in flavivirus infection

by Vinicius Pinho dos Reis

The *Flavivirus* genus (*Flaviviridae* family) comprises the most important arboviruses in the world such as dengue virus, West Nile virus (WNV), Zika virus (ZIKV), Japanese encephalitis virus and yellow fever virus (YFV). Every year, several outbreaks caused by flaviviruses are reported worldwide (i.e.: ZIKV and YFV outbreaks in South America) with a huge impact on economy and public health. In the last few decades, many aspects of the flavivirus biology and the interaction of flaviviruses with host cells have been elucidated. However, many underlying mechanisms concerning receptor usage, entry process and viral interaction with host cell factors are still not completely understood. Integrins, the major class of cell adhesion molecules have been implicated in the infectious cycle of different viruses including flaviviruses. A previous report proposed that a particular integrin, the $\alpha V\beta 3$ integrin, might act as a cellular receptor for WNV. However, this hypothesis was not confirmed by other groups. In the present study, murine cell lines lacking the expression of one or more integrin subunits were used to evaluate the involvement of different integrins in the flavivirus infection cycle. Mouse fibroblasts lacking the expression of $\beta 1$ integrin (MKF-$\beta 1^{-/-}$) or $\beta 3$ integrin (MEF-$\beta 3^{-/-}$) subunits or $\alpha V\beta 3$ integrin (MEF-$\alpha V\beta 3^{-/-}$) as well as their corresponding wild-type cells were utilized. A second model using Chinese hamster ovary cells (CHO-K1), a cell line that has been described to be refractory to some flaviviruses, were modified to express either αV (CHO-$\alpha V^{+/+}$) or $\beta 3$ (CHO-$\beta 3^{+/+}$) integrin subunits. All cell lines were first characterized by confocal laser microscopy, flow cytometry and functional assays prior to infection to assess their integrin expression. The cell lines were then inoculated with different flaviviruses of public health relevance: WNV, YFV-17D, Usutu virus (USUV), Langat virus (LGTV) and ZIKV. Infection assays were designed in order to evaluate whether integrins influence i) cell susceptibility; ii) binding; iii) internalization and iv) replication of the investigated flaviviruses. Our findings clearly demonstrate that $\beta 1$, $\beta 3$ and $\alpha V\beta 3$ integrins do not act as flavivirus cellular receptor or attachment factor since their ablation does not completely abrogate flavivirus infection in the investigated cell lines. Flavivirus binding to the cell surface of MEFs, MKFs and CHO cells was not disturbed by the genomic deletion of the above-mentioned integrins. The deletion of $\beta 1$ and $\beta 3$ integrin subunit did not affect internalization of any of the flaviviruses tested. In contrast to that, loss of $\alpha V\beta 3$ integrin in the MEF-$\alpha V\beta 3^{-/-}$ cells showed a statistically significant decrease in WNV and USUV internalization while ZIKV, YFV-17D and LGTV internalization remained unaffected suggesting that $\alpha V\beta 3$ integrin might be involved in the internalization process of at least some flaviviruses.

On the other hand, flavivirus replication was substantially impaired in the integrin-deficient cell lines in comparison to their corresponding wild-type cells. Both, MEF-β3$^{-/-}$ and MKF-β1$^{-/-}$ cells showed a statistically significant reduction on viral load for all flaviviruses tested in comparison to their respective wild-type cells. The MEF-αVβ3$^{-/-}$ cells in particular, showed a strong inhibition of flavivirus replication with a reduction of up to 99% on viral loads for all flaviviruses tested. Levels of flavivirus negative-strand RNA were substantially decreased in MEF-αVβ3$^{-/-}$ cells indicating that integrins might influence flavivirus RNA replication. The ectopic expression of either αV or β3 integrin subunits in CHO cells slightly increased the replication of all flaviviruses tested. Taken together, this is the first report highlighting the involvement of integrins in ZIKV, USUV, LGTV and YFV infection. The results strongly indicate that the investigated integrins play an important role in flavivirus infection and might represent a novel host cell factor that enhances flavivirus replication. Although the exact mechanism of interaction between integrins and flaviviruses is currently unknown, the results provided in this study deepen our insight into flavivirus - host cell interactions and open doors for further investigations.

Zusammenfassung

The role of integrins in flavivirus infection

von Vinicius Pinho dos Reis

Die Gattung der Flaviviren (Familie *Flaviviridae*) beinhaltet einige der wichtigsten Arboviren weltweit, beispielsweise das Dengue Virus, das West-Nil Virus (WNV), das Zika Virus (ZIKV), das Japanische-Enzephalitis Virus sowie das Gelbfieber Virus (YFV). Jedes Jahr kommt es zu zahlreichen, durch Flaviviren verursachten Ausbrüchen (u.a. Zika und Gelbfieber Virus Ausbrüche in Südamerika), die mit immensen Auswirkungen auf die Ökonomie und das öffentliche Gesundheitswesen einhergehen. Obwohl die Interaktion von Flaviviren mit verschiedenen Wirtszellen in den letzten Jahrzehnten intensiv untersucht wurde und wichtige Fragen in der Flavivirus Biologie bereits geklärt werden konnten, sind viele zugrundeliegende Mechanismen, u.a. die virale Rezeptornutzung, der Eintrittsprozess sowie die Interaktion mit verschiedenen Wirtszellfaktoren nicht vollständig verstanden. Integrine, eine der wichtigsten Klasse von Zelladhäsionsmolekülen, wurden bereits in der Literatur beschrieben, eine Rolle im Infektionszyklus verschiedener Viren, u.a. auch der Flaviviren, zu spielen. Es gibt zudem Hinweise, dass ein bestimmtes Integrin, das αVβ3 Integrin, als Zellrezeptor für WNV fungieren kann, wobei diese Hypothese bislang nicht weiter bestätigt werden konnte. In dieser Arbeit wurde der Einfluss von bestimmten Integrinen auf die Flavivirusinfektion in verschiedenen, genetisch modifizierten Maus- und Hamsterzelllinien untersucht. Hierfür wurden zum einen Mausfibroblasten verwendet, die für die Expression von β1 oder β3 Integrin Untereinheiten oder für das αVβ3 Integrin deletiert sind (MKF-β1$^{-/-}$; MEF-β3$^{-/-}$ und MEF-αVβ3$^{-/-}$), um diese in Infektionsexperimenten mit den entsprechenden Wildtypzellen zu vergleichen. Zum anderen wurde die Chinese Hamster Ovary (CHO) Zelllinie genutzt, welche in der Literatur als refraktär gegenüber bestimmten Flaviviren beschrieben wurde. Diese Zelllinie wurde im Rahmen der Studie genetisch so modifiziert, dass entweder die αV (CHO-αV$^{+/+}$) oder die β3 (CHO-β3$^{+/+}$) Integrin Untereinheit exprimiert wurde. Alle rekombinanten Zelllinien sowie deren Wildtyp wurden mittels Konfokalmikroskopie, Durchflusszytometrie und funktionalen Assays bezüglich der Integrinexpression charakterisiert. Anschließend wurden die Zellen mit den folgenden, Public Health relevanten Flaviviren inokuliert: WNV, YFV, ZIKV, Usutu Virus (USUV) und Langat Virus (LGTV). In diesen Experimenten wurde der Einfluss der beschriebenen Integrine auf i) zelluläre Empfänglichkeit; ii) Bindung; iii) Internalisierung und iv) Replikation der verwendeten Flaviviren untersucht. Die Ergebnisse der Studie zeigen, dass die untersuchten Integrine in den verwendeten Maus- und Hamsterzelllinien weder als Zellrezeptor noch als Attachment-Faktor dienen. Die fehlende Expression der Integrine verhindert in keinem Fall die Infektion der Zellen. Unabhängig von der Integrinexpression können alle untersuchten Flaviviren an die

x

entsprechenden Zellen binden und internalisiert werden. Die Deletion der β1 und β3 Integrin Untereinheiten zeigt keinen Effekt auf die Internalisierung der untersuchten Flaviviren. Das Fehlen des αVβ3 Integrins in den MEF-αVβ3$^{-/-}$ Zellen hingegen resultiert in einem statistisch signifikanten Unterschied in der Internalisierung von WNV und USUV im Vergleich zu den entsprechenden Wildtypzellen während die Internalisierung von ZIKV, YFV-17D und LGTV unbeeinträchtigt bleibt. Diese Ergebnisse deuten darauf hin, dass αVβ3 Integrin in die Internalisierung bestimmter Flaviviren involviert sein könnte.

Die Flavivirusreplikation zeigt sich in den Integrin-defizienten Zellen in dieser Studie stark beeinträchtigt im Vergleich zu den Wildtypzellen. Die Deletion der β1 und β3 Untereinheiten resultiert in einer statistisch signifikant verminderten Replikation in den entsprechenden Mausfibroblasten. Eine noch deutlichere Beeinträchtigung der Replikation aller untersuchter Flaviviren mit einer Reduktion der Viruslast um bis zu 99% wird zudem in den MEF-αVβ3$^{-/-}$ Zellen beobachtet. Diese Ergebnisse werden zusätzlich durch deutlich reduzierte Mengen an detektierbarer Negativstrang-RNA in den MEF-αVβ3$^{-/-}$ Zellen unterstützt, was auf einen Einfluss der Integrine auf die Flavivirusreplikation hinweist. Die ektopische Expression der beschriebenen Integrine in CHO Zellen resultiert ebenfalls in einem leichten Anstieg der Flavivirusreplikation. Insgesamt ist dies der erste Bericht, der die Beteiligung von Integrinen in ZIKV, USUV, LGTV und YFV Infektionen beschreibt. Die Ergebnisse dieser Studie deuten stark darauf hin, dass bestimmte Integrine eine entscheidende Rolle in der Flavivirusinfektion spielen und möglicherweise einen neuen Wirtszellfaktor für Flaviviren darstellen. Auch wenn ein eindeutiger Mechanismus für die Interaktion von Integrinen mit Flaviviren bislang nicht bekannt ist, können die gewonnenen Ergebnisse dieser Studie den Anstoß für weiterführende Untersuchungen geben.

1) Introduction

1.1) Arboviruses: a brief overview

Arthropod-borne viruses, or in short arboviruses, are a group of viruses transmitted by arthropods such as mosquitoes, ticks and sandflies (Kuno *et al.*, 2005). According to the World Health Organization (WHO) arboviruses possess the ability to replicate in their arthropod vectors as well as in their vertebrate hosts leading to efficient virus amplification that enables subsequent transmission to a new host (WHO, 1985). Up to now, there are more than 530 arboviruses described, of which more than 100 cause disease in humans. In addition, a majority of arboviruses are considered to be zoonotic viruses (Gubler, 2001; Lequime *et al.*, 2016; Liang *et al.*, 2015). Arboviruses belong mainly to eight virus families namely *Peribunyaviridae*, *Phenuiviridae, Nairoviridae, Togaviridae*, *Reoviridae*, *Asfarviridae*, *Rhabdoviridae* and *Flaviviridae* (Adams *et al.*, 2017; Lequime *et al.*, 2016; Liang *et al.*, 2015; Weaver *et al.*, 2010).

Arboviruses are maintained in the nature in enzootic cycles which include non-human vertebrates (especially birds, non-human primates and rodents) as their reservoir hosts and arthropods as vectors. In some cases, arboviruses may have more than one vertebrate host or arthropod vector (Davis *et al.*, 2008; Weaver *et al.*, 2004). In most of the cases, humans, domestic animals, livestock and a variety of wild animals are considered incidental hosts that sustain low and short viremia, which does not contribute to the ongoing arbovirus cycle (Gubler, 2001). In case of infections with dengue virus (DENV), yellow fever virus (YFV), Zika virus (ZIKV) and some alphaviruses, humans and primates may develop high viremia and clinical symptoms leading to potential infection of mosquitoes which then contributes to the maintenance of the arbovirus cycle in nature (Gubler, 2001).

Arboviral diseases are found in all six continents (with the exception of the Arctic and Antarctic) and billions of people are living in areas with high risk of arboviral transmission and disease (Beck *et al.*, 2013; Huang *et al.*, 2014). In the particular context of flaviviruses, DENV, the most important arbovirus in the world, is today present in 128 countries, with more than 4 billion of people living in areas with its transmission (Duong *et al.*, 2015). Every year, several flavivirus outbreaks are reported around the world: ZIKV, DENV and YFV in South America; West Nile virus (WNV), St. Louis encephalitis virus (SLEV) and Powassan virus (POWV) in North America; Usutu virus (USUV), WNV, Tick Borne encephalitis virus (TBEV) and Louping ill virus (LIV) in Europe; Japanese encephalitis virus (JEV), DENV and ZIKV in Asia; Murray Valley encephalitis virus (MVEV), WNV and DENV in Australia and YFV, DENV, WNV and several other flaviviruses in Africa (Artsob, 2000; Beck *et al.*, 2013; Lima-Camara, 2016; Lindsey *et al.*, 2014; Mackenzie *et al.*, 2009; Smith *et al.*, 2011; Tompkins *et al.*, 2013).

1.2) The *Flaviviridae* family

Although the theory that mosquitoes could transmit diseases was first proposed in 1881 by Carlos Finnlay, a Cuban physician, it was Walter Reed who isolated the first human arbovirus, the YFV, at the beginning of the 1900's and empirically demonstrated that YFV is a mosquito-borne virus (Tomori, 2004). The family's name came from the latin word *flavus* that means yellow, in reference to the yellow fever disease (Huang *et al.*, 2014). Today, the *Flaviviridae* family comprises more than 60 viral species distributed along the four genera: *Flavivirus*, *Pestivirus*, *Hepacivirus* and *Pegivirus* (**Figure 1**) (Simmonds *et al.*, 2017). The *Pestivirus* genus includes among others the bovine viral diarrhea virus (BVDV) and the classic swine fever virus (CSFV); the *Hepacivirus* genus includes the Hepatitis C virus (HCV) as well as canine, equine and rodent hepaciviruses and the *Pegivirus* genus includes human, rodent, bat, equine and simian pegiviruses (Drexler *et al.*, 2013; Lindenbach, 2013).
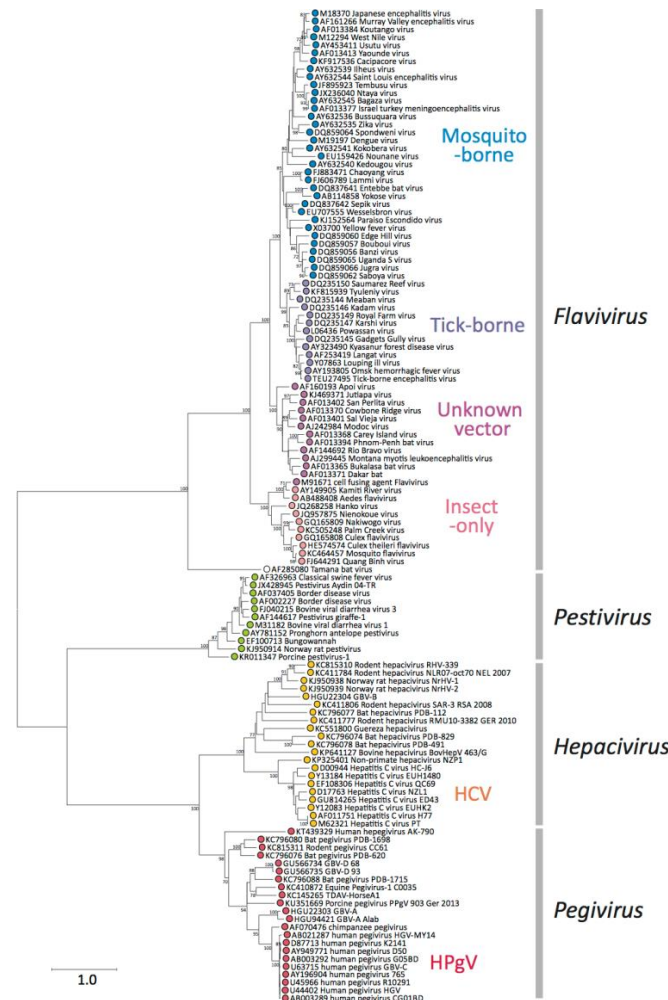
Figure 1: Phylogenetic classification of the *Flaviviridae* family. The phylogenetic tree shows the four genera included within the *Flaviviridae* family: *Flavivirus*, *Pestivirus*, *Hepacivirus* and *Pegivirus*. Figure source: Simmonds *et al.*,(2017). Originally published in https://talk.ictvonline.org/ictv-reports/ictv_online_report/positive-sense-rna-viruses/w/flaviviridae (no modifications) This picture is under Creative Commons Attribution 4.0 (CC.BY-SY.4.0).

1.3) The *Flavivirus* genus

1.3.1) Taxonomy and classification

The *Flavivirus* genus is represented by more than 70 viruses and most of them are arboviruses of medical and veterinary importance such as DENV, WNV, TBEV, JEV, ZIKV and YFV as the prototype of this genus (Huang *et al.*, 2014; Simmonds *et al.*, 2017). Phylogenetic studies divided the *Flavivirus* genus in three major clades according to their mechanism of transmission and genetic similarity: mosquito-borne flaviviruses (MBFV), tick-borne flaviviruses (TBFV) and no-known vector flaviviruses (NKVF) (Gaunt *et al.*, 2001; Lindenbach, 2013). More recently, an additional group has been included and named insect-specific flaviviruses (ISF) (Blitvich *et al.*, 2015). The MBFV clade includes important pathogens of human and animals which may be also classified according to the disease they cause: i) hemorrhagic disease viruses (DENV and YFV); ii) neurotropic and encephalitis viruses (WNV, JEV, SLEV and ZIKV) and iii) acute febrile disease viruses (DENV, ZIKV, WNV) (Grard *et al.*, 2007; Lindenbach, 2013). Infections with some members of the TBFV clade might lead to encephalitis and neurological manifestations (LIV, TBEV and POWV) as well as to hemorrhagic fever (Omsk hemorrhagic fever virus; OHFV, Kyasanur forest disease virus; KFDV) (Grard *et al.*, 2007). The NKVF clade includes several flaviviruses such as the Yokose virus, Entebbe bat virus and the Modoc virus. Their biology and disease manifestation in humans and animals are unclear (Blitvich *et al.*, 2017).

Another flavivirus classification is based on antigenic similarity and the presence of serological cross-reactivity. WNV, JEV and USUV are classified into the Japanese Encephalitis complex; LIV, TBEV and KFDV are classified into the TBEV complex, ZIKV is grouped into the Spondweni serocomplex and DENV is grouped in a separated complex (Calisher *et al.*, 1989; Kuno *et al.*, 1998).

1.3.2) Structure and physical properties of flaviviruses

Virions are spherical and enveloped and contain an icosahedral nucleocapsid that surrounds the virus genome (**Figure 2 A and B**). They have a diameter of around 40-60 nm and are structurally composed by multiple copies of the capsid (C) protein, the envelope (E) protein and the membrane (M) protein (**Figure 2 A and B**) (Lindenbach, 2013; Oliveira *et al.*, 2017; Schweitzer *et al.*, 2009). The nucleocapsid is assembled by multiple copies of the C protein (12-14 kDa). The largest structural protein, the E protein (50-54 kDa), is highly glycosylated, responsible to interact with cellular receptors and elicits most of the neutralizing antibodies against the virus. The M protein is synthesized as a precursor-membrane protein (prM) of 18-20 kDa and is also highly glycosylated. Together with the E protein, it is responsible to form the outer surface of the virions. Its cleavage from prM to M is mediated by furin and constitutes an important step in virus maturation (Chambers *et al.*, 1990; Lindenbach, 2013).

The virus particle can be displayed in two physical states: mature particles (fully prM cleavage) and immature particles (no prM cleavage) (Pierson *et al.*, 2012). The immature particles (**Figure 2 C**) show approximately 60 spikes that are E/prM protein trimers while the mature particles are smooth and plane (**Figure 2 D**) with no spike projections on the surface (Pierson *et al.*, 2012).

Like most enveloped viruses, the flavivirus particle is sensitive to low pH, detergents, alcohols, aldehydes and beta-propiolactone as well as UV light and temperatures above 60°C (Muller *et al.*, 2016).
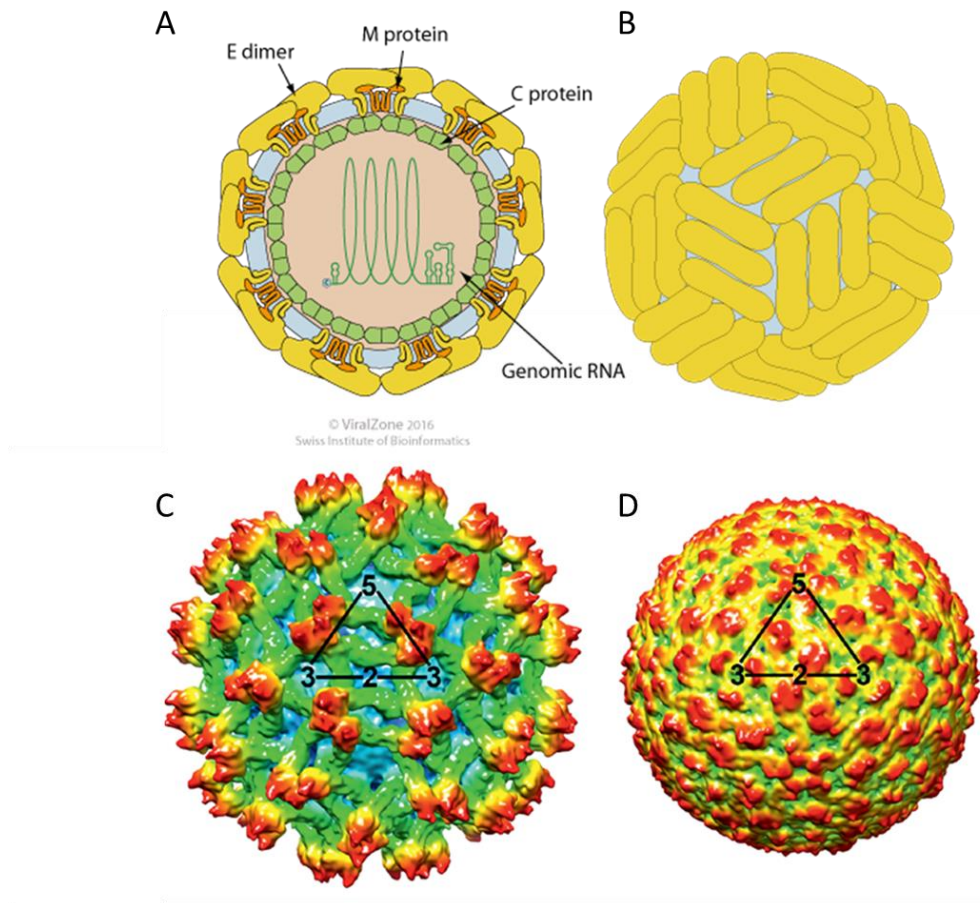
Figure 2: Schematical representation of flavivirus particles. Sagittal illustration showing the C protein, M protein as well as dimers of the E protein and the +ssRNA genome inside the capsid (A); outer surface of a mature virion (B); immature virus particle is depicted showing a rough structure of accumulated prM proteins (C) and smooth mature flavivirus particle (E). References: Figure 2 A and 2 B: http://viralzone.expasy.org/24?outline=all_by_species, modified. This picture is under Creative Commons Attribution 4.0 (CC.BY-NC.4.0); image 2 C and 2 D: Simmonds *et al.*, 2017, (no modifications). Republished with permission from Microbiology Society from Simmonds *et al.* 2017 DOI: https://doi.org/10.1099/jgv.0.000672.

1.3.3) Genome organization

The flavivirus genome is a single stranded RNA of positive polarity (+ssRNA) with approximately 11 Kb (9,500 to-12,500 nucleotides) that encodes for 10 proteins: three structural (C-prM-E) and seven non-

structural proteins (NS1-NS2a-NS2b-NS3-NS4a-NS4b-NS5; **Figure 3**) (Bollati *et al.*, 2010). The viral RNA functions as a messenger RNA (mRNA) and is immediately translated into a polyprotein (Mukhopadhyay *et al.*, 2005). The genome is arranged into a single open reading frame (ORF) that encodes a polyprotein of 3,300 to 3,500 amino acids which is cleaved by viral and host proteases (Chambers *et al.*, 1990).

The flavivirus genome is flanked by non-coding regions (NCR), with the 5' region being generally smaller than the 3' region (Chambers *et al.*, 1990; Gebhard *et al.*, 2011). The majority of flavivirus genomes lack a polyadenylation tail (poly A) at the 3' region. The only exception found among the flavivirus genomes is a European strain of TBEV (strain Neudörfl) that harbors a poly A tail in the 3' region. The function of the poly A tail in this specific strain of TBEV is still unclear (Asghar *et al.*, 2016; Mandl *et al.*, 1991). At the 5' region of all flaviviruses a type I cap structure (m7GpppAmp) is found (Gebhard *et al.*, 2011). In general, for most of the flaviviruses, in both 5' and 3' regions the RNA shows secondary structures resembling "hairpins" that are important for RNA transcription, translation and stability (Gebhard *et al.*, 2011).
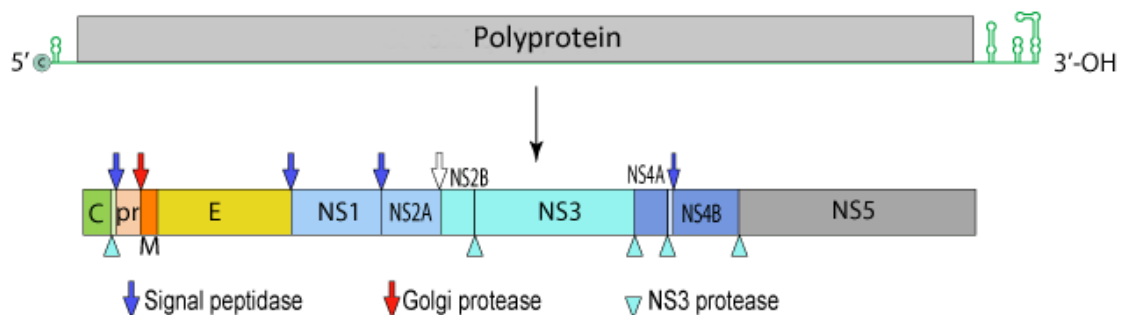
Figure 3: Genome organization for the members of the *Flavivirus* genus. The +ssRNA contains two non-coding regions at the 5' and 3' ends flanking a single open reading frame (ORF) that encodes a single polyprotein. The polyprotein is cleaved by viral and host proteases (arrows) resulting in three structural proteins (C-prM-E) and seven non-structural proteins (NS1-NS2a-NS2b-NS3-NS4a-NS4b-NS5). The structural protein encoding sequences are located downstream of the 5' end and the non structural protein encoding sequences upstream of the 3' end. Reference: Originally published in http://viralzone.expasy.org/24?outline=all_by_species, modified. This picture is under Creative Commons Attribution 4.0 (CC.BY-NC.4.0).

1.3.4) Functions of structural and non-structural proteins

1.3.4.1) Structural proteins

The C protein has the major function to shape the viral particle and to protect the viral RNA from degradation. However, other functions of the C protein still remain broadly unknown (Oliveira *et al.*, 2017). It is unclear how and at which point of the flavivirus replication the C protein recruits and packs the viral RNA (Samsa *et al.*, 2009). A study demonstrated that regions within the alpha-4 helix of the C protein are responsible for RNA packing (Ma *et al.*, 2004). The C protein was also found in the nucleus of infected cells

and is reported to interact with nuclear proteins and enhances replication of JEV (Mori *et al.*, 2005; Tsuda *et al.*, 2006). In addition to that, WNV C protein might interact with other cellular proteins and may induce apoptosis (Yang *et al.*, 2002). Since many functions and underlying mechanisms associated with the C protein have been studied in recent years, the C protein has been considered as an important target for antiviral drug design (Oliveira *et al.*, 2017).

The prM/M protein is associated with the E protein building heterodimers that are anchored into the lipid bilayers to form the outer viral surface (Zhang *et al.*, 2003). Studies have demonstrated the prM/M protein to be involved in apoptosis induction and interactions with host cells during virus entry, replication and assembly (Brabant *et al.*, 2009; Brault *et al.*, 2011; Catteau *et al.*, 2003; Gao *et al.*, 2010; Wong *et al.*, 2012). During the infection, antibodies are raised against the prM protein. Interestingly, those antibodies were reported to mediate entry of immature WNV and DENV virions via Fc receptor, thus enhancing the virus infection via a phenomenon known as antibody-dependent enhancement (ADE) (Colpitts *et al.*, 2011; Halstead, 1979; Rodenhuis-Zybert *et al.*, 2010a). However, it has not been elucidated whether the presence of those antibodies might be associated with a poor prognosis or with severe clinical manifestations of DENV infection (Rodenhuis-Zybert *et al.*, 2015).

The flavivirus E protein is a transmembrane protein and a class II fusion protein. Structurally, the E protein has three domains: E-DI, E-DII and E-DIII. In response to an acidic pH, the E protein undergoes irreversible conformational changes that eventually lead to the fusion of the virus particle with the endosomal membrane and consequently genome delivery into the cytoplasm (Kielian, 2014; Modis *et al.*, 2004; Smit *et al.*, 2011). The E-DI is the central domain of the E protein structure. E-DII contains a hydrophobic fusion loop, a peptide that is responsible for viral fusion with the cell membrane (Zhang *et al.*, 2004). In the immature virus particle, the fusion loop is covered by a portion of prM peptides impairing the virus fusion (Li *et al.*, 2008; Lindenbach, 2013). Studies on DENV and WNV have demonstrated that antibodies raised against the fusion loop are highly cross-reactive and might trigger ADE and internalization of immature particles via Fc receptor (Lai *et al.*, 2008; Rodenhuis-Zybert *et al.*, 2011a). Finally, the E-DIII is an immunoglobulin like domain and the most exposed domain of the E protein, forming projections along the virion. It also contains the receptor binding domain that mediates binding to the host cell (Lindenbach, 2013; Zhang *et al.*, 2004). Interestingly, some flaviviruses such as MVEV, YFV-17D and JEV have an integrin binding motif in their E-DIII, namely the RGD (Arg-Gly-Asp) motif, raising speculations that these viruses might use integrins as cellular receptors (van der Most *et al.*, 1999). In addition to that, among all other E protein domains, E-DIII is the most immunogenic domain and forms a major target for neutralizing antibodies. This domain has thus been used in several vaccine candidates as a target for antiviral drugs and as antigen in serological assays (Chavez *et al.*, 2010; Perera *et al.*, 2008). A vaccine harboring the YFV-17D backbone and the structural proteins of WNV is commercially available for horses. For humans, DENV

and JEV chimeric-based vaccines are available (Arroyo *et al.*, 2004; Chin *et al.*, 2013; Guy *et al.*, 2015; Monath *et al.*, 2002).

1.3.4.2) Non-structural proteins

The non-structural (NS) 1 protein is highly glycosylated and highly conserved among flaviviruses. Upon infection, the NS1 protein may be localized intracellularly or may be secreted. The NS1 protein is dimeric in case of intracellular localization and hexameric when secreted. The intracellular form of NS1 seems to be involved in immune evasion and interacts with host cell proteins (Rastogi *et al.*, 2016; Somnuke *et al.*, 2011). In association with NS4b, NS1 is also reported to be involved in virus replication (Muller *et al.*, 2013; Rastogi *et al.*, 2016). The secreted form of NS1 is highly immunogenic and has been detected in antigen capture based assays during early infection. Furthermore, some authors have proposed that NS1 is a biomarker and that high levels of anti-DENV NS1 antibodies might be correlated with more severe disease (Hermann *et al.*, 2014; Paranavitane *et al.*, 2014; Singh *et al.*, 2010). Several studies have also demonstrated that soluble NS1 from different flaviviruses can inhibit the complement system by interacting with C4b complement protein and factor H (Avirutnan *et al.*, 2010; Avirutnan *et al.*, 2011; Chung *et al.*, 2006).

The NS2 protein is cleaved into two different proteins: NS2A and NS2B. The NS2A is a hydrophobic protein that is involved in RNA replication and virus assembly (Leung *et al.*, 2008; Lindenbach, 2013). NS2A was also reported to interact with the 3' NCR of the viral genome and to modulate the interferon responses (Liu *et al.*, 2005; Mackenzie *et al.*, 1998). NS2B interacts as a cofactor with NS3 and this complex has been demonstrated to be the main viral protease and is involved in the processing of viral structural proteins (Bessaud *et al.*, 2006; Murray *et al.*, 2008). This complex has been targeted as candidate for antiviral drugs (Aguilera-Pesantes *et al.*, 2017). The NS3 is a multifunctional protein involved in RNA replication. Studies further demonstrated protease, helicase and NTPase activities of this protein (Lindenbach, 2013; Wu *et al.*, 2005). A study with YFV demonstrated that NS3 alone is also involved in virus assembly (Patkar *et al.*, 2008).

Similar to NS2, the NS4 protein is cleaved into two proteins: NS4A and NS4B. Although their exact functions are unclear, both proteins are membrane associated and have been shown to be linked to flavivirus replication complexes (FRC) (Lindenbach, 2013; Miller *et al.*, 2007; Nemesio *et al.*, 2012). A study suggested that the NS4A of WNV is an essential co-factor for NS3, leading to NS3 helicase activity (Shiryaev *et al.*, 2009).

The NS5 protein is the largest flavivirus protein (103 kDa) and the most conserved protein among the flaviviruses (Lindenbach, 2013). Due to its high similarity among the members of *Flavivirus* genus, the NS5

protein nucleotide sequence is widely used for phylogenetic and flavivirus evolution analysis (Baleotti *et al.*, 2003; Kuno *et al.*, 1998). Several functions have been attributed to NS5. The most important one is its RNA-dependent RNA polymerase (RdRp) activity. In this case, NS5 plays an essential role in the RNA replication, being involved in the synthesis of both negative and positive strand RNAs during the flavivirus replication cycle (Bollati *et al.*, 2010; Klema *et al.*, 2015). Another important function associated to NS5 is its methyltransferase activity being important for adding the cap structure to the 5' NCR (Ray *et al.*, 2006). This process constitutes an important mechanism of viral immune evasion not only for flaviviruses but for other viruses as well (Dong *et al.*, 2014).

1.4) Flavivirus interaction with the host cell

1.4.1) Flavivirus entry into the host cell

The flavivirus entry is a complex process involving the usage of multiple receptors and accessory molecules. Initially, virions bind to the host cell via electrostatic, non-specific and low affinity interactions with cell membrane molecules. The interaction with those molecules does not mediate virus entry but virus attachment leading to accumulation of virions on the cell membrane (Grove *et al.*, 2011; Smit *et al.*, 2011). Upon attachment, flaviviruses move along the cell membrane in order to find their specific receptor(s) that will mediate entry into the host cell. Flaviviruses mainly enter the host cell by receptor-mediated endocytosis, i.e. clathrin-mediated endocytosis (Kaufmann *et al.*, 2011; Smit *et al.*, 2011; van der Schaar *et al.*, 2008). However, alternative routes have been reported by other authors. For example, DENV might enter the cells alternatively by caveolae, dynamin or macropinocytosis (Acosta *et al.*, 2009; Suksanpaisan *et al.*, 2009). WNV has been described to enter the cell by lipid rafts (Medigeshi *et al.*, 2008). A study with TBEV suggested an alternative entry route by macropinocytosis in Caco-2 cells (Yu *et al.*, 2014).

Flavivirus internalization is a relatively fast event according to two studies with DENV and WNV, demonstrating that virions were internalized within less than five minutes after binding to a cellular receptor (Chu *et al.*, 2004a; van der Schaar *et al.*, 2008). Upon internalization, virions are located in the early and late endosomes until they finally fuse with the lysosomes (Smit *et al.*, 2011; Yamauchi *et al.*, 2013). The intracellular trafficking of the virion along the endosomes is controlled by a group of GTPases called Rab (Jordens *et al.*, 2005; Yamauchi *et al.*, 2013). Rab 5 and Rab 7 proteins have been shown to be required for DENV and WNV entry into Hela cells (Krishnan *et al.*, 2007).

Fusion of late endosomes with the lysosomes causes endosomal acidification leading to pH-dependent irreversible changes in the E protein conformation and consequently, to fusion of the viral and endosomal membrane (Kaufmann *et al.*, 2011). Studies demonstrated that the E protein changed its conformation by

mild-acidic environment (pH 5.0 to 6.0) leading to E protein trimerization and consequently fusion loop exposition (Stiasny *et al.*, 2007). Treatment with drugs that inhibit endosomal acidification such as chloroquine led to inhibition of DENV-2 fusion and consequently replication in both *in vitro* and *in vivo* models (Farias *et al.*, 2013; Farias *et al.*, 2014; Farias *et al.*, 2015). Other *in vitro* studies using drugs that inhibited endosomal acidification also showed inhibition of WNV and JEV replication (Chu *et al.*, 2006; Chu *et al.*, 2004a; Kalia *et al.*, 2013). Fusion of the viral and endosomal membrane is then followed by virus uncoating and releasing the viral RNA into the cytoplasm where the replication cycle is initiated (Mukhopadhyay *et al.*, 2005; van der Schaar *et al.*, 2008).

1.4.2) Flavivirus replication

Flavivirus replication takes place in membrane-induced vesicles located in the cytoplasm of infected cells (Bartholomeusz *et al.*, 1999; Brinton, 2013; Romero-Brey *et al.*, 2014). Within the cytosol, the viral +ssRNA is immediately translated into a single polyprotein that is cleaved at first by host proteases (Murray *et al.*, 2008; Natarajan, 2010). The flavivirus non-structural proteins induce modifications in the cellular membranes of the endoplasmatic reticulum (ER), building compartments, the FRC. Inside the FRC, the viral proteins necessary to support viral replication accumulate and the viral RNA is then replicated (Klema *et al.*, 2015; Saeedi *et al.*, 2013). The NS5 then transcribes +ssRNA template into a negative-strand RNA and a transitory double strand RNA (dsRNA) structure is formed. Thus, the dsRNA is separated by NS3 helicase activity and the negative-strand RNA is used as template for the synthesis of new +ssRNA (Klema *et al.*, 2015; Natarajan, 2010). The newly synthesized +ssRNA is then translated into a single polyprotein that is cleaved by host and viral proteases. Following that, post-translational cleavage of C-prM-E proteins takes place mediated by the NS2B/NS3 complex and host proteases. The structural proteins remain anchored in the membrane of the ER while more +ssRNA is synthesized (Klema *et al.*, 2015; Lindenbach, 2013). Assembly of new virus particles occurs in the lumen of the ER when the C protein physically interacts with the +ssRNA leading to packing of viral RNA and formation of the nucleocapsid. The nucleocapsid containing the viral RNA is budding through the ER which consists the prM-E protein heterodimers forming the immature virus particle (Fernandez-Garcia *et al.*, 2009; Murray *et al.*, 2008). In this immature state, the prM hides the fusion loop located at the E-DII protein to avoid self-fusion with the Golgi membranes during the trans-Golgi pathway. Following the trans-Golgi pathway, the prM protein is cleaved by furin exposing the fusion loop and dissociation of prM-E complexes giving the virions a status of mature particles (Heinz *et al.*, 1994; Stadler *et al.*, 1997; Yu *et al.*, 2008; Zhang *et al.*, 2003). Infectious mature virus particles are released by exocytosis pathway (Fernandez-Garcia *et al.*, 2009). An overview of the flavivirus replication cycle and genome replication is shown in **Figure 4**.
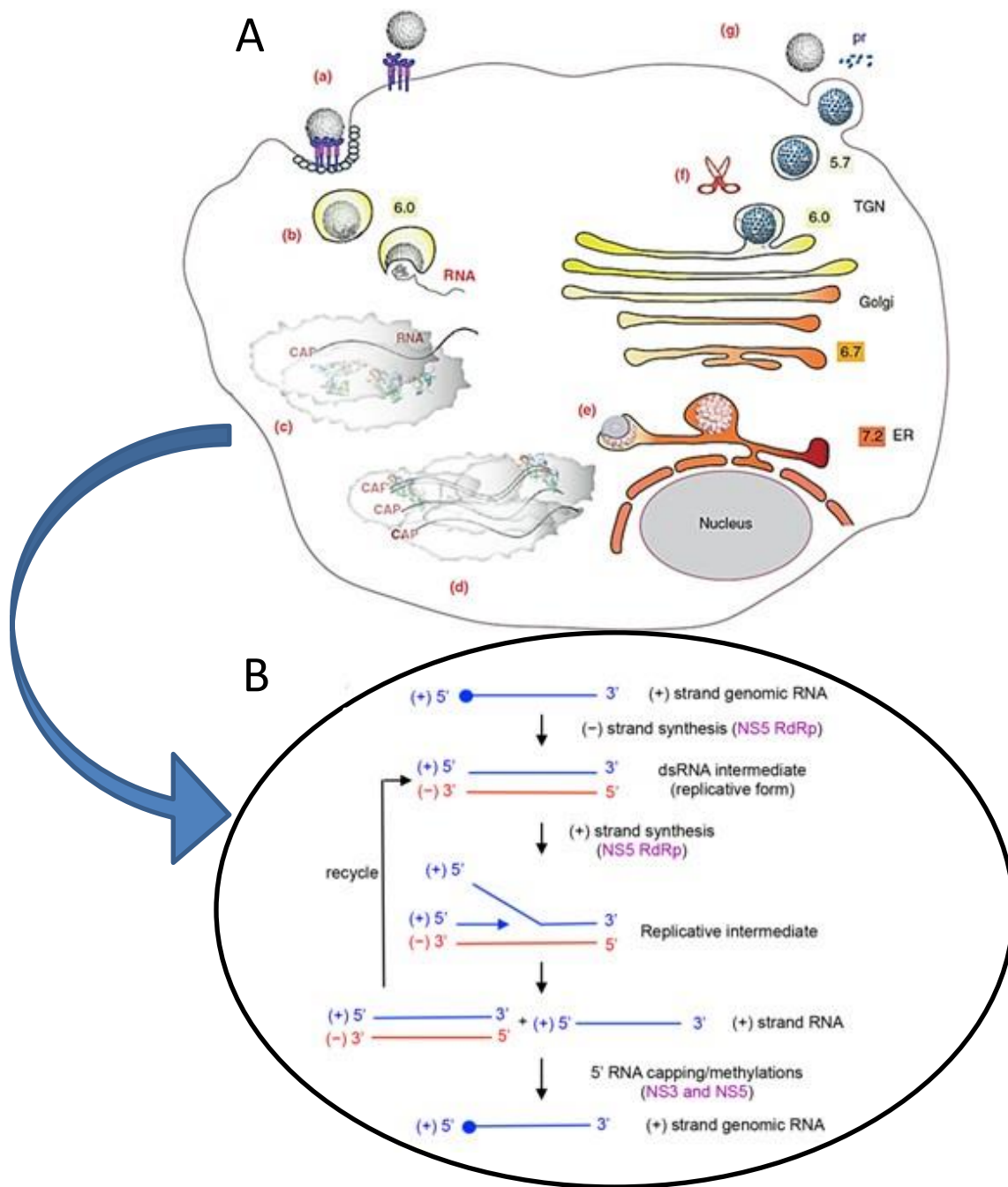
Figure 4: Flavivirus replication cycle. **(A)** After binding, flaviviruses are internalized by receptor mediated endocytosis (a), the low endosomal pH triggers irreversible changes in the E protein leading to fusion of viral membrane with endosome, uncoating and delivery of viral genome (b); the viral positive single stranded RNA (+ssRNA) is subsequently translated and replicated in the perinuclear region inside the flavivirus replication complex (c); virus assembly occurs in the endoplasmatic reticulum following a final glycosylation in the Golgi complex (e); the cleavage of prM to M and consequent final maturation is mediated by furin along the trans-Golgi network (f) and the virus is secreted by exocytosis (g). **(B)** The +ssRNA is immediately translated into a polyprotein that is cleaved first by host proteases and later by viral proteases. The +ssRNA is then transcribed in a negative-strand RNA and the viral genome acquires an intermediate double strand (ds) RNA state. The negative-strand RNA serves as a template for synthesis of new +ssRNA. A final 5' CAP is added to the newly synthesized viral +ssRNA. References: Figure A: Reprinted from Rodenhuis-Zybert *et al.,*(2011b) with permission from Elsevier (Rodenhuis-Zybert *et al*. 2011b, DOI: https://doi.org/10.1016/j.tim.2011.02.002, modified; Figure B: Klema *et al.,*(2015), no modifications. This picture is under Creative Commons Attribution 4.0 (CC.BY.4.0)

10

1.5) Epidemiology

In North America, the circulation of WNV, SLEV and POWV have been reported in USA and Canada. DENV has been also reported in parts of USA (Texas, Hawai and Puerto Rico) and Mexico (Davis *et al.*, 2008). In Central and South America, especially in Brazil, the circulation of several flaviviruses has been described, among them DENV, WNV, SLEV, ZIKV, YFV, Rocio virus, Bussuquara virus, Cacipacoré virus, Iguape virus and Ilhéus virus. Thereof, in particular DENV, ZIKV and YFV are of greater importance for publich health (Figueiredo, 2000; Zanluca *et al.*, 2015). DENV is responsible for large outbreaks in Brazil and surrounding countries in South and Central America (Ramos-Castaneda *et al.*, 2017). In 2015, ZIKV was first detected in the northeast from Brazil (Zanluca *et al.*, 2015). In the following years, more than 210,000 cases of ZIKV infection were recorded with more than 10,000 suspected cases of microcephaly (Brazillian Ministry of Health - MS 2016a; Brazillian Ministry of Health - MS 2016b).

In Europe, WNV, USUV and TBEV are the major flaviviruses circulating within the continent (Papa, 2017). In 2016, the European Center for Disease Control (ECDC) recorded 225 cases of WNV in humans with most of the cases in South and Southeast Europe (ECDC, 2016). USUV was first detected in 1996 in Italy, from a dead Eurasian blackbird (*Turdus merula*) (Weissenbock *et al.*, 2013). Since then, USUV has been spreading throughout Europe and has been detected in birds in Austria, Belgium, Czech Republic, England, Germany, Greece, Hungary, Spain and Switzerland (Ashraf *et al.*, 2015; Engel *et al.*, 2016). TBEV is the causative agent of severe encephalitis in humans in Europe and its circulation is reported in 27 European countries. Although an effective vaccine is available, the number of cases have recently increased (Amicizia *et al.*, 2013).

JEV, DENV, WNV, ZIKV, MVEV and Kunjin virus (KUJV) are the flaviviruses of major concern in Asia and Australia (Kindhauser *et al.*, 2016; Mackenzie *et al.*, 2009; Russell *et al.*, 2000). JEV is present in 24 countries in Asia, Western Pacific and Northern Australia (Wang *et al.*, 2015b). It is estimated that more than 67,000 human cases of JEV infection occur every year (Campbell *et al.*, 2011a). DENV represents a public health problem especially in Southeast Asia and the Western Pacific region with up to 187,000 cases in 2010 (Murray *et al.*, 2013). MVEV has caused sporadic encephalitis cases in humans in Australia (Russell *et al.*, 2000). KUJV is classified within the WNV group and has been reported to circulate in Australia. In general, most of the infections are asymptomatic and result in mild clinical manifestations (Prow, 2013). ZIKV is endemic in eight countries in Asia, but ZIKV infections seem to be very sporadic and outbreaks have been rarely reported (Kindhauser *et al.*, 2016; Posen *et al.*, 2016; Wiwanitkit, 2016). In the federal states of Micronesia, ZIKV is endemic with huge outbreaks in Yap Islands and French Polynesia. Serological surveys estimated that 73% of the Yap Island population have antibodies against ZIKV (Duffy *et al.*, 2009).

1.6) Flavivirus transmission and ecology

Most of the flaviviruses are maintained in nature by two distinct transmission cycles: the enzootic (= sylvatic) or urban (= human) cycle (Vasilakis *et al.*, 2011). The sylvatic cycle involves mosquitoes and wild animals such as birds and/or non-human primates or, for TBFV, ticks, rodents and apparently wild deer (Mansfield *et al.*, 2009; Weaver *et al.*, 2004). The urban cycle, especially important for DENV, YFV and ZIKV, involves humans and the *Aedes* spp. mosquitoes in urban and peri-urban areas. In this case, humans play an important role in facilitating the infection of naïve mosquitoes (Vasilakis *et al.*, 2011; Vasilakis *et al.*, 2017).

1.6.1) Transmission vectors

The majority of flaviviruses are transmitted by mosquitoes and only a few flaviviruses are transmitted by ticks (Huang *et al.*, 2014; Lasala *et al.*, 2010). Several studies have demonstrated that many mosquito species such as *Aedes* spp. and *Culex* spp. are susceptible to flaviviruses and transmit them to other hosts (Conway *et al.*, 2014). *Aedes aegypti* and *Aedes albopictus* are the most widespread mosquitoes being found in the Americas, Africa, Europe, Asia and Australia and are competent vector of DENV, YFV, ZIKV and many other flaviviruses (Kraemer *et al.*, 2015). *Culex* spp. have the similar global distribution as *Aedes* spp. and are vectors of WNV, KUJV, JEV, MVEV and SLEV (Prow, 2013; Samy *et al.*, 2016).

Ticks transmit flaviviruses such as TBEV, LIV, POWV, KFDV and OHFV (Dobler, 2010). The genus *Ixodes* spp. is globally widespread and responsible for the transmission of POWV, LIV and TBEV in North America, Europe and Asia (Dobler, 2010; Pettersson *et al.*, 2014).

Although the majority of flaviviruses are transmitted via arthropods, a small number of human infections happens without any vector. The majority of non-vectored infections occurs by blood transfusion, bone marrow as well as solid organ transplantations (Chen *et al.*, 2016). Sexual transmission of flaviviruses has also been reported, especially for ZIKV (Foy *et al.*, 2011; Grischott *et al.*, 2016). Perinatal transmission of DENV and ZIKV was reported in endemic areas (Besnard *et al.*, 2014; Chen *et al.*, 2016; Grischott *et al.*, 2016).

1.6.2) Flavivirus reservoirs

Birds, rodents, other small mammals and some reptiles are known to be a reservoir for flaviviruses (Weaver *et al.*, 2004). Humans, horses and some livestock and domestic animals are usually considered to be dead-end hosts as they normally do not transmit the virus to other vertebrates. Since they do not sustain strong and persistent viremia, these hosts do not function as a reservoir for re-infection of

12

mosquitoes which impedes the arbovirus transmission cycle (van den Hurk *et al.*, 2009; Weaver *et al.*, 2004).

Birds are the main reservoir for flaviviruses, especially for those that belong to the Japanese encephalitis serocomplex such as WNV, JEV and USUV. WNV infects more than 100 different bird species while JEV is able to infect more than 90 and USUV more than 30 bird species (Ashraf *et al.*, 2015; Campbell *et al.*, 2002; van den Hurk *et al.*, 2009). This broad avian host range and the migratory behavior might contribute to the emergence and introduction of flaviviruses to new environments such as observed for WNV in North America and JEV in Australia (van den Hurk *et al.*, 2009; Weaver *et al.*, 2004). In general, flavivirus infection in birds leads to high and long-lasting viremia. For this reason birds are often considered to be amplifying hosts of many flaviviruses. For JEV, pigs may also act as amplifying hosts (van den Hurk *et al.*, 2009; Weaver *et al.*, 2004).

Ticks are the main reservoir for TBEV nevertheless, rodents and other wildlife animals such as deers are important in the maintenance of TBEV in nature (Lindquist, 2014; Lindquist *et al.*, 2008). Although the role of birds in the TBEV life cycle has not yet been unravelled, birds might spread TBEV infected ticks into distant areas (Mansfield *et al.*, 2009). A study conducted by Waldenstrom *et al.*,(2007) found TBEV infected ticks on birds migrating from Western Russia to Sweden.

Finally, although not considered reservoir, non-human primates are an important amplifying host for several flaviviruses such as DENV, ZIKV and in special for YFV in the Americas and Africa (Barrett *et al.*, 2007; Kuno *et al.*, 2017).

1.7) Flavivirus pathogenesis

Following inoculation by mosquito or tick bite, flaviviruses initiate a prompt replication at the inoculation site infecting mainly fibroblasts, epithelial cells, resident macrophages and migratory dendritic cells (Langerhans cells) (Bustos-Arriaga *et al.*, 2011; Samuel *et al.*, 2006). This early replication in local tissues enables the flaviviruses to increase the viral load allowing further migration to target tissues/cells. Infected Langerhans cells and resident macrophages migrate to the draining lymph node where the virus initiates the spreading through the lymphatic system, consequently reaching the blood stream and disseminating to the target cells and tissues (Kaufmann *et al.*, 2011; Martina *et al.*, 2009).

Viremia in birds is detected within less than 24 hours after infection with a recent study demonstrating viremia even 30-45 minutes after infection (Gamino *et al.*, 2013; Reisen *et al.*, 2007). In humans, viremia for WNV and DENV is observed between 2-4 and 1-7 days after infection, respectively (Busch *et al.*, 2008; Vaughn *et al.*, 2000).

The mechanisms for neuroinvasion of neurotropic flaviviruses are poorly understood. There have been four routes proposed: i) hematogenic dissemination; ii) blood brain barrier disruption; iii) infected leukocyte mediated migration ("Trojan-horse") and iv) transneural route (Sips *et al.*, 2012; Suen *et al.*, 2014). The pathogenesis of hemorrhagic diseases observed in DENV, KFDV and OHFV infections seems to be rather immune-mediated than directly caused by the infection of endothelial cells. In this case, the strong activation of the immune response would alter the vascular permeability leading to hemorrhagic manifestations (Back *et al.*, 2013). High levels of Tumor Necrosis Factor alpha, interleukin (IL-) 6 and IL-8 were found in patients with dengue hemorrhagic fever (Martina *et al.*, 2009).

1.8) Clinical manifestations

Flavivirus infections may lead to four distinct manifestations: i) asymptomatic infection (or sub-clinical infection); ii) acute febrile disease; iii) hemorrhagic fever and iv) meningoencephalitis (Cobo, 2016; Martina *et al.*, 2009; Turtle *et al.*, 2012). Asymptomatic infections account for approximately 80 % of flavivirus infection cases in humans in special for WNV and DENV (Hayes *et al.*, 2005; Reiter, 2010). DENV, YFV and KFDV are more related to hemorrhagic fever and manifestations related to hemodynamic disorders (Holbrook, 2012; Martina *et al.*, 2009). Most of the members of the Japanese encephalitis complex such as WNV, JEV, MVEV and SLEV are more reported to cause encephalitis in humans and animals (Niven *et al.*, 2017; Turtle *et al.*, 2012). Horses infected by WNV seem to develop neurological manifestations in more than 10% of the infections and less than 1% of humans develop neurological manifestations (Castillo-Olivares *et al.*, 2004). Symptomatic USUV infections in humans are rare and more confined to immunocompromised individuals. However, antibodies against USUV were found in asymptomatic blood-donor individuals in Italy (Allering *et al.*, 2012; Gaibani *et al.*, 2012). POWV, LIV and TBEV infections result in most of the cases in neurological manifestations such as encephalitis and meningoradiculitis (Bogovic *et al.*, 2015; Turtle *et al.*, 2012). Several case reports have described atypical clinical manifestations of flavivirus infections especially in hyper-endemic areas such as South and North America, Asia and Australia. In case of DENV infections, hepatitis, pneumonia, optical neuritis, pancreatitis, nephritis and myocarditis have been reported (Gulati *et al.*, 2007; Nimmagadda *et al.*, 2014). Atypical clinical manifestations due to WNV infection are more related to central nervous system disorders. Those include acute flaccid paralysis, Guillain-Barré Syndrome, meningoradiculitis and a polio-like syndrome (Ahmed *et al.*, 2000; Josekutty *et al.*, 2013; Leis *et al.*, 2012; Sejvar *et al.*, 2003). Recently, ZIKV was linked to abnormal malformations in newborns (microcephaly) and spontaneous abortions as well as atypical clinical manifestations in adults such as the Guillain-Barré syndrome and encephalitis (Cao-Lormeau *et al.*, 2016; Martines *et al.*, 2016; Paixao *et al.*, 2016).

1.9) Flavivirus receptors and host cell factors

During the initial steps of infection, viruses must cross the cell membrane to deliver their genome into the cytoplasm and complete the replication cycle. Prior to entry, viruses interact with a diverse repertoire of cellular molecules in order to find their receptor to mediate virus particle internalization, fusion and genome delivery (Bhella, 2015; Yamauchi *et al.*, 2013).

Over the last few decades, the knowledge concerning the mechanisms of flavivirus interaction with the host cells have increased dramatically. However, many aspects of these flavivirus-host interactions still remain unclear. To date, many flavivirus receptor candidates as well as host cell factors have been identified and suggested to interact with flaviviruses during the course of infection (Fernandez-Garcia *et al.*, 2009; Pastorino *et al.*, 2010; Perera-Lecoin *et al.*, 2013).

Host cell factors are defined as molecules that may interact with (flavi)viruses during the early steps of infection, during RNA replication or may be involved in virus assembly and egress (Foo *et al.*, 2015; Wang *et al.*, 2017; Ward *et al.*, 2016).

1.9.1) Flavivirus receptors

According to the literature, flaviviruses might either use an ubiquitously expressed molecule or multiple receptor molecules to invade the host cell. In this process, molecules such as attachment factors and the putative receptor(s) act synergistically to promote flavivirus entry into the host cell (Perera-Lecoin *et al.*, 2013; Smit *et al.*, 2011).

Notably, glycoaminoglycans (GAG), in particular heparan sulfate, are widely expressed in most of cell lines and have been demonstrated to interact with flaviviruses during the initial steps of infection. Interactions between flavivirus particles and GAGs are mainly mediated by negatively charged carbohydrates such as GAGs that bind to the positively charged flavivirus E protein (Afratis *et al.*, 2012; Perera-Lecoin *et al.*, 2013; Smit *et al.*, 2011). The importance of heparan sulfate on flavivirus binding to the cell surface was extensively demonstrated by several studies: heparin (a heparan sulfate analogue) or lactoferrin (a molecule that binds GAGs), were both able to block entry of several flaviviruses such as DENV, YFV, WNV, JEV ,TBEV and ZIKV (Chen *et al.*, 2017; Chen *et al.*, 1997; Chien *et al.*, 2008; Germi *et al.*, 2002; Hilgard *et al.*, 2000; Kim *et al.*, 2017; Kroschewski *et al.*, 2003; Lee *et al.*, 2004; Tan *et al.*, 2017). Although the role of GAGs in flavivirus attachment and entry was extensively shown, this characteristic seems to be related to virus attenuation, adaptation to cell culture and loss of virulence *in vivo* as reported in some studies with DENV, JEV, MVEV and TBEV (Lee *et al.*, 2002; Lee *et al.*, 2006a; Mandl *et al.*, 2001).

Dendritic cell-specific intercellular adhesion molecule-3 grabbing non-integrin (DC-SIGN) is a C-type lectin that has also been implicated to play a role in attachment and entry of WNV and DENV in human cell lines

such as monocytes and dendritic cells (Davis *et al.*, 2006; Navarro-Sanchez *et al.*, 2003; Tassaneetrithep *et al.*, 2003). More recently, HEK293 cells expressing the DC-SIGN receptor were reported to greatly enhance ZIKV infection in up to 50% (Hamel *et al.*, 2015).

TIM and TAM receptors belong to a class of transmembrane phosphatidylserine binding receptors that have been involved in entry of several enveloped viruses including flaviviruses such as WNV, DENV, and ZIKV (Hamel *et al.*, 2015; Jemielity *et al.*, 2013; Meertens *et al.*, 2012). In the case of ZIKV, a study demonstrated that both TIM and TAM mediated ZIKV entry into human fibroblasts with TAM being more effective in mediating ZIKV infection than TIM (Hamel *et al.*, 2015). However, a recent study using a group of mice deficient for TAM receptors demonstrated that expression of TAM receptors are not required for ZIKV infection *in vivo,* reinforcing the multitude of flavivirus receptor usage and the hypothesis that flaviviruses use multiple receptors to gain access to the target cells (Hastings et al., 2017)*.*

The high affinity laminin receptor has been described to play a role in flavivirus entry in mammalian as well as in mosquito cells. A study conducted by Tio *et al.*,(2005) using a virus overlay binding protein assay identified that DENV serotypes 1, 2 and 3 but not DENV serotype 4 interacted with the laminin receptor. Thepparit *et al.*,(2004b) also identified the laminin receptor as potential DENV receptor in a human hepatic cell line (HepG2). In this study, entry of DENV serotype 1 into HepG2 cells was blocked by anti-laminin antibodies as well as by soluble laminin in a dose-dependent manner. Interestingly, this phenomenon was only shown for DENV serotype 1 but not for DENV serotypes 2, 3 and 4 serotypes in this study (Thepparit *et al.*, 2004b). In C6/36 mosquito cells, soluble laminin and antibodies against the laminin receptor were shown to abrogate binding and internalization of DENV serotypes 3 and 4, but had no impact on DENV serotype 1 and 2 (Sakoonwatanyoo *et al.*, 2006).

Similarly, the laminin receptor has been identified to play a role in JEV entry into neural cells and anti-laminin receptor antibodies disrupted JEV infection in up to 25% (Thongtan *et al.*, 2012). Vimentin was also implicated to be involved in JEV binding and internalization. A study demonstrated that silencing the human vimentin gene greatly impaired the binding and entry of RP9, a pathogenic JEV strain (Liang *et al.*, 2011).

1.9.2) Flavivirus host cell factors

Over the last few years, several molecules have been reported as flavivirus host cell factors. Recently, a CRISPR genetic screening based strategy was used to unravel host cell factors for DENV and HCV in a hepatic human cell line (Huh 7) (Marceau *et al.*, 2016). This study identified many families of proteins associated to the ER such as the translocon associated protein complex, ER associated protein degradation (ERAD) and oligosaccharyltransferase protein complex (OST) (Marceau *et al.*, 2016). Further validation by

cell infection assays with several flaviviruses demonstrated that DENV, WNV, ZIKV and YFV replication was completely abrogated by the deletion of the above mentioned molecules, implicating that flaviviruses share mutual host cell factors (Marceau *et al.*, 2016).

More recently, a family of proteins called "reticulon" have been reported to be involved in flavivirus replication. This family of proteins is mostly found in the ER and is associated with the formation of vesicles and membranes in the ER (Aktepe *et al.*, 2017). By downregulating the expression of reticulon 3.1A protein, the authors showed that WNV, ZIKV and DENV replication was substantially impaired but not completely abrogated. The authors suggested that the presence of this family of proteins in the ER is of great importance for the flavivirus membrane induced remodeling, a process that is essential for the flavivirus RNA replication (Aktepe *et al.*, 2017).

Another study reported a total of 96 genes to be involved in WNV replication using a large scale siRNA screening in *Drosophila melanogaster* cells (Yasunaga *et al.*, 2014). Among those host cell factors, several identified proteins were involved in WNV endocytosis and endosomal acidification. Although lacking functional validation, this work provides important insights into the multitude of flavivirus host cell factors in different hosts (Yasunaga *et al.*, 2014).

The RNA binding protein AUF1 p45, a cellular chaperone, has been reported to be a common flavivirus host cell factor. Silencing of AUF1 p45 in Huh7 cells significantly dropped WNV, ZIKV and DENV replication by destabilizing the viral genome and impeding its cyclisation (Friedrich *et al.*, 2017).

The Golgi ERI3 protein belongs to a family of RNA binding proteins that was reported to be a host cell factor for DENV and YFV (Ward *et al.*, 2016). Though ERI3 was not required for DENV and YFV RNA stability, the authors concluded that ERI3 is essential for flavivirus RNA synthesis (Ward *et al.*, 2016).

A class of ribosomal proteins including RPLP1 and RPLP2, has been found to be required for RNA translation of a number of flaviviruses such as DENV, ZIKV and YFV in human and mosquito cell lines (Campos *et al.*, 2017).

1.10) Cell Adhesion molecules and their involvement in flavivirus infection

1.10.1) Brief overview

Tissues are composed of cells and an extracellular matrix (ECM) that is vital to sustain the architecture and conformation of the tissue (Gumbiner, 1996). The major function of cell adhesion molecules is to mediate contact between the cell surface and the ECM or mediate cell-cell contacts (Chothia *et al.*, 1997). There are mainly four families of cell adhesion molecules: cadherins, immunoglobulins, selectins and integrins (Lodish H, 2000). The cadherins are a family of cell surface proteins that are important for shaping the tissue architecture. The major function of cadherins is to mediate cell-cell adhesion (Shapiro *et al.*, 2009).

The immunoglobulin superfamily comprises molecules such as antibodies, major histocompatibility complex (MHC) and membrane associated proteins of T and B cell receptor complex (Wai Wong *et al.*, 2012). Immunoglobulin-like proteins are associated with cell adhesion functions. Representatives are neural cell adhesion molecule (NCAM), junctional cell adhesion molecule (JAM), intercellular cell adhesion molecule (ICAM) and vascular cell adhesion molecule (VCAM) (Aricescu *et al.*, 2007). The selectin family of cell adhesion molecules is represented by P-, E-, and L-selectins that stand for platelet-, endothelial- and leukocyte- selectins, respectively. Their major function is to mediate leukocyte and platelet adhesion to the vascular endothelium (Bendas *et al.*, 2012). Integrins were first described in 1986 when fibronectin was found to bind to a group of transmembrane proteins that functioned as respective receptors (Hynes, 1987; Tamkun *et al.*, 1986). The name "*integrin*" was then proposed to these newly discovered transmembrane proteins due to their ability to link the ECM with the cytoskeleton (Hynes, 2002; Hynes, 2004).

1.10.2) The integrin family

Integrins are characterized as a large family of cell adhesion molecules expressed in almost all cell lines that display a diverse repertoire of integrins depending on their function and localization (Hynes, 2002). For example, while leukocytes express high levels of β2 integrin subunits (known as "leukocyte integrin"), epithelial cells and fibroblasts lack the expression of this integrin subunit (Harris *et al.*, 2000). Integrins are expressed in mammalian cells as well as in sponges, corals, arthropods and nematodes and share a high degree of similarity among the species (Brower *et al.*, 1997; Burke, 1999; Hughes, 2001).

Integrins are heterodimeric molecules composed of two subunits, alpha (α) and beta (β). Both subunits are non-covalently bound. Up to now, there are 18 α subunits and 8 β subunits known that are able to create 24 different integrin combinations (**Figure 5**) (Campbell *et al.*, 2011b; Hynes, 2002).
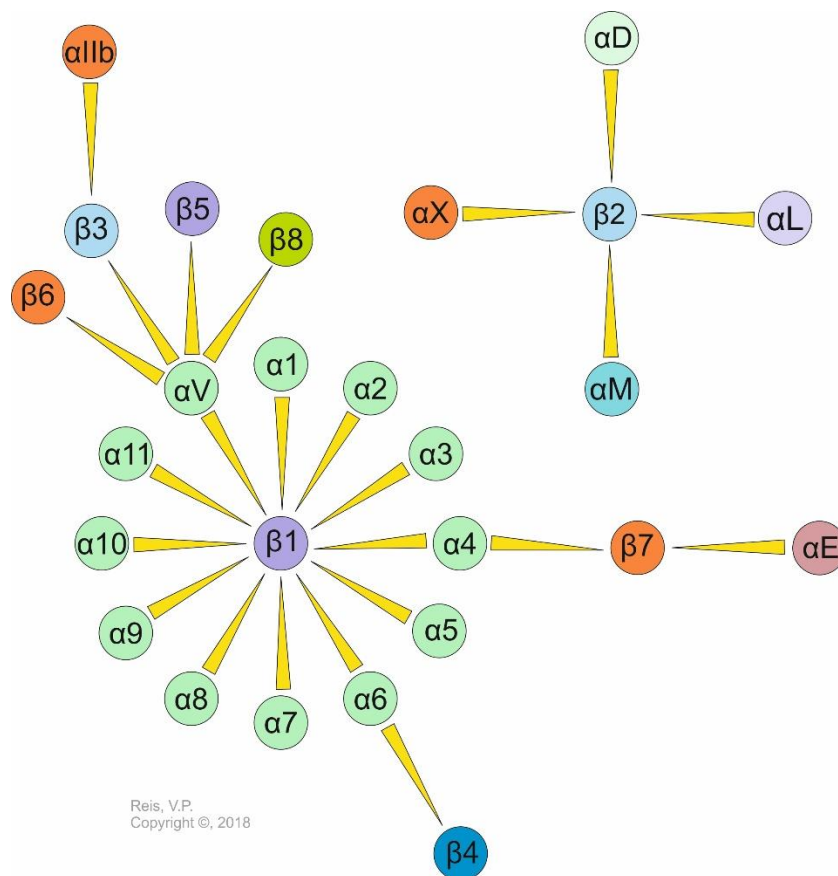
Figure 5: The integrin family and their possible α and β integrin subunits combinations. There are 18 α integrin subunits and 8 β integrin subunits. The αβ integrin combination enables to form 24 distinct integrin molecules. The β1 integrin subunit is the more promiscuous integrin subunit enabling more possible combinations.

Integrins are type I transmembrane molecules (**Figure 6**) with an ectodomain (extracellular part), a transmembrane domain and a short cytoplasmatic tail that is responsible for signal transduction (Hynes, 2002; Ulmer, 2010). Integrins are allosteric proteins and can be found in three different states (**Figure 6**): i) inactive state (also called "bent" state) at which they show low affinity and are unable to bind the ligands (**Figure 6 A**); ii) "extended" state in which they show some affinity to the ligands (**Figure 6 B**) and iii) active state ("ligand occupied" state or "high affinity" state) in which they display a high affinity to the ligands (**Figure 6 C**) (Askari *et al.*, 2009; Evans *et al.*, 2009; Srichai, 2010).
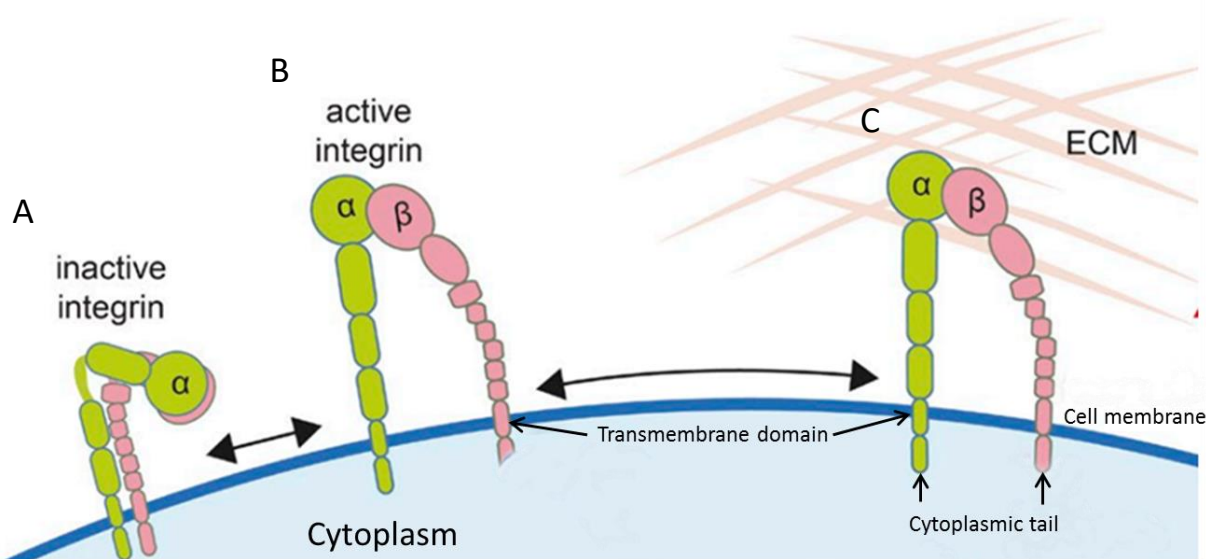
Figure 6: Integrin structure and conformations: bent inactive integrin state (A); active, extended integrin state (B) and active, high affinity integrin state bound to the extracellular matrix (ECM); C). The α integrin subunit is represented in green while the β integrin subunit is represented in pink. Each integrin subunit is composed of a large extracellular domain, a transmembrane molecule and the cytoplasmatic tail. Reference: © Georgiadou *et al.*,(2017), modified. Originally published in The Journal of Cell Biology, 216:1107-1121. DOI: 10.1083/jcb.201609066.

Integrins are also classified as metalloproteins because their functions are highly regulated by divalent cations such as Mg^{++}, Mn^{++} and Ca^{++} (Zhang *et al.*, 2012). Divalent cations in particular Mg^{++} and Mn^{++}, have stimulatory effects on the integrin activation substantially increasing the integrin-ligand affinity. Opposite to that, Ca^{++} ions have inhibitory effects on the integrins. These stimulatory and inhibitory effects mediated by divalent cations are especially important in the case of leukocytes where the integrins are most of the time in the inactive state (Leitinger *et al.*, 2000; Mitroulis *et al.*, 2015; Zhang *et al.*, 2012).

The most important integrin functions are to mediate cell adhesion to the ECM and to transduce intracellular cell signaling (Harburger *et al.*, 2009; Hynes, 2002). Since their discovery, several other important physiological functions have been attributed to integrins. Those functions include cell migration and differentiation during embryogenesis and organogenesis and leukocyte migration during inflammatory response (Darribere *et al.*, 2000; Hyun *et al.*, 2009; Lammermann *et al.*, 2008; Merviel *et al.*, 2001; Schmidt *et al.*, 2013b). Integrins are able to control cell mitosis by the activation of mitogen activated protein kinase (MAP) and many other intracellular proteins involved in the progression of cell cycle (Streuli, 2009). On the other hand, integrins can also control the apoptotic mechanisms in different cells. Integrins can trigger anoikis, a type of apoptosis induced when cells are not properly attached to the ECM. This mechanism seems to be especially important to control tumor metastasis (Gilmore, 2005). Furthermore, integrins are involed in hemostasis, healing processes and platelets aggregation (Bennett, 2005; Bergmeier *et al.*, 2012; Koivisto *et al.*, 2014; Longmate *et al.*, 2014).

Since integrins are closely connected to the cytoskeleton, these connections mediate several cellular responses that will culminate in changes in cell morphology, adhesion and spreading (Calderwood *et al.*, 2000; Choquet *et al.*, 1997). One classical example of cell response driven by cytoskeleton rearrangement is the formation of structures called focal adhesion sites. These structures consist of integrin agglomerations and intracellular signaling proteins that connect the ECM to the actin cytoskeleton (Wehrle-Haller *et al.*, 2002; Wozniak *et al.*, 2004).

One important characteristic of integrins is their ability to bind to different ligands like fibronectin, vitronectin, fibrinogen, laminin, von Willebrand factor and collagen. The recognition of an integrin ligand is mediated by conserved amino acid sequences within the ligand (Humphries *et al.*, 2006; Plow *et al.*, 2000). One of the main ligand motifs involved in the recognition by integrins is the RGD (Arg-Gly-Asp) motif which is found in fibronectin, vitronectin and fibrinogen. Another integrin ligand motif is GFOGER which is present in collagen (Humphries *et al.*, 2006).

1.10.3) Integrin signaling

Integrin molecules are very specialized in transducing intracellular signaling via its cytoplasmatic tail leading to distinct changes in cell response (Harburger *et al.*, 2009; Miranti *et al.*, 2002). Integrins are called "bi-directional" molecules due to their ability to transduce signals from inside the cell (called "inside-out" signaling) or from outside of the cell (called "outside-in" signaling) (Hynes, 2002; Shen *et al.*, 2012). Inside-out signaling is particularly important in the context of leukocyte and platelet activation during immune and inflammatory responses. During this process, integrin activation increases the affinity to their ligands. Outside-in signaling happens in response to ligand binding to integrins subsequently leading to intracellular events that might end in different cell responses such as migration, differentiation, division or apoptosis (Harburger *et al.*, 2009; Kim *et al.*, 2011). Downstream intracellular signaling involves several molecules such as focal adhesion kinase (FAK) which is phosphorylated upon integrin activation and is a pivotal marker of integrin signaling (Mitra *et al.*, 2005; Zhao *et al.*, 2011) Several other intracellular signalling proteins have been reported to be involved in the integrin signaling such as Rho family proteins, Src-kinase family proteins, talin, kindlins, paxilin, vinculin and many others (Harburger *et al.*, 2009).

1.10.4) Integrins as virus receptors

Since integrins are widely expressed in many cell lines, are conserved among the species and represent essential receptors involved in different important cellular processes, not surprising that viruses also explore the integrin machinery with several benefits for their infection cycle. Although some viruses

harbor canonical integrin ligand motifs, other viruses use the integrin machinery independently of these motifs (Hussein *et al.*, 2015; Triantafilou *et al.*, 2001) .

Adenoviruses (*Adenoviridae* family, *Mastadenovirus* genus) are the classical example of virus-integrin interaction. These viruses can enter the cells by using αVβ3 or αVβ5 integrin. Many adenovirus strains harbor an RGD motif loop in the penton base that is reported to interact with integrins mediating adenovirus internalization (Nemerow *et al.*, 2016; Wickham *et al.*, 1993).

Foot and mouth disease virus (FMDV – *Picornaviridae* family, *Aphthovirus* genus) is another example for an RGD-dependent manner integrin usage. FMDV was shown to interact with at least four RGD binding integrins (αvβ1, αvβ6, αvβ3 and αvβ8) to promote virus attachment and internalization (Berinstein *et al.*, 1995; Jackson *et al.*, 2004; Jackson *et al.*, 2002; Wang *et al.*, 2015a). In one of these studies, ectopic expression of the αv integrin subunit in Chinese Hamster Ovary (CHO) cells, a cell line that is non-permissive to FMDV infection, enabled FMDV binding to the cells and subsequent infection of the CHO cells (Jackson *et al.*, 2002).

Several herpesviruses of medical importance were shown to use integrins as cellular receptors. The Kaposi's sarcoma associated herpesvirus (KSHV – *Herspesviridae* family, *Rhadinovirus* genus) was shown to use the α3β1 integrin, a laminin receptor, to mediate binding and entry in human foreskin fibroblasts (Akula *et al.*, 2002). Another study reported that KSHV also interacts with αVβ3 integrin mediating attachment and entry into salivary gland epithelial cells (Garrigues *et al.*, 2014). The human herpex simplex virus 1 (HHV-1 – *Herpesviridae* family, *Simplexvirus* genus) glycoprotein H (gH), a protein involved in herpesvirus fusion, harbors an RGD motif that was demonstrated to mediate binding to αVβ3 integrin in Vero and CHO cells (Parry *et al.*, 2005). Another study demonstrated binding of soluble HHV-1 gH and glycoprotein L (gL) to αVβ6 and αVβ8 with high affinity reinforcing the physical interaction between HHV-1 glycoproteins and integrins (Gianni *et al.*, 2013). The human cytomegalovirus (HCMV – *Herpesviridae* family, *Cytomegalovirus* genus) glycoprotein B (gB) does not posses any canonical integrin ligand motif but holds a disintegrin-like domain instead which is a conserved motif known to be recognized by integrins (Feire *et al.*, 2010). The disintegrin-like domain was found to interact directly with the β1 integrin subunit. Soluble recombinant gB fragments blocked HCMV infection (Feire *et al.*, 2010).

Hantaviruses (*Hantaviridae* family, *Orthohantavirus* genus) have a particular and distinct interaction with integrins. It was proposed that pathogenic hantaviruses such as Sin Nombre virus (SNV) and New York 1 virus (NYV-1) use the β3 integrin subunit as cellular receptor while non-pathogenic hantaviruses like Prospect Hill virus (PHV) were shown to use β1 integrin subunit to infect the host cell (Gavrilovskaya *et al.*, 1999; Gavrilovskaya *et al.*, 1998). These studies demonstrated that expression of both αIIbβ3 and αvβ3 integrins rendered CHO cells permissive to SNV and NYV-1 but not PHV, indicating a particular usage of integrins by pathogenic hantaviruses (Gavrilovskaya *et al.*, 1999; Gavrilovskaya *et al.*, 1998).

The arbovirus Ross river virus (RRV – *Togaviridae* family, *Alphavirus* genus) was reported to use α1β1 integrin as cellular receptor in human epithelial cells (HeLa) and mosquito cells (C6/36) (La Linn *et al.*, 2005). In this study, type IV collagen as well as monoclonal and polyclonal antibodies against the β1 integrin subunit inhibited RRV infection. RRV was also shown to interacted physically with soluble α1β1 integrin (La Linn *et al.*, 2005).

The CSFV (*Flaviviridae* family, *Pestivirus* genus) has been reported to upregulate the expression of β3 integrin subunit in swine endothelial cells upon infection (Tang *et al.*, 2010). More recently, Li et al., (2014) reported that expression of β3 integrin subunit enhanced CSFV infection and proliferation. By comparing a set of porcine cell lines, the authors demonstrated a more efficient virus infection and proliferation in cell lines expressing high amounts of β3 integrin subunit (Li *et al.*, 2014).

1.10.5) Integrins and flaviviruses

The first study reporting the involvement of integrins in flavivirus infection goes back to 1997. The authors proposed that α3β1 integrin, a laminin receptor, could be involved in TBEV infection (Protopopova *et al.*, 1997).

The presence of the integrin binding RGD motif in the E protein of YFV-17D, MVEV and JEV led to speculations whether these viruses might use integrins as a cellular receptor (van der Most *et al.*, 1999). By introducing amino acid exchanges in the YFV-17D RGD motif, the authors demonstrated that those amino acid exchanges did not affect YFV-17D infection in human adrenal gland cells (SW13 cells) but rather resulted in instability of the YFV-17D E protein which consequently impaired virus spread at 37°C. Additionally, RGD modification to RAD and RAE strongly impaired the YFV-17D titers in mosquito C6/36 cells. These results provided additional evidence of integrin interaction with flaviviruses (van der Most *et al.*, 1999).

In 2003, the isolation of a 105 kDa cellular protein from Vero and murine neuroblastoma cells was reported. The unidentified 105 kDa cellular protein interacted with WNV promoting virus binding and infection of the cells. In the same study, antibodies raised against the unknown 105 kDa protein strongly abrogated WNV and KUJV infection in Vero cells (Chu *et al.*, 2003). Further characterization of the unknown 105 kDa protein by peptide sequencing revealed a member of the integrin family, namely the integrin αVβ3 (Chu *et al.*, 2004b). The authors demonstrated that specific antibodies against the αV and β3 integrin subunits strongly impaired WNV binding to Vero cells by 50% and 60%, respectively. In addition, these antibodies inhibited WNV internalization in Vero cells by 50% (αV) and 75% (β3) (Chu *et al.*, 2004b). Silencing of β3 integrin subunit in Hela cells reduced WNV entry by about 60%. Binding and infection of WNV in CS-1 melanoma cells, a WNV non-susceptible cell line that does not express the β3 integrin

subunit, was substantially increased upon ectopic expression of β3 integrin subunit. Finally, WNV binding to αVβ3 integrin triggered the FAK phosphorylation, giving reasonable evidence that integrin αVβ3 integrin might act as a putative WNV receptor (Chu *et al.*, 2004b). Further studies demonstrated that WNV recombinant E-DIII protein bound with high specificity to αVβ3 but not to αVβ5 or heparan sulfate (Lee *et al.*, 2006b). Moreover, treatment of β3 integrin expressing CS-1 cells with WNV recombinant E-DIII protein resulted in αVβ3-E-DIII complex formation and precipitation, suggesting that WNV E-DIII physically interacts with αVβ3 integrin (Lee *et al.*, 2006b). In strong contrast to the results reported by other authors, Medigeshi *et al.* (2008) demonstrated that WNV entry into the host cell is completely independent of αVβ3 integrin but instead depends on lipid-raft microdomains (Medigeshi *et al.*, 2008). Using CS-1 cells as well as mouse embryonic fibroblasts (MEF) deficient for β3 integrin subunit and FAK, the authors showed that WNV infects CS-1 cells regardless of the αVβ3 integrin expression. Virus titers in both β3 integrin subunit and FAK deficient MEFs did not differ significantly from their respective wild type cell lines (Medigeshi *et al.*, 2008).

More recently, Schmidt *et al.*,(2013a) showed that the αV, β1 and β3 integrin subunit were not involved in WNV binding to MEFs. Furthermore, antibodies raised against the β1 and β3 integrin subunits did neither affect binding nor replication of WNV. However, the deletion of β1 and β3 integrin subunits, strongly impaired the replication of all WNV strains in the integrin deficient MEFs. Once the respective integrin subunit was rescued, WNV yields were recovered up to 90% (Schmidt *et al.*, 2013a). Moreover, Fan *et al.,* (2017) suggested that αVβ3 integrin could promote JEV infection in baby hamster kidney cells strain 21 (BHK-21). Downregulation of both, αV and β3 integrin subunits in BHK-21 cells reduced the JEV plaque formation by 4- fold and 2-fold in αV and β3 integrin subunit siRNA silenced BHK cells. Moreover, synthetic RGD peptides as well as antibodies raised against the αV and β3 integrin subunits reduced the plaque formation by up to 58% and 33%, respectively (Fan *et al.*, 2017). Since CHO cells have been demonstrated to be not or only poorly permissive to several viral agents including flaviviruses (Berting *et al.*, 2010) and to lack the expression of αV and β3 integrin subunits at the cell surface (Gianni *et al.*, 2010a; Gianni *et al.*, 2010b; Xu *et al.*, 2011), Fan et al. (2017) established a CHO cell line expressing the β3 integrin subunit to investigate the involvement of this integrin in JEV infection. The expression of β3 integrin subunit increased JEV replication in CHO cells suggesting that this specific integrin subunit might play a role in the JEV replication cycle (Fan *et al.*, 2017).

2) Objectives

The current knowledge on integrin usage by flaviviruses is scarce and most of the previous studies were performed with WNV and JEV. In these reports, integrins were demonstrated to be involved in WNV and JEV binding and internalization into the host cell as well as in RNA replication.

To our knowledge, there are no other studies demonstrating the involvement of integrins in other flavivirus infections despite WNV and JEV. Therefore, the main objective of this study was to evaluate the potential role of selected integrins, the αVβ3 integrin and the β1 and β3 integrin subunits, for the infection cycle of several other medically important flaviviruses.

For this purpose the study aimed:

(i)   to develop cell lines expressing the integrins and corresponding deficient cell lines,

(ii)   to evaluate the potential of integrins as flavivirus receptor,

(iii)   to prove the ability of integrin to act as flavivirus attachment factor,

(iv)   to investigate the potential role of integrins in flavivirus internalization,

(v)   to characterize the role of integrins in flavivirus RNA replication.

3) Materials and Methods

3.1) Materials

All materials, reagents, solution protocols, equipments, softwares and databases are listed in Appendices I, II, III, VII, IX.

3.2.) Cell culture methods

3.2.1.) Cell lines and cultivation methods

All cell lines used in this study are described in **Table 1** and Appendix VIII. Generally, cells were maintained in medium containing 10 % fetal bovine serum (FBS). Cells were cultivated under standard conditions in a 37°C incubator with 5% carbon dioxide. Prior to experiments, cells were cultivated with 5% FBS. For splitting, cells were washed twice with 1X phospate buffered saline (PBS) followed by adding 5ml of 0.25% trypsin solution into the flasks and incubation at 37°C for 5 minutes. Trypsin inactivation was performed by adding 5 ml of the usual cell culture medium supplied with FBS.

Table 1: Cell lines used in this study

Designation	Species	Background	Organ/Tissue	Reference/Source
MEF-WT	*Mus musculus*	C57/BL6	Embryonal	Dr. Markus Keller, INNT, Friedrich-Loeffler Institut, Insel Riems
MEF-αVβ3$^{-/-}$	*Mus musculus*	C57/BL6	Embryonal	
MEF-β3$^{+/+R}$	*Mus musculus*	C57/BL6	Embryonal	Hodivala-Dilke *et al.*,(1999); Schmidt *et al.*,(2013a)
MEF-β3$^{-/-}$	*Mus musculus*	C57/BL6	Embryonal	
MKF-β1Flox	*Mus musculus*	C57/BL6X 129SV	Kidney	Fassler *et al.*,(1995a)
MKF-β1$^{-/-}$	*Mus musculus*	C57/BL6X 129SV	Kidney	
CHO-K1	*Cricetulu. griseus*	-	Ovary	Puck *et al.*,(1958)
Vero	*Chlorocebus aethiops*	-	Kidney	see references 1 and 2 in Osada *et al.*,(2014)
Vero B4	*Chlorocebus sabaeus*	-	Kidney	German Collection of microorganisms and cel culture - DSMZ
Vero E6	*Chlorocebus aethiops*	-	Kidney	see reference 13 in Osada *et al.*,(2014)
Vero 76	*Chlorocebus aethiops*	-	Kidney	

MEF: mouse embryonic fibroblasts; MKF: mouse kidney fibroblasts; CHO: Chinese Hamster Ovary cells; R: rescue

3.2.2) Mouse embryonic fibroblasts (MEFs)

Wild type mouse embryonic fibroblasts (MEF-WT) and MEFs lacking the expression of either β3 integrin subunit (MEF-β3$^{-/-}$) or αVβ3 integrin (MEF-αVβ3$^{-/-}$) as well as MEFs rescued (R= rescue) for the expression of β3 integrin subunit (MEF-β3$^{+/+R}$) were cultivated in Dulbecco's Modified Essential Medium (DMEM) supplied with 10% FBS and 1% antibiotic-antimycotic mix composed of penicillin (10,000 U /ml), streptomycin (10 mg/ml) and amphotericin B (25 µg/ ml). Cells were cultivated until confluence of approximately 80% (MEF-WT) and 90% (MEF-αVβ3$^{-/-}$) was reached. Cultures were routinely split at ratios of 1:10 for MEF-WT and MEF-αVβ3$^{-/-}$ and 1:3 for MEF-β3$^{-/-}$ and MEF-β3$^{+/+R}$. For the MEF-β3$^{+/+R}$ transfected cells, the zeocin antibiotic was added into the medium at a final concentration of 10 µg per ml.

3.2.3) Mouse kidney fibroblasts (MKFs)

Wild type mouse kidney fibroblasts (MKF-β1^{flox}) and mouse kidney fibroblasts lacking the expression of β1 integrin subunit (MKF-β1$^{-/-}$) were cultivated in DMEM supplied with 5% FBS and 1% antibiotic-antimycotic mix composed of penicillin (10,000 U/ml), streptomycin (10 mg/ml) and amphotericin B (25 µg/ml). Cells were cultivated until confluence of approximately 80% was reached. Cultures were routinely split at a ratio of 1:10.

3.2.4) Chinese hamster ovary cells

Chinese Hamster Ovary cells clone K1 (CHO-K1) were cultivated in Eagle's Modified Essential Medium (E-MEM) supplied with 10% FBS and 1% antibiotics-antimycotic mix composed of penicillin (10,000 U/ml), streptomycin (10 mg/ml) and amphotericin B (25 µg/ml). Cells were cultivated until confluence of approximately 80% was reached. Cultures were routinely split at a ratio of 1:5. For CHO-β3$^{+/+R}$ and CHO-αV$^{+/+R}$ transfected cells, the selection antibiotics zeocin or hygromycin were added into the medium at a final concentration of 50 µg per ml and 5 µg per ml, respectively.

3.2.5) Vero cells

Vero cells from different lineages referred to as Vero-76, Vero-B4, Vero-E6 and Vero were cultivated in E-MEM supplied with 10% FBS and 1% antibiotic-antimycotic mix (100 µg/ml). Cells were cultivated until confluence of approximately 80% was reached. Cultures were routinely split at a ratio of 1:5.

3.2.6) Cryopreservation methods

For long-lasting storage of eukaryotic cells in liquid nitrogen, cells were detached from the flasks by trypsin as described above. The detached monolayers were resuspended in fresh medium and centrifuged at 900 rotations per minute (RPM) for 10 minutes. Then, supernatants were discarded and the cell pellet was gently resuspended in fresh cold medium containing 10% of cell culture grade dimethylsulfoxide (DMSO) prepared shortly before the freezing procedure. Cell suspension was aliquoted in cryogenic storage vials and placed into Mr Frosty™ cell freezing container filled with isopropanol and stored overnight at -80°C. Finally, cells were transferred into liquid nitrogen tanks for long-term storage.

For thawing cryopreserved cells, cryogenic storage vials were removed from liquid nitrogen tanks and placed into a portable small liquid nitrogen container. Cryogenic tubes were quickly thawed in a pre-warmed water bath (37°C). Afterwards, cell suspension was gently resuspended and cells were seeded in fresh cell culture medium (10 ml) in T25 cm² flasks and incubated at 37°C. The day after, cells were washed with 1X PBS to remove cell debris and DMSO remains and fresh medium was added.

3.2.7) Determination of cell number

Determination of total cell number was achieved by counting the cells in a Neubauer chamber. All the four quadrants (16 squares) were counted and the average number of cells was calculated. The number of cells per ml was calculated using the formula

$$N° \text{ of cells/ml } = \frac{A}{B} \text{ x C x } 10000$$

where A is the average of cells counted in each quadrant; B is the number of quadrants counted and C is the dilution factor.

3.2.8) Determination of cell viability

Routinely, prior to cell plating and all cell infection assays, cell viability was determined using the trypan blue exclusion method. In order to evaluate cell metabolism and consequently cell viability, the MTS-tetrazolium colorimetric assay was applied. While the first method measures cell membrane selectiveness, the second method measures the ability of cells to metabolize tetrazolium metabolites.

Determination of cell viability by trypan blue exclusion method was performed as described by Strober,(2015). Briefly, cells were detached as described above and resuspended in a total volume of 10 ml fresh medium. An aliquot of 100 µl of cell suspension was transferred into a microtube containing 0.4% trypan blue dye solution diluted in 1X PBS (1:10 dilution) to a final volume of 1 ml. After two minutes at room temperature, 10 µl of cell suspension was loaded into a Neubauer chamber and counted using inverted light microscope. Blue stained cells (i.e.: no cell membrane selectiveness) were considered dead and cells that did not acquire blue staining (i.e.: cell membrane selectiveness) were considered vital. Determination of viability was calculated by the following formula:

$$\text{Viability (\%)} = \frac{\text{number of vital cells}}{\text{total number of cells}} \times 100\%$$

Determination of cell viability was also performed using the CellTiter 96® AQueous One Solution Cell Proliferation Assay (Promega) following instructions of the manufacturer. Briefly, cells were detached as described above and resuspended in a total volume of 10 ml of fresh medium. Cell number was determined by counting in a Neubauer chamber as described before. Different cell concentrations (ranging from 10^3 to 10^6 cells per well) were seeded in duplicate into the 96-well cell culture plates to a final volume of 100 µl. After addition of 20 µl of MTS-tetrazolium reagent to each well, the plates were gently mixed and incubated at 37°C with 5% carbon dioxide atmosphere under light protection for 4 hours with gently mixing every hour. Thereafter, absorbance was measured at 490 nm by an Enzyme-linked immunosorbent assay (ELISA) plate reader. Vero cells and Vero cells treated with 10% sodium azide (100 µl per ml of cells) were used as positive and negative control, respectively. Background wells (only MTS-tetrazolium reagent) as well as blank wells (no reagent) were added into the plate as internal controls. Absorbance was plotted by mean value of respective cell amount subtracted by the background absorbance. Two independent experiments were performed in duplicate (*n*=2).

3.3) Viruses and virological techniques

All viruses used in this study are described in **Table 2**.

Table 2: Flaviviruses used in this study

Virus	Abbreviation (ICTV)	Strain	Source	Reference
Yellow Fever virus	YFV	17D	Dr. Ute Ziegler, FLI,INNT	Theiler *et al.*,(1937)
West Nile virus	WNV	PreVnile™	Dr. Katja Schmidt, FLI,INNT	Arroyo *et al.*,(2004)
Usutu virus	USUV	Germany	Dr. Ute Ziegler, FLI,INNT	Jöst *et al.*,(2011)
Langat virus	LGTV	TP-21	Dr. Ute Ziegler, FLI,INNT	Smith,(1956)
Zika virus	ZIKV	MR-766	Dr. Ute Ziegler, FLI,INNT	Dick *et al.*,(1952)

3.3.1) Preparation of viral stocks

For flavivirus propagation, confluent monolayers of Vero-76 cells were seeded in T75 cm^2 flasks. Virus stocks were thawed on ice and diluted in E-MEM without FBS at a ratio of 1:10. Prior to inoculation, cell monolayers were washed once with 1X PBS and virus inoculum was added to the cell monolayers and incubated for 1 hour at 37°C with constant agitation every 20 minutes. After this period, the inoculum was removed and replaced with E-MEM 2% FBS. Inoculated monolayers were incubated at a 37°C incubator with 5% carbon dioxide for a period of 5 to 7 days until the cytopathic effects (syncytia formation, cell death and total or focal degeneration of cell monolayers) were clearly observed. Cell supernatants were harvested and centrifuged at 5,000 RPM for 10 minutes to remove cell debris. Virus stocks were aliquoted and stored at -80°C.

3.3.2) Virus purification and concentration

For the binding studies, viruses were purified by sucrose gradient density centrifugation. Briefly, virus stocks were propagated in Vero cells as described above. For virus purification, cells were cultivated in T162 cm² flasks. Supernatants from infected Vero cells were clarified by centrifugation at 5,000 RPM for 10 minutes at 4°C. Cell debris was removed and the supernatant was mixed with 50% polyethylene glycol (PEG) 6000 and incubated for 30 minutes on ice. Afterwards, flasks were incubated overnight at 4 °C for

virus precipitation. In parallel, sucrose gradient was prepared with two densities: 30% and 60% of sucrose (30 g of sucrose per 100 ml of TNE buffer and 60 g of sucrose per 100 ml of TNE buffer). Then, 4 ml of 60% solution and 6 ml of 30% solution were added into ultracentrifugation tubes and incubated overnight at 4°C. The day after, the virus/PEG 6000 mixture was centrifuged at 5,000 RPM for 30 minutes at 4°C. The pellet containing the precipitated virus particle was resuspended in TNE buffer, carefully added into the centrifugation tube containing the sucrose gradient and centrifuged at 28,000 RPM for 2 hours at 4°C. Afterwards, a visible band containing the precipitated virus was collected and centrifuged again using the same conditions described above. Finally, purified virus was resuspended in 500 μl of TNE buffer, aliquoted and stored at -80°C until use.

3.3.3) Plaque assay

The plaque assay was performed as previously described by Dulbecco *et al.*,(1953) with some modifications. For the plaque assay, specific Vero cells for each flavivirus were seeded into 6-well plates at a confluence of $1x10^5$ cells per well in E-MEM 10% FBS, 24 hours prior to inoculation. On the day of inoculation, virus stocks were 10-fold serially diluted ranging from 1:10 to $1:10^8$ in E-MEM without FBS and inoculated into the wells in duplicate. A negative control well (no virus) was also included in the assay. Infected monolayers were incubated for 1 hour at 37°C with constant agitation every 20 minutes. After this period, the inoculum was removed and monolayers were covered with an overlay medium composed of E-MEM 2% FBS supplied with 1.8% bacteriological agar.Plates were incubated at 37°C for a period of 5 to 7 days. After this period, monolayers were fixed with buffered 10% formalin for 1 hour and stained with 1% crystal violet solution overnight. The day after, monolayers were washed to remove excess of dye and agarose clumps, dried and plaques were counted. The plaque forming units (PFU) were calculated following the formula:

$$PFU/ml = n° \text{ of plaques x 2 x inverse of dilution}$$

3.3.4) Tissue culture infectious dose determination

The tissue culture infectious dose ($TCID_{50}$) assay was performed as previously described by Reed,(1938) with modifications. For the assay, Vero cells were seeded in E-MEM 10% FBS at a confluence of $1x10^4$ cells per well in 96-well plates at 24 hours prior to inoculation. Virus stocks were 10-fold serially diluted ranging from 1:10 to $1:10^{10}$ in E-MEM without FBS and incubated on ice until inoculation. Medium was removed from the wells and 100 μl of inoculum was added into the wells in quadruplicate. Inoculated monolayers

32

were incubated at 37°C for 1 hour for virus adsorption and infection. After this period, the inoculum was removed, the wells washed once with 1X PBS and the wells were replaced with fresh E-MEM 2% FBS. Plates were checked daily for the presence of cytopathic effect (i.e.: monolayer devastation) with an estimated time of 4 to 6 days post inoculation. Once the cytopathic effects were visualized, monolayers were fixed with buffered 10% formalin for 1 hour, washed twice with distilled water and stained with 1% crystal violet solution overnight. The following day, plates were washed and the end-point titer was calculated according to the Spearman-Kaerber method (Kärber, 1931; Spearman, 1908). The following formula was applied for determination of end-point titers:

$$M = X_k + d/2 - \Sigma P_i$$

Where,

M = Logarithm of titer in relation to the testing volume
X_k = Negative common logarithm of the highest dilution level where all wells are positive
d = Negative common logarithm of the dilution factor
P_i = Positive wells/well rate in a row starting with the dilution X

3.4) Cloning of heterologous DNA in expression vectors

All vectors, sequences, reagents and buffers are listed in Appendices I, II, IV and V. The *Escherichia coli* (*E. coli*) strain DH5α was used as standard strain for all cloning procedures. Further information concerning its genetic background and the manufacturer is displayed in Appendix VIII.

3.4.1) Preparation of competent bacterial cells

Preparation of competent *E. coli* cells was performed using the calcium-magnesium method (Hanahan *et al.*, 1991). Frozen bacteria glycerol stocks were scraped and inoculated into Luria Bertani (LB) medium without antibiotics and incubated overnight at 37°C in a bacterial shaker at 200 RPM. The day after, 1 ml of the overnight bacterial culture suspension was added into 40 ml of LB medium without antibiotics. Cultures were incubated at 37°C with continuous agitation (200 RPM) and the optical density of 600 nm (OD_{600}) was measured systematically. When the culture reached the OD_{600} value of 0.5, the bacterial suspension was transferred to a 50 ml centrifuge tube, incubated on ice for 10 minutes and centrifuged at 2,000 RPM for 10 minutes at 4°C. After centrifugation, supernatants were discarded and the pellet was gently resuspended in 2 ml of ice-cold calcium-magnesium buffer, filled with 18 ml of the same buffer (final volume of 20 ml) and incubated on ice for 30 minutes. Afterwards, bacterial suspension was

centrifuged at 1,800 RPM for 10 minutes at 4°C. The supernatant was discarded and the pellet resuspended in 3 ml of ice-cold calcium-magnesium buffer plus 500 µl of glycerol. After gentle mixing suspension was aliquoted (100 µl) into microtubes and quickly frozen by liquid nitrogen. Stocks of competent bacteria were then transferred to -80°C and stored until use.

3.4.2) Transformation of bacterial cells

Bacteria were transformed by heat shock method as described by Froger *et al.*,(2007) with modifications. For this, competent *E. coli* (strain DH5α) cells were thawed on ice and 100-500 ng of vector or constructs were added, gently mixed and incubated for 30 minutes on ice. Following this incubation, bacterial cells were incubated at 42°C for 2 minutes followed by 5 minutes incubation on ice. After this, 1 ml of LB medium without antibiotics was added and bacterial cells were incubated for 1 hour and 30 minutes at 37°C with constant shaking (300 RPM). Then, cells were centrifuged at 8,000 RPM for 3 minutes and resuspended in 100 µl of LB medium and gently mixed by pipetting. Bacteria were then seeded on LB agar plates containing either ampicillin (100 µg/ml) or kanamycin (50 µg/ml) according to the resistance gene assigned to the vector and incubated at 37°C for 12-16 hours in incubator.

3.4.3) Selection of bacterial transformants

Bacterial cells grown on the LB agar plate containing the selection antibiotic were considered to be transformed (containing the vector) and were selected for cultivation in LB medium. For this, 5-10 colonies were picked from each plate and inoculated individually in LB medium containing the antibiotics mentioned above. Cultures were incubated for 12-16 hours at 37°C with constant agitation at 200 RPM in a bacteriological shaker. The next day, cultures were centrifuged at 5,000 RPM for 30 minutes, supernatant discarded and the bacterial pellet lysed for DNA plasmid isolation or frozen at -20°C for further use.

3.4.4) Purification of plasmid DNA

For purification of plasmid DNA at small and medium scale, the QIAprep Spin Miniprep Kit (Qiagen) and QIAprep Plasmid Midi Kit (Qiagen) were used respectively, following manufacturer's instructions. Bacterial pellets were resuspended in P1 buffer and subsequently lysed with P2 buffer and mixed by inversion 4 to 6 times. Suspension was neutralized by addition of P3 buffer and centrifuged at 5,000 RPM for 30 minutes. After this, the supernatant was loaded into filter cartridges for filtration and loaded into gravity flow columns. After flow through of the supernatant, columns were washed twice with QC buffer and DNA was

eluted in QF buffer. DNA was precipitated by addition of absolute isopropanol at room temperature. The mixture was mixed and centrifuged at 5,000 RPM for one hour at 4°C. After this, the pellet was washed with 70% isopropanol and centrifuged again at 5,000 RPM for 30 minutes at 4°C. Pellets were dried and resuspended in 100-200 µl of TE buffer. Plasmid DNA concentrations were determined by micro-volume spectrophotometer (NanoDrop®).

3.4.5) Agarose gel electrophoresis

Separation of plasmid DNA and restriction fragments was achieved by agarose gel electrophoresis using gels with different agarose concentrations (0.8%, 1.0% and 1.8%) according to the DNA fragment size. For separation of large DNA fragments, lower agarose concentrations were used and for small DNA fragment size higher agarose concentrations instead. The 50x Tris-acetate-EDTA buffer concentrate (50x TAE) was used as standard electrophoresis buffer in a working concentration of 1X (1X TAE). The same fresh-prepared 1X TAE buffer was used to dissolve the agarose powder. Agarose powder was weighed and dissolved in 100 ml of 1X TAE buffer and melted by heating the mixture under constant agitation. After, the homogeneous agarose mixture was added into an electrophoresis tray coupled with a 1.5 mm comb. Thereafter, the gels were transferred to an electrophoresis chamber and the chamber loaded with 1X TAE. In parallel, samples were diluted in 5 µl of 6x loading buffer dye and loaded into the gel slots. Alongside, a molecular size marker was loaded in the first slot to estimate the size of fragments. The separation took place at 110 volts for 1 hour. After electrophoresis, the gels were stained with ethidium bromide (1 mg/liter). DNA fragments were visualized by ultraviolet (UV) light excitation using a transilluminator and documented with an integrated camera system and thermal printer. If necessary, the desired bands were excised and subjected to purification.

3.4.6) Enzymatic digestion of plasmid DNA

Vectors as well as constructs were digested by restriction endonucleases. High fidelity (HF) restriction enzymes from New England Biolabs were used for all experiments according to the manufacturer's guidelines. Shortly, 20 units of restriction endonucleases (1 µl of each enzyme) were added to digest 1-2 µg of DNA together with the 5X Cutsmart buffer (New England Biolabs). Water was added to complete the final volume to 50 µl. Reactions were run in a thermocycler for 2 hours at 37°C, followed by endonucleases heat inactivation at 65°C for 10 minutes. After digestion, DNA fragments were visualized by agarose gel electrophoresis as mentioned in the section above.

3.4.7) Vector DNA dephosphorylation

To avoid spontaneous vector re-circularization, vector DNA was subjected to dephosphorylation to remove the phosphate groups from the 5' ends soon after digestion. The New England Biolabs Antartic Phosphatase system was used since it allows high compatibility with the buffer used for previous digestion. For this, 1 µl of 10X Antarctic Phosphatase reaction buffer and 1 unit of Antarctic Phosphatase were added.per 10 µl of digestion reaction mixture. The reaction mix was incubated for 1 hour at 37 °C before inactivation of the enzyme for five minutes at 65 °C.

3.4.8) Gel extraction of plasmid DNA

For isolation of plasmid DNA from agarose gels, the QIAquick gel extraction kit (Qiagen) was used according to the manufacturer's guidelines. Shortly, after electrophoresis and staining with ethidium bromide, fragments were excised from the agarose gels with a clean-sterile scalpel and added into 2.0 ml microtubes. The fragments were weighed and 100 µl of QG buffer per 100 mg of gel was added. The mixture was incubated at 50°C for approximately 10 minutes until complete gel dissolution. Then 1 volume of isopropanol was added to the mixture, mixed and loaded into QIAquick spin column and centrifuged at 13,000 RPM for 1 minute. Subsequently, columns were washed with 750 µl PE buffer and centrifuged again at 13,000 for 1 minute. Finally, 50 µl of RNAse/DNAse free water was added onto the column, incubated for 5 minutes and transferred to a sterile 1.5 ml microtube for centrifugation at 13,000 RPM for 1 minute. The plasmid DNA concentration was measured by micro-volume spectrophotometer (Nanodrop®) and stored at -20° C until use.

3.4.9) DNA clean-up and nucleotide removal

In order to remove excess of salts, enzymes and nucleotides from the digestion reaction, vector DNA clean-up was performed upon digestion and/or dephosphorylation using the QIAquick Nucleotide Removal Kit (Qiagen). Shortly, the digestion reaction was mixed with 10 volumes of PNI buffer, applied to a spin column and centrifuged at 6,000 RPM for 1 minute. The flow-through was discarded and the column washed with 750 µl PE buffer and centrifuged again for 1 minute at 6,000 RPM. The flow-through was discarded and the column centrifuged again to remove excess of buffers. The DNA was eluted by adding 50 µl of water to the column, incubation for 5 minutes at room temperature and centrifugation at 13,000 RPM for 1 minute. The plasmid DNA concentration was measured by micro-volume spectrophotometer (Nanodrop®) and stored at -20° C until use.

3.4.10) Ligation

Ligation reaction was performed using the Rapid DNA Ligation kit (ThermoFisher) following manufacturer's instructions. Based on the plasmid (vector) DNA and insert concentration ratios were calculated as 1:1, 1:3, 1:5. Then, the vector, insert, buffer and the T4 ligase were mixed and a final volume of 20 µl was completed with water. Reaction was incubated at room temperature for 1 hour and 5-10 µl of ligation reaction was used to transform competent bacteria as described above. For selection of recombinant bacteria, the procedure described in **section 3.4.3** was applied. Constructs were confirmed by restriction endonuclease digestion (**section 3.4.6**) and sequencing (see below).

3.4.11) DNA sequencing methods

Plasmid DNA as well as PCR amplicons were submitted to sequencing to confirm their identities with the original sequences. The dideoxy chain-termination method according to Sanger *et al.*,(1977) was used to sequence all samples in this study. Samples were prepared and shipped to Eurofins Genomics, Ebersberg, Germany, following instructions of the company. Shortly, samples containing 50-100 ng/µl of purified plasmid DNA or 2-5 ng/µl of purified PCR product were diluted in water to a total volume of 15 µl. If necessary, forward and reverse primers were shipped together with the samples in a separate mix containing a primer concentration of 10 pmol and final volume of 15 µl.

3.4.12) Synthesis of integrin coding sequences

The mouse αV and β3 integrin (ITG-αV and ITG-β3) subunit coding sequences (GenBank, accession no. KP296148.1 and NM016780.2) were commercially synthesized by GeneArt, Regensburg, Germany. The sequences were codon-optimized to enable maximal expression in murine cell lines. Additionally, to increase the expression of recombinant modified genes, the Kozak consensus sequence (5'-GCCACC-3') was added at the 5' region upstream of the integrin coding sequence. The cleavage sites for the restriction endonucleases BamHI and NotI were added at 5' and 3' regions, respectively. The integrin genes were cloned into a standard vector (pMK-RQ) harboring the kanamycin resistance gene. The final constructs named pMK-ITGαV and pMK-ITGβ3 were 5,450 base pairs and 4,678 base pairs, respectively. The genes corresponding to ITG-αV had 3,172 base pairs and ITG-β3 had 2,400 base pairs. These genes were used for subcloning into the pcDNA 3.1 vector system.

3.4.13) Cloning of integrin genes

The respective pMK vectors harboring the ITG-αV and ITG-β3 genes were digested with HF *Bam*HI and *Not*I restriction endonuclease enzymes as described in **section 3.4.6**. The integrin corresponding fragments, 3,172 bp for the ITG-αV and 2,400 bp ITG-β3 were excised from the gels and subjected to gel extraction clean-up as described in **section 3.4.8**. Concentration of DNA fragments was measured by micro-volume spectrophotometer (Nanodrop®).

The pcDNA 3.1 (+) Zeo and pcDNA 3.1 (+) Hygro plasmid DNA referred to as pcDNA 3.1 (Z) and pcDNA 3.1 (H), respectively, were digested with HF-*Bam*HI and HF-*Not*I as described in **section 3.4.6.** After digestion, the linearized vectors were immediately dephosphorylated as outlined in **3.4.7** and purified as mentioned in section **3.4.9**. After purification, plasmid DNA and insert were subjected to ligation as described in section **3.4.10**. After that, the procedures for bacterial transformation and selection of bacterial transformants were performed according to section **3.4.2** and **3.4.3**. To confirm the successful subcloning of integrin genes, the putative recombinant plasmids were digested as described in **3.4.6**. Selected recombinant plasmids were confirmed by DNA sequencing as mentioned in **section 3.4.11**.

3.5) Transfection methods and antibiotic selection

Transfection of plasmid DNA was performed using a cationic lipid based chemical, commercially known as Lipofectamine®. To deliver the respective foreign target genes into MEFs, Lipofectamine® LTX-Plus was used preferentially due to its low toxicity and high transfection efficiency. To create CHO-K1 cells expressing the αV or β3 integrin subunits, CHO-K1 cells were transfected with Lipofectamine® 3000.

3.5.1) Transfection protocol optimization

Transfection procedures were performed as recommended by the manufacturer's (Invitrogen). The optimal DNA/Lipofectamine® ratios were evaluated in the cell lines to achieve the highest transfection efficiency with the lowest toxicity. Initially, cells were transfected with a vector harboring the green fluorescent protein (GFP) coding sequence. For the Lipofectamine® LTX, pcDNA-GFP was tested at ratios of 1:3, 1:5, 1:7 and 1:9 (DNA : Lipofectamine®). Best results were achieved with the ratio of 1:9. For the Lipofectamine® 3000, the ratios 2:3 and 2:5 (DNA : Lipofectamine®) were tested. Best results were achieved with the ratio 2:3.

3.5.2) Transfection of mouse embryonic fibroblasts

MEF-β3$^{-/-}$ and MEF-αVβ3$^{-/-}$ cells were seeded into 12-well plates 12-16 hours prior to transfection with DMEM 10% FBS without antibiotics. The next day, the medium was replaced with fresh cell culture medium (500 µl per well) and incubated at 37°C until transfection. A mix containing the Lipofectamine® LTX reagent (18 µl), the Plus reagent (5 µl), the plasmid DNA (2 µg) and Opti-MEM® medium (to a final volume of 500 µl) were prepared in duplicate. The mixture was incubated for 10 minutes at room temperature and then added dropwise to the cells. Plates were gently rocked and incubated at 37°C with 5% carbon dioxide for 24 hours. The medium was then replaced with fresh cell culture medium and cells were incubated for additional 24 hours before they were split and subjected to antibiotic selection.

3.5.3) Transfection of CHO-K1 cells

The CHO-K1 cells were seeded into 12-well plates 12-16 hours prior to transfection with E-MEM 5% FBS without antibiotics. The next day, the medium was replaced with fresh cell culture medium (500 µl per well) and incubated at 37°C until transfection. A mix containing the Lipofectamine® 3000 (6 µl), the P3000 reagent (4 µl), the plasmid DNA (2 µg) and Opti-MEM® medium (to a final volume of 500 µl) was prepared in duplicate. The mixture was incubated for 10 minutes at room temperature and then added dropwise to the cells. Plates were gently rocked and incubated at 37°C with 5% carbon dioxide for 24 hours. The medium was then replaced with fresh cell culture medium and cells were incubated for additional 24 hours before they were split and subjected to antibiotic selection.

3.5.4) Antibiotic selection

Cells were split and subjected to antibiotic selection 48 hours after transfection. Cells were detached from the 12-well plates as described in **3.2.1.** and seeded into 6-well plates. The MEFs transfected with pcDNA 3.1 (H)-ITG-αV and pcDNA 3.1 (Z)-ITG-β3 were resuspended in DMEM 10% FBS supplied with hygromycin (100 µg/ml) and zeocin (500 µg/ml). For the CHO-K1 cells transfected with the pcDNA3.1(H)-ITG-αV and pcDNA3.1(Z)-ITG-β3, cells were resuspended in E-MEM 10% FBS containing the hygromycin (200 µg/ml) and zeocin (1000 µg/ml). Cells were kept under antibiotic selection for several (approximately 15) passages and sorted by magnetic cell sorting in order to reach a homogeneous cell population expressing the integrin genes.

3.6) Cell sorting

In order to obtain a homogenous cell population of integrin expressing cells, transfected cells were sorted magnetically using the MACS system following the instructions of the manufacturer. A positive selection, i.e. the selection of integrin expressing cells, was chosen. The system is composed of the MS magnetic columns, the MACS multiStand and the anti-biotin Microbeads. The procedure was performed under sterile conditions. Cells were detached from the flasks and resuspended in 1X MACSQuant Running buffer and the cell number was determined ($1x10^7$ cells per column). Cells were then incubated with biotinylated anti-αV and anti-β3 integrin subunit specific antibodies (1 µg per $1x10^7$ cells) for one hour and 30 minutes at 4°C with slight rotation (20 RPM). After this, cells were centrifuged at 1,000 RPM at 4°C for 10 minutes and the pellet washed twice with 1X MACSQuant Washing buffer. The cell pellet was resuspended in 100 µl of 1X MACSQuant Running buffer. Thereafter, 50 µl of anti-biotin Microbeads were added, mixed carefully and incubated at 4°C with constant agitation (20 RPM) for 1 hour at 4°C. Then, cells were washed twice with washing buffer and centrifuged at 1,000 RPM for 10 minutes at 4°C and resuspended in 500 µl of MACSQuant Running buffer. MS columns were placed in the MACS multiStand and equilibrated with MACSQuant Washing buffer followed by careful loading of cells into MS columns. The first fraction containing the unlabeled cells (flow-through) was collected and placed at 4°C. Subsequently, columns were washed three times with MACSQuant Washing buffer. Finally, columns were removed from the magnetic stand, loaded with 500 µl of MACSQuant Running buffer and cells were eluted by pressure with a plunger. This elution procedure was repeated twice. The positively selected cells were again centrifuged at 1,000 RPM for 10 minutes and seeded into T25 cm² cell culture flasks with medium containing the selection antibiotics. To analyze the percentage of integrin expressing cells and separation efficiency, flow cytometry analysis was performed

3.7) Flow cytometry analysis

Further details about the antibodies used in this experiment are shown in Appendix III. Flow cytometry analysis was performed to measure the integrin expression on the cell surface. Briefly, cells were detached from flasks and passed through a 0.22 µm cell strainer. Cell number was determined and a concentration of $1x10^6$ cells per tube was used. Tubes were incubated on ice for 30 minutes, centrifuged and incubated with anti mouse αV, β1 and β3 integrin-subunit specific antibodies for 1 hour at 4°C. After this incubation, cells were washed twice with ice-cold 1X PBS and centrifuged at 2,000 RPM for 5 minutes. Secondary antibodies labelled with Alexa 488 and Alexa 647 fluorescent dyes were added into the tubes and incubated for 1 hour at 4°C. Subsequently, cells were washed twice with ice-cold 1X PBS and centrifuged

at 2,000 RPM for 5 minutes. Cell pellets were resupended in 300 µl of ice-cold 1X PBS and analyzed by BD FACSCanto II flow cytometer with BD FACSDiva Software. A number of 10,000 events was determined. Data were processed and post-analyzed by Flowing software (Perttu Terho – Turku Centre for Biotechnology, University of Turku, Finland).

3.8) Indirect Immunofluorescence

Further details about the antibodies used in this experiment are shown in Appendix III. Cells were grown on glass coverslips 12-16 hours prior to the experiment. Thereafter, cells were fixed with 3 % paraformaldehyde for 15 minutes, followed by incubation with 50 mM ammonium chloride for 30 minutes. After this, cells were permeabilized with 0.5 % TritonX-100, washed twice with 1X PBS and subsequently blocked with 0.5 % skim milk. Antibodies were diluted in blocking buffer and cells were incubated with anti mouse αV, β1 and β3 integrin-subunit specific antibodies for 1 h at room temperature followed by three washes with 1X PBS and subsequent incubation with Alexa-488 and Alexa-647 labelled secondary antibodies for 1 hour at 4°C. For nucleus staining, the glass cover slips were quickly rinsed with 2 mg/ml 4',6-Diamidino-2-Phenylindole (DAPI) solution diluted at 1:5,000 in 1X PBS followed by a final wash with 1X PBS and a quick wash with distilled water. Finally, coverslips were dried and fixed upside down on microscopy slides with VectaShield® anti-fade mounting medium. Cells were visualized in the laser Confocal Leica DMI600 CS microscope and using the LAS AF Leica Application Suite software. Images were processed with ImageJ software (National Institutes of Health, NIH, USA).

3.9) Cell adhesion assay

In order to verify the presence of other RGD binding integrins and confirm the functionality of these integrins, a cell adhesion assay was performed as described by Miao *et al.*,(2000) with modifications. Enzyme-linked mmunosorbent assay (ELISA) Maxisorp® plates were coated overnight at 4°C with 1 µg/ml of recombinant mouse vitronectin or Poly-L-Lysin (Poly-L-Lsy) diluted in carbonate buffer (pH 8.0). The next day, plates were washed once with 1X PBS and blocked with 2% bovine serum albumin (BSA) prepared in 1X PBS and incubated for 1 hour at 37°C. Cell monolayers were detached from the flasks using 5 mM EDTA, counted and added at a concentration of $1x10^5$ cells per well in serum free E-MEM with 0.1% BSA fraction V. Cells were incubated for 30 minutes (MKF-β1^{Flox} and MKF-β1$^{-/-}$) or 45 minutes (all other cells) at 37°C to allow for cell adhesion. Vero cells were used as control for the assay. After this incubation, plates were washed to remove non-adherent cells and adherent cells were fixed with 3% paraformaldehyde for 1 hour at room temperature. After fixation, plates were washed and cells were stained with 1% crystal

violet prepared in 20% methanol for 1 hour. After extensive washing, plates were dried and the dye was extracted from the adhered cells with a dye removal solution (50% ethanol in 50 mM sodium citrate buffer, pH 4.5). Absorbances (OD 550 nm) were measured using ELISA plate reader.

3.10) Development of synthetic RNA and production of standard curves for RT-qPCR

Synthetic *in vitro* transcribed RNAs were produced to enable quantification of viral RNA load in the infection experiments. All sequences, their respective accession numbers as well as a schematic organization of these constructs are displayed in Appendix X. Sequences were collected from the online database GenBank® provided by the National Center for Biotechnology Information (NCBI). Geneious® software was used to process and modify the sequences. The *in vitro* transcription reactions were perfomed using the Riboprobe System SP6/T7 kit (Promega).

3.10.1) Sequence design and synthesis

Sequences from YFV-17D (NS5 gene), USUV (NS1 gene), WNV (E gene), LGTV (NS5 gene) and ZIKV (NS1 gene) were collected from the GenBank database and the primer/probe binding regions from the virus sequences were tested *in silico* to certify the correct primer/probe annealing. In the 5' extremity, the bacteriophage SP6 RNA polymerase promoter sequence was added upstream to the specific virus primer/probe binding regions. Between the SP6 promoter sequence and the virus primer/probe binding region a "spacer" region containing 8 nucleotides was added. Finally the specific virus primer/probe binding region was added. In addition to that, if the sequence length allowed modifications, an "identification" region was introduced to certify sequence authenticity and avoid and rapidly identify cross-contamination. Sequences were then commercially synthesized by Eurofins Genomics and cloned into pEX-A2 vector (Eurofins Genomics).

3.10.2) Vector linearization and clean-up

Four micrograms of each construct were linearized by restriction endonuclease cleavage using the HF-*Not*I as described in **3.4.6.** Afterwards, linearization was confirmed by agarose gel electrophoresis and the linearized construct was purified using the QIAquick PCR Purification Kit following manufacturer's instructions. Linearized vectors were eluted in 50 µl of DNAse/RNAse free water and stored at -20°C until use.

3.10.3) Production of synthetic RNAs

Linearized vectors were *in vitro* transcribed using the Riboprobe system SP6/T7 kit (Promega) following manufacturer's guidelines. Briefly, the reaction was scaled-up to a final volume of 40 µl. Then, a mix was prepared containing the transcription buffer, DTT, RNase inhibitors, the ribonucleotides (rATP, rGTP, rCTP and rUTP), the SP6 polymerase, the linearized vector and water to a final volume of 40 µl (**Table 3**) and the reactions were incubated at 37°C for 2 hours.

Table 3: Protocol for *in vitro* synthesis of RNA

Reagent	Volume
Transcription Optimized 5X Buffer	8.0 µl
DTT (100mM)	4.0 µl
Recombinant RNasin Ribonuclease Inhibitor (20–40 units)	1.0 µl
rATP, rGTP and rUTP (2.5 mM each)	8.0 µl
100 µM rCTP (diluted from stock)	4.8 µl
Linearized template DNA (0.2–1.0 mg/ml in water or TE buffer)	X
SP6, T3 or T7 RNA Polymerase (15–20 units)	4.0 µl
Water	X
	Final Volume 40 µl

3.10.4) Removal of DNA template

To completely remove remaining template DNA, reactions were digested with 2 units (2 µl) of DNAse turbo per µg of DNA template and incubated at 37°C for 1 hour.

3.10.5) RNA purification

The *in vitro* transcribed RNAs were cleaned up using the RNeasy Mini Kit (Qiagen) following manufacturer's instructions. Briefly, the *in vitro* transcription reaction was resuspended in 350 µl of RLT buffer and 250 µl of absolute ethanol. Samples were loaded into spin columns and centrifuged at 8,000 RPM for 1 minute. The flow-through was discarded and the columns were washed twice with 500 µl RPE buffer. To remove remaining buffer, the columns were centrifuged at 13,000 RPM for 1 minute. Then, columns were loaded with 50 µl of DNase/RNase free water and incubated for 5 minutes and then centrifuged again at 13,000 RPM for 1 minute. Synthetic RNAs were quantified by micro-volume spectrophotometer (Nanodrop®) and stored at -80°C until use.

3.10.6) Determination of RNA copy numbers

RNA copy numbers were determined as described by Hoffmann *et al.*,(2005). The following formula was applied for this calculation:

$$\text{Copy numbers} = \frac{\text{conc of RNA (g)/(µl)}}{\text{transcript length in nucleotides x 340}} \text{ x } 6.022\text{x}10^{23}$$

3.10.7) Preparation of standard curve

To quantify the absolute viral RNA copy numbers, a standard curve was developed based on serial dilutions of the respective synthetic RNAs. Shortly, samples were diluted serially in RNA-safe-buffer (RSB) ranging from 1:10 to 1:10^8 to a final volume of 250 µl. After dilution, samples were stored at -80°C and once thawed, stored at -20°C with a maximum of 5 freeze- and thaw-cycles.

3.11) Isolation of nucleic acids

3.11.1) Isolation of viral RNA from cell culture supernatant

Virus RNA was isolated using the QIAamp Viral RNA Mini Kit (Qiagen) following manufacturer's protocol. Briefly, 140 µl of cell culture supernatant were collected and mixed with 560 µl AVL buffer. Afterwards, suspensions were spin-centrifuged to remove droplets from the lid and 560 µl of absolute ethanol were added to the mixture, mixed and shortly spun-down to remove lid droplets. Then 630 µl were loaded to a spin column and centrifuged at 8,000 RPM for 1 minute, the flow-through was discarded and the step

repeated again. Columns were first washed with 500 µl of AW1 and subsequently with 500 µl of AW2 buffer, centrifuged at 8,000 RPM for 1 minute and 3 minutes, respectively. Finally, the spin columns were transferred to a sterile 1.5 ml microtube, 50 µl of AVE buffer were added to the columns, incubated for 5 minutes and then centrifuged at 13,000 RPM for 1 minute. The eluted RNA was stored at -80°C until use.

3.11.2) Isolation of total RNA from cell monolayers

Total RNA was isolated using the RNeasy Mini Kit (Qiagen) following manufacturer's instructions. Cell culture monolayers were resusupended in 350 µl of RLT buffer and frozen overnight at -80°C. Suspensions were spun-down to remove droplets from the lid and 350 µl of 70% ethanol were added, mixed and shortly spun-down again. Then 700 µl of the mixture were loaded to a spin column and centrifuged at 8,000 RPM for 1 minute, the flow-through discarded and the step repeated, if necessary. Columns were washed with 700 µl of RW1 buffer and subsequently with 500 µl of RPE buffer before centrifugation at 10,000 RPM for 1 minute (RW1 buffer) and 2 minutes (RPE buffer). Finally, the spin columns were transferred to a sterile 1.5 ml microtube, 50 µl of AVE buffer was added to the columns, incubated for 5 minutes and then centrifuged at 13,000 RPM for 1 minute. The eluted RNA was stored at -80°C until use.

3.12) Polymerase chain reaction

Primer sequences and reagents are all listed in Appendices VI, IV.

3.12.1) One-step reverse transcription-polymerase chain reaction (RT-PCR)

To detect the gene expression by reverse transcription (RT) followed by polymerase chain reaction (PCR) two systems are available: one-step and two-step RT-PCR. Basically, the first system performs both, the RT and PCR reaction in a single reaction while in the second system, each reaction must be performed separately. For detection of integrin mRNA expression, we chose the one-step RT-PCR method using the Superscript III™ One-Step RT-PCR kit. Total RNA was isolated as described in **section 3.11.2**. A master mix containing 1.0 µl of each forward and reverse primers (at a concentration of 10 pmol), 25 µl of the PCR buffer (containing dNTPs, magnesium and DTT) and 2.0 µl of the enzyme mix containing both RT (Moloney murine leukemia virus RT) and *Thermus aquaticus* (Taq) DNA polymerase enzymes were added into a 1.5 ml microcentrifuge tube. Sterile RNase/DNase free water was added into the tube to complete the reaction to a final volume of 45 µl. The master mix was then gently homogenized and aliquoted into a 0.2

ml PCR reaction tube. After this, the total RNA (5 μl) was added into each tube separately and reactions were mixed and submitted to thermal cycling as shown in **Tables 4, 5 and 6**.

Table 4: RT-PCR cycling conditions used for detection of the mouse αV integrin gene

Stage	Temperature	Time	Cycles
Reverse Transcription	55° C	60 min	1x
	94° C	2 min	
PCR	94°C	15 sec	40 x
	56°C	30 sec	
	68°C	60 sec	
Final Elongation	68°C	10 min	

Table 5: RT-PCR cycling conditions used for detection of the mouse β3 integrin gene

Stage	Temperature	Time	Cycles
Reverse Transcription	60° C	60 min	1x
	94° C	2 min	
PCR	94°C	15 sec	40 x
	62°C	30 sec	
	68°C	60 sec	
Final Elongation	68°C	10 min	

Table 6: RT-PCR cycling conditions used for detection of the mouse β1 integrin gene

Stage	Temperature	Time	Cycles
Reverse Transcription	55° C	60 min	1x
	94° C	2 min	
PCR	94°C	15 sec	40 x
	60°C	30 sec	
	68°C	60 sec	
Final Elongation	68°C	10 min	

3.12.2) Quantitative reverse transcription-polymerase chain reaction (RT-qPCR)

Quantification of viral genome by quantitative reverse transcription-polymerase chain reaction (RT-qPCR) was performed in a *one-step* system. The detection method used in this study was based on DNA probes labelled with fluorescent dyes (commonly known as *Taqman* system). Primers and probes were diluted to a final concentration of 10 pmol in 0.1X TE buffer. The primer/probe mix was stored at -20°C under light protection. The RT-qPCR reactions were set using the QuantiTec Probe RT-PCR kit (Qiagen). The standard protocol was used for all RT-qPCR reactions. Viral RNA was isolated from supernatants or cell culture monolayers as outlined in **3.11**. A mastermix containing 12.5 µl of the PCR buffer (supplied with dNTPs, magnesium and the *Taq* DNA polymerase), 2.0 µl of the primers/probe mix, 0.25µl of the RT enzyme mix (Omniscript® Reverse Transcriptase and Sensiscript® Reverse Transcriptase) and water was added up to a final volume of 20 µl. The mastermix was homogenized by agitation and a quick spin-centrifugation was done to collect droplets from the lid. Then, the mastermix was aliquoted into 96-well PCR plates. Finally, 5 µl of RNA template were added into the respective wells, plates were sealed with adhesive optical PCR sealing film, centrifuged and submitted to thermal cycling as shown in **Table 7**. A standard curve based on *in vitro* transcribed RNA was used to quantify the absolute copy number. Positive controls as well as negative and blank controls were also added in every RT-qPCR experimental run. All RT-qPCR reactions were run in the CFX96™ Real-Time PCR Detection System (Biorad).

Table 7: Cycling conditions for RT-qPCR

Stage	Temperature	Time	Cycles
Reverse Transcription	50° C	30 min	1x
	95° C	15 min	
PCR	95°C	15 sec	45 x
	55°C	30 sec	
	72°C	15 sec	

3.12.3) Detection of flavivirus RNA by RT-qPCR

The pan-flavivirus detection and identification assay was used for the detection and quantification of YFV and LGTV genomes (Vina-Rodriguez *et al.*, 2017). In this assay, a primer pair was designed targeting the NS5 region of different flaviviruses, enabling the detection of almost all flavivirus species. Aside in this study, a DNA-based probe labelled with fluorescence dye was designed separately targeting the inter-

regions between forward and reverse primers. The YFV and LGTV DNA-probes were labelled with 6'carboxyfluorescein (FAM) reporter at the 5' region and with a tetramethylrhodamine (TAMRA) quencher at the 3' region. FAM-specific fluorescences were excited at 450-490 nm and detected at 515-530 nm. Detection of USUV genome was performed as described by Jöst *et al.*,(2011) with modifications. The DNA-based probe was labelled with a Hexachlorofluorescein (HEX) at the 5' region and Black Hole Quencher 1 (BHQ-1) as quencher at the 3' region. HEX specific fluorescences were excited at 515-535 nm and detected at 560-580 nm. The WNV genome detection was performed as described by Lanciotti *et al.*,(2000) with modifications. The DNA-based probe was labelled with FAM reporter at the 5' region and with TAMRA quencher at the 3' region. FAM specific fluorescences were excited at 450-490 nm and detected at 515-530 nm. ZIKV genome was detected using primers and probe described by Lanciotti *et al.*,(2008) with modifications. The DNA-based probe was labelled with FAM reporter at the 5' region and TAMRA quencher at the 3' region. FAM specific fluorescences were excited at 450-490 nm and detected at 515-530 nm.

3.13) Cell infection assays

Generally, all cell infection assays were performed in 12-well plates except the binding inhibition assay that was performed in 24-well plates. Unless specified, all integrin deficient MEFs and MKFs, their respective wild-type cells and the CHO cells expressing the αV and β3 integrin subunits were seeded at a concentration of $1x10^5$ cells per well. Cells were cultivated in DMEM or E-MEM supplied with 2% FBS unless further specified. Prior to inoculation, cell concentrations as well as cell viability (Trypan Blue method) were determined to ensure correct multiplicity of infection (MOI) calculation. For virus inoculation, serum and antibiotic free DMEM or E-MEM were used.

3.13.1) Virus binding assay

For the binding assay, cell culture medium was replaced with serum-free DMEM or E-MEM medium and cells were pre-incubated at 4°C for 30 minutes prior to inoculation. After this, plates were placed on ice and cells inoculated with sucrose gradient purified flaviviruses at an MOI of 10. Then, cells were incubated for one hour on ice with agitation every 15 minutes. After this period, the inoculum was removed and the wells were washed four times with ice-cold 1X PBS to remove unbound virus particles. Cell monolayers were resuspended in RLT buffer and stored at -80°C. Three independent experiments were performed in triplicate.

3.13.2) Replication Assay

For the replication assay, cells were inoculated at an MOI of 10 and incubated at 37°C for virus adsorption for one hour. After this period, the inoculum was removed and monolayers were washed four times with 1X PBS to remove unbound virus particles. Finally, either fresh E-MEM or DMEM 2% FBS medium was added into the wells and plates were incubated at 37°C with 5% carbon dioxide. Supernatants were harvested 48 hours after inoculation and stored at -80°C until use. Three independent experiments were performed in triplicate.

3.13.3) Virus internalization assay

For the internalization assay, cell culture medium was replaced with serum-free DMEM and cells were pre-incubated at 4°C for 30 minutes prior to inoculation. After this, plates were placed on ice and cells inoculated with different flaviviruses at an MOI of 10. Cells were incubated for one hour on ice with agitation every 15 minutes. After this period, inoculum was removed and cells washed four times with ice-cold 1X PBS to removed unbound virus particles and serum-free DMEM was added into the wells. Cells were shifted to 37°C for 40 minutes to allow virus internalization. After this period, medium was removed and cell monolayers were washed once with 1X PBS and treated with acidic glycine (pH 2.5) for 2 minutes to inactivate non-internalized virions as described elsewhere (Hung *et al.*, 1999; Suksanpaisan *et al.*, 2009; Thepparit *et al.*, 2004a). Following this treatment, monolayers were washed twice with 1X PBS and cell monolayers were resuspended in RLT buffer and stored at -80°C. Three independent experiments were performed in triplicate.

3.13.4) Detection of flavivirus negative-strand RNA

For the detection of flavivirus negative-strand RNA, cells were inoculated as detailed in **3.13.2**. Supernatants were removed and cell monolayers were extensively washed with 1x PBS to remove excess of virus. Cell monolayers were resuspended in RLT buffer and stored at -80°C. Three independent experiments were performed in triplicate. Levels of flavivirus negative-strand RNA were calculated using the 2^ddCT method as described by Pfaffl,(2001).

3.13.5) Binding inhibition assay

For the binding inhibition assay, cells were seeded in 24-well plates with DMEM supplied with 2% FBS at a concentration of 1×10^4 cells per well, 12-16 hours prior to inoculation. Medium was replaced with serum-free DMEM and cells were pre-incubated at 4°C for 15 minutes prior to inoculation. Subsequently, type I collagen (0-500 µg/ml), synthetic RGD motif peptide (0-250 µg/ml) and recombinant mouse vitronectin (0-50 µg/ml) were added into the wells in serum-free DMEM supplied with 1 mM $MnCl_2$ and 1 mM $MgCl_2$ and incubated at 4°C for 30 minutes to allow ligand binding. After this, plates were placed on ice, washed twice and cells inoculated at an MOI of 10. Cells were incubated for 1 hour on ice with constant agitation every 15 minutes. After this period, the inoculum was removed and the wells were washed four times with ice-cold 1X PBS to remove unbound virus particles. Cell monolayers were resuspended in RLT buffer and stored at -80°C. Experiments were performed in duplicate. Percentage of binding inhibition was calculated using the following formula:

$$\text{Percentage of binding inhibition} = \frac{\text{Ct value of infected cell} - \text{Ct value of treated control cells}}{\text{Ct value of infected cell}} \; x \; 100$$

3.14) Graphical design and statistical analysis

Graphics were designed using Graphpad Prism software version 6. Statistical analysis was also performed using Graphpad Prism software version 6. if necessary, prior to statistical analysis, the D'Agostino & Pearson and Shapiro-Wilk normality tests were performed in order to assure normal distribution. The non-parametric Mann-Whitney test was used to evaluate statistical significance between the two groups (Wild-type vs.Knock-out cells) in the binding experiments. The parametric Student's t-test was used to evaluate statistical significance between the two groups (Wild-type vs.Knock-out cells) in the internalization and replication experiments. The parametric One-way ANOVA with Bonferroni's correction was used to compare three or more groups. Indication of statistical significance is represented by asterisks (*) as follows: * = $p \leq 0.05$; ** = $p \leq 0.01$; *** = $p \leq 0.001$; **** = $p = \leq 0.0001$. The abbreviation "ns" stands for "not significant" with $p > 0.05$.

4.) Results

4.1) Generation of integrin expressing cells

4.1.1) Cloning of integrin genes into mammalian expression vectors

The constructs pMK-ITGαV and pMK-ITGβ3 were digested separately with the HF-*Bam*HI and HF-*Not*I restriction endonucleases. In a subsequent step, the mouse ITG-αV and ITG-β3 genes were inserted into pcDNA 3.1 (H) (5,600 bp) and pcDNA 3.1 (Z) (5,000 bp) vectors, respectively, and transformed into *E. coli* strain DH5α. Constructs containing the correct insert were subjected to DNA sequencing. Sequence analysis showed the absence of mutations and confirmed in-frame orientation of the inserted sequences (data not shown).

As demonstrated in **Figure 7**, gel electrophoresis showed fragments of 5,600 bp and 3,172 bp (lane 2) corresponding to the pcDNA 3.1 (H) vector and mouse ITG-αV gene, respectively, and fragments of 5,000 bp and 2,400 bp (lane 3) corresponding to the pcDNA 3.1 (Z) vector and the mouse ITG-β3 gene.
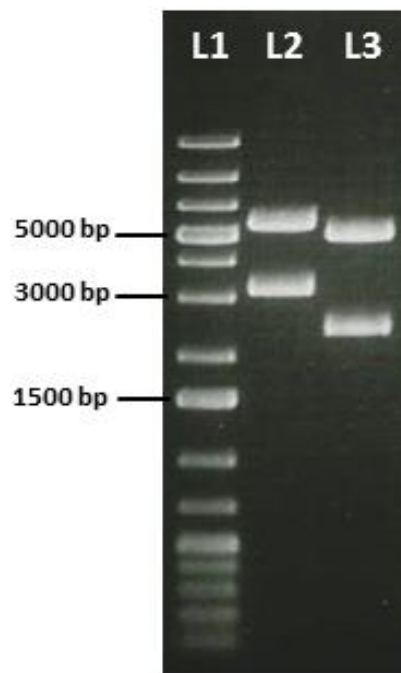
Figure 7: Restriction digestion analysis of pcDNA 3.1 (H) and pcDNA 3.1 (Z) derived integrin gene constructs. The constructs were digested by restriction endonucleases HF-*Bam*HI and HF-*Not*I. Agarose electrophoresis showing fragments of 5,600 and 3,172 bps (lane 2; L2) corresponding to the pcDNA 3.1 (H) and the mouse ITG-αV gene; fragments of 5,000 and 2,400 bps corresponding to the pcDNA 3.1 (Z) vector and the mouse ITG-β3 gene (lane 3; L3). Agarose concentration: 0.8%; electrophoresis conditions: 110V, 70 minutes; ethidium bromide staining; L1: GeneRuler 1 Kb DNA ladder (Fermentas). Abbreviation: bp: base pairs.

4.1.2) Recovery of αVβ3 integrin expression in MEF-αVβ3$^{-/-}$ cells

To recover the expression of αVβ3 in MEF-αVβ3$^{-/-}$cells, both vectors harboring the mouse αV and β3 integrin subunit genes were transfected simultaneously into MEF-αVβ3$^{-/-}$ cells. Forty-eight hours after transfection with the vectors harboring the mouse ITG-αV and mouse ITG-β3 integrin subunit genes, antibiotic selection using hygromycin B and zeocin was initiated. Within the first 3 days, more than 80% of the cells died due to the antibiotic selection. Resistant cell populations were kept under antibiotic selection for approximately 6-12 weeks or until a confluent cell monolayer was achieved that allowed splitting to T25 cm² flasks. Several clones showed the presence of both αV and β3 integrin subunit genes at the cellular DNA level (data not shown). However, the expression levels of αV and β3 integrin subunits at the cell surface measured by FACS were less than 10% (data not shown). Positive selection by magnetic cell sorting was performed in order to obtain a homogeneous cell population expressing the respective integrin subunits. The cell sorting resulted in a cell population of very low density that was further maintained under cultivation. After reaching the confluence, cells were tested again by PCR and FACS. Most cells of the population lost the expression of one or both integrin subunits but still grew under antibiotic selection. Several modifications and different strategies were applied in order to recover the αVβ3 integrin expression in MEF-αVβ3$^{-/-}$ cells such as i) decrease of antibiotic concentration; ii) removal of antibiotics after cell sorting until the sorted cells reach confluence of more than 60% and iii) use of other transfection reagents and transfection techniques such as electroporation. Indeed, all these modifications resulted in cell populations with low or absent αVβ3 integrin expression. In turn, the recovery of αVβ3 integrin expression in the MEF-αVβ3$^{-/-}$ cells was not achieved (data not shown). Thus, the MEF-WT cells were used as the respective wild-type cells.

4.1.4) Establishment of CHO cells expressing the integrin subunits

Transfection efficiency in CHO cells reached more than 80% as determined by the GFP-encoding vector control. Forty-eight hours after transfection with the vectors harboring the mouse ITG-αV and mouse ITG-β3 integrin subunit genes, CHO cells were split into T25 cm² flasks and set under antibiotic selection with either zeocin or hygromycin. Hygromycin resistant cell populations were observed after three days of antibiotic selection. Zeocin resistant cell populations were observed after one week. Cells were successively passed for up to 20 passages. These cell populations were then subjected to positive selection by magnetic cell sorting and further characterized for expression of ectopic integrins

4.2) Characterization of integrin expressing cells

4.2.1) Cell morphology and growth

4.2.1.1) Cell morphology and growth of MEF and MKF cells

Integrin deficient cells as well as their respective wild-type cells were characterized by indirect immunofluorescence, FACS and RT-PCR. Initial morphological analyses of the integrin deficient cells as well as their respective wild-type cells revealed slight differences in cell morphology (**Figure 8**). The MKF-β1$^{-/-}$ cells showed to be more round-shaped than the parental wild-type cells, the MKF-β1^{Flox}. Both cell lines showed similar growth rates and were split more often than MEFs. Interestingly, the MEF-αVβ3$^{-/-}$ cells showed morphological changes by forming more cell aggregations than their respective wild-type cells. MEF-αVβ3$^{-/-}$ cells showed to be more round-shaped and the cell density was much lower than for the MEF-WT and MKF cells (**Figure 8**). The MEF-β3$^{+/+R}$ cells showed a discrete decrease in the growth rate when compared to MEF-β3$^{-/-}$ cells. No substantial differences on cell morphology were observed between MEF-β3$^{+/+R}$ and MEF-β3$^{-/-}$ cells.
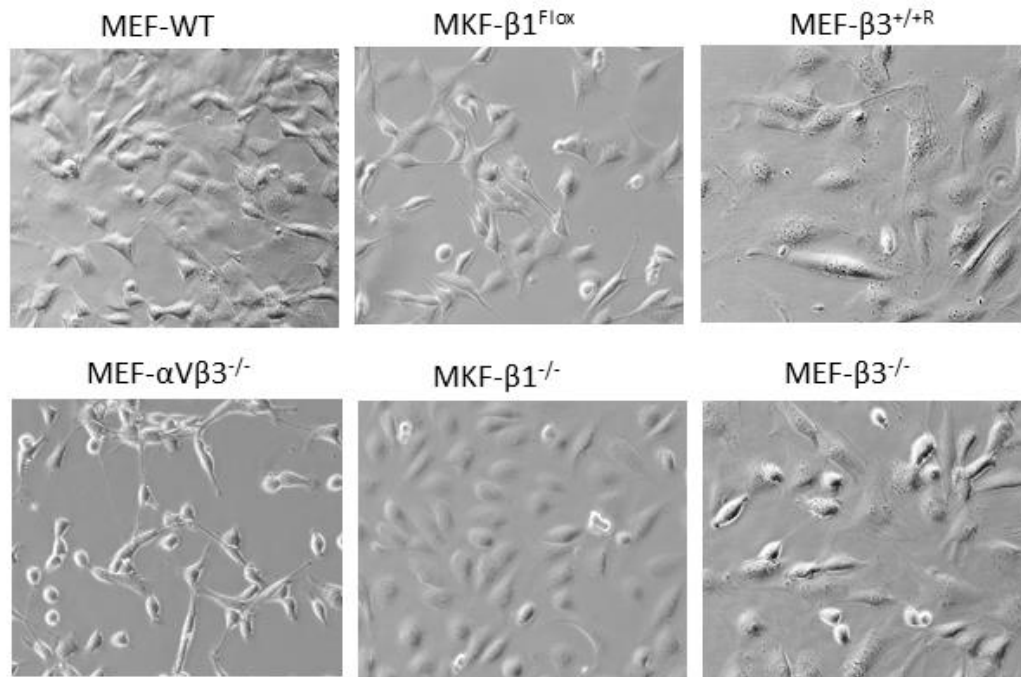
Figure 8: Morphology of integrin deficient MEFs and MKFs and their respective wild-type cells. Cells were visualized by inverted light microscopy 72 hours after seeding in T25 cm² cell culture flasks. Magnification: 20X. Abbreviations: MEF-WT: mouse embryonic fibroblasts wild-type; MEF-αVβ3$^{-/-}$: mouse embryonic fibroblasts deficient for αVβ3 integrin; MKF-β1^{Flox}: mouse kidney fibroblasts expressing the β1 integrin subunit; MKF-β1$^{-/-}$: mouse kidney fibroblasts deficient for the β1 integrin subunit; MEF-β3$^{+/+R}$: mouse embryonic fibroblasts expressing the β3 integrin subunit (R = rescue; rescued by ITG-β3 gene transfection) and MEF-β3$^{-/-}$: mouse embryonic fibroblasts deficient for the β3 integrin subunit.

4.2.1.2) Cell morphology and growth of CHO cells

CHO-K1 cells were transfected with pcDNA plasmids harboring the mouse αV or mouse β3 integrin subunit genes. Upon transfection and establishment of CHO cells expressing the mouse αV or β3 integrin subunits, referred to as CHO-αV$^{+/+}$ and CHO-β3$^{+/+}$, cells were characterized for their morphology and growth. As demonstrated in **Figure 9**, expression of mouse αV and β3 integrin subunits in CHO cells did not alter cell morphology in comparison with the CHO-K1 cells. The cell growth of CHO-αV$^{+/+}$ and CHO-β3$^{+/+}$ cells was substantially slower than that of CHO-K1 cells as observed by different split rates during the maintenance of the cell cultures (data not shown).
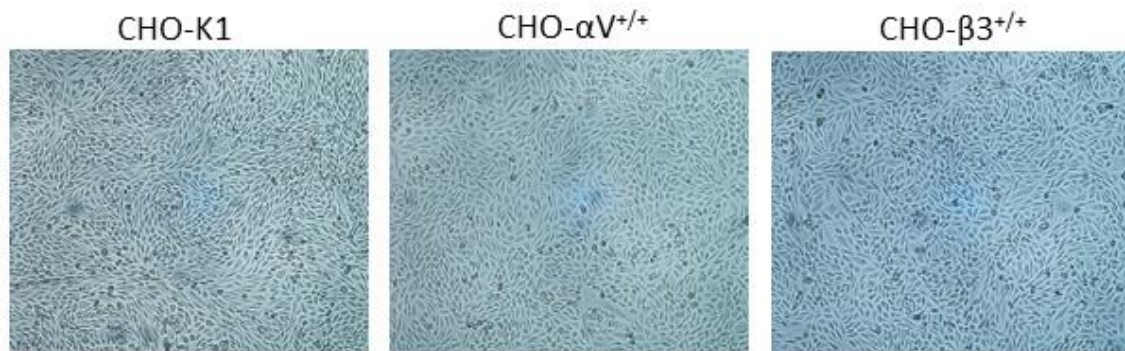
Figure 9: Morphology of wild-type CHO-K1 cells and CHO cells expressing mouse αV or mouse β3 integrin subunits. Cells were visualized by inverted light microscopy 72 hours after seeding in T25 cm² cell culture flasks. Magnification: 10X. Abbreviations: CHO-K1: Chinese hamster ovary cell clone K1; CHO-αV$^{+/+}$: Chinese hamster ovary cells expressing the mouse αV integrin subunit; CHO-β3$^{+/+}$: Chinese hamster ovary cells expressing the mouse β3 integrin subunit. αV: alpha V integrin subunit; β3: beta 3 integrin subunit.

4.2.2) Detection of integrin mRNA by RT-PCR

4.2.2.1) Detection of integrin mRNA by RT-PCR in MEFs and MKFs

RT-PCR was performed to test for the mRNA expression of αV, β1 and/or β3 integrin subunits in the integrin deficient, rescued and WT cells. As shown in **Figure 10 A** (**right panel**), the detection of αV, β1 and β3 integrin subunit mRNA in MEF-WT cells was confirmed by amplification of fragments of 300 bp, 500 bp and 200 bp corresponding to the αV, β1 and β3 integrin subunit mRNAs, respectively. In contrast to that, MEF-αVβ3$^{-/-}$ cells only expressed the β1 integrin subunit mRNA (**Figure 10 A, left panel**).

The MKF-β1^{Flox} and MEF-β3$^{+/+R}$ cells showed an expression pattern of αV, β1 and β3 integrin subunit mRNA identical to the MEF-WT cells (**Figure 10 B, right panel and Figure 10 C, right panel**). The MKF-β1$^{-/-}$ cells were demonstrated to express αV and β3 integrin subunit mRNA while lacking β1 integrin subunit mRNA (**Figure 10 B, left panel**). Last, the analysis of MEF-β3$^{-/-}$ cells revealed the expression of αV and β1 integrin subunit mRNAs in the absence of β3 integrin subunit mRNA (**Figure 10 C, left panel**).
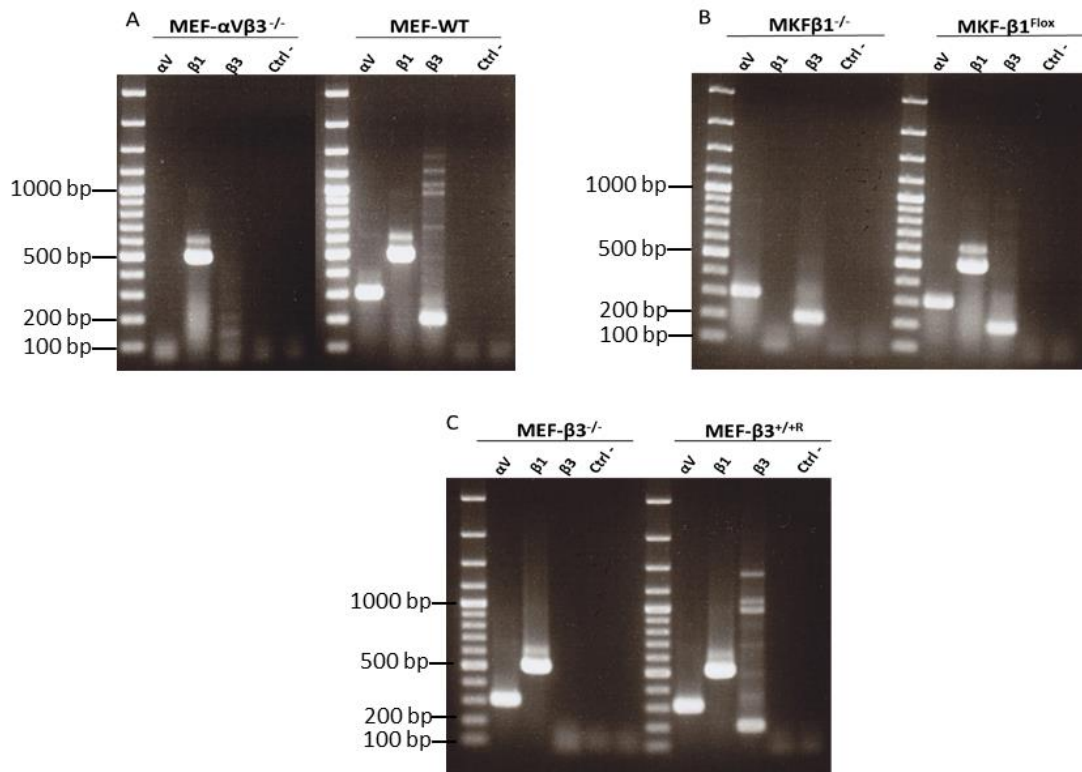
Figure 10: Expression of integrin mRNA in MEF-WT and MEF-αVβ3$^{-/-}$ (A); MKF-β1^{Flox} and MKF-β1$^{-/-}$ (B) and MEF-β3$^{+/+R}$ and MEF-β3$^{-/-}$ (C) cells. The RT-PCR resulted in amplification of 300 bp (αV integrin), 500 bp (β1 integrin) and 200 bp (β3 integrin) products. Agarose concentration: 2.5%; electrophoresis conditions: 110 V, 70 minutes; ethidium bromide staining; Ladder: GeneRuler 100 bp DNA ladder (Fermentas). Abbreviations: MEF-WT: mouse embryonic fibroblasts wild-type; MEF-αVβ3$^{-/-}$: mouse embryonic fibroblast deficient for αVβ3 integrin; MKF-β1^{Flox}: mouse kidney fibroblasts expressing the β1 integrin subunit (wild-type); MKF-β1$^{-/-}$: mouse kidney fibroblasts deficient for the β1 integrin subunit; MEF-β3$^{+/+R}$: mouse embryonic fibroblasts expressing the β3 integrin subunit (R = rescue); MEF-β3$^{-/-}$: mouse embryonic fibroblasts deficient for the β3 integrin subunit; αV: alpha V integrin subunit; β1: beta 1 integrin subunit; β3: beta 3 integrin subunit, Ctrl-: negative control; bp: base pairs.

4.2.2.1) Detection of integrin mRNA by RT-PCR in CHO cells

To confirm the expression of αV and β3 integrin subunit mRNAs in transfected CHO cells, RT-PCR was performed. As shown in **Figure 11**, the CHO-K1 cells express only the β1 integrin subunit. Obviously, the endogenous hamster β1 integrin subunit was also expressed in the CHO cells transfected with either the mouse αV or the mouse β3 integrin subunit genes (**Figure 11**). CHO-αV$^{+/+}$ cells that were transfected with a DNA plasmid harboring the mouse αV integrin gene expressed the respective αV integrin subunit mRNA (**Figure 11**). Finally, the CHO-β3$^{+/+}$ cells expressed the β3 integrin subunit mRNA (**Figure 11**). In conclusion, the CHO cells transfected with the mouse αV and β3 integrin subunits genes expressed the respective mRNAs.
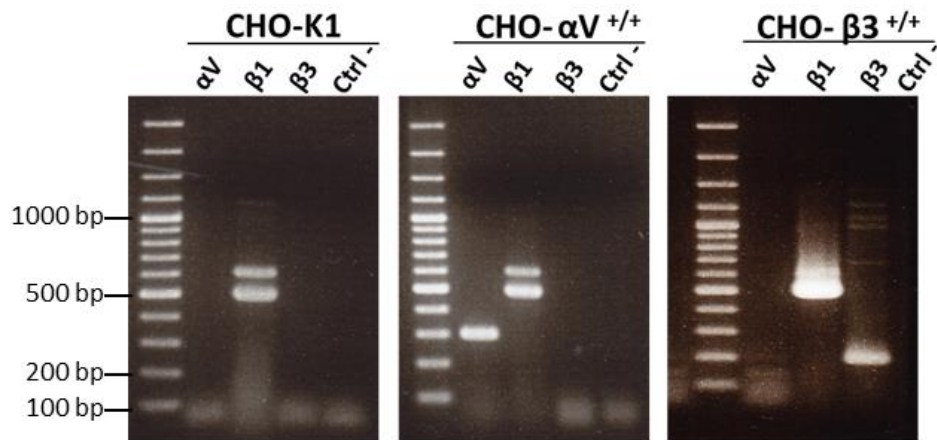
Figure 11: Expression of integrin mRNA in CHO-K1, CHO-αV$^{+/+}$ and CHO-β3$^{+/+}$ cells. The RT-PCR resulted in amplification of 300 bp (αV integrin), 500 bp (β1 integrin) and 200 bp (β3 integrin) products. Agarose concentration: 2.5%; electrophoresis conditions: 110 V, 70 minutes; ethidium bromide staining; Ladder: GeneRuler 100 bp DNA ladder (Fermentas). Abbreviations: CHO-K1: Chinese hamster ovary cell clone K1; CHO-αV$^{+/+}$: Chinese hamster ovary cells expressing the mouse αV integrin subunit; CHO-β3$^{+/+}$: Chinese hamster ovary cells expressing the mouse β3 integrin subunit; αV: alpha V integrin subunit; β1: beta 1 integrin subunit; β3: beta 3 integrin subunit; Ctrl-: negative control; bp: base pairs.

4.2.3) Characterization of integrin expressing cells by indirect immunofluorescence assay

4.2.3.1) Characterization of MEFs and MKFs

In order to visualize the integrin expression pattern and to determine its sub-cellular localization, indirect immunofluorescence assays were performed using antibodies raised against the αV, β1 and β3 integrin subunits.

Images analyzed by confocal laser microscopy revealed that all of the expressed integrin subunits are globally distributed along the cell membrane with the formation of focal adhesion sites intensively stained at the cell surface (**Figure 12**). As expected, MEF-WT, MEF-β3$^{+/+R}$ and MKF-β1^{Flox} cells expressed the αV (shown in red, left panel, **Figure 12**), β1 and β3 integrin subunits (shown in green, middle and right panel, **Figure 12**). When analyzing the integrin deficient cells, the MEF-αVβ3$^{-/-}$ cells expressed only the β1 integrin subunit (**Figure 12**) while the MEF-β3$^{-/-}$ cells expressed the αV and β1 (**Figure 12**). The MKF-β1$^{-/-}$ cells showed no expression of β1 but readily expressed the αV and β3 integrin subunits (**Figure 12**). Interestingly, the formation of focal adhesion sites was also observed in the MEF-αVβ3$^{-/-}$, the MEF-β3$^{-/-}$ and the MKF-β1$^{-/-}$ cells indicating that the absence of a certain integrin subunit had no impact on the functional expression of other integrin heterodimers. In summary, these results further confirm the results obtained by RT-PCR.
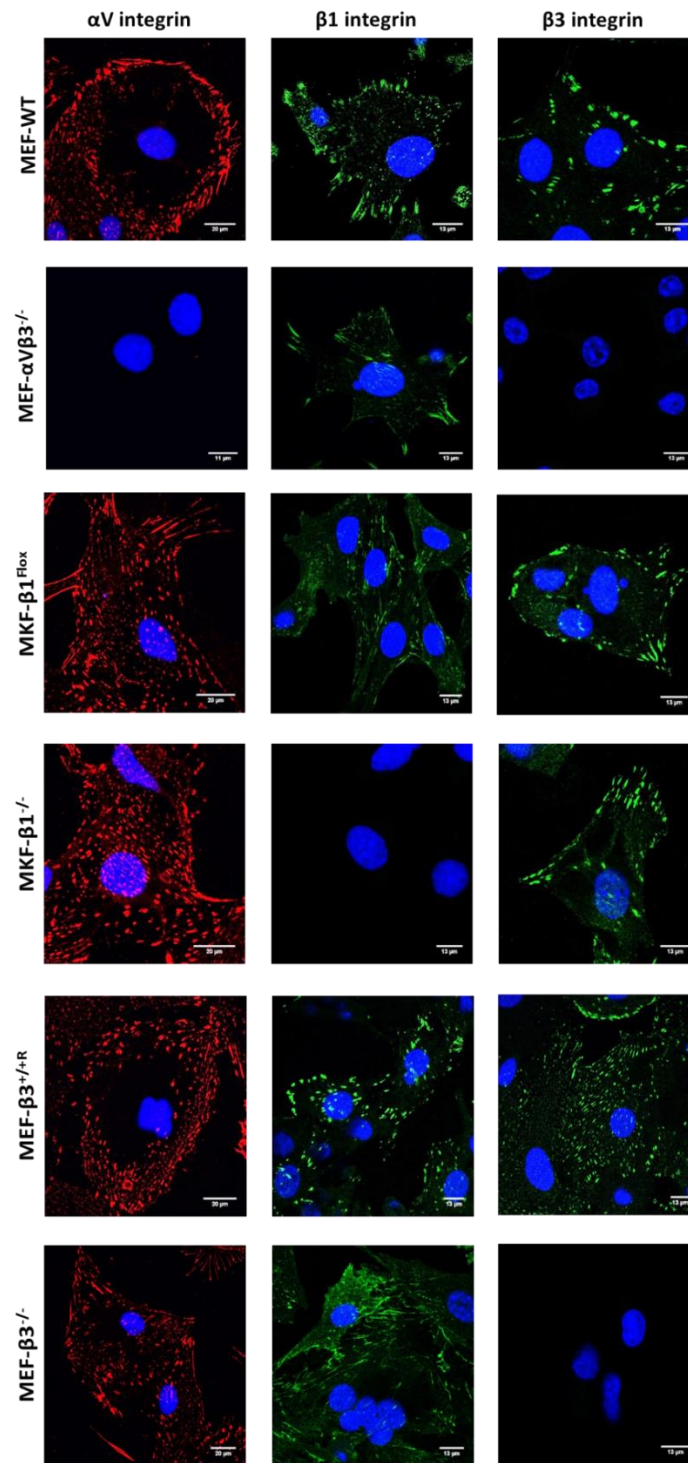
Figure 12: Immunofluorescence-based detection of αV, β1 and β3 integrin subunits in MEF and MKF cells. Antibodies raised against mouse αV (red), β1 and β3 (green) integrin subunits were used to detect the integrin expression on the cell surface. Nuclei were stained using DAPI (blue). Images were captured by Leica laser scanning confocal microscope and processed with LAS AF, Leica. Images were edited using ImageJ software. Scale bar: 20 µm (αV staining) and 13 µm (β3 and β1 staining). Abbreviations: MEF-WT: mouse embryonic fibroblasts wild-type; MEF-αVβ3^{-/-}: mouse embryonic fibroblasts deficient for αVβ3 integrin; MKF-β1^{Flox}: mouse kidney fibroblasts expressing the β1 integrin subunit (wild-type); MKF-β1^{-/-}: mouse kidney fibroblasts deficient for the β1 integrin subunit; MEF-β3^{+/+R}: mouse embryonic fibroblasts expressing the β3 integrin subunit (R = rescue); MEF-β3^{-/-}: mouse embryonic fibroblasts deficient for the β3 integrin subunit; αV: alpha V integrin subunit; β1: beta 1 integrin subunit; β3: beta 3 integrin subunit.

4.2.3.1) Characterization of CHO cells

To confirm the expression of mouse αV and β3 integrin subunits in CHO cells at the cell membrane, the same immunofluorescence protocol as described for MEF/MKF cells was applied here. As shown in **Figure 13**, the respective mouse integrin subunits were detected at the cell surface forming characteristic focal adhesion sites in both CHO-αV$^{+/+}$ and CHO-β3$^{+/+}$ cells indicating the formation of chimeric integrin heterodimers in CHO-αV$^{+/+}$ as well as in CHO-β3$^{+/+}$ cells.
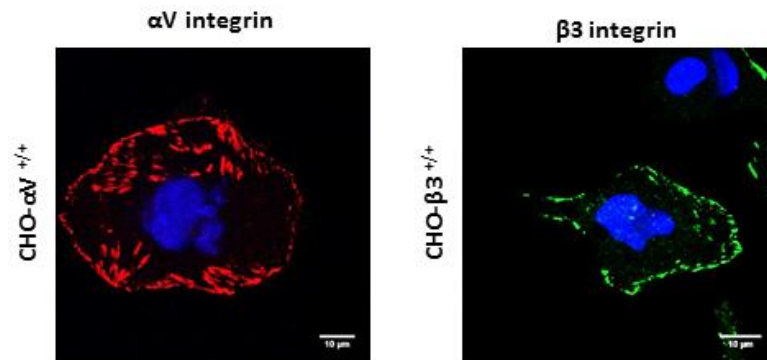
Figure 13: Immunofluorescence-based analysis of CHO-αV$^{+/+}$ and CHO-β3$^{+/+}$ cells for the expression of αV and β3 integrin subunits on the cell surface. Antibodies raised against mouse αV (red) or β3 (green) integrin subunits were used to detect the respective integrin subunits. Nuclei were stained using DAPI (blue). Images were captured by Leica laser scanning confocal microscope and processed with LAS AF, Leica. Images were edited using ImageJ software. Scale bar: 13 μm. Abbreviations: CHO-αV$^{+/+}$: Chinese hamster ovary cells expressing the mouse αV integrin subunit; CHO-β3$^{+/+}$: Chinese hamster ovary cells expressing the mouse β3 integrin subunit; αV: alpha V integrin subunit; β3: beta 3 integrin subunit.

4.2.4) Characterization of integrin expressing cells by flow cytometry

4.2.4.1) Characterization of MEFS and MKFs by flow cytometry

In order to verify the indirect immunofluorescence results as well as to quantify integrin expression on the cell surface, flow cytometry was applied. As shown in **Figure 14**, all wild-type MEFs and MKFs expressed high levels of αV, β1 and β3 integrin subunit on the cell surface. The expression levels ranged from 98% to 100% for all integrin subunits (**Table 8**). MEF-αVβ3$^{-/-}$ cells showed no expression of both αV and β3 integrin subunits but expressed considerable amounts of β1 integrin subunits (**Figure 14 and Table 8**). MEF-β3$^{-/-}$ cells showed high expression of αV and β1 integrin subunits but complete absence of β3 integrin subunit expression (**Figure 14**). MKF-β1$^{-/-}$ cells expressed high levels of αV and β3 integrin subunits but no detectable levels of β1 integrin subunits (**Figure 14**). In summary, the results achieved by flow cytometry analysis are in accordance with the previous results obtained by indirect immunofluorescence assay and RT-PCR.
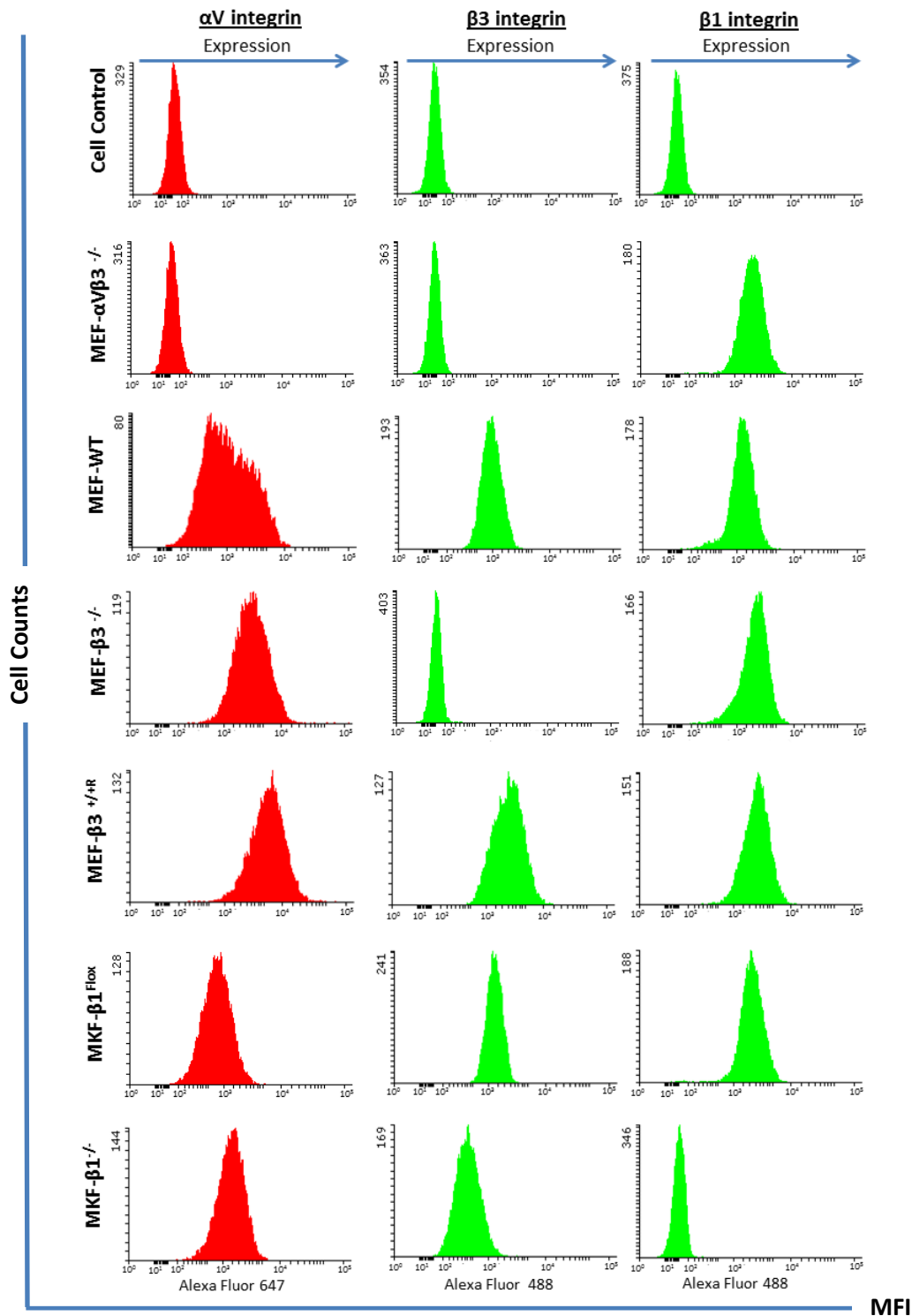
Figure 14: Flow cytometry analysis of MEF and MKF cells for αV, β1 and β3 integrin subunit expression. The figure shows the flow cytometry histograms based on the mean fluorescence intensity (MFI). Cells were incubated with anti-integrin subunit specific antibodies followed by isotype specific secondary antibodies labelled with Alexa-647 (αV integrin) or Alexa-488 (β3 and β1 integrin). Unlabelled cells as well as mouse IgG isotype (not shown) were used as controls. MFI is represented in log scale. Abbreviations: MEF-WT: mouse embryonic fibroblasts wild-type; MEF-αVβ3$^{-/-}$: mouse embryonic fibroblasts deficient for αVβ3 integrin; MKF-β1^{Flox}: mouse kidney fibroblasts expressing the β1 integrin subunit (wild-type); MKF-β1$^{-/-}$: mouse kidney fibroblasts deficient for the β1 integrin subunit; MEF-β3$^{+/+R}$: mouse embryonic fibroblasts expressing the β3 integrin subunit (R = rescue); MEF-β3$^{-/-}$: mouse embryonic fibroblasts deficient for the β3 integrin subunit; αV: alpha V integrin subunit; β3: beta 3 integrin subunit; β1: beta 1 integrin subunit.

Table 8: Percentage of integrin expression in MEFs and MKFs measured by flow cytometry

Cell Line	Percentage of cells expressing respective integrin subunits		
	αV	β3	β1
MEF-WT	99.2	99	99.8
MEF-αVβ3$^{-/-}$	nd	nd	99.4
MEF-β3$^{+/+R}$	99.9	100	99.9
MEF-β3$^{-/-}$	99.9	nd	99.9
MKF-β1^{Flox}	99.7	99	99
MKF-β1$^{-/-}$	99.9	98.7	nd

Abbreviations: nd: not detected; MEF-WT: mouse embryonic fibroblasts wild-type; MEF-αVβ3$^{-/-}$: mouse embryonic fibroblasts deficient for αVβ3 integrin; MKF-β1^{Flox}: mouse kidney fibroblasts expressing the β1 integrin subunit (wild-type); MKF-β1$^{-/-}$: mouse kidney fibroblasts deficient for the β1 integrin subunit; MEF-β3$^{+/+R}$: mouse embryonic fibroblasts expressing the β3 integrin subunit; MEF-β3$^{-/-}$: mouse embryonic fibroblasts deficient for the β3 integrin subunit; αV: alpha V integrin subunit; β1: beta 1 integrin subunit; β3: beta 3 integrin subunit.

4.2.4.1) Characterization of CHO cells by flow cytometry

The levels of integrin expression were measured by flow cytometry using the same antibodies raised against the mouse αV and β3 integrin subunit. As seen in **Figure 15**, CHO-αV$^{+/+}$ and CHO-β3$^{+/+}$ cells expressed high amounts of mouse αV and β3 integrin subunits while the respective wild-type CHO-K1 cells showed no expression of these integrin subunits. The percentage of αV or β3 integrin expressing cells ranged from 99.7% to 99.9% for CHO-αV$^{+/+}$ and CHO-β3$^{+/+}$ cells, respectively (**Table 9**).
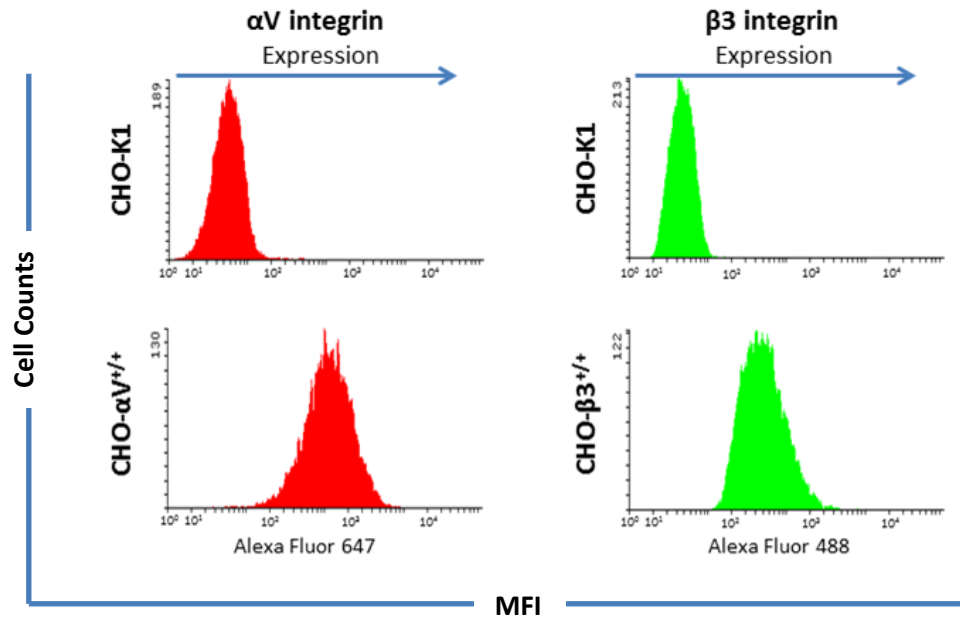
Figure 15: Flow cytometry analysis of CHO-K1, CHO-αV$^{+/+}$ and CHO-β3$^{+/+·}$cells for αV and β3 integrin subunit expression. Flow cytometry histograms are based on the mean fluorescence intensity (MFI). Cells were incubated with αV (red) and β3 (green) anti-integrin subunit specific antibodies followed by incubation with isotype specific secondary antibody labelled with Alexa-647 (αV integrin) or Alexa-488 (β3 integrin). Abbreviations: CHO-αV$^{+/+}$: Chinese hamster ovary cells expressing the mouse αV integrin subunit; CHO-β3$^{+/+}$: Chinese hamster ovary cells expressing the mouse β3 integrin subunit; αV: alpha V integrin subunit; β3: beta 3 integrin subunit.

Table 9: Percentage of integrin expression in CHO-K1, CHO-αV$^{+/+}$ and CHO-β3$^{+/+}$ cells measured by flow cytometry

Cell Line	Percentage of cells expressing respective integrin subunits	
	αV	β3
CHO-K1	nd	nd
CHO-αV$^{+/+}$	99.7	nt
CHO-β3$^{+/+}$	nt	99.9

Abbreviations: nd: not detected; nt: not tested; CHO-αV$^{+/+}$: Chinese hamster ovary cells expressing the mouse αV integrin subunit; CHO-β3$^{+/+}$: Chinese hamster ovary cells expressing the mouse β3 integrin subunit; αV: alpha V integrin subunit; β3: beta 3 integrin subunit.

4.3) Effect of integrin ablation on cell viability

Loss of integrin expression might lead to the inability of the cell to attach to the ECM and potentially triggering anoikis, a type of apoptosis triggered by the inability of cells to bind to the ECM (Gilmore, 2005). In order to determine whether the deletion of αVβ3 integrin and the β1 and β3 integrin subunits affects viability of MEFs and MKFs, a colorimetric cell viability assay based on MTS-tetrazolium was applied. There was no difference in cell viability detected for MEF-αVβ3$^{-/-}$ and MEF-β3$^{-/-}$ cells when compared to their respective wild-type, MEF-WT and MEF-β3$^{+/+R}$ cells (**Figure 16 A and C**). Similarly, the loss of β1 integrin subunit expression in MKF-β1$^{-/-}$ cells did not influence cell viability in comparison to MKF-β1^{Flox} as their respective wild-type cells (**Figure 16 B**).
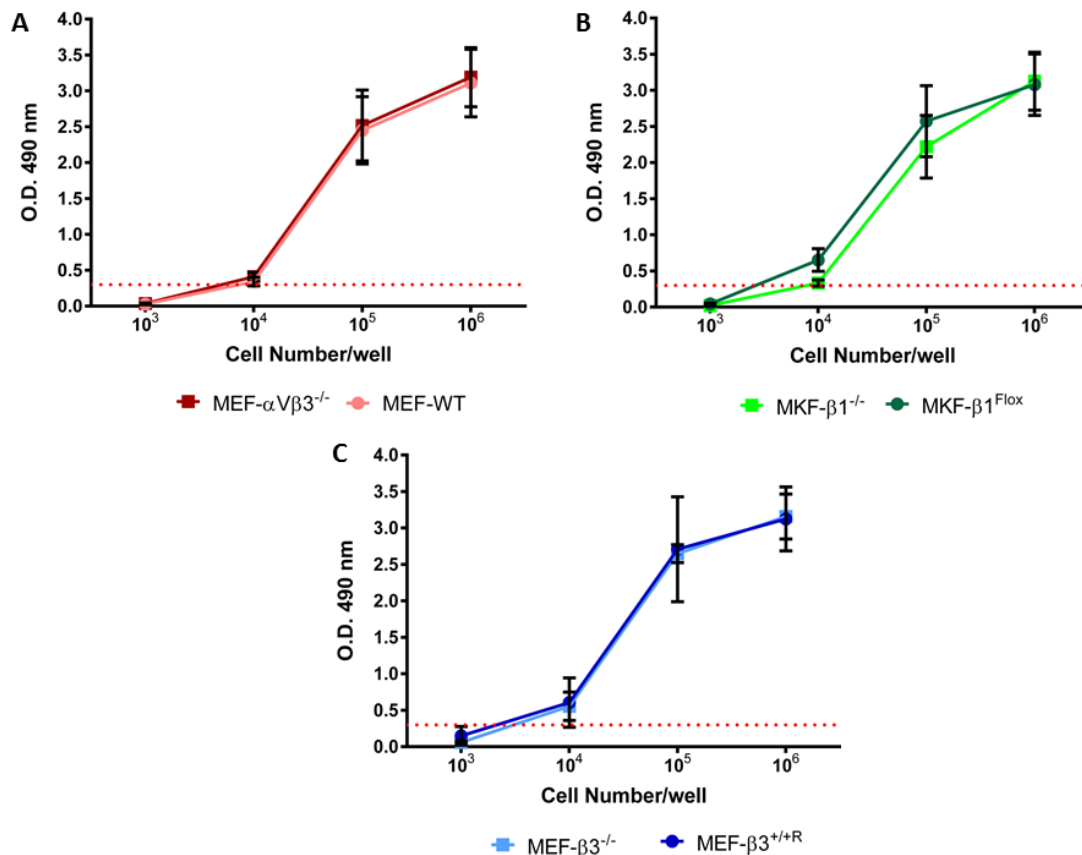
Figure 16: Tetrazolium cell viability assay for MEF-αVβ3$^{-/-}$ and MEF-WT (A); MKF-β1$^{-/-}$ and MKF-β1^{Flox} (B) and MEF-β3$^{-/-}$ and MEF-β3$^{+/+R}$ (C) cells. Cells were seeded at different concentrations (10^3 to 10^6 cells per well) and incubated with the tetrazolium reagent for 4 hours at 37°C with 5% carbon dioxide. Optical density was measured at 490 nm. Two independent experiments were each performed in duplicate (n=2). Square and circle represent the mean values, bars represent the standard deviation (means ± standard deviation). Dashed lines indicate the detection limit of the test. Abbreviations: MEF-WT: mouse embryonic fibroblasts wild-type; MEF-αVβ3$^{-/-}$: mouse embryonic fibroblasts deficient for αVβ3 integrin; MKF-β1^{Flox}: mouse kidney fibroblasts expressing the β1 integrin subunit (wild-type); MKF-β1-/-: mouse kidney fibroblasts deficient for the β1 integrin subunit; MEF-β3$^{+/+R}$: mouse embryonic fibroblasts expressing the β3 integrin subunit (R = rescue); MEF-β3$^{-/-}$: mouse embryonic fibroblasts deficient for the β3 integrin subunit; αV: alpha V integrin subunit; β1: beta 1 integrin subunit; β3: beta 3 integrin subunit.

In addition to that, routine observation of MEF and MKF cells by light microscopy did not show any signs of cell viability reduction such as nuclear retraction, loss of nucleus/cytoplasm ratio, loss of cell adherence or excessive number of dead cells (data not shown). In conclusion, the ablation of αVβ3 integrin and β1 and β3 integrin subunits did not interfere with cell viability.

4.4) Functional characterization of integrin deficient and corresponding wild-type cells

In order to analyze whether the deletion of integrins affects the ability of the integrin deficient cells to bind to their ligands, a cell adhesion assay was performed. Poly-L-Lsy, a positively charged polymer, served as positive control for cell adhesion since it facilitates binding via electrostatic interactions and is independent of integrins (Salmela *et al.*, 2017). All tested cell lines bound to the Poly-L-Lsy (**Figure 17 A - C**). Interestingly, integrin deficient cells bound less efficiently to Poly-L-Lsy coated wells. BSA coated wells, used as a control to prove sufficient blocking of the wells showed no cell adhesion for any of the tested cells (**Figure 17 A - C**). Vero cells, known to express a broad variety of different integrins, served as positive control and bound efficiently to the vitronectin (**Figure 17 A – C**). As demonstrated in **Figure 17 A**, MEF-αVβ3$^{-/-}$ cells bound to a less extent to mouse vitronectin in comparison to the wild-type cells (MEF-WT). The binding activity of MEF-αVβ3$^{-/-}$ cells to vitronectin was reduced by approximately 37.6% (**Figure 17 A**). In a similar manner, the deletion of the β3 integrin subunit in the MEF-β3$^{-/-}$ cells reduced the binding to vitronectin to approximately 40.5% compared to the MEF-β3$^{+/+R}$ cells (**Figure 17 C**). The deletion of β1 integrin subunit affected poorly the ability of MKF-β1$^{-/-}$ cells to bind to vitronectin (**Figure 17 B**). In this case, a reduction of approximately 8.0% on binding to mouse vitronectin compared to the MKF-β1^{Flox} cells was observed (**Figure 17 B**). In turn, in both integrin deficient MEF and MKF cells, the deletion of one or two integrin subunits impaired the recognition and binding to vitronectin.
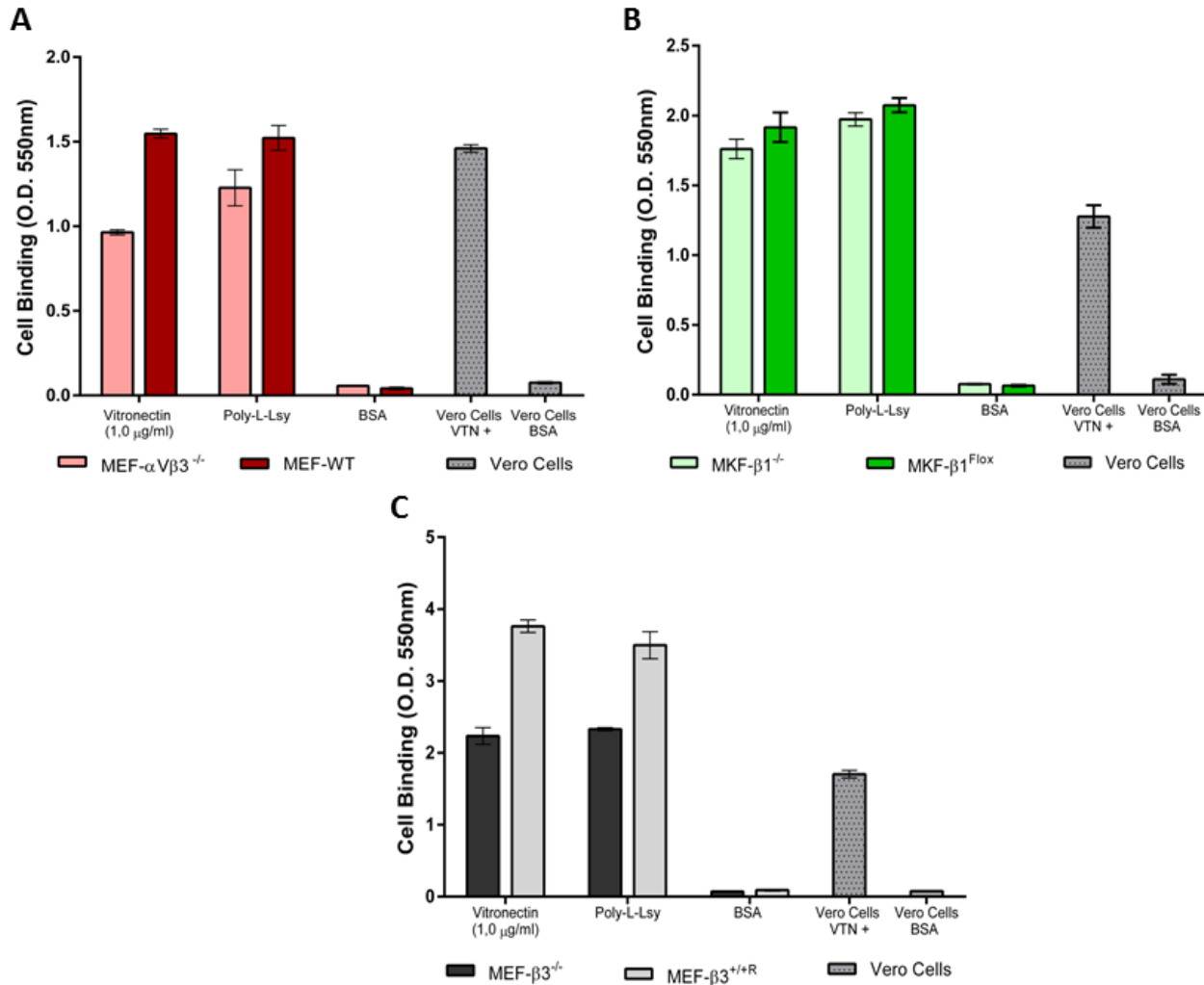
Figure 17: Vitronectin cell adhesion assay with MEF-αVβ3$^{-/-}$ and MEF-WT (A); MKF-β1$^{-/-}$ and MEF-β1^{Flox} (B) and MEF-β3$^{-/-}$ and MEF-β3$^{+/+R}$ cells (C). Plates were coated overnight with 1 µg/ml of mouse vitronectin. Then, plates were blocked with 1% BSA and cells were seeded and incubated at 37°C with 5% carbon dioxide for 30 minutes. Plates were washed carefully, fixed with 3% PFA and cells were stained with 1% crystal violet. Dye was extracted and optical density was measured at 550 nm. Vero cells, Poly-L-Lsy and BSA were used as controls for the assay. The experiment was performed in triplicate. Bars represent the mean values and error bars represent the standard deviation (means ± standard deviation). Abbreviations: MEF-WT: mouse embryonic fibroblasts wild-type; MEF-αVβ3$^{-/-}$: mouse embryonic fibroblasts deficient for αVβ3 integrin; MKF-β1^{Flox}: mouse kidney fibroblasts expressing the β1 integrin subunit (wild-type); MKF-β1$^{-/-}$: mouse kidney fibroblasts deficient for the β1 integrin subunit; MEF-β3$^{+/+R}$: mouse embryonic fibroblasts expressing the β3 integrin subunit (R = rescue); MEF-β3$^{-/-}$: mouse embryonic fibroblasts deficient for the β3 integrin subunit; αV: alpha V integrin subunit; β1: beta 1 integrin subunit; β3: beta 3 integrin subunit; Poly-L-Lsy: Poly-L-Lysine; BSA: bovine serum albumin; VTN: vitronectin; O.D.: optical density.

Next, it was evaluated whether the mouse αV and β3 integrin subunits expressed in CHO-αV$^{+/+}$ and CHO-β3$^{+/+}$ cells are functional and able to recognize their ligands such as vitronectin. For this, CHO cells expressing either the αV or β3 integrin subunits were subjected to the same cell adhesion assay as applied to the integrin deficient MEF and MKF cells.

As shown in **Figure 18**, the binding to mouse vitronectin was higher in CHO-αV$^{+/+}$ and CHO-β3$^{+/+}$ cells in comparison to the CHO-K1 cells. The increase in vitronectin binding was 41.9% and 44.5% for the CHO-αV$^{+/+}$ and CHO-β3$^{+/+}$ cells, respectively. In conclusion, the chimeric integrins formed by the ectopic expression of mouse αV and β3 integrin subunits associated with the corresponding hamster integrin subunits showed to be functional by binding to vitronectin.
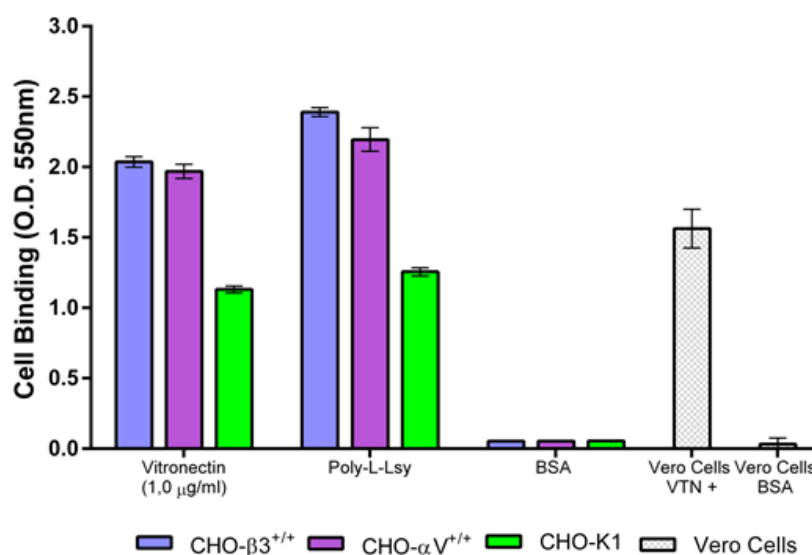
Figure 18: Vitronectin cell adhesion assay with CHO-K1, CHO-αV$^{+/+}$ and CHO-β3$^{+/+}$ cells. Plates were coated overnight with 1 μg/ml of mouse vitronectin. Plates were then blocked with 1% BSA and cells were seeded and incubated at 37°C with 5% carbon dioxide for 30 minutes. Plates were washed carefully, fixed with 3% PFA and cells were stained with 1% crystal violet. Dye was extracted and optical density was measured at 550 nm. Vero cells, Poly-L-Lsy and BSA were used as controls for the assay. The experiment was performed in triplicate. Bars represent the mean values and error bars represent the standard deviation (means ± standard deviation). Abbreviations: CHO-αV$^{+/+}$: Chinese hamster ovary cells expressing the mouse αV integrin subunit; CHO-β3$^{+/+}$: Chinese hamster ovary cells expressing the mouse β3 integrin subunit; αV: alpha V integrin subunit; β3: beta 3 integrin subunit; Poly-L-Lsy: Poly-L-Lysine; BSA: bovine serum albumin; VTN: vitronectin; O.D.: optical density.

4.5) Cell infection assays

In order to investigate whether integrins are involved in the early or late steps of flavivirus infection, experiments were designed to analyze these steps separately. Basically it was the aim of this study to assess: i) susceptibility and permissiveness of integrin deficient cells for different flaviviruses by analyzing the flavivirus replication kinetics; ii) flavivirus binding to integrin deficient cells; iii) virus internalization and iv) virus RNA replication.

4.5.1) Flavivirus replication kinetics in MEFs, MKFs and CHO cells

In order to evaluate if the absence of αV, β1 and β3 integrin subunits affects cell permissiveness and/or influences replication efficiency of different flaviviruses, all integrin deficient MEFs and MKFs as well as the respective wild-type cells were inoculated with YFV-17D, WNV, USUV and LGTV at an MOI of 0.1. Vero cells, known to be highly permissive and susceptible to flaviviruses, were used as control in all assays. Inoculation of CHO-K1 cells with the flaviviruses mentioned above resulted in no detectable virus titers (data not shown).

As shown in **Figure 19 A – D**, all four cell lines were permissive for the four flaviviruses investigated. However, the replication kinetics of different flaviviruses differed distinctly among the cell lines. Flavivirus-inoculated Vero cells, the most permissive cell line for flaviviruses, displayed the highest titers for all flaviviruses tested 96 hours post inoculation (**Figures 19 A – D**). Surprisingly, YFV-17D replication in MEF-β3$^{-/-}$ cells reached similar titers as in Vero cells (6.0 vs. 6.25 log TCID$_{50}$/ml; **Figure 19 A**). In addition, YFV-17D showed to replicate more efficiently in MEF-WT than in Vero cells within the first 72 hours (**Figures 19 A**). Among the MEFs, MEF-WT cells produced the highest titers for all flaviviruses tested in this study. In these cells, the highest titers were observed for USUV reaching a maximum of up to 9 log TCID$_{50}$/ml after 96 hours (**Figure 19 C**) and LGTV (7 log TCID$_{50}$/ml, **Figure 19 D**) followed by YFV-17D (6.50 TCID$_{50}$/ml **Figure 19 A)** and WNV (4.5 TCID$_{50}$/ml **Figure 19 B**).

In contrast to that, MEF-αVβ3$^{-/-}$ cells displayed low viral titers for all flaviviruses tested (**Figure 19 A – D**). After 96 hours, titers reached 3.0 log TCID$_{50}$/ml for YFV-17D, 3.75 log TCID$_{50}$/ml for WNV, 5.0 log TCID$_{50}$/ml for USUV and 3.25 log TCID$_{50}$/ml for LGTV. In MEF-β3$^{-/-}$ cells, LGTV and USUV titers were even lower reaching only a maximum of 3.75 and 4.75 log TCID$_{50}$/ml at 96 hours post inoculation, respectively (**Figure 19 C and D**). As mentioned above, YFV-17D showed to moderately replicate in MEF-β3$^{-/-}$ cells in comparison to the MEF-WT cells (**Figure 19 A**). Finally, LGTV showed to replicate more efficiently in MKF-β1$^{-/-}$ cells than the other flaviviruses tested, reaching titers comparable to MEF-WT cells after 96 hours post-infection (MKF-β1$^{-/-}$ 6.75 log TCID$_{50}$/ml vs. MEF-WT 7.0 log TCID$_{50}$/ml; **Figure 19 D**). In sum, the

deletion of one or two integrin subunits was not able to abrogate flavivirus infection, but substantially impaired replication of some flaviviruses.
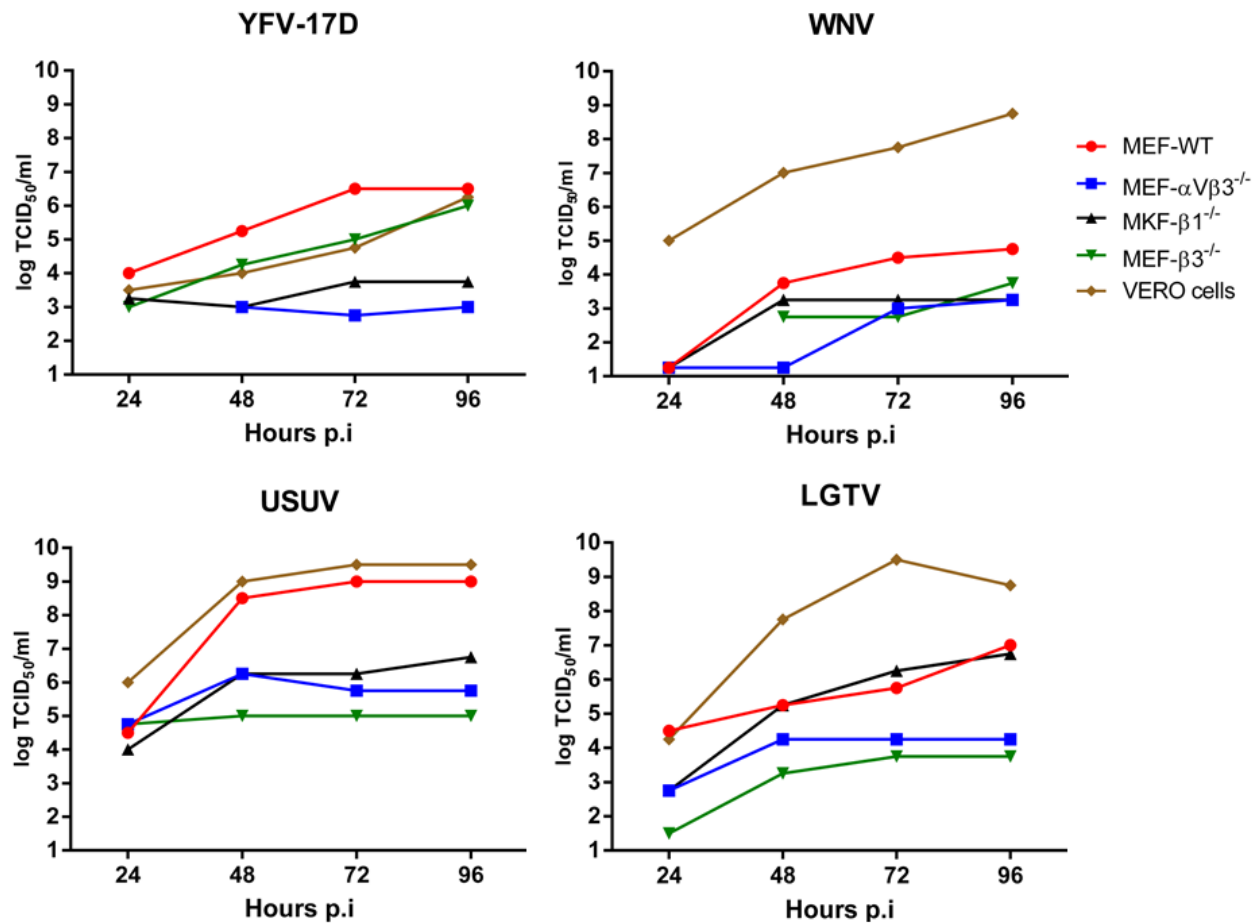
Figure 19: Replication kinetics of YFV-17D, WNV, USUV and LGTV in MEF-WT (red), MEF-αVβ3$^{-/-}$ (blue), MKF-β1$^{-/-}$ (black), MEF-β3$^{-/-}$ (green) and Vero (brown) cells. Cells were seeded into 24-well plates and infected with MOI of 0.1. Supernatants were harvested every 24 hours over a period of 4 days post inoculation. Virus titers were measured by TCID$_{50}$ in Vero cells. Virus titers were expressed as log of TCID$_{50}$ per ml of supernatant. Three independen experiments were performed. Abbreviations: MEF-WT: mouse embryonic fibroblasts wild-type; MEF-αVβ3$^{-/-}$: mouse embryonic fibroblasts deficient for αVβ3 integrin; MKF-β1$^{-/-}$: mouse kidney fibroblasts deficient for the β1 integrin subunit; MEF-β3$^{-/-}$: mouse embryonic fibroblasts deficient for the β3 integrin subunit; αV: alpha V integrin subunit; β1: beta 1 integrin subunit; β3: beta 3 integrin subunit; YFV-17D: Yellow fever virus strain 17D; WNV: West Nile virus; USUV: Usutu virus and LGTV: Langat virus; p.i.:post-inoculation; TCID$_{50}$: tissue culture infectious dose 50%.

4.5.2) Influence of integrins on flavivirus binding

Several viruses such as FMDV, echovirus and hantaviruses bind to integrins mediating virus internalization into the host cell (Hussein *et al.*, 2015). To investigate whether integrins are involved in flavivirus binding to MEFs and MKFs, a virus binding assay was performed.

First, flavivirus binding to the Vero cells was evaluated by RT-qPCR. As expected, all flaviviruses bound to Vero cells but to a different extent (**Figure 20**). Among all the viruses tested, USUV bound to Vero cells to the highest amount displaying mean Ct values of 17.1 followed by WNV (mean Ct value of 21) and YFV-17D with a mean Ct value of 25.5 (**Figure 20**). Unexpectedly, LGTV, a cell culture adapted TBEV strain bound to Vero cells less efficiently (mean Ct value of 29.9, **Figure 20**).
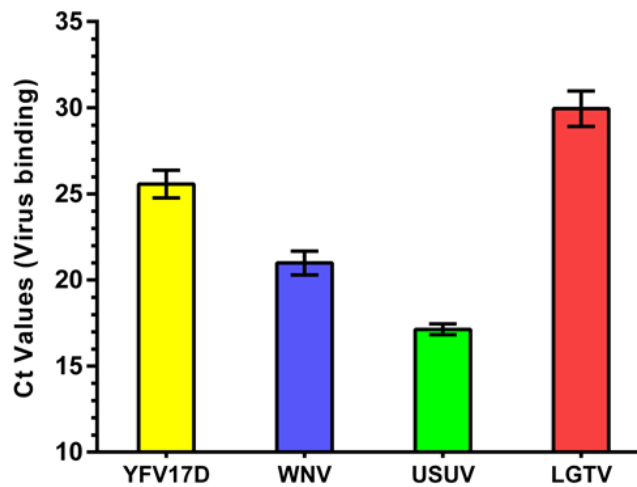
Figure 20: Flavivirus binding to Vero cells measured by RT-qPCR. Cells were seeded into 12-well plates, placed on ice and inoculated with different flaviviruses at an MOI of 10. After one hour, monolayers were washed, harvested and lysed with RLT buffer. Total RNA was isolated and RT-qPCR was performed to indirectly measure virus binding to the cell surface by detection of viral RNA. Virus binding values are expressed in cycle threshold values (Ct values). Bars represent the mean of Ct values and error bars represent the standard deviation (means ± standard deviation). Abbreviations: YFV-17D: Yellow fever virus strain 17D; WNV: West Nile virus; USUV: Usutu virus; LGTV: Langat virus; Ct: cycle threshold.

4.5.2.1) Influence of integrins on flavivirus binding to MEF and MKF cells

Next, it was evaluated if the deficiency of one or two integrin subunits could affect flavivirus binding to MEFs and MKFs. As shown in **Figure 21 A-C**, the deletion of αVβ3 integrin, β1 or β3 integrin subunits did not affect the flavivirus binding to integrin deficient MEFs and MKFs in comparison to the respective wild-type cells. Statistical analysis did not infer any statistical significance ($p > 0.05$) in all groups tested with different flaviviruses (**Figure 21 A-C**). Taken together, these results indicate that αVβ3 integrin, β1 or β3 integrin subunits are not involved in flavivirus binding to the MEF and MKF cells.
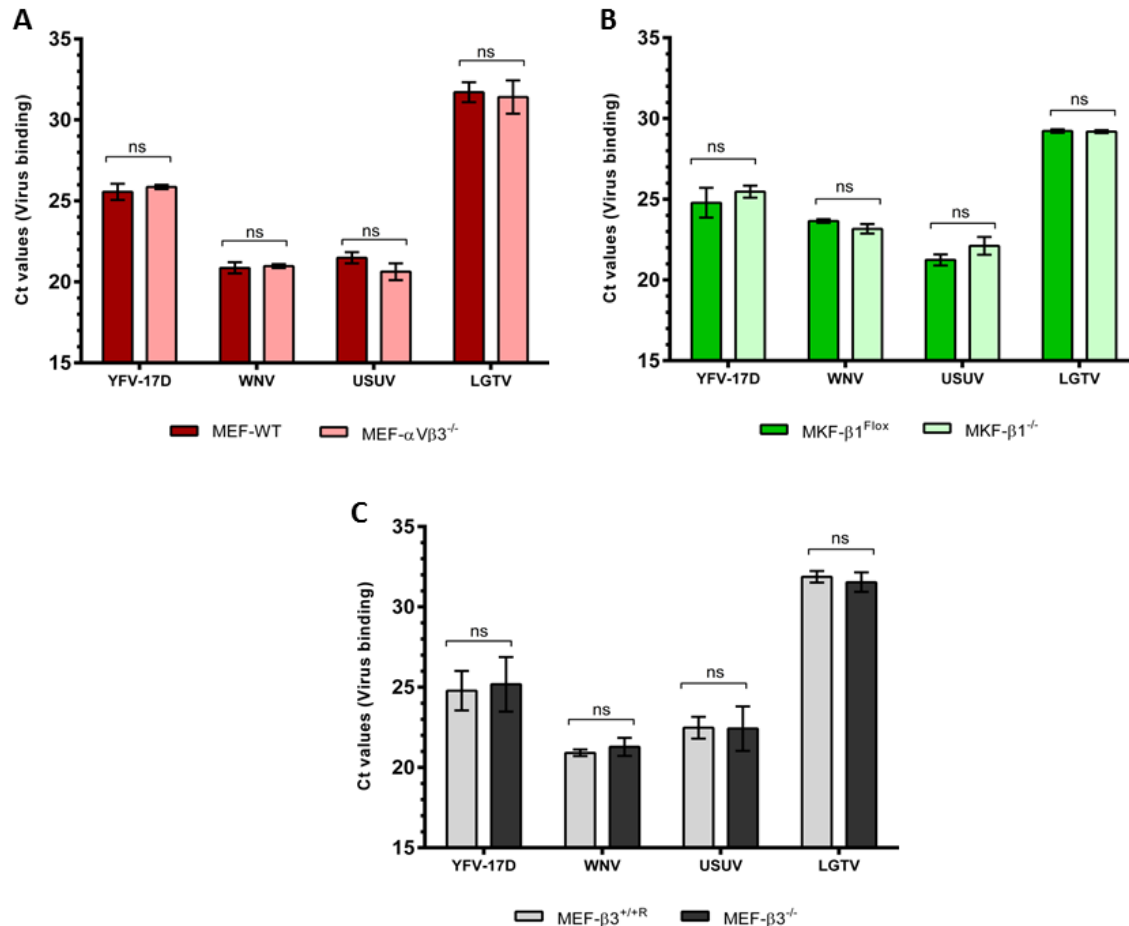
Figure 21: Flavivirus binding to MEF-WT and MEF-αVβ3$^{-/-}$ (A); MKF-β1^{Flox} and MKF-β1$^{-/-}$(B) and MEF-β3$^{+/+R}$ and MEF-β3$^{-/-}$ (C) cells. Cells were seeded into 12-well plates, placed on ice and inoculated with different flaviviruses at an MOI of 10. After one hour, monolayers were washed, harvested and lysed with RLT buffer. Total RNA was isolated and RT-qPCR was performed to indirectly measure virus binding to the cell surface by detection of viral RNA. Virus binding values are expressed in cycle threshold values (Ct values). Three independent experiments were each performed in triplicate (n=3). Bars represent the mean Ct values and error bars represent the standard deviation (means ± standard deviation). Statistical analysis: Mann-Whitney test; ns: not significant (p> 0.05). Abbreviations: MEF-WT: mouse embryonic fibroblasts wild-type; MEF-αVβ3$^{-/-}$: mouse embryonic fibroblasts deficient for αVβ3 integrin; MKF-β1^{Flox}: mouse kidney fibroblasts expressing the β1 integrin subunit (wild-type); MKF-β1$^{-/-}$: mouse kidney fibroblasts deficient for the β1 integrin subunit; MEF-β3$^{+/+R}$: mouse embryonic fibroblasts expressing the β3 integrin subunit (R = rescue); MEF-β3$^{-/-}$: mouse embryonic fibroblasts deficient for the β3 integrin subunit; αV: alpha V integrin subunit; β1: beta 1 integrin subunit; β3: beta 3 integrin subunit; YFV-17D: Yellow fever virus strain 17D; WNV: West Nile virus; USUV: Usutu virus; LGTV: Langat virus; Ct: cycle threshold.

4.5.2.2) Influence of integrins on flavivirus binding to CHO cells

To further investigate the influence of integrins on flavivirus infection, CHO cells expressing the mouse αV or mouse β3 integrin subunits, CHO-αV$^{+/+}$ and CHO-β3$^{+/+}$, and the respective wild-type cells, CHO-K1, were used. It was investigated whether the ectopic expression of mouse αV and β3 integrin subunits in CHO-αV$^{+/+}$ and CHO-β3$^{+/+}$ cells influences flavivirus binding to the cell surface.

As demonstrated in **Figure 22**, expression of both αV and β3 integrin subunits had no impact on flavivirus binding to CHO cells. The statistical analysis also failed to show any significant differences between CHO-K1 and CHO cells expressing either the αV or the β3 integrin subunit ($p > 0.05$).

Together, the expression of mouse αV and mouse β3 integrin subunits in CHO cells *per se* did not influence flavivirus binding to CHO cells.
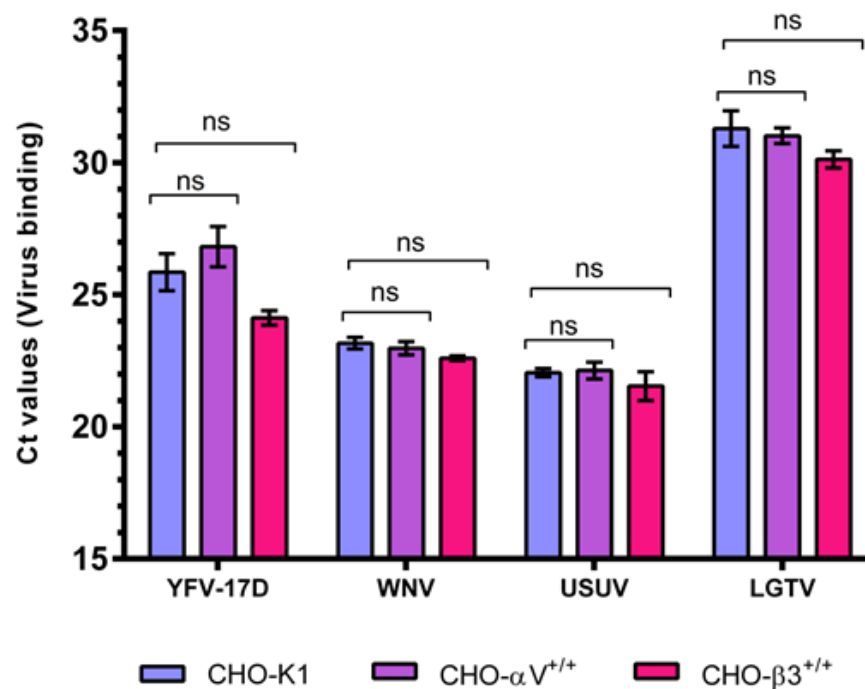
Figure 22. Flavivirus binding to CHO-K1, CHO-αV$^{+/+}$ and CHO-β3$^{+/+}$ cells. Cells were seeded into 12-well plates, placed on ice and inoculated with an MOI of 10. After one hour, monolayers were extensively washed, harvested and lysed with RLT buffer. Total RNA was isolated and RT-qPCR was performed to indirectly measure virus binding to the cell surface by detection of viral RNA. Virus binding values are expressed in cycle threshold (Ct) values. Three independent experiments were performed in triplicate (n=3). Bars represent the mean Ct values and error bars represent the standard deviation (means ± standard deviation). Statistical analysis: Mann-Whitney test; ns: not significant ($p > 0.05$). Abbreviations: YFV-17D: Yellow fever virus strain 17D; WNV: West Nile virus; USUV: Usutu virus; LGTV: Langat virus; CHO-K1: Chinese hamster ovary cells clone K1; CHO-αV$^{+/+}$: Chinese hamster ovary cells expressing the mouse alpha V integrin subunit; CHO-β3$^{+/+}$: Chinese hamster ovary cells expressing the mouse beta 3 integrin subunit.

4.5.3) Effect of integrin ligands on flavivirus binding to MEF and MKF cells

For a functional blocking assay, MEF-αVβ3$^{-/-}$ and the respective MEF-WT cells were selected for treatment with different integrin ligands. For this assay, three integrin ligands were selected: i) the synthetic RGD peptide that represents the minimum residual sequence that integrins recognize; ii) the vitronectin that binds with high affinity to RGD binding integrins such as α5β5 and α8β1 and iii) the type I collagen that binds to collagen binding integrins such as α1β1, α2β1 and α10β1 integrins (Humphries *et al.*, 2006). A pilot experiment was performed in Vero cells to evaluate whether the experimental conditions allowed efficient integrin ligand binding. Cells were first treated on ice with 50 μg of a recombinant his-tagged vitronectin that was subsequently detected on the cell surface using monoclonal anti-his-tag antibodies. As observed in **Figure 23**, recombinant mouse vitronectin was detected on the cell surface of Vero cells in high amounts.
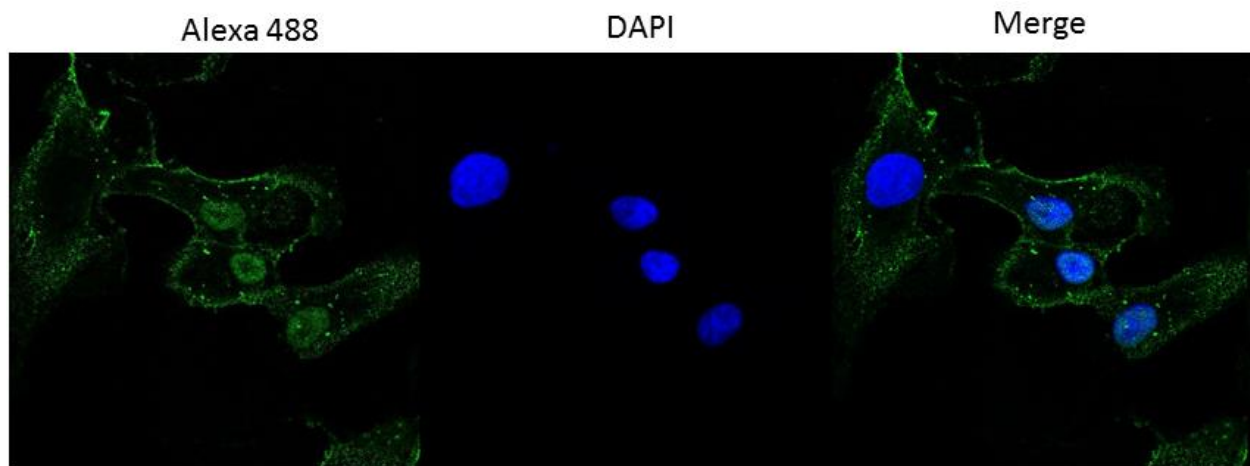
Figure 23: Detection of recombinant his-tagged mouse vitronectin on the cell surface of Vero cells. Vero cells were treated with recombinant mouse vitronectin (50 μg/ml) for 30 minutes, and then washed and fixed with PFA for 15 minutes. Then, monoclonal antibodies raised against the his-tag motif were used followed by an anti-mouse Alexa 488 secondary antibody (green). Nuclei were stained using DAPI (blue). Images were visualized by laser scanning confocal microscopy and edited using ImageJ software.

The established protocol was then applied to MEF-WT and MEF-αVβ3$^{-/-}$ cells that, after treatment with the integrin ligands mentioned above, were inoculated with different flaviviruses. As demonstrated in **Figure 24** (panel A, B and C) none of the integrin ligands were able to disrupt flavivirus binding to the cell surface of MEF-WT or MEF-αVβ3$^{-/-}$ cells as determined by RT-qPCR. Treatment with recombinant mouse vitronectin had almost no impact on flavivirus binding (**Figure 24, panel A**). The maximum inhibitory effect of recombinant mouse vitronectin on virus binding observed for MEF-WT and MEF-αVβ3$^{-/-}$ cells was 6.3% for the YFV-17D, 7.6% for the WNV, 4.8% for the USUV and 4.9% for the LGTV compared to the untreated controls (**Figure 24, panel A**). The treatment of MEF-WT and MEF-αVβ3$^{-/-}$ cells with a synthetic cyclic RGD peptide equally resulting in no substantial binding inhibition of the investigated flaviviruses (**Figure 24, panel B**). Pre-treatment of the cells with type I collagen did not affect flavivirus binding in both, MEF-WT and MEF-αVβ3$^{-/-}$ cells (**Figure 24, panel C**). The maximum binding inhibition achieved was 5.1% for YFV-17D, 7.8 % for WNV, 4.5% for USUV and 3.4% for LGTV when compared to the untreated control. Taken together, the results of these assays including the binding assay reinforce that integrins are not involved in flavivirus binding to the MEF and MKF cells.
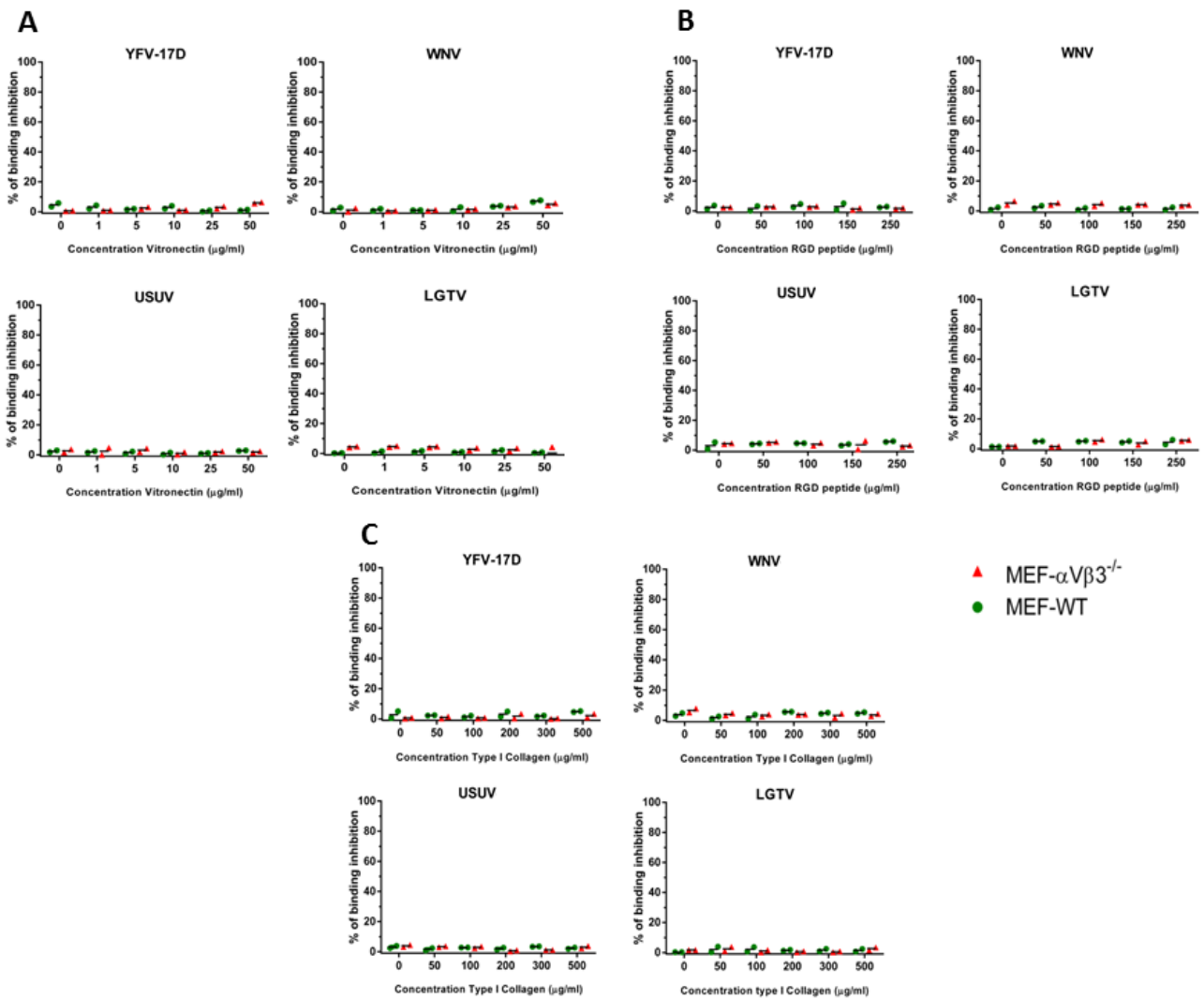
Figure 24: Binding inhibition assay with MEF-WT and MEF-αVβ3$^{-/-}$ cells. Cells were first treated with increasing concentrations of recombinant mouse vitronectin (0-50 µg/ml) (panel A); synthetic cyclic RGD peptide (0-250 µg/ml) (panel B) and type I collagen (0-500 µg/ml) (panel C) for 30 minutes prior to virus inoculation. Then, treated cells were shifted to 4°C and inoculated with different flaviviruses at an MOI of 10 for 1 hour. Monolayers were extensively washed and resuspended in RLT buffer. The total RNA was isolated and RT-qPCR was performed. Percentage of binding inhibition was calculated based on cycle threshold values. Two independent experiments were performed in duplicate. Dots represent the mean of individual values from each independent experiment. Dashes represent the median. Abbreviations: MEF-WT: mouse embryonic fibroblasts wild-type; MEF-αVβ3$^{-/-}$: mouse embryonic fibroblasts deficient for αVβ3 integrin; αV: alpha V integrin subunit; β3: beta 3 integrin subunit; YFV-17D: Yellow fever virus strain 17D; WNV: West Nile virus; USUV: Usutu virus; LGTV: Langat virus; RGD: Arginine-Glycine-Aspartic acid.

4.5.4) Effect of integrins on flavivirus internalization by MEF and MKF cells

In order to investigate whether the lack of integrin expression influences flavivirus internalization, the integrin deficient MEF and MKF cells as well as their respective wild-type cells were inoculated with different flaviviruses. As shown in **Figures 25, 26 and 27 A – D**, the absence of integrin expression did not abrogate flavivirus internalization by MEF and MKF cells.

Internalization of YFV-17D and LGTV was not affected by the loss of αVβ3 integrin expression in MEF-αVβ3$^{-/-}$ cells when compared to MEF-WT cells (**Figures 25 A and D**). Statistical analysis using the Student's *t*-test revealed no significant differences ($p > 0.05$) between the two cell lines with 4.3% and 6.3% of differences in internalization for YFV-17D and LGTV, respectively. On the other hand, statistical analysis using the unpaired Student's *t*-test revealed a significant difference between MEF-WT and MEF-αVβ3$^{-/-}$ cells concerning the internalization of WNV ($p = 0.0007$) and USUV ($p = 0.0001$) (**Figure 25 B and C**). Data analysis demonstrated the differences in internalization of USUV and WNV to be rather low between the two cell lines. The differences in virus internalization between MEF-WT and MEF-αVβ3$^{-/-}$ cells for WNV and USUV were 3.6% and 7.6%, respectively. These results indicate that αVβ3 integrin might be involved in the internalization of some flaviviruses.

Our findings for MKF-β1^{Flox} and MKF-β1$^{-/-}$ cells demonstrated that deletion of β1 integrin subunit did not influence flavivirus internalization (**Figure 26 A-D**). The differences in virus internalization were 2.25% for YFV-17D, 0.59% for WNV, 1.16% for USUV and 7.16% for LGTV resulting in no statistical significance for all the viruses tested ($p > 0.05$) suggesting that β1 integrin subunit is not involved in flavivirus internalization. Internalization of YFV-17D ($p = 0.2254$), WNV ($p = 0.9880$) and USUV ($p = 0.0779$) by MEF-β3$^{-/-}$ and MEF-β3$^{+/+R}$ cells was not affected by the deletion of the β3 integrin subunit (**Figure 27 A-D**). Statistical analysis showed only a small but significant difference in internalization of LGTV ($p = 0.0318$) between the two cell lines with a difference in virus internalization of 11.34%. The difference in virus internalization was extremely low for YFV-17D ($p=0.2254$) and USUV with 1.71% and 2.21%, respectively. These findings suggest that the β3 integrin subunit might be involved in the internalization of LGTV.

Collectively, these results implicate that αVβ3 integrin and the β3 integrin subunit might have an effect on the internalization of some flaviviruses in MEF cells.
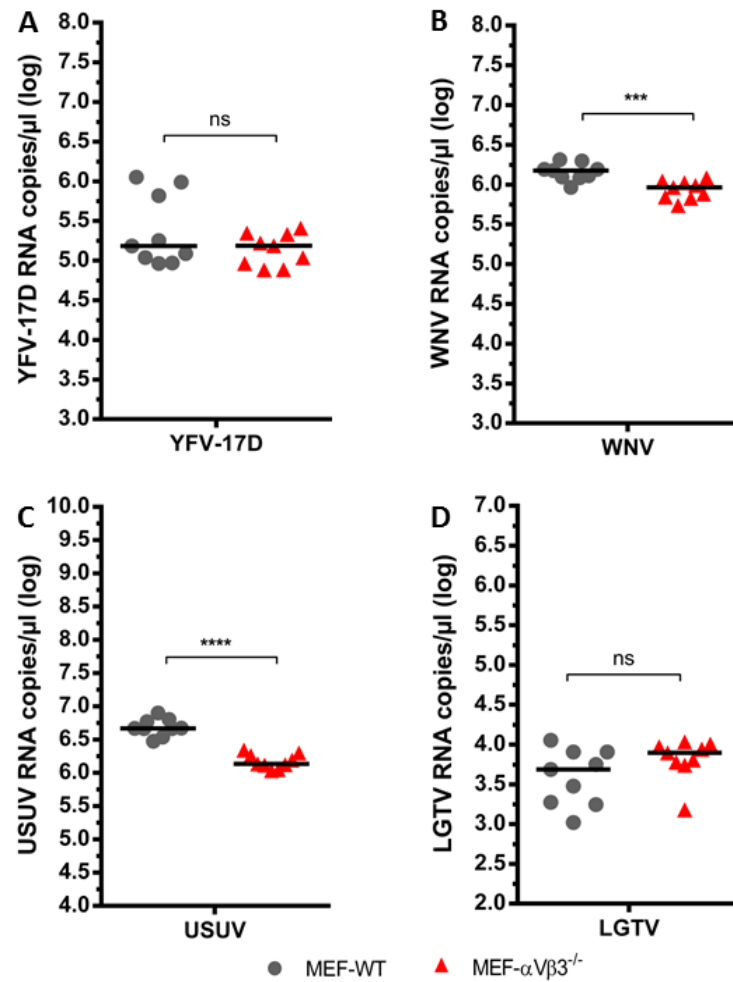
Figure 25: Internalization of YFV-17D (A), WNV (B), USUV (C) and LGTV (D) by MEF-WT and MEF-αVβ3$^{-/-}$ cells. Cells were seeded into 12-well plates, placed on ice and inoculated with different flaviviruses at an MOI of 10. After one hour, monolayers were extensively washed and shifted to 37°C for 30 minutes. Cell monolayers were then washed once with acidic glycine (pH 2.5) and incubated for 2 minutes, washed twice with 1X PBS and monolayers harvested and lysed with RLT buffer. Total RNA was isolated and RT-qPCR was performed to measure internalized virus particles by detection of viral RNA. The amount of internalized virus is expressed as copy numbers per microliter (log transformed). Three independent experiments were performed in triplicate (n=3). Dot plots represent each individual replicate from the three independent experiments. Statistical analysis: Unpaired Student's *t*-test with Welch's correction; (***) $p \leq 0.001$; (****) $p \leq 0.0001$; ns: not significant ($p > 0.05$). Abbreviations: MEF-WT: mouse embryonic fibroblasts wild-type; MEF-αVβ3$^{-/-}$: mouse embryonic fibroblasts deficient for αVβ3 integrin; αV: alpha V integrin subunit; β3: beta 3 integrin subunit; YFV-17D: Yellow fever virus strain 17D; WNV: West Nile virus; USUV: Usutu virus; LGTV: Langat virus.

Figure 26: Internalization of YFV-17D (A), WNV (B), USUV (C) and LGTV (D) by MKF-β1^{Flox} and MKF-β1$^{-/-}$ cells. Cells were seeded into 12-well plates, placed on ice and inoculated with different flaviviruses at an MOI of 10. After one hour, monolayers were extensively washed and shifted to 37°C for 30 minutes. Cell monolayers were then washed once with acidic glycine (pH 2.5) and incubated for 2 minutes, washed twice with 1X PBS and monolayers harvested and lysed with RLT buffer. Total RNA was isolated and RT-qPCR was performed to measure internalized virus particles by detection of viral RNA. The amount of internalized virus is expressed as copy numbers per microliter (log transformed). Three independent experiments were performed in triplicate (n=3). Dot plots represent each individual replicate from the three independent experiments. Statistical analysis: Unpaired Student's *t*-test with Welch's correction; ns: not significant ($p > 0.05$). Abbreviations: MKF-β1^{Flox}: mouse kidney fibroblasts expressing the β1 integrin subunit (wild-type); MKF-β1$^{-/-}$: mouse kidney fibroblasts deficient for the β1 integrin subunit; MEF-β3$^{+/+R}$: mouse embryonic fibroblasts expressing the β3 integrin subunit (R = rescue); MEF-β3$^{-/-}$: mouse embryonic fibroblasts deficient for the β3 integrin subunit; αV: alpha V integrin subunit; β1: beta 1 integrin subunit; β3: beta 3 integrin subunit; YFV-17D: Yellow fever virus strain 17D; WNV: West Nile virus; USUV: Usutu virus; LGTV: Langat virus.
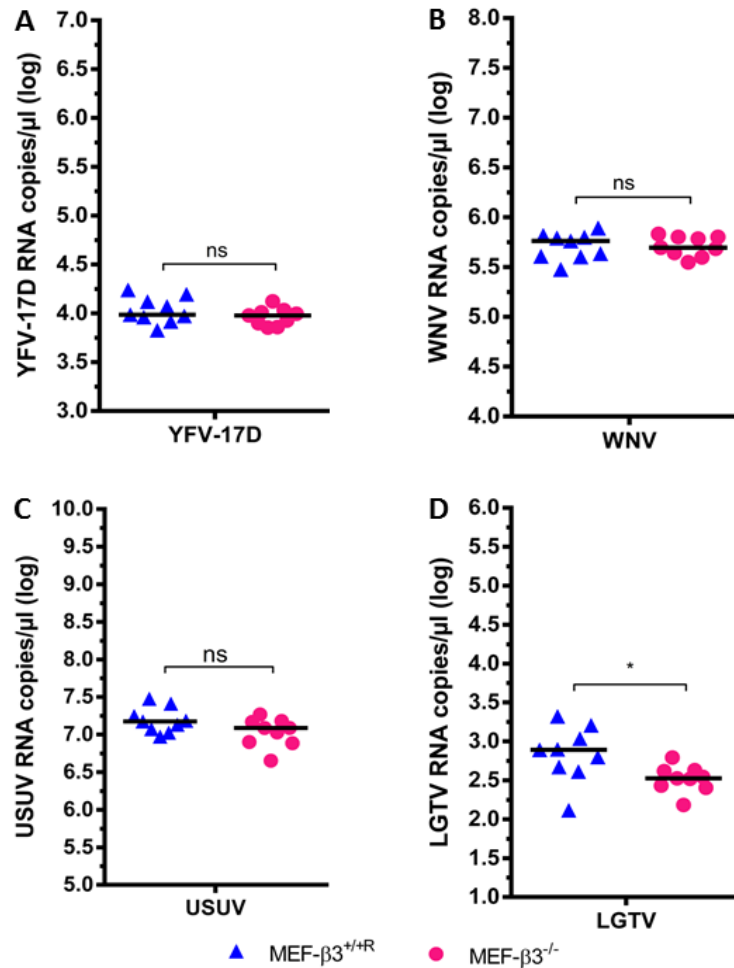
Figure 27: Internalization of YFV-17D (A), WNV (B), USUV (C) and LGTV (D) by MEF-β3[+/+R] and MEF-β3^{-/-} cells. Cells were seeded into 12-well plates, placed on ice and inoculated with different flaviviruses at an MOI of 10. After one hour, monolayers were extensively washed and shifted to 37°C for 30 minutes. Cell monolayers were then washed once with acidic glycine (pH 2.5) and incubated for 2 minutes, washed twice with 1X PBS and monolayers harvested and lysed with RLT buffer. Total RNA was isolated and RT-qPCR was performed to measure internalized virus particles by detection of viral RNA. The amount of internalized virus is expressed as copy numbers per microliter (log transformed). Three independent experiments were performed in triplicate (n=3). Dot plots represent each individual replicate from the three independent experiments. Statistical analysis: Unpaired Student's *t*-test with Welch's correction; (*) $p \leq 0.05$; ns: not significant ($p > 0.05$). Abbreviations: MEF-β3[+/+R]: mouse embryonic fibroblasts expressing the β3 integrin subunit (R = rescue); MEF-β3^{-/-}: mouse embryonic fibroblasts deficient for the β3 integrin subunit; β3: beta 3 integrin subunit; YFV-17D: Yellow fever virus strain 17D; WNV: West Nile virus; USUV: Usutu virus; LGTV: Langat virus.

4.5.5) Influence of integrins on flavivirus replication in MEFs, MKFs and CHO cells

So far, this study has shown that integrins are not involved in binding of flaviviruses to MEFs, MKFs and CHO cells. On the other hand, internalization of some flaviviruses was slightly affected by the loss of integrins. Next, it was evaluated whether the deletion of one or two integrin subunits affects flavivirus replication in MEF, MKF and CHO cells by RT-qPCR and virus titration.

4.5.5.1) Effect of β1 integrin subunit deletion on flavivirus replication

As seen in **Figure 28 A and B**, the deletion of β1 integrin subunit in MKF-β1$^{-/-}$ cells affected the replication of YFV-17D and WNV reducing viral loads by 65.1% and 45.5%, respectively, as determined by quantification of viral genome. On the other hand, replication of USUV was not affected by the deletion of β1 integrin subunit (**Figure 28 C**). Statistical analysis using the parametrical Student's *t*-test showed a statistically significant reduction in the viral loads of YFV-17 (p = 0.0003), WNV (p = 0.0001) but not for USUV (p = 0.4086) in MKF-β1$^{-/-}$ cells (**Figure 28 A – C**). Virus titers measured by TCID$_{50}$ were also decreased in MKF-β1$^{-/-}$ cells infected with YFV-17D (MKF-β1$^{-/-}$ vs MKF-β1^{flox}: 4.55 vs 4.13 log TCID$_{50}$/ml) and WNV (MKF-β1$^{-/-}$ vs MKF-β1^{flox}: 5.58 vs 5.33 log TCID$_{50}$/ml) **(Figure 28 A and B).** USUV titers were slightly increased in MKF-β1^{flox} cells in comparison to MKF-β1$^{-/-}$ cells (MKF-β1$^{-/-}$ vs MKF-β1^{flox}: 7.25 vs 6.33 log TCID$_{50}$/ml) **(Figure 28 C)**. Unexpectedly, the LGTV replication in MKF-β1$^{-/-}$ cells was increased up to 335% resulting in a higher viral load compared to wild-type MKF-β1^{Flox} cells (**Figure 28 D**). This increase of viral load observed in MKF-β1$^{-/-}$ cells showed to be statistically significant (p = 0.0001). LGTV titers were also substantially higher in MKF-β1$^{-/-}$ than in MKF-β1^{Flox} cells (MKF-β1$^{-/-}$ vs MKF-β1^{flox}: 5.91 vs 6.83 log TCID$_{50}$/ml).

Taken together, these results suggest that the deletion of β1 integrin subunit might impair the replication of YFV-17D and WNV and, in case of LGTV, potentially enhance the replication.
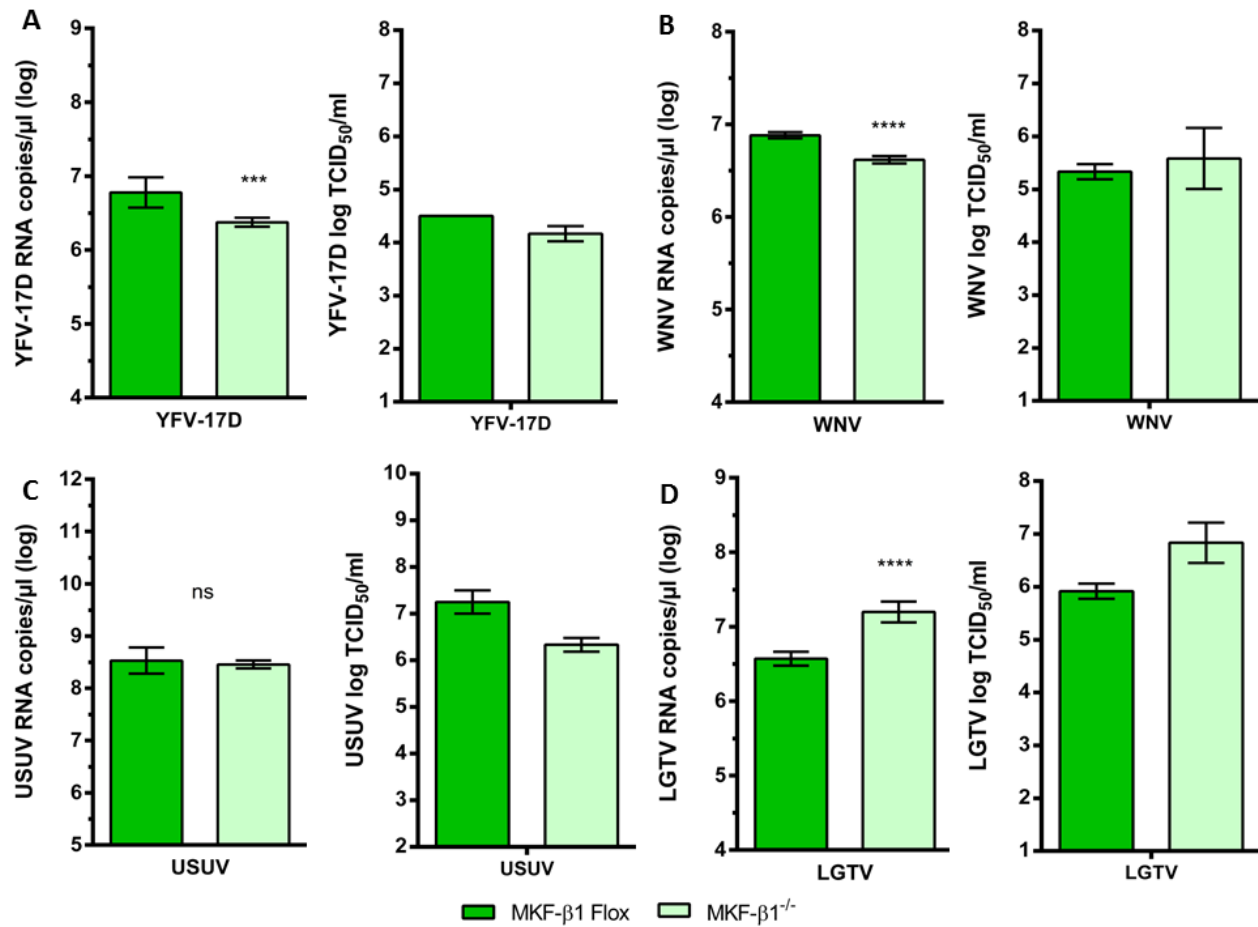
Figure 28: Replication analysis of YFV-17D (A), WNV (B), USUV (C) and LGTV (D) in integrin deficient MKF-β1$^{-/-}$ and corresponding wild-type MKF-β1^{Flox} cells. RNA yields and virus titers were measured 48 hours post inoculation. Cells were seeded into 12-well plates and inoculated with different flaviviruses at an MOI of 10. After one hour, monolayers were extensively washed and shifted to 37°C for 48 hours. Supernatants were harvested, total RNA was isolated and RT-qPCR was performed to determine the yield of viral RNA. The amount of virus genome is expressed as copy numbers per microliter (log transformed). Virus titers were determined by TCID$_{50}$. End-point determinations of virus titers were calculated using the Spearman-Kaerber method. Titers are expressed in log values. Three independent experiments were performed in triplicate (n=3). Bars represent mean values and error bars represent the standard deviation (mean ± standard deviation). Statistical analysis: Unpaired Student's *t*-test with Welch's correction; (***) $p \leq 0.001$; (****) $p \leq 0.0001$; ns: not significant ($p > 0.05$). Abbreviations: YFV-17D: Yellow fever virus strain 17D; WNV: West Nile virus; USUV: Usutu virus; LGTV: Langat virus; MKF-β1^{Flox}: mouse kidney fibroblasts expressing the beta 1 integrin subunit; MKF-β1$^{-/-}$: mouse kidney fibroblasts deficient for the beta 1 integrin subunit.

4.5.5.2) Effect of β3 integrin subunit deletion on flavivirus replication in MEFs

Similar results were also found for MEF-β3$^{+/+R}$ and MEF-β3$^{-/-}$ cells (**Figure 29 A – D**). Quantification of viral RNA revealed decrease in flavivirus replication for WNV, USUV and LGTV in MEF-β3$^{-/-}$ cells in comparison to MEF-β3$^{+/+R}$ cells (**Figure 29 B, C and D**). The reduction of viral RNA yields for WNV, USUV and LGTV were 28.2%, 63.5% and 43.9%, respectively (**Figure 29 B, C and D**). Statistical analysis indicated that these differences are significant (WNV p = 0.0001; USUV p = 0.0001 and LGTV p = 0.0001). Viral titers measured by TCID$_{50}$ also showed a decrease for WNV (MEF-β3$^{+/+R}$ vs MEF-β3$^{-/-}$: 5.16 vs 4.25 log TCID$_{50}$/ml), USUV (MEF-β3$^{+/+R}$ vs MEF-β3$^{-/-}$: 6.33 vs 5.08 log TCID$_{50}$/ml) and LGTV (MEF-β3$^{+/+R}$ vs MEF-β3$^{-/-}$: 6.25 vs 6.33 log TCID$_{50}$/ml) (**Figure 29 B, C and D**).

On the other hand, viral load of YFV-17D showed to be lower in MEF-β3$^{+/+R}$ cells than in the integrin deficient MEF-β3$^{-/-}$ cells (**Figure 29 A**). The increase of YFV-17D replication in MEF-β3$^{-/-}$ cells was 116% compared to MEF-β3$^{+/+R}$ cells. Statistical analysis also demonstrated that the differences observed in YFV-17D replication in the two cell lines were significant (p = 0.0001). YFV-17D titers were also higher in MEF-β3$^{-/-}$ in comparison to MEF-β3$^{+/+R}$ cells (MEF-β3$^{+/+R}$ vs MEF-β3$^{-/-}$: 4.66 vs 4.83 log TCID$_{50}$/ml) (**Figure 29 A**). Together, these results indicate that the deletion of β3 integrin subunit might impair replication of USUV, LGTV and WNV.
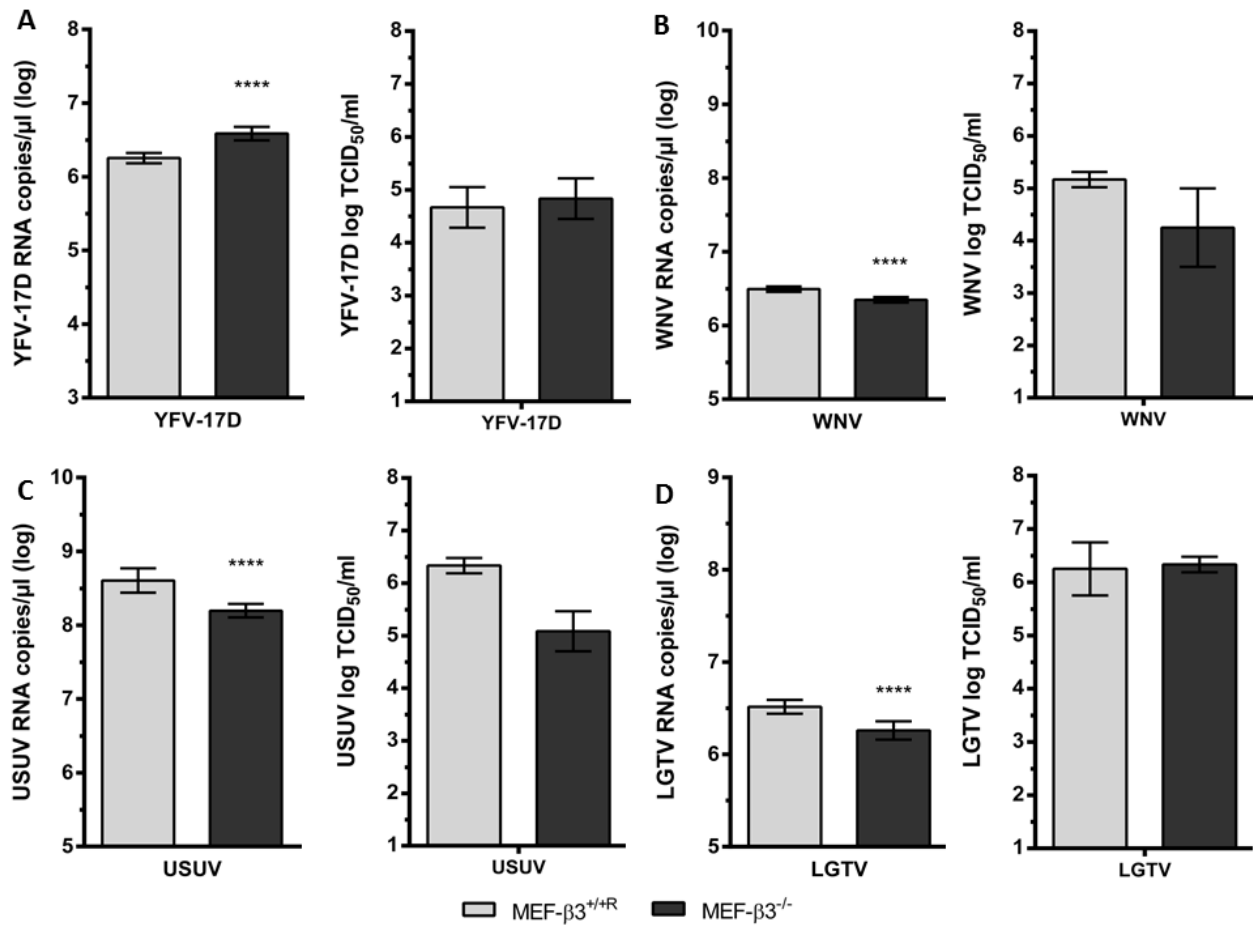
Figure 29: Replication analysis of YFV-17D (A), WNV (B), USUV (C) and LGTV (D) in integrin deficient MEF-β3$^{-/-}$ and corresponding wild-type MEF-β3$^{+/+R}$ cells. RNA yields and virus titers were measured 48 hours post inoculation. Cells were seeded into 12-well plates and inoculated with different flaviviruses at an MOI of 10. After one hour, monolayers were extensively washed and shifted to 37°C for 48 hours. Supernatants were harvested, total RNA was isolated and RT-qPCR was performed to determine the yield of viral RNA. The amount of virus genome is expressed as copy numbers per microliter (log transformed). Virus titers were determined by TCID$_{50}$. End-point determinations of virus titers were calculated using the Spearman-Kaerber method. Titers were expressed in log values. Three independent experiments were performed in triplicate (n=3). Bars represent mean values and error bars represent the standard deviation (mean ± standard deviation). Statistical analysis: Unpaired Student's t-test with Welch's correction; (****) $p \leq 0.0001$; ns: not significant ($p > 0.05$). Abbreviations: YFV-17D: Yellow fever virus strain 17D; WNV: West Nile virus; USUV: Usutu virus; LGTV: Langat virus; MEF-β3$^{+/+R}$: mouse embryonic fibroblasts expressing the beta 3 integrin subunit (R = rescue); MEF-β3$^{-/-}$: mouse embryonic fibroblasts deficient for the beta 3 integrin subunit.

4.5.5.3) Effect of αVβ3 integrin deletion on flavivirus replication in MEFs

As demonstrated in **Figure 30 A – D**, flavivirus replication in MEF-αVβ3$^{-/-}$ cells was strongly impaired by the lack of αVβ3 integrin expression when compared to MEF-WT cells (**Figure 30 A – D**). The reduction of viral RNA yields was 99.2% for YFV-17D, 99.9% for WNV, 99.5% for USUV and 99.0% for LGTV (**Figure 30 A - D**). The statistical analysis (Student's *t*-test) evidenced that the differences observed in flavivirus replication between MEF-WT and MEF-αVβ3$^{-/-}$ cells were highly significant (p = 0.0001) for all the viruses analyzed. Virus titers were also strongly reduced in MEF-αVβ3$^{-/-}$ cells in comparison to MEF-WT cells (**Figure 30 A -**

D). The viral titers were 5.24-fold decreased for YFV-17D (MEF-WT vs MEF-αVβ3$^{-/-}$: 6.08 vs 1.16 log TCID$_{50}$/ml), 2.6-fold decreased for WNV (MEF-WT vs MEF-αVβ3$^{-/-}$: 5.41 vs 2.08 vs log TCID$_{50}$/ml), 1.82-fold decreased for USUV (MEF-WT vs MEF-αVβ3$^{-/-}$: 8.66 vs 4.75 log TCID$_{50}$/ml) and 1.68-fold decreased for LGTV (MEF-WT vs MEF-αVβ3$^{-/-}$: 7.16 vs 4.25 log TCID$_{50}$/ml). In sum, the deletion of αVβ3 integrin strongly affected flavivirus replication.
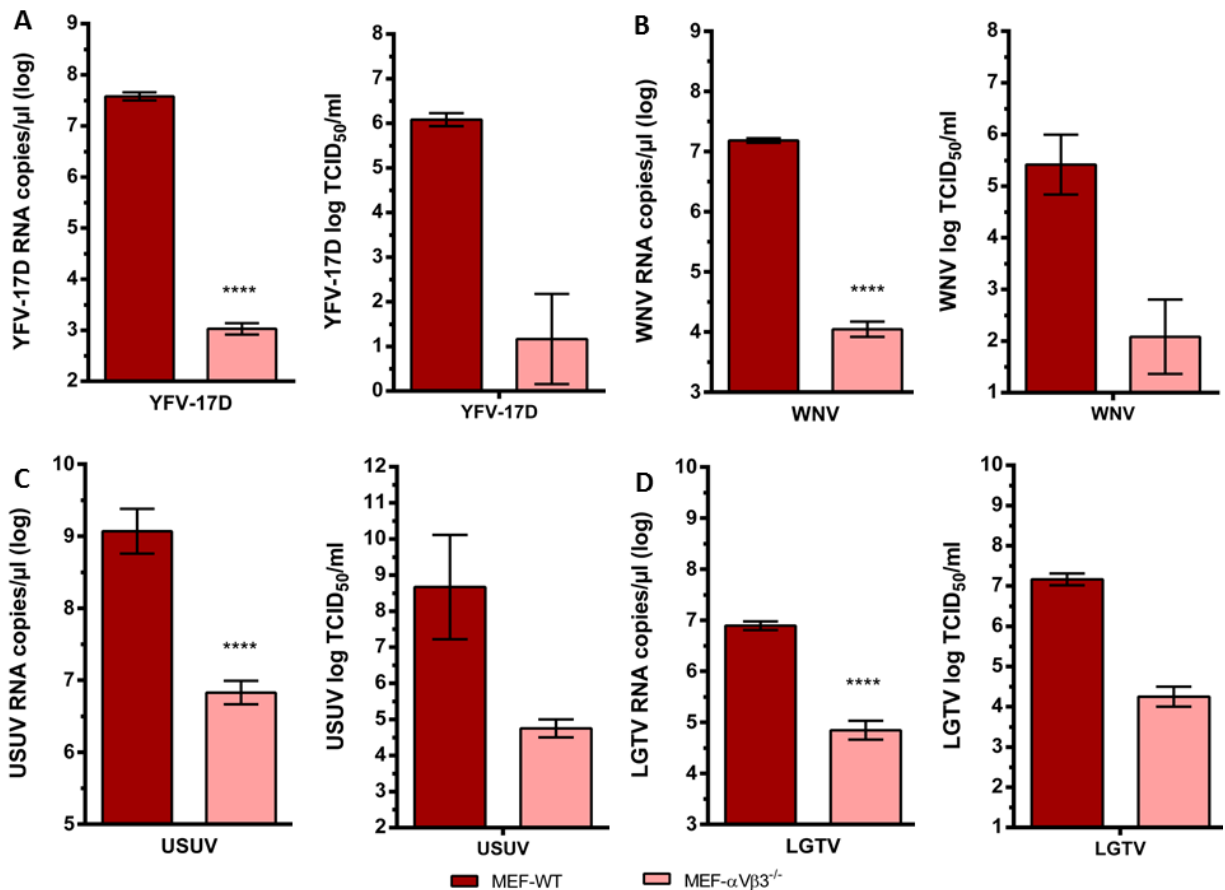
Figure 30: Replication analysis of YFV-17D (A), WNV (B), USUV (C) and LGTV (D) in the integrin deficient MEF-αVβ3$^{-/-}$ and corresponding wild-type MEF-WT cells. RNA yields and virus titers were measured 48 hours post inoculation. Cells were seeded into 12-well plates and inoculated with different flaviviruses at an MOI of 10. After one hour, monolayers were extensively washed and shifted to 37°C for 48 hours. Supernatants were harvested, total RNA was isolated and RT-qPCR was performed to determine the yield of viral RNA. The amount of virus genome is expressed as copy numbers per microliter (log transformed). Virus titers were determined by TCID$_{50}$. End-point determinations of virus titers were calculated using the Spearman-Kaerber method. Titers were expressed in log values. Three independent experiments were performed in triplicate (n=3). Bars represent mean values and error bars represent the standard deviation (mean ± standard deviation). Statistical analysis: Unpaired Student's *t*-test with Welch's correction; (****) $p ≤ 0.0001$; ns: not significant ($p > 0.05$). Abbreviations: YFV-17D: Yellow fever virus strain 17D; WNV: West Nile virus; USUV: Usutu virus; LGTV: Langat virus; MEF-WT: mouse embryonic fibroblasts wild-type; MEF-αVβ3$^{-/-}$: mouse embryonic fibroblasts deficient for the alpha V beta 3 integrin.

As demonstrated in **Figure 30 A - D**, the deletion of αVβ3 integrin strongly impairs flavivirus replication. In order to further investigate whether the deletion of αVβ3 integrin influences the flavivirus RNA replication, the level of flavivirus negative-strand RNA was measured. As shown in **Figure 31**, the level of negative-strand RNA in MEF-αVβ3$^{-/-}$ cells was strongly reduced in comparison to MEF-WT cells. LGTV showed the strongest reduction of negative-strand RNA with 98.2% of reduction (**Figure 31 D**). The other flaviviruses showed reductions of 94% (YFV-17D), 65.7% (WNV) and 85% (USUV). Together, these results suggest that integrin expression might influence flavivirus RNA replication.
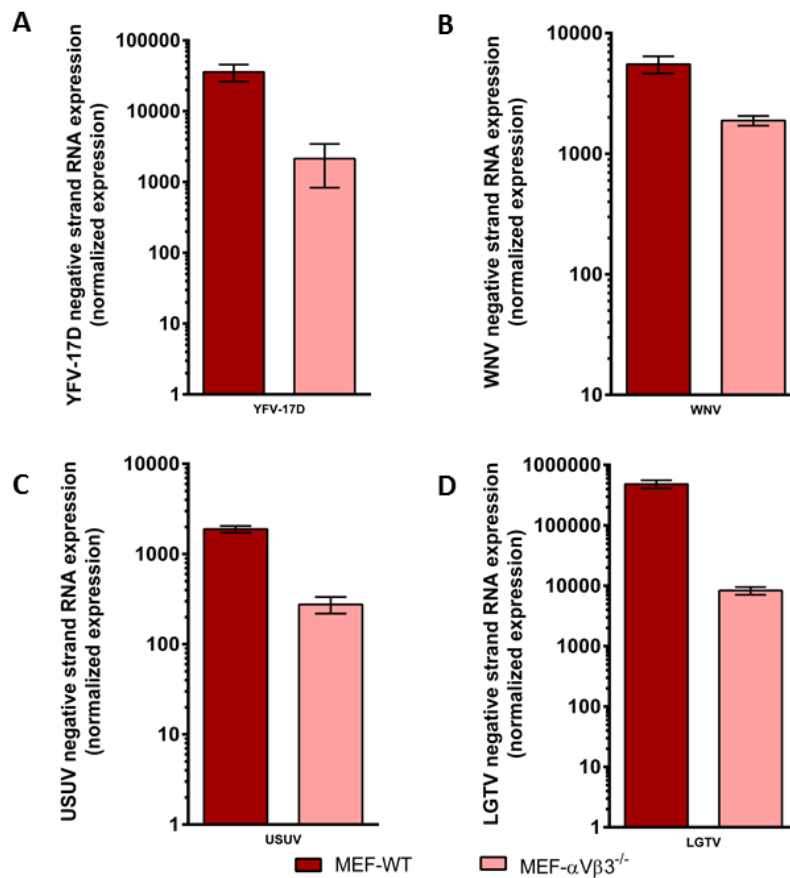
Figure 31: Detection of flavivirus negative-strand RNA in MEF-WT and MEF-αVβ3$^{+/+}$ cells. Cells were inoculated with YFV-17D (A), WNV (B), USUV (C) and LGTV (D) at an MOI of 10. After 48 hours post inoculation, monolayers were washed and then harvested, lysed and total RNA was extracted. RT-qPCR was performed to quantify the amount of negative-strand RNA. The levels of flavivirus negative-strand RNA were normalized against beta-actin, a housekeeping gene, and the relative gene expression was calculated by 2^ddCT method. Levels of flavivirus negative-strand RNA were expressed as fold amplification in relation to the housekeeping gene. Three independent experiments were performed in triplicate (n=3). Bars represent mean values and error bars represent the standard deviation (mean ± standard deviation). Abbreviations: YFV-17D: yellow fever virus strain 17D; WNV: West Nile virus; USUV: Usutu virus; LGTV: Langat virus; MEF-WT: mouse embryonic fibroblasts wild-type; MEF-αVβ3$^{-/-}$: mouse embryonic fibroblasts deficient for the alpha V beta 3 integrin.

4.5.5.4) Effect of αV or β3 integrin expression on flavivivirus replication in CHO cells

In order to analyze whether the expression of αV and β3 integrin subunits could influence flavivirus replication in CHO cells, the CHO-K1 as well as the CHO cells expressing the αV and β3 integrin subunits were inoculated with YFV-17D, WNV, USUV and LGTV at an MOI of 10.

The **Figures 32 A – D** show the replication profile of different flaviviruses in CHO cells expressing the mouse αV or β3 integrin subunit as well as in the CHO-K1 cells. Despite the high MOI (10) used in this study, flaviviruses only replicated poorly in all CHO cell lines tested. However, replication was slightly increased in CHO cells expressing either αV or β3 integrin subunits (**Figures 32 A – D)**. The expression of αV integrin subunit resulted in a slight increase of YFV-17D (**Figure 32 A**) and USUV RNA yields (**Figures 32 C**) in CHO-αV$^{+/+}$ cells in comparison with the CHO-K1 cells. YFV-17D and USUV replication was increased by 82.8% and 142.5%, respectively. Statistical analysis demonstrated that those differences were highly significant in both cases, YFV-17D (p = 0.0045) and USUV (p = 0.0001). In contrary to the αV integrin subunit, the expression of β3 integrin subunit in CHO cells did neither influence YFV-17D nor USUV (p = 0.8407 for YFV-17D and p = 0.2685 for USUV) (**Figures 32 A and C**).

For LGTV however, an increase of 72.5% in replication in CHO-β3$^{+/+}$ cells in comparison to CHO-K1 cells was observed (**Figure 32 D**). This increase in LGTV replication in CHO-β3$^{+/+}$ cells showed to be significant (p = 0.0069). The expression of αV integrin subunit in CHO cells did not influence LGTV replication (**Figure 32 D**). Unexpectedly, in the case of WNV, the replication seemed to be more efficient in CHO-K1 cells than in CHO-αV$^{+/+}$ cells (**Figures 32 B**) and this difference showed to be statistically significant (p = 0.0024). WNV replication in CHO-αV$^{+/+}$ cells was decreased by only 24.3 % compared to wild-type CHO-K1 cells. On the other hand, the replication of WNV in CHO-β3$^{+/+}$ cells was slightly increased compared to CHO-K1 cells (**Figures 32 B**). The increase of WNV replication was 21.58% and showed to be significant (p = 0.0251).

In conclusion, these cell infection assays demonstrate that expression of either αV or β3 integrin subunits in CHO-K1 cells might positively affect the replication of some flaviviruses.
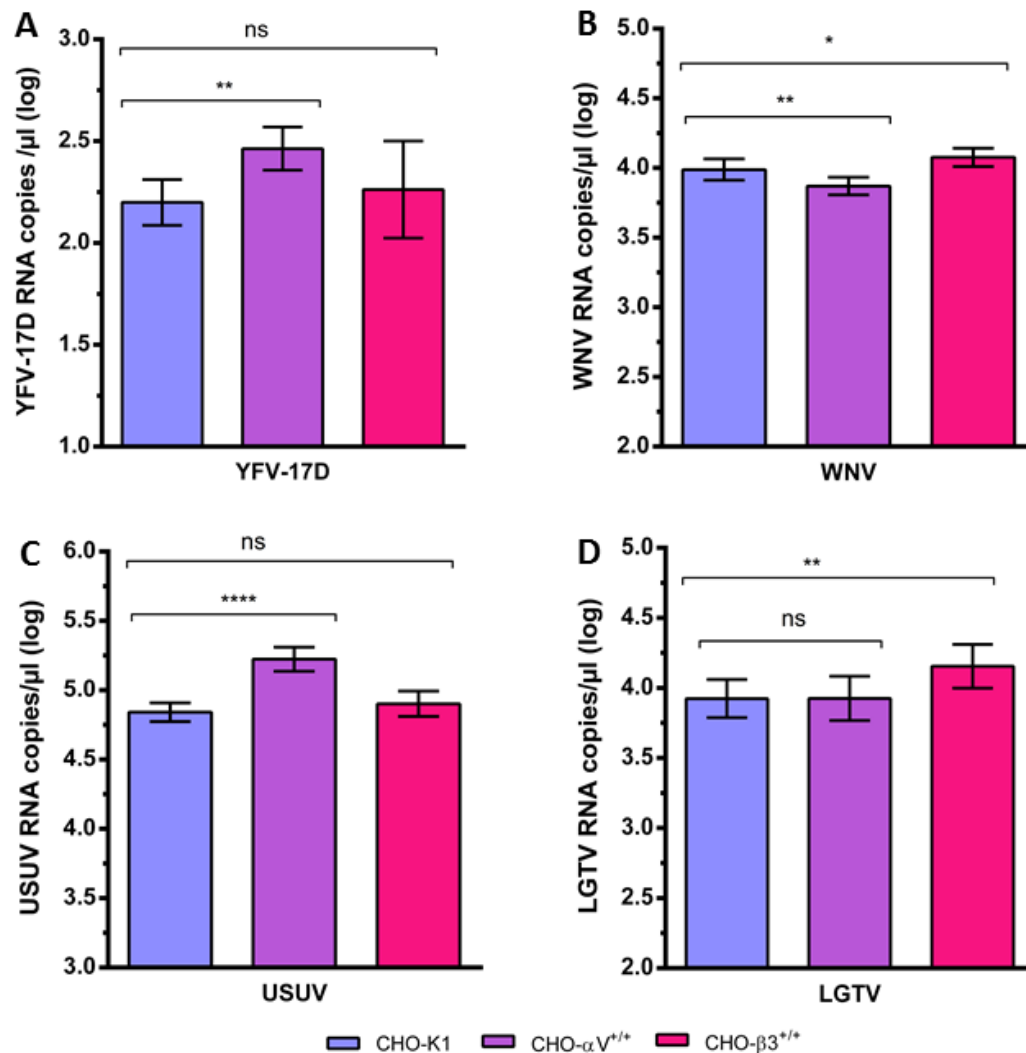
Figure 32: Replication analysis of YFV-17D (A); WNV (B); USUV (C) and LGTV (D) in CHO-K1, CHO-αV$^{+/+}$ and CHO-β3$^{+/+}$ cells. The figure shows RNA yields 48 hours post-inoculation. Cells were seeded into 12-well plates and inoculated with different flaviviruses at an MOI of 10. After one hour, monolayers were extensively washed and shifted to 37°C for 48 hours. Supernatants were harvested and total RNA was isolated and RT-qPCR was performed to determine the yield of viral RNA. The amount of virus genome is expressed as copy numbers per microliter (log transformed). Three independent experiments were performed in triplicate (n=3). Bars represent mean values and error bars represent the standard deviation (mean ± standard deviation). Statistical analysis: One-Way ANOVA with Bonferroni correction; (*) $p \leq 0.05$; (**) $p \leq 0.01$; (****) $p \leq 0.0001$; ns: not significant ($p > 0.05$). Abbreviations: YFV-17D: Yellow fever virus strain 17D; WNV: West Nile virus; USUV: Usutu virus; LGTV: Langat virus; CHO-K1: Chinese hamster ovary cells clone K1; CHO-αV$^{+/+}$: Chinese hamster ovary cells expressing the mouse alpha V integrin subunit; CHO-β3$^{+/+}$: Chinese hamster ovary cells expressing the mouse beta 3 integrin subunit.

4.6) Cell infection assays to investigate the effect of integrin ablation on Zika virus infection

4.6.1) Influence of integrins on ZIKV binding to MEFs and MKFs

First, it was evaluated whether the genomic deletion of integrins affects ZIKV binding to the surface of integrin deficient MEFs and MKFs. As demonstrated in **Figure 33**, the absence of αVβ3 integrin in MEF-αVβ3$^{-/-}$ cells as well as the β1 and β3 integrin subunit in MKF-β1$^{-/-}$ and MEF-β3$^{-/-}$ cells did not influence ZIKV binding to the cell surface of these cells. No statistical significance was shown for any of the cells tested ($p > 0.05$).

In conclusion, similar to other flaviviruses, the absence of integrin expression did not affect ZIKV binding to the surface of MEFs and MKFs.
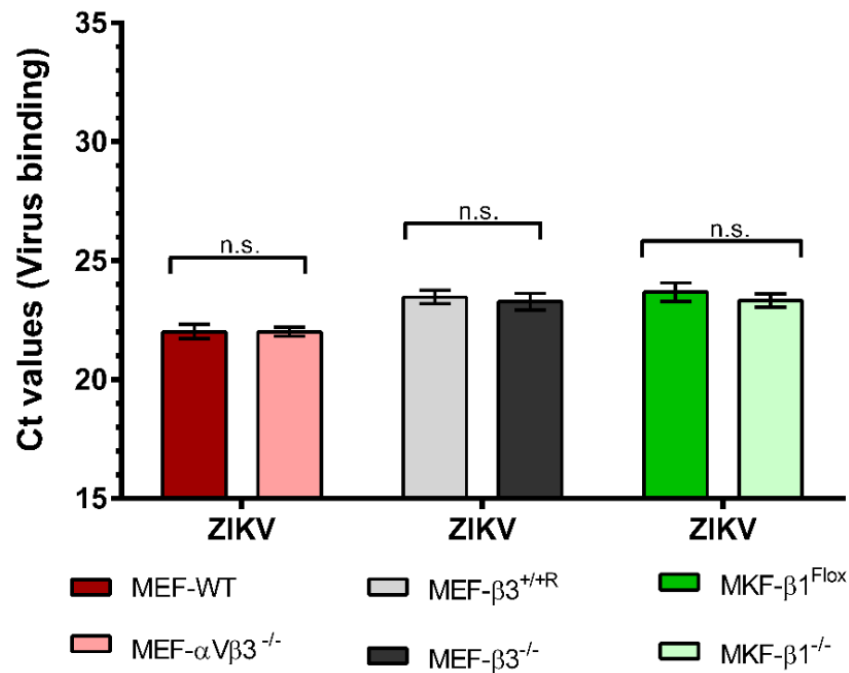
Figure 33. Zika virus (ZIKV) binding to the integrin deficient MEFs and MKFs and the corresponding wild-type cells. Cells were seeded into 12-well plates, placed on ice and inoculated with ZIKV at an MOI of 10. After one hour, monolayers were extensively washed, harvested and lysed with RLT buffer. Total RNA was isolated and RT-qPCR was performed to indirectly measure virus binding to the cell surface by detection of viral RNA. Virus binding values are expressed in cycle threshold (Ct) values. Three independent experiments were performed in triplicate (n=3). Bars represent the mean Ct values and error bars represent the standard deviation (means ± standard deviation). Statistical analysis: Mann-Whitney test; ns: not significant ($p > 0.05$). Abbreviations: MEF-WT: mouse embryonic fibroblasts wild-type; MEF-αVβ3$^{-/-}$: mouse embryonic fibroblasts deficient for αVβ3 integrin; MKF-β1^{Flox}: mouse kidney fibroblasts expressing the β1 integrin subunit (wild-type); MKF-β1$^{-/-}$: mouse kidney fibroblasts deficient for the β1 integrin subunit; MEF-β3$^{+/+R}$: mouse embryonic fibroblasts expressing the β3 integrin subunit (R = rescue); MEF-β3$^{-/-}$: mouse embryonic fibroblasts deficient for the β3 integrin subunit.

4.6.2) Influence of integrins on ZIKV internalization by MEFs and MKFs

Next, we evaluated whether the lack of integrin expression could affect ZIKV internalization into MEFs and MKFs. As shown in **Figure 34**, ZIKV was equally internalized into MEFs and MKFs regardless of integrin expression (**Figure 34**). No statistically significant difference was found between MKF-β1^{Flox} vs MKF-β1$^{-/-}$ cells (p = 0.1605; **Figure 34 B**). Statistical analysis however revealed a difference in ZIKV internalization between MEF-β3$^{+/+R}$ and MEF-β3$^{-/-}$ cells (p = 0.0341; **Figure 34 C**). Although the statistical analysis demonstrated a significant difference, the total RNA copy numbers indicating ZIKV internalization differed only by 2.9% for MEF-β3$^{+/+R}$ vs MEF-β3$^{-/-}$ cells (**Figure 34 C**). Statistical analysis also indicated significant differences in ZIKV internalization between MEF-αVβ3$^{-/-}$ and MEF-WT cells (p = 0.0007; **Figure 34 A**) while viral RNA copy numbers between MEF-αVβ3$^{-/-}$ vs MEF-WT cells differed only by 2.0%. Together, our results demonstrated that integrins are most likely not involved in ZIKV internalization.
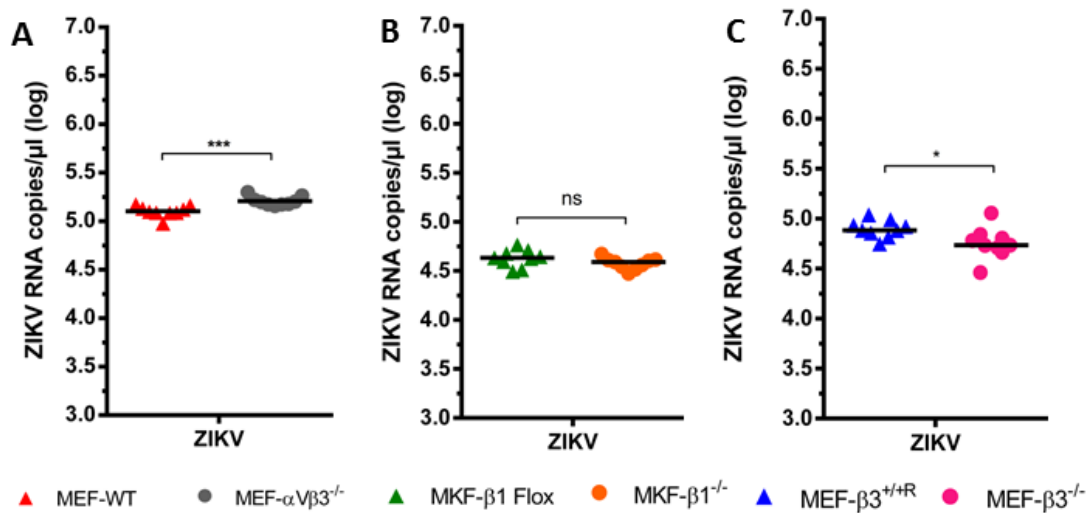
Figure 34: Zika virus (ZIKV) internalization by MEF-WT and MEF-αVβ3$^{-/-}$ (A); MKF-β1^{Flox} and MKF-β1$^{-/-}$ (B) and MEF-β3$^{+/+R}$ and MEF-β3$^{-/-}$ (C) cells. Cells were seeded into 12-well plates, placed on ice and inoculated with ZIKV at an MOI of 10. After one hour, monolayers were extensively washed and shifted to 37°C for 30 minutes. Cell monolayers were then washed once with acidic glycine (pH 2.5) and incubated for 2 minutes, washed twice with 1X PBS. Monolayers were harvested and lysed with RLT buffer. Total RNA was isolated and RT-qPCR was performed to determine the amount of internalized virus particles. The amount of virus internalization is expressed in copy numbers per microliter (log transformed). Three independent experiments were performed in triplicate (n=3). Dot plots represent each individual replicate from the three independent experiments. Statistical analysis: Unpaired Student's t-test; (*) $p \leq$ 0.05; (***) $p \leq 0.001$; ns: not significant ($p > 0.05$). Abbreviations: MEF-WT: mouse embryonic fibroblasts wild-type; MEF-αVβ3$^{-/-}$: mouse embryonic fibroblasts deficient for αVβ3 integrin; MKF-β1^{Flox}: mouse kidney fibroblasts expressing the β1 integrin subunit (wild-type); MKF-β1$^{-/-}$: mouse kidney fibroblasts deficient for the β1 integrin subunit; MEF-β3$^{+/+R}$: mouse embryonic fibroblasts expressing the β3 integrin subunit (R = rescue); MEF-β3$^{-/-}$: mouse embryonic fibroblasts deficient for the β3 integrin subunit; αV: alpha V integrin subunit; β1: beta 1 integrin subunit; β3: beta 3 integrin subunit.

4.6.3) Influence of integrins on ZIKV replication in MEFs, MKFs and CHO cells

Subsequent experiments to evaluate the influence of integrins on ZIKV replication were performed in MEF, MKF and CHO cells expressing the αV and β3 integrin subunits. As demonstrated in **Figure 35 C**, deletion of β3 integrin subunit affected ZIKV replication with a reduction of ZIKV RNA yields by 54.06% in MEF-β3$^{-/-}$ cells in comparison to MEF-β3$^{+/+R}$ cells. This reduction of ZIKV yields in MEF-β3$^{-/-}$ cells showed to be statistically significant (p = 0.0002). Surprisingly, the lack of β1 in MKF-β1$^{-/-}$ cells had a positive effect on ZIKV replication with an increase in ZIKV RNA yields of more than 77% in comparison to the MKF-β1^{Flox} cells (**Figure 35 B**). This finding also showed to be statistically significant (p = 0.0001). On the other hand, and similar to what was observed for the other flaviviruses, the deletion of αVβ3 integrin in MEF-αVβ3$^{-/-}$ cells had a significant impact on ZIKV replication with a reduction of almost 98% (p = 0.0001) in ZIKV RNA yields compared to MEF-WT cells (**Figure 35 A**).
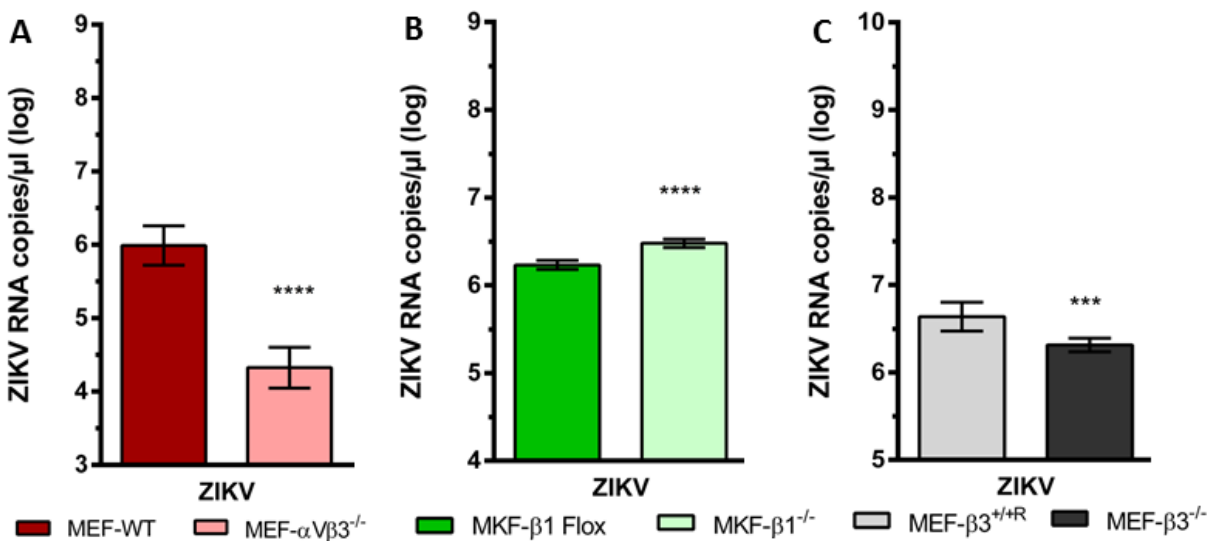
Figure 35: Zika virus (ZIKV) replication analysis in MEF-WT and MEF- αVβ3$^{-/-}$ (A); MKF-β1^{Flox} and MKF-β1$^{-/-}$ (B); MEF-β3$^{+/+R}$ and MEF-β3$^{-/-}$ (C) cells. Cells were seeded into 12-well plates and inoculated with ZIKV at an MOI of 10. After one hour, monolayers were extensively washed and shifted to 37°C for 48 hours. Supernatants were harvested and total RNA was isolated. RT-qPCR was performed to determine the yields of viral RNA. The amount of virus genome is expressed as copy numbers per microliter (log transformed). Three independent experiments were performed in triplicate (n=3). Bars represent mean values and error bars represent the standard deviation (mean ± standard deviation). Statistical analysis: unpaired students t-test; (***) $p \leq 0.001$; (****) $p \leq 0.0001$. Abbreviations: MEF-WT: mouse embryonic fibroblasts wild-type; MEF-αVβ3$^{-/-}$: mouse embryonic fibroblasts deficient for αVβ3 integrin; MKF-β1^{Flox}: mouse kidney fibroblasts expressing the β1 integrin subunit (wild-type); MKF-β1$^{-/-}$: mouse kidney fibroblasts deficient for the β1 integrin subunit; MEF-β3$^{+/+R}$: mouse embryonic fibroblasts expressing the β3 integrin subunit (R = rescue); MEF-β3$^{-/-}$: mouse embryonic fibroblasts deficient for the β3 integrin subunit; αV: alpha V integrin subunit; β1: beta 1 integrin subunit; β3: beta 3 integrin subunit.

Since MKF-β1$^{-/-}$ cells only showed a slight increase in ZIKV replication while MEF-β3$^{-/-}$ cells only displayed a small decrease, the ZIKV titers were not further determined by TCID$_{50}$ due to the very small differences in RT-qPCR based RNA quantification. However, the titers of ZIKV in MEF-WT cells and MEF-αVβ3$^{-/-}$ cells were determined by TCID$_{50}$ to further confirm the inhibition of ZIKV replication observed in these cells. Titers of ZIKV in MEF-αVβ3$^{-/-}$ cells were reduced by almost 2 logs in comparison to MEF-WT cells (MEF-WT vs MEF-αVβ3$^{-/-}$: 6.29 vs 4.37 log TCID$_{50}$/ml; **Figure 36**), reinforcing the involvement of αVβ3 integrin in ZIKV replication.
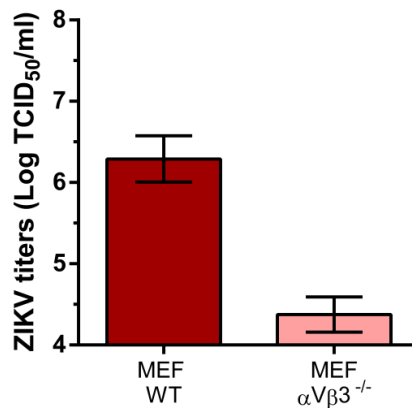
Figure 36: Zika virus (ZIKV) titers after inoculation of MEF-αVβ3$^{-/-}$ and MEF-WT cells. Cells were seeded into 12-well plates and infected with ZIKV at an MOI of 10. After one hour, monolayers were extensively washed and shifted to 37°C for 48 hours. Supernatants were harvested and ZIKV titers were determined by TCID$_{50}$. End-point titers were calculated using the Spearman-Kaerber method. Titers are expressed in log values. Experiment was performed in triplicate. Bars represent mean values and error bars represent the standard deviation (mean ± standard deviation). Abbreviations: MEF-WT: mouse embryonic fibroblasts wild-type; MEF-αVβ3$^{-/-}$: mouse embryonic fibroblasts deficient for αVβ3 integrin; αV: alpha V integrin subunit; β3: beta 3 integrin subunit.

To confirm that ablation of integrins, in particular the αVβ3 integrin, interferes in flavivirus RNA replication, the level of ZIKV negative-strand RNA was measured.

As shown in **Figure 37**, no significant differences in the levels of ZIKV negative-strand RNA expression in MKF-β1$^{-/-}$ and the MEF-β3$^{-/-}$ cells in comparison to the respective wild-type cells, MKF-β1^{Flox} and MEF-β3$^{+/+R}$, were detected. In contrast, synthesis of ZIKV negative-strand RNA in MEF-αVβ3$^{-/-}$ cells was reduced almost 1000-fold compared to MEF-WT cells (**Figure 37**). In conclusion, deletion of αVβ3 integrin affects ZIKV replication at RNA replication level.
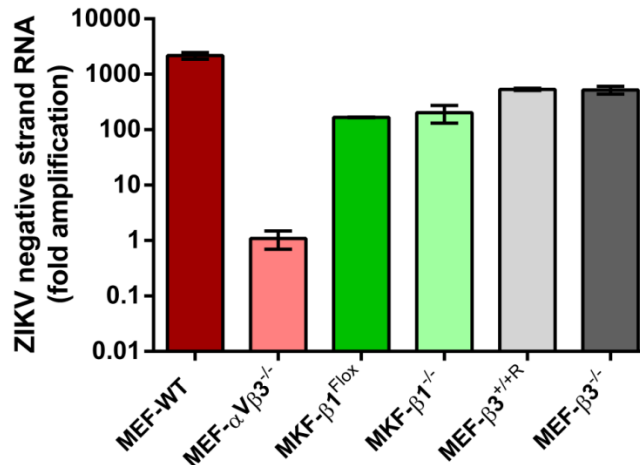
Figure 37. Levels of Zika virus (ZIKV) negative-strand RNA in integrin deficient MEFs and MKFs and corresponding wild-type cells. Cells were inoculated with ZIKV at an MOI of 10 at 37°C for 1 hour. After inoculation, cells were washed 6 times and incubated at 37°C for 48 hours. Monolayers were harvested 48 hours after inoculation and levels of ZIKV negative-strand RNA were measured by RT-qPCR. The levels of ZIKV negative-strand RNA were normalized against beta-actin, a housekeeping gene, and the relative gene expression was calculated by 2^ddCT method. Levels of ZIKV negative-strand RNA were expressed as fold amplification in relation to the housekeeping gene. Three independent experiments were performed in triplicate (n=3). Bars represent mean values and error bars represent the standard deviation (mean ± standard deviation). Scale was log-transformed. Abbreviations: MEF-WT: mouse embryonic fibroblasts wild-type; MEF-αVβ3$^{-/-}$: mouse embryonic fibroblast deficient for αVβ3 integrin; MKF-β1^{Flox}: mouse kidney fibroblasts expressing the β1 integrin subunit (wild-type); MKF-β1$^{-/-}$: mouse kidney fibroblasts deficient for the β1 integrin subunit; MEF-β3$^{+/+R}$: mouse embryonic fibroblasts expressing the β3 integrin subunit (R = rescue); MEF-β3$^{-/-}$: mouse embryonic fibroblasts deficient for the β3 integrin subunit; αV: alpha V integrin subunit; β1: beta 1 integrin subunit; β3: beta 3 integrin subunit

In order to assess whether the expression of αV and β3 integrin subunits in CHO cells could enhance ZIKV replication, CHO cells expressing the αV or β3 integrin subunits as well as the corresponding CHO wild-type cells were inoculated with ZIKV. In contrast to what was observed for the other flaviviruses in the replication assays in CHO cells, the expression of αV or β3 integrin subunits did not enhance ZIKV replication in CHO cells (**Figure 38 A**). Statistical analysis (One-Way ANOVA) failed to demonstrate any statistical significance between the groups.

Next, the level of ZIKV negative-strand RNA was measured by RT-qPCR. The levels of negative-strand ZIKV RNA were similar in all CHO cells tested regardless of the expression of αV or β3 integrin subunits in these cells (**Figure 38 B**). In conclusion, these results demonstrate that the ectopic expression of integrins in CHO cells does not influence ZIKV replication.
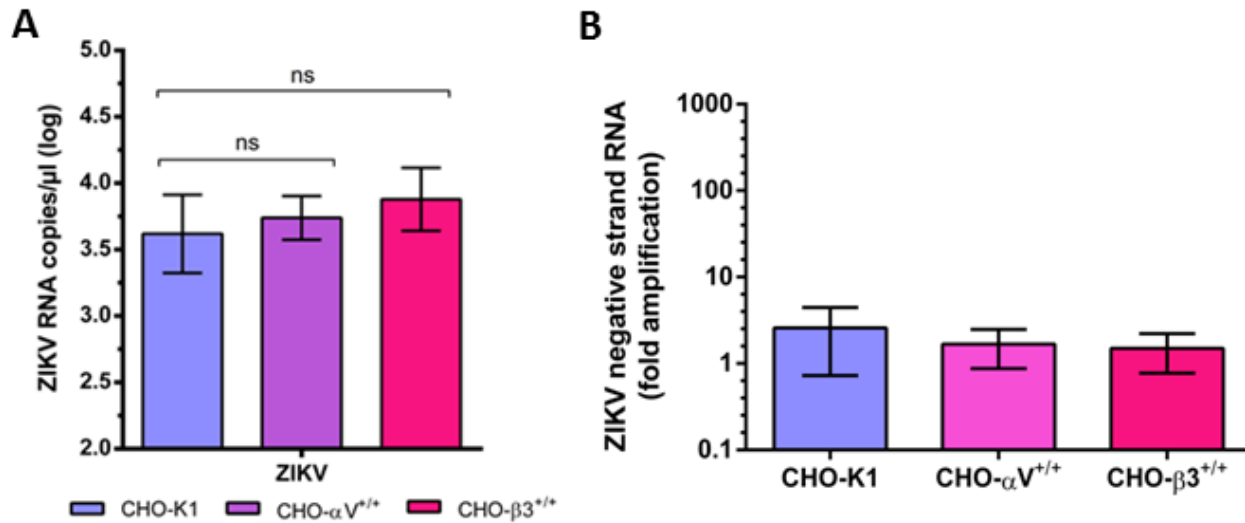
Figure 38: Zika virus (ZIKV) replication analysis in CHO-K1, CHO-αV$^{+/+}$ and CHO-β3$^{+/+}$ cells. Figure A shows RNA yields after 48 hours post-inoculation and Figure B shows the level of ZIKV negative strand RNA measured by RT-qPCR. Cells were seeded into 12-well plates and inoculated with ZIKV at an MOI of 10. After one hour, monolayers were extensively washed and shifted to 37°C for 48 hours. Supernatants were harvested and total RNA was isolated. RT-qPCR was performed to determine the yield of viral RNA. (A) The amount of virus genome is expressed as copy numbers per microliter (log transformed). (B) The levels of ZIKV negative-strand RNA were normalized against beta-actin, a housekeeping gene, and the relative gene expression was calculated by 2^ddCT method. Levels of ZIKV negative-strand RNA were expressed as fold amplification in relation to the housekeeping gene. Three independent experiments were performed in triplicate (n=3). Bars represent mean values and error bars represent the standard deviation (mean ± standard deviation). Statistical analysis: One–way ANOVA with Bonferroni correction; ns: not significant ($p > 0.05$). Abbreviations: CHO-K1: Chinese hamster ovary cells clone K1; CHO-αV$^{+/+}$: Chinese hamster ovary cells expressing the mouse alpha V integrin subunit CHO-β3$^{+/+}$: Chinese hamster ovary cells expressing the mouse beta 3 integrin subunit.

5) Discussion

Flaviviruses have an extraordinary ability to infect a huge diversity of hosts. Thus, for many years, it was proposed that flaviviruses use a single common receptor to infect the host cell. However, since many molecules have been recently characterized to function as potential flavivirus receptors in different cell lines from different hosts, the idea of one common receptor has been rejected (Gould *et al.*, 2008; Kaufmann *et al.*, 2011; Perera-Lecoin *et al.*, 2013; Rodenhuis-Zybert *et al.*, 2010b; Smit *et al.*, 2011). Thus, today the main hypothesis claims that flaviviruses use multiple receptors to get access into the host cell and that the receptor repertoire might change according to the host and/or the cell line (Kaufmann *et al.*, 2011; Perera-Lecoin *et al.*, 2013).

Another subject that has been extensively studied over the last few years are host cell factors that modulate virus infection. Those host cell factors might not function as the cellular receptor but might act as accessory molecules that influence the virus infection (Fernandez-Garcia *et al.*, 2009; Pastorino *et al.*, 2010; Wang *et al.*, 2017).

In the past, several groups have proposed and investigated the involvement of cell adhesion molecules, in particular integrins, in the flavivirus infection cycle (Chu *et al.*, 2004b; Medigeshi *et al.*, 2008; Protopopova *et al.*, 1997) since integrins are highly conserved among vertebrate and invertebrate species and constitutively expressed in all cell lines (Hynes, 1992).

A recent study by Schmidt et al. (2013) concluded that WNV entered the cells independently of the integrin expression and regardless of the WNV strain used. For this study, a MEF cell line lacking the expression of different integrin subunits was infected with different WNV strains. For all these WNV strains, the lack of integrin expression did not affect binding or internalization into the MEFs. However, the deletion of β1 or β3 integrin subunits affected WNV replication suggesting a role of integrins in WNV infection (Schmidt *et al.*, 2013a). More recently, integrin αVβ3 has been demonstrated to play a role in JEV infection reinforcing the importance of integrins in the flavivirus infection cycle (Fan *et al.*, 2017).

In the present study, a similar model based on MEFs deficient for the expression of one or more integrin subunits and their respective wild-type cells were used to assess the influence of integrins in the flavivirus infection cycle. Additionally, CHO cells expressing the mouse αV or β3 integrin subunits were generated to investigate the involvement of these cell adhesion molecules in the flavivirus infection cycle. All these cell lines were used to assess their permissiveness and susceptibility to different flaviviruses, namely YFV-17D, USUV, LGTV, WNV and ZIKV.

5.1) Development of suitable cell models

In this study, several cell models were established to investigate the involvement of integrins in the flavivirus infection cycle. Those models were based on (i) MEFs lacking the expression of αVβ3 integrin or β3 integrin subunit; (ii) MKFs lacking the expression of β1 integrin subunit and iii) CHO cells expressing either αV or β3 integrin subunits.

The deletion of these specific integrin subunits in MEFs and MKFs enabled us to evaluate whether one specific integrin heterodimer or specific integrin subunit(s) were involved in the flavivirus infection cycle. The ablation of the respective integrin genes in the integrin deficient MEFs and MKFs occurred at the genomic level by homologous recombination (Fassler *et al.*, 1995a; Hodivala-Dilke *et al.*, 1999; Schmidt *et al.*, 2013a). The advantage of this method is that by deleting the target genes at the DNA level, most of the off-target effects caused by other gene silencing methods such as siRNA are avoided and/or abrogated (Boettcher *et al.*, 2015). Those effects would include residual expression of target genes and activation of the innate immunity by introducing foreign nucleic acids into the target cell cytoplasm (Angart *et al.*, 2013; Jackson *et al.*, 2010). Another advantage of using MEFs is that these cells are easily isolated and maintained and have a high rate of proliferation *in vitro* (Ruiz-Ojeda et al., 2016). Although no study has fully described the whole integrin profile in MEFs, a few studies have demonstrated that they express a diverse repertoire of integrins such as α5β1, α11β1, α2β1 and α1β1 (Carracedo *et al.*, 2010; Guo *et al.*, 2005; Lu *et al.*, 2014; Popova *et al.*, 2004; Zhu *et al.*, 2007). Due to the embryonic origin of MEFs used in the present study, the expression of integrins might be substantially upregulated in these cells to mediate important cellular processes during embryonic stages such as migration, attachment and differentiation of the cells (Bokel *et al.*, 2002; Hertle *et al.*, 1991; Schmid *et al.*, 2003; Sutherland *et al.*, 1993).

In contrast to that, CHO cells express only a limited integrin repertoire and have been reported to be unsusceptible to several viral agents including members of the *Flavivirus* genus which makes these cells a suitable model to study the involvement of integrins in flavivirus infection (Berting *et al.*, 2010; Garrigues *et al.*, 2008; Symington *et al.*, 1993; Takagi *et al.*, 1997; Xu *et al.*, 2011).

Lastly, although mice and hamster are not a natural flavivirus reservoir, a number of cell lines derived from these species have been reported to be susceptible to flavivirus infection and support efficient replication (Chan *et al.*, 2016; Rossi *et al.*, 2016; Tesh *et al.*, 2005; Wang *et al.*, 2011). In this study, we demonstrated that some flaviviruses such as YFV-17D and USUV replicated to comparable levels in MEF-WT cells as in Vero cells, the most flavivirus permissive cell line. These results strongly support the usage of MEFs and MKFs to investigate flavivirus susceptibility and replication *in vitro*.

5.1.1) Recovery of αVβ3 integrin in MEF-αVβ3$^{-/-}$ cells

MEFs deficient for αVβ3 integrin were subjected to recover their respective integrin genes. For that, cells were transfected with vectors carrying the mouse αV and β3 integrin subunit genes. Though several transfection strategies were followed, the expression of αVβ3 integrin in MEF-αVβ3$^{-/-}$ cells was not recovered. Different cationic lipid based transfection reagents and several transfection methods such as electroporation were attempted but only resulted in low transfection efficiency and high cell toxicity leading to excessive cell death. By transfecting the integrin subunit encoding plasmids one after another into MEF-αVβ3$^{-/-}$ cells, the recovered integrin expression was very low. After a few passages, the level of integrin expression even decreased which made it necessary to base the following work on MEF wild-type cells. *Per se*, primary cells such as MEFs are known to be hard to transfect and several authors have experienced low transfection efficiencies using cationic lipid based transfection as performed in our study (Han *et al.*, 2015; Lee *et al.*, 2017). The antibiotic selection reagents used for selection of transgenic resistant cells might also play a crucial role in the establishment of transgenic cell lines (Lanza *et al.*, 2013). Unsuccessful recovery of expression of both integrin subunits in MEF-αVβ3$^{-/-}$ cells might therefore be attributed to the toxic effects of the antibiotics used for selection of resistant clones. However, the zeocin selection marker used in our study showed to be superior in selecting resistant clones compared to other antibiotic selection markers (Lanza *et al.*, 2013). Since MEF-αVβ3$^{-/-}$ cells were transfected with two vectors either harboring the antibiotic resistance gene for zeocin or hygromycin, cells were selected by adding both antibiotics to the cell culture medium. It remains unclear whether both antibiotic resistance genes were expressed at their maximum level to allow complete cell resistance to both antibiotics. This might also explain the observation of some transfected MEF-αVβ3$^{-/-}$cell populations that expressed different levels of αV and β3 integrin subunits and later succumbed to antibiotic selection. To transduce the target genes into MEF-αVβ3$^{-/-}$ cells and recover the expression of αVβ3 integrin, viral vector-based methods might be an interesting approach for future studies.

5.2) Cell morphology, growth rates and viability of MKFs, MEFs and CHO cells

Since MEFs and MKFs originate from different tissues, differences on cell morphology, growth rate and integrin expression were expected.
The double deficient MEF-αVβ3$^{-/-}$ cells revealed a remarkable difference in cell morphology and growth rates compared to their wild-type cells. These differences in cell morphology and growth rates are certainly due to the genomic deletion of αVβ3 integrin. A study conducted by Cruet-Hennequart *et al.*,(2003) reported that αVβ3 and αVβ5 integrins regulate cell proliferation by activating the integrin-linked kinase leading to cell cycle progression. Functional blocking of these integrins by epitope blocking antibodies as

well as synthetic RGD peptides led to inhibition of the cell cycle with consequent reduction of cell proliferation (Cruet-Hennequart *et al.*, 2003). Despite the reduction of cell growth and density, the MEF-αVβ3$^{-/-}$ cells showed an abnormal morphology by forming cell aggregations. This abnormal morphology might be attributed to the loss of αVβ3 integrin and the increased need of the close cell-to-cell contact to promote growth. A number of publications have further demonstrated that the absence of αVβ3 and α5β1 integrins disturbs cell spreading and expansion on extracellular matrices (Balcioglu *et al.*, 2015; Charo *et al.*, 1990; Cruet-Hennequart *et al.*, 2003). These observations might also account for the formation of "cellular islets" observed in MEF-αVβ3$^{-/-}$ cells in our study.

Notably, the MKF-β1$^{-/-}$ cells displayed a more rounded shape compared to the parental cell line, the MKF-β1^{Flox} cells. This morphological effect is most likely attributed to the deletion of β1 integrin subunit and was also observed by others (Fassler *et al.*, 1995b; Hou *et al.*, 2016). Interestingly, in our study, the loss of β1 integrin subunit did not affect the MKF-β1$^{-/-}$ cell growth rate as observed by similar split ratios compared to MKF-β1^{Flox} cells. However, their growth rate was still higher than that observed for MEFs. These characteristics concerning morphology and cell growth are in accordance with reports from other authors (Fassler *et al.*, 1995b; Hou *et al.*, 2016; Schmidt *et al.*, 2013a).

Unexpectedly, the loss of β3 integrin subunit expression in MEF-β3$^{-/-}$ cells did neither influence cell morphology nor cell growth. However, the rescued β3 expressing cells (MEF-β3$^{+/+}$) showed a strong decrease of growth rate. This special characteristic observed in MEF-β3$^{+/+}$ cells is most probably attributed to the usage of zeocin as antibiotic selection marker and was also observed in the CHO-β3$^{+/+}$ cells treated with zeocin. Last, ectopic expression of either αV or β3 integrin in CHO cells did not influence cell morphology. However, similar to what was observed in MEF-β3$^{+/+}$ cells, we experienced a decline in the split ratio for maintenance in the CHO-β3$^{+/+}$ cells when compared to the CHO-K1 cells. Again, this effect might be attributed to the use of zeocin as selection antibiotic and was also reported by another author (Hwang *et al.*, 2005).

Despite the fact that the deletion of integrins might influence cell morphology, spread and growth, deleting one or more integrin subunits does not seem to influence cell viability in our study.

Our metabolic viability assay (MTS assay) clearly demonstrated that loss of integrin expression did not affect cell viability regardless of the cell line tested. Within the course of the study and prior to infection experiments, cells were routinely checked by trypan blue staining which did not reveal any decrease in cell viability. Though several publications have reported that integrin ablation or *knock-down* might trigger apoptotic pathways consequently leading to cell death in certain cell types (Koistinen *et al.*, 2004; Popov *et al.*, 2011; Simirskii *et al.*, 2007), we did not observe such an effect in any of our cell lines.

This might be attributed to the expression of alternative integrin heterodimers that counterbalance the lack of αVβ3 integrin, β1 and β3 integrin subunits in our MEFs and MKFs. Other authors have reported that

expression of integrins in certain cell types rescued these cells from entering into apoptosis by triggering intracellular signaling with the result of cell survival (Montgomery *et al.*, 1994; Zhang *et al.*, 1995).

5.3) Characterization of integrin expression in MEFs, MKFs and CHO cells

In order to characterize the integrin expression among our cell lines, several methods were applied. Confocal laser microscopy analysis was performed to determine the sub-cellular localization of integrins and/or the loss of $\alpha V\beta 3$ integrin and $\beta 1$ and $\beta 3$ integrin subunits.

Integrins were homogeneously distributed along the cell membrane in all analyzed MEF and MKF cell lines which is in accordance to the literature (Geiger *et al.*, 2011). As expected, MEF and MKF wild-type cells expressed αV, $\beta 3$ or $\beta 1$ integrin subunits in high amounts evidenced by the presence of multiple focal adhesion sites. The presence of these structures visualized in wild-type MEFs and MKFs indicated the formation of functional integrin heterodimers as reported by other authors (Schmidt *et al.*, 2013a). Interestingly, by staining the integrin deficient cells, we also observed the presence of focal adhesion sites indicating that other functional integrin heterodimers were indeed expressed in the deficient cell lines. For example, the deletion of $\beta 1$ in MKF-$\beta 1^{-/-}$ cells did not affect the expression of αV and $\beta 3$ subunits in these cells in our study. This fact can be explained by the structural composition of integrins as heterodimers that are composed of one α and one β integrin subunit (Hynes, 2002). The genomic ablation of $\beta 1$ integrin subunit in these cells obviously impairs the formation of all $\beta 1$ integrin heterodimer combinations at the cell surface level whereas other heterodimers remain unaffected as described by other groups (Fassler *et al.*, 1995b; Hynes, 2002; Schmidt *et al.*, 2013a). Similarly, the deletion of $\alpha V\beta 3$ integrin in MEF-$\alpha V\beta 3^{-/-}$ cells disrupts the expression of six integrins ($\alpha V\beta 1$, $\alpha V\beta 3$, $\alpha V\beta 4$, $\alpha V\beta 5$, $\alpha V\beta 6$ and $\alpha V\beta 8$) while the deletion of $\beta 3$ integrin subunit in MEF-$\beta 3^{-/-}$ cells only impairs the expression of $\alpha V\beta 3$ in this specific cell line according to the literature (Hynes, 2002; Schmidt *et al.*, 2013a).

Confocal microscopy analysis in CHO-$\beta 3^{+/+}$ and CHO-$\alpha V^{+/+}$ cells revealed an integrin expression at the cell surface similar to the pattern observed in MEFs/MKFs. This indicates the formation of integrin heterodimers by combining endogenous hamster integrin subunits with ectopic mouse integrin subunits. Due to the fact that integrins share a high similarity among the mammalian species, the formation of hybrid integrins is possible and was reported by other authors (Briesewitz *et al.*, 1995; Symington *et al.*, 1993; Takagi *et al.*, 1997). In the case of CHO cells expressing the mouse αV integrin subunit (CHO-$\alpha V^{+/+}$) the probable integrin combination is $\alpha V\beta 1$ integrin, as a previous report showed the expression of endogenous $\beta 1$ integrin subunit in CHO cells (Takagi *et al.*, 1997). For CHO cells expressing the mouse $\beta 3$ integrin subunit, the only heterodimer combination possible is the $\alpha V\beta 3$ integrin since the αIIb is exclusively expressed in platelets and megakaryocytes (Bennett, 2005; Hynes, 2002).

In order to measure the level of integrin expression in our cell lines, RT-PCR and flow cytometry analysis were performed. The wild-type MEFs and MKFs expressed high levels (> 90%) of αV, β1 and β3 integrin subunits which is in accordance with a previous report (Schmidt *et al.*, 2013a). Concerning the integrin deficient cells, flow cytometry results demonstrated the total absence of either αVβ3 integrin (MEF-αVβ3$^{-/-}$), β3 (MEF-β3$^{-/-}$) or β1 (MKF-β1$^{-/-}$) integrin subunits in the respective cell lines which has been described before (Fassler *et al.*, 1995a; Schmidt *et al.*, 2013a).

There have been controversies in the literature whether the deletion of one specific integrin could up- or down-regulate the expression of other integrins. In our study, we did not determine up- or down-regulation of other integrin subunits in response to deletion of αV, β1 or β3 integrin subunits. However, our observations demonstrated that levels of β1 integrin expression in MEF-αVβ3$^{-/-}$ and MEF-β3$^{-/-}$ cells or αV and β3 integrin expression in MKF-β1$^{-/-}$ cells remained constant according to the flow cytometry analysis. A study using human cardiac fibroblasts reported that β3 integrin gene *knock-down* by siRNA upregulated the expression of β5 integrin subunit. The opposite effect of β3 integrin upregulation was observed when β5 integrin subunit was silenced, demonstrating a compensatory effect between both integrin subunits (Sarrazy *et al.*, 2014). Another study showed that α2β1 integrin in keratinocytes was substituted by other collagen binding integrins such as α1β1 or α11β1 integrin in α2 *knock-out*-mice (Zhang *et al.*, 2006). On the other hand, two studies reported no compensatory effects in αV and β3 integrin-null mice (Bader *et al.*, 1998; Hodivala-Dilke *et al.*, 1999). As the level of integrin subunits other than αV, β1 and β3 was not determined in our study, a compensatory effect can only be assumed.

Transfection of CHO cells with a vector carrying either the mouse αV or β3 integrin subunit genes resulted in clones stably expressing mouse αV or β3 integrin subunits as demonstrated by RT-PCR and flow cytometry analysis. Flow cytometry revealed expression of high levels of mouse αV and β3 integrin subunits. As mentioned above, CHO cells are known to express only a few integrins. However, a study demonstrated the expression of endogenous β1 integrin and αV integrin subunits (Takagi *et al.*, 1997). Due to unknown reasons, this hamster αV integrin subunit was not expressed on the cell surface (Takagi *et al.*, 1997). In our study, we assume that the ectopic expression of mouse β3 integrin subunit in CHO cells was able to rescue the expression of hamster αV since we detected the mouse β3 integrin subunit at the cell surface. This assumption is supported by the fact that β3 integrin subunit is only described to form heterodimers with αV or αIIb integrin subunits, the latter being exclusively expressed in megakaryocytes and platelets (Bennett, 2005; Hynes, 2002). The formation of hamster/mouse "hybrid" integrins such as α5β1, α3β1, αVβ1 and αVβ3 was also reported by other authors (Balzac *et al.*, 1993; Felding-Habermann *et al.*, 1997; Laukaitis *et al.*, 2001; Zhang *et al.*, 1993).

Finally, to confirm whether the integrins expressed in CHO cells are functional and able to recognize their ligands, a cell adhesion assay was performed. In this assay, both CHO cell lines expressing hamster/mouse

hybrid integrins showed to recognize vitronectin as their integrin ligand while CHO-K1 cells bound less efficiently to vitronectin. This observation confirmed the functionality of the hybrid integrins expressed in CHO cells and is also reported by other authors (Balzac *et al.*, 1993; Felding-Habermann *et al.*, 1997; Zhang *et al.*, 1993).

In the same assay, integrin-deficient MEFs and MKFs bound less efficiently to vitronectin than their respective wild-type cells. However, binding was observed for all cell lines regardless of absence or presence of αV, β1 or β3 integrin subunits. Though the present study was focused on αV, β1 and β3 integrin subunits, these results provide evidence that MEF-αVβ3^{-/-}, MEF-β3^{-/-} and MKF-β1^{-/-} cells may indeed express other RGD binding integrins. However, the expression level of these RGD binding integrin heterodimers in our MEF and MKF cell lines is unknown.

5.4) Cell infection assays

5.4.1) Flavivirus binding to the cell surface is not enhanced by the presence of integrins

In order to analyze the influence of integrins in flavivirus binding to the cell surface, binding assays were performed by infecting the cells at 4°C which allows virus binding but prevents virus internalization. In our study, we clearly demonstrate that αVβ3, β1 and β3 integrin subunits are not involved in flavivirus binding to the cell surface of MEFs, MKFs and CHO cells expressing either αV or β3 integrin subunits. Even in the case of YFV-17D that harbors the RGD motif which is an integrin binding motif, the virus binding to the cell surface of MEF and MKF cells was not affected by the deletion of integrin subunits in the respective cells. Interestingly, van der Most *et al.*,(1999) explicitly demonstrated that, by introducing mutations in the RGD motif of YFV-17D, the absence of this motif had no impact on YFV-17D binding and infectivity (van der Most *et al.*, 1999). These observations are consistent with the results from our study demonstrating that the presence of RGD motif in YFV-17D does not affect YFV-17D binding to integrins. Our results rather suggest that other molecules than integrins are used by flaviviruses to promote binding. Several other molecules were reported as flavivirus binding/attachment receptor such as laminin, DC-SIGN and GAGs (Perera-Lecoin *et al.*, 2013). Among those, GAGs have been reported to mediate flavivirus binding to a variety of cells (Chen *et al.*, 1997; Chien *et al.*, 2008; Germi *et al.*, 2002; Hilgard *et al.*, 2000; Kim *et al.*, 2017; Kroschewski *et al.*, 2003; Lee *et al.*, 2004; Lin *et al.*, 2002). Since GAGs are expressed in a wide variety of cells, including MEFs and CHO cells (Bame *et al.*, 1989; Bernfield *et al.*, 1999; Cuellar *et al.*, 2007; Kraushaar *et al.*, 2013; Llorente-Cortes *et al.*, 2002), the presence of these molecules might overlap the interaction of integrins with flaviviruses during the early steps of infection. As a result, flaviviruses might preferentially bind to GAGs rather than integrins. The GAG interactions with E-DIII proteins are characterized by electrostatic interaction that generally lacks specificity and shows low affinity (Smit *et al.*,

2011). A few studies have documented that the presence of GAGs on the cell surface of CHO cells mediate virus binding. A study with WNV using a derivative CHO cell line deficient for GAGs demonstrated that WNV binding to the cell surface was strikingly impaired in comparison with the CHO wild-type cells further supporting the role of GAGs in flavivirus attachment in CHO cells (Schmidt, 2012). In addition to that, Jan *et al.*,(1999) demonstrated that Sindbis virus, an arbovirus in the *Alphavirus* genus (*Togaviridae* family) bound to the cell surface of CHO cells. Upon CHO cell treatment with heparinase I, virus binding was decreased by more than 20% compared to the untreated control, demonstrating that GAGs also act as an attachment factor for other arboviruses such as Sindbis virus in CHO cells (Jan *et al.*, 1999).

Another important issue to be mentioned is the flavivirus strains used in this study. With the exception of USUV and ZIKV, all other strains are considered vaccine strains (YFV-17D and WNV-chimerivax) or attenuated strains (LGTV). It was previously reported that serial *in-vitro* passages of flaviviruses raise cell culture-adapted viral populations with GAG binding residues in the flavivirus E-DIII protein. This characteristic has been attributed to virus attenuation, a desired feature in virus vaccine strains (Lee *et al.*, 2002; Lee *et al.*, 2006a). In our study, we did not compare wild-type viruses with their respective vaccine/attenuated strains. Thus, comparisons between flavivirus vaccine strains and their respective virulent strains might be helpful to further elucidate a potential role of integrins in flavivirus binding to the host cell. So far, all our observations suggest the presence of a common attachment factor in MEFs/MKFs and CHO cells that mediate flavivirus binding.

In order to verify whether other integrins are involved in flavivirus binding, we performed a binding inhibition assay in MEFs using three different integrin ligands: synthetic RGD peptide and vitronectin that bind to RGD binding integrins and type-I collagen that binds all collagen-binding integrins. Binding inhibition assays using integrin ligands as well as integrin epitope blocking antibodies are widely used to test the ability of these molecules to block integrin-mediated virus binding and internalization. For example, FMDV uses αvβ8 integrin to mediate binding to and internalization into SW40 cells, a human colon cancer cell line. Cell treatment with synthetic RGD motif as well as antibodies against the αv integrin subunit completely abrogated FMDV binding and infection of the cells (Jackson *et al.*, 2004). Similarly, Berinstein *et al.*,(1995) demonstrated that αvβ3 integrin was implicated in FMDV binding to the host cell and internalization. In this study, antibodies against the αvβ3 integrin inhibited binding and plaque formation upon infection in *Macaca mulatta* kidney (LLC-MK) cells while antibodies against the α5β1 integrin could not inhibit FMDV binding and plaque formation (Berinstein *et al.*, 1995).

In our study, cell treatment with the synthetic integrin ligands had clearly no influence on flavivirus binding to the cell surface of MEFs. These results strikingly contradict those of two other groups who demonstrated that cell treatment with synthetic RGD motif or epitope blocking antibodies inhibited WNV and JEV binding to Vero and BHK cells, respectively (Chu *et al.*, 2004b; Fan *et al.*, 2017). Instead, our results

100

are in accordance with those proposed by two groups who demonstrated that WNV binding to the target cells is not inhibited by integrin epitope-blocking antibodies and is rather independent of integrins (Medigeshi *et al.*, 2008; Schmidt *et al.*, 2013a). A similar assay used in our study to evaluate the ability of integrin ligands to inhibit virus infection was also used by other authors for different viruses (Jackson *et al.*, 2002; La Linn *et al.*, 2005; Wickham *et al.*, 1993). Taken together, the results provided by the binding assay as well as by the binding inhibition assay strongly suggest that integrins are not involved in flavivirus binding to the cell surface.

5.4.2) Lack of integrins does not abrogate flavivirus internalization

Due to the fact that integrin activation promotes internalization of several viruses (Hussein *et al.*, 2015; Triantafilou *et al.*, 2001), it was hypothesized whether flaviviruses might also use this route to enter the host cell. In the present study, the absence of αVβ3 integrin and β1 and β3 integrin subunits did not abrogate flavivirus entry. However, we found evidences that the internalization of some flaviviruses into MEFs might be affected by the deletion of integrins. To assess the statistical significance between these groups, a parametric Student's *t*-test was applied since the samples were unpaired and the measured values were normally distributed. Although statistical analyses demonstrated significant differences in internalization of USUV, WNV and ZIKV ($p < 0.001$, $p < 0.0001$, and $p < 0.001$ respectively) in MEF-WT cells compared to MEF-αVβ3$^{-/-}$ cells, the absolute differences observed were modest and have apparently a limited biological relevance. The same effect was observed for LGTV ($p = 0.0318$) in MEF-β3$^{+/+R}$ cells and for ZIKV in MEF-β3$^{+/+R}$ cells ($p = 0.0341$) and MEF-αVβ3$^{-/-}$ cells ($p = 0.0007$) compared to the respective integrin deficient cells. These significant differences might be explained by the fact that each of the compared groups had only small standard deviations among their sample values. Therefore, even small differences between the mean values of the two compared groups might result in statistical significance. Analysis of measurements from RT-qPCR showed clearly that the differences between the compared groups were substantially small even before log transformation.

Since the αVβ3, β1 and β3 integrin deficient cells used in our study express other integrins, we cannot definitely exclude the involvement of these other integrins in flavivirus internalization. In the case of adenoviruses that have multiple RGD sequences displayed in the adenovirus penton base, αVβ3 and αVβ5 integrins were shown to mediate virus internalization (Wickham *et al.*, 1993). However, these integrins have no influence on adenovirus attachment suggesting that other molecules such as heparan sulfate are utilized as attachment factor (Wickham *et al.*, 1993). Thus, similar to what was described for adenoviruses, it might be conceivable that flaviviruses first bind to an unspecific attachment factor and then subsequently to integrins to promote virus internalization. Another study demonstrated that upon

adenovirus binding, virus interaction with αV integrin subunit leads to FAK phosphorylation and virus internalization (Li *et al.*, 1998). Moreover, Chu *et al.*,(2004a) reported that upon WNV binding to αVβ3 integrin, FAK was phosphorylated indicating an activation of intracellular signaling (Chu *et al.*, 2004a). In contrast to these results, another group demonstrated that WNV infectivity is independent of FAK phosphorylation by using FAK deficient mouse embryonic fibroblasts (Medigeshi *et al.*, 2008). Whether other flaviviruses rather than WNV lead to FAK phosphorylation should be further investigated.

Since integrin recognition motifs are not required for viruses to interact with integrins as described for hantaviruses, it might be possible that flaviviruses still use intergrins for internalization. Neither pathogenic nor non-pathogenic hantaviruses have integrin ligand motifs although hantavirus interaction with integrins was demonstrated by several studies (Gavrilovskaya *et al.*, 1999; Gavrilovskaya *et al.*, 1998). However, another study demonstrated that hantaviruses bind to another integrin region, the plexin-semaphorin-integrin domain (PSI), which then mediates hantavirus infection in CHO cells (Raymond *et al.*, 2005). Whether these atypical interactions occur during flavivirus internalization is unknown and should be further addressed.

Interestingly, studies demonstrated that HCMV gB and gH proteins do not display any canonical integrin ligand motifs such as RGD but only a highly conserved disintegrin-like domain that mediates interactions with integrins (Feire *et al.*, 2004; Feire *et al.*, 2010) and use αVβ3 integrin as co-receptor (Wang *et al.*, 2005). This is then followed by the activation of integrin intracellular signaling and consequent virus entry into human embryonic lung fibroblasts (Wang *et al.*, 2005). Another study demonstrated that integrins are not involved in the attachment of HCMV but rather in a post-attachment step mediating HCMV internalization into the host cell (Feire *et al.*, 2004). According to these results, one might speculate whether flaviviruses use integrins as co-receptor to mediate flavivirus internalization in a similar manner as to what was observed for HCMV. In addition, these two studies mentioned above highlight an interaction of viruses containing a disintegrin-like domain. According to our knowledge, the presence of a disintegrin-like domain in the flavivirus E protein has never been reported and should be further investigated.

In sum, the results provived by our internalization assay suggest that αVβ3 integrin and β3 integrin subnit might be involved in the internalization of some flaviviruses (WNV, USUV, LGTV) tested in this study. However, the results should be interpreted carefully since i) the absolute differences between wild-type and integrin deficient cells were considered to be modest although statistically significant; ii) flavivirus species-specific differences in integrin usage might occur and iii) the involvement of other integrins in flavivirus internalization cannot be completely excluded. Therefore, further investigations should be performed in order to elucidate the role of integrins in flavivirus internalization.

5.4.3) Integrins modulate flavivirus replication

In the viral replication kinetics assay, MEFs and MKFs were infected with different flaviviruses at a very low MOI which in turn allowed to analyze the permissiveness and replication efficiency in both integrin deficient and their respective wild-type cells. All cell lines including the integrin-deficient MEFs and MKFs were susceptible and permissive to flavivirus infection. Regardless of the integrin expression, viral infection led to production of infectious viruses that were later quantified by $TCID_{50}$. In the case of CHO cells, infection at a very low MOI did not produce detectable viral titers confirming the hypothesis that CHO cells are refractory and not permissive to flavivirus infection. This resistance to flavivirus infection is also reported by other authors (Berting *et al.*, 2010; Fan *et al.*, 2017). Based on the observations in MEFs and MKFs in our replication kinetics experiments, we can however reject the hypothesis that αVβ3 integrin, β1 or β3 integrin subunits act as flavivirus receptors. These observations were also reported by other authors (Medigeshi *et al.*, 2008; Schmidt *et al.*, 2013a). Although all flaviviruses in our study were able to infect MEF and MKF cell lines independent of the integrin expression, the replication efficiency in the integrin deficient cells was substantially impaired compared to the respective wild-type cells. Most notably, in the replication assay, ablation of integrins in MEF-αVβ3^{-/-} cells influenced the flavivirus replication efficiency with a reduction of viral load by more than 90% as well as a strong decrease on virus titers for all the viruses tested indicating that integrins indeed play a role in flavivirus replication. The involvement of αVβ3 integrin in virus infection has been extensively reported for several other viruses such as HCMV, HHV-1, FMDV and adenoviruses (Berinstein *et al.*, 1995; Parry *et al.*, 2005; Wang *et al.*, 2005; Wickham *et al.*, 1993).

Moreover, we demonstrated that ablation of integrins had a negative effect on flavivirus RNA replication by measuring the amount of flavivirus negative-strand RNA in MEF-αVβ3^{-/-} cells. These findings implicate that integrins might be indirectly involved in flavivirus RNA replication and may thus serve as a host cell factor. Several host cell factors have been described to influence the flavivirus RNA replication including the synthesis of flavivirus negative-strand RNA such as the reticulon protein (Aktepe *et al.*, 2017) and AUF1p45 chaperone proteins (Friedrich *et al.*, 2017) for DENV, ZIKV and WNV. To our knowledge, this is the first study reporting the involvement of αVβ3 integrin in YFV, USUV, LGTV and ZIKV RNA replication. Although the exact mechanism of how integrins modulate flavivirus RNA replication is currently unknown, we provide strong evidence that integrin expression, in particular the αVβ3 integrin, influences flavivirus RNA replication. The integrin-mediated modulatory effects on members of the *Flaviviridae* family in virus infection have also been explored by other authors (Fan *et al.*, 2017; Li *et al.*, 2014; Schmidt *et al.*, 2013a). The total loss of αVβ3 integrin in MEF-αVβ3^{-/-} cells profoundly impaired WNV replication in our study indicating that both integrin subunits might be fundamental for WNV replication. However, we did not observe a very strong inhibition in MEF-β3^{-/-} cells infected with the WNV vaccine strain. Nonetheless,

Schmidt *et al.*,(2013a) demonstrated that the replication of four different pathogenic WNV strains was indeed impaired in β3 integrin *knock-out* MEFs suggesting that the β3 integrin subunit plays an important role in WNV replication. In the same study, the authors reported that rescue of β3 integrin subunit in the *knock-out* cell line enhanced viral RNA yields by more than 90% (Schmidt *et al.*, 2013a). These discrepancies observed between the two studies might be explained by the different WNV strains used.

Silencing or blocking of αV and β3 integrin subunits substantially impaired JEV replication in two different cell lines according to studies performed by Fan *et al.*,(2017). Similar to what was found in our study, the downregulation of either αV or β3 integrin subunits in BHK-21 cells led to a 2-4 fold decrease of JEV replication, stressing the importance of αVβ3 integrin in flavivirus replication (Fan *et al.*, 2017).

CSFV was demonstrated to profit from the expression of β3 integrin subunit enhancing infection and proliferation in porcine cells. One study showed that, upon infection, CSFV up-regulated the expression of β3 integrin subunit in porcine endothelial cells (Tang *et al.*, 2010). In another study, the authors reported that CSFV replicated and proliferated efficiently in cells expressing high levels of β3 integrin subunits (Li *et al.*, 2014). Moreover, silencing of β3 integrin subunit mRNA inhibited more than 90% of CSFV replication as well as virus dissemination indicating that expression of this specific integrin subunit is beneficial for CSFV replication (Li *et al.*, 2014). It remains unclear whether the αV integrin subunit is still expressed after downregulation by siRNA in the porcine cell line used in this study and at which step of the CSFV infection cycle integrins are required. However, these results are consistent with the results from our study suggesting that αVβ3 integrin might be an important mutual factor that modulates replication efficiency of certain members within the *Flaviviridae* family.

The replication assay with MKF-β1$^{-/-}$ cells demonstrated that deletion of β1 integrin subunit negatively affected the replication of YFV-17D and WNV. To our knowledge, besides the present study and the study by Schmidt *et al.*,(2013a) who demonstrated that β1 integrin subunit is important for WNV replication, there are no publications highlighting the importance of β1 integrin subunit in flavivirus infection. Interestingly, USUV, LGTV and ZIKV did not require the expression of β1 integrin subunit for their replication. On the contrary, LGTV and ZIKV replication in MKF-β1$^{-/-}$ cells was clearly increased compared to MKF-β1^{Flox} cells resulting in a higher viral load and viral titers. Similar results were described by another group for the deletion of β3 integrin subunit in MEFs which led to higher WNV titers in comparison to the wild-type cells (Medigeshi *et al.*, 2008). One possible explanation for these effects might be the presence of αVβ3 integrin expression in MKF-β1$^{-/-}$ cells as demonstrated by flow cytometry and immunofluorescence assay in this study. Further, the replication assays indicated that αVβ3 integrin expression is of great importance for the replication of all investigated flaviviruses. Thus, one might speculate whether the expression of αVβ3 integrin in MKF-β1$^{-/-}$ cells might compensate for the lack of β1

integrin subunit expression thus enhancing the replication of LGTV and ZIKV. Additionally, the deletion of β1 integrin might upregulate other integrins potentially affecting replication of LGTV and ZIKV.

In sum, the results provided from the replication assays indicate that integrins, in particular the αVβ3 integrin, are of great importance for flavivirus replication in mouse fibroblasts.

We also investigated the involvement of integrins in flavivirus infection by generating CHO cells expressing either mouse αV or β3 integrin subunits. Our results demonstrated that flaviviruses are able to bind to CHO cells, regardless of the expression of integrins indicating that a binding receptor or attachment factor for flaviviruses is present in CHO cells. Replication of investigated flaviviruses in CHO-K1 wild-type cells was substantially impaired which is in accordance to the literature where CHO cells are described to be non-permissive to several viral agents including flaviviruses (Berting *et al.*, 2010). Interestingly, upon ectopic expression of mouse αV or β3 integrin subunits in CHO cells, the flavivirus replication was slightly increased upon inoculation with a high MOI (10). The expression of αV integrin subunit increased the replication of USUV and YFV-17D whereas expression of β3 integrin subunit increased replication of WNV and LGTV. For ZIKV, ectopic expression of either αV or β3 integrin subunits in CHO cells did not enhance replication. Similar to our results, Fan *et al.*,(2017) demonstrated slightly increased JEV replication in CHO cells expressing the β3 integrin subunit suggesting a beneficial effect of β3 integrin subunit in JEV replication (Fan *et al.*, 2017).

Genomic analysis revealed that CHO cells lack the expression of 158 important genes that are involved in virus entry and replication including integrin genes (Xu *et al.*, 2011). The absence of all these genes in CHO cells might explain their remarkable resistance to viral agents including flaviviruses as previously reported by Berting *et al.*,(2010). Taking that into account, we assume that flavivirus entry and replication in CHO cells cannot be fully recovered only by ectopic expression of integrins. Thus, in the specific case of CHO cells, integrins might only play a minor role in CHO cell susceptibility and permissiveness to flaviviruses. Although our results demonstrate that integrin expression in CHO cells increases flavivirus replication, these effects were only modest and should be interpreted carefully. Further studies should be performed in order to elucidade the CHO cell resistance to flaviviruses, and to determine at which step of flavivirus infection cycle the blockade occurs.

It is well-understood that integrins control several cellular downstream pathways that might culminate in diverse cellular responses such as cytoskeleton rearrangments and changes in the cellular environment (Harburger *et al.*, 2009). In this sense, it might be possible that the expression of several host cell factors which influence virus replication might be directly or indirectly under control of the integrin expression. For example, Ebola virus (EBOV - *Filoviridae* family, *Ebolavirus* genus) was shown to benefit from the expression of integrins to complete its replication cycle. Although integrins are not required for EBOV

binding and internalization, integrins regulate the expression of cathepsin B and L, two proteases that are necessary to prime EBOV glycoprotein triggering virus fusion with the host cell (Schornberg *et al.*, 2009). These results stress the possible influence of integrins on other cellular organelles and in regulating the expression of certain genes that may influence the outcome of a viral infection. The magnitude of interactions between integrins and several cellular molecules have been continuously described in the literature: these interactions are described as the so-called "Integrin adhesome" which comprises more than 200 molecules resulting in more than 690 interactions of integrins with numerous cellular proteins (Horton *et al.*, 2016; Zaidel-Bar *et al.*, 2007). Based on these facts, it is easily conceivable that other cellular proteins affecting flavivirus replication might be under the control of integrins.

Taken together, the expression of integrins clearly affected flavivirus replication in the investigated cell lines from our study suggesting integrins as a new flavivirus host cell factor. A mechanism of how integrins influence flavivirus replication in MEFs, MKFs or CHO cells has not yet been elucidated. However, in this study, the integrin-mediated modulation of flavivirus replication in different integrin deficient cells was clearly demonstrated by the following findings:

(i)   the deletion of αVβ3 integrin significantly affected the replication of YFV-17D, WNV, USUV, LGTV and ZIKV with a reduction of more than 90% on viral RNA yields;

(ii)   the levels of flavivirus negative-strand RNA were strongly reduced in αVβ3 integrin deficient cells;

(iii)   the deletion of β1 or β3 integrin subunits had a small and/or no effect on flavivirus replication depending on the flavivirus tested and

(iv)   although ectopic expression of integrins in CHO cell had no impact on flavivirus binding, their expression slightly increased flavivirus replication

5.5) Conclusions and outlook

The present study is the first that demonstrates the involvement of integrins in flavivirus infection for four medically relevant flaviviruses (YFV, USUV, LGTV and ZIKV) while this had been described for WNV and JEV before. The major findings of the present study are:

(i)   the deletion of either αVβ3 integrin, β3 or β1 integrin subunit in MEFs and MKFs did not affect flavivirus binding to the cell surface;

(ii)   the expression of either αV or β3 integrin subunit in CHO cells did not enhance flavivirus binding to the cell surface;

(iii)   the internalization of some flaviviruses was impaired by the deletion of αVβ3 integrin and β3 integrin subunit while the deletion of β1 integrin subunit had no effect;

(iv)   the replication of all flaviviruses tested in this study was strongly inhibited in αVβ3 integrin deficient cells with a reduction of more than 90% on viral load;

(v)   the deletion of β1 or β3 integrin subunits resulted only in slightly reduced flavivirus replication;

(vi)   the ectopic expression of αV or β3 integrin subunits in CHO cells slightly increased the replication of some flaviviruses.

The mechanism of how integrins modulate flavivirus replication has not yet been completely elucidated. There are some specific aspects in regard to integrins and their modulation of flavivirus infection that should be addressed in future:

(i)   to analyze whether the activation of integrin-associated intracellular pathways is triggered upon flavivirus infection;

(ii)   to investigate whether the downregulation or ablation of integrins, in particular αVβ3 integrin, impairs or downregulates the expression of other molecules that will influence flavivirus infection/replication;

(iii)   to examine whether the replication of other flaviviruses including virulent and low-passage strains is also disrupted by integrin *knock-out*;

(iv)   to investigate whether the integrin-mediated effect on flavivirus replication also applies to other cell lines from different host species and

(v)   to closely monitor flavivirus replication by usage of replicon systems in order to better understand how integrins modulate flavivirus RNA replication.

In conclusion, the results achieved in the present study provided strong evidence that integrins play a role in flavivirus infection, particularly in replication and thus might act as a new flavivirus host cell factor modulating the flavivirus infection cycle.

6) References

Acosta, E. G.; Castilla, V. and Damonte, E. B. (2009). Alternative infectious entry pathways for dengue virus serotypes into mammalian cells. Cell Microbiol **11**(10): 1533-1549.

Adams, M. J.; Lefkowitz, E. J.; King, A. M. Q.; Harrach, B.; Harrison, R. L.; Knowles, N. J.; Kropinski, A. M.; Krupovic, M.; Kuhn, J. H.; Mushegian, A. R.; Nibert, M.; Sabanadzovic, S.; Sanfacon, H.; Siddell, S. G.; Simmonds, P.; Varsani, A.; Zerbini, F. M.; Gorbalenya, A. E. and Davison, A. J. (2017). Changes to taxonomy and the International Code of Virus Classification and Nomenclature ratified by the International Committee on Taxonomy of Viruses (2017). Arch Virol **162**(8): 2505-2538.

Afratis, N.; Gialeli, C.; Nikitovic, D.; Tsegenidis, T.; Karousou, E.; Theocharis, A. D.; Pavao, M. S.; Tzanakakis, G. N. and Karamanos, N. K. (2012). Glycosaminoglycans: key players in cancer cell biology and treatment. FEBS J **279**(7): 1177-1197.

Aguilera-Pesantes, D.; Robayo, L. E.; Mendez, P. E.; Mollocana, D.; Marrero-Ponce, Y.; Torres, F. J. and Mendez, M. A. (2017). Discovering key residues of dengue virus NS2b-NS3-protease: New binding sites for antiviral inhibitors design. Biochem Biophys Res Commun **492**(4): 631-642.

Ahmed, S.; Libman, R.; Wesson, K.; Ahmed, F. and Einberg, K. (2000). Guillain-Barre syndrome: An unusual presentation of West Nile virus infection. Neurology **55**(1): 144-146.

Aktepe, T. E.; Liebscher, S.; Prier, J. E.; Simmons, C. P. and Mackenzie, J. M. (2017). The Host Protein Reticulon 3.1A Is Utilized by Flaviviruses to Facilitate Membrane Remodelling. Cell Rep **21**(6): 1639-1654.

Akula, S. M.; Pramod, N. P.; Wang, F. Z. and Chandran, B. (2002). Integrin alpha3beta1 (CD 49c/29) is a cellular receptor for Kaposi's sarcoma-associated herpesvirus (KSHV/HHV-8) entry into the target cells. Cell **108**(3): 407-419.

Allering, L.; Jost, H.; Emmerich, P.; Gunther, S.; Lattwein, E.; Schmidt, M.; Seifried, E.; Sambri, V.; Hourfar, K. and Schmidt-Chanasit, J. (2012). Detection of Usutu virus infection in a healthy blood donor from south-west Germany, 2012. Euro Surveill **17**(50).

Amicizia, D.; Domnich, A.; Panatto, D.; Lai, P. L.; Cristina, M. L.; Avio, U. and Gasparini, R. (2013). Epidemiology of tick-borne encephalitis (TBE) in Europe and its prevention by available vaccines. Hum Vaccin Immunother **9**(5): 1163-1171.

Angart, P.; Vocelle, D.; Chan, C. and Walton, S. P. (2013). Design of siRNA Therapeutics from the Molecular Scale. Pharmaceuticals (Basel) **6**(4): 440-468.

Aricescu, A. R. and Jones, E. Y. (2007). Immunoglobulin superfamily cell adhesion molecules: zippers and signals. Curr Opin Cell Biol **19**(5): 543-550.

Arroyo, J.; Miller, C.; Catalan, J.; Myers, G. A.; Ratterree, M. S.; Trent, D. W. and Monath, T. P. (2004). ChimeriVax-West Nile virus live-attenuated vaccine: preclinical evaluation of safety, immunogenicity, and efficacy. J Virol **78**(22): 12497-12507.

Artsob, H. (2000). Arthropod-borne disease in Canada: A clinician's perspective from the 'Cold Zone'. Paediatr Child Health **5**(4): 206-212.

Asghar, N.; Lee, Y. P.; Nilsson, E.; Lindqvist, R.; Melik, W.; Kroger, A.; Overby, A. K. and Johansson, M. (2016). The role of the poly(A) tract in the replication and virulence of tick-borne encephalitis virus. Sci Rep **6**: 39265.

Ashraf, U.; Ye, J.; Ruan, X.; Wan, S.; Zhu, B. and Cao, S. (2015). Usutu virus: an emerging flavivirus in Europe. Viruses **7**(1): 219-238.

Askari, J. A.; Buckley, P. A.; Mould, A. P. and Humphries, M. J. (2009). Linking integrin conformation to function. J Cell Sci **122**(Pt 2): 165-170.

Avirutnan, P.; Fuchs, A.; Hauhart, R. E.; Somnuke, P.; Youn, S.; Diamond, M. S. and Atkinson, J. P. (2010). Antagonism of the complement component C4 by flavivirus nonstructural protein NS1. J Exp Med **207**(4): 793-806.

Avirutnan, P.; Hauhart, R. E.; Somnuke, P.; Blom, A. M.; Diamond, M. S. and Atkinson, J. P. (2011). Binding of flavivirus nonstructural protein NS1 to C4b binding protein modulates complement activation. J Immunol **187**(1): 424-433.

Back, A. T. and Lundkvist, A. (2013). Dengue viruses - an overview. Infect Ecol Epidemiol **3**.

Bader, B. L.; Rayburn, H.; Crowley, D. and Hynes, R. O. (1998). Extensive vasculogenesis, angiogenesis, and organogenesis precede lethality in mice lacking all alpha v integrins. Cell **95**(4): 507-519.

Balcioglu, H. E.; van Hoorn, H.; Donato, D. M.; Schmidt, T. and Danen, E. H. (2015). The integrin expression profile modulates orientation and dynamics of force transmission at cell-matrix adhesions. J Cell Sci **128**(7): 1316-1326.

Baleotti, F. G.; Moreli, M. L. and Figueiredo, L. T. (2003). Brazilian Flavivirus phylogeny based on NS5. Mem Inst Oswaldo Cruz **98**(3): 379-382.

Balzac, F.; Belkin, A. M.; Koteliansky, V. E.; Balabanov, Y. V.; Altruda, F.; Silengo, L. and Tarone, G. (1993). Expression and functional analysis of a cytoplasmic domain variant of the beta 1 integrin subunit. J Cell Biol **121**(1): 171-178.

Bame, K. J. and Esko, J. D. (1989). Undersulfated heparan sulfate in a Chinese hamster ovary cell mutant defective in heparan sulfate N-sulfotransferase. J Biol Chem **264**(14): 8059-8065.

Barrett, A. D. and Higgs, S. (2007). Yellow fever: a disease that has yet to be conquered. Annu Rev Entomol **52**: 209-229.

Bartholomeusz, A. and Thompson, P. (1999). Flaviviridae polymerase and RNA replication. J Viral Hepat **6**(4): 261-270.

Beck, C.; Jimenez-Clavero, M. A.; Leblond, A.; Durand, B.; Nowotny, N.; Leparc-Goffart, I.; Zientara, S.; Jourdain, E. and Lecollinet, S. (2013). Flaviviruses in Europe: complex circulation patterns and their consequences for the diagnosis and control of West Nile disease. Int J Environ Res Public Health **10**(11): 6049-6083.

Bendas, G. and Borsig, L. (2012). Cancer cell adhesion and metastasis: selectins, integrins, and the inhibitory potential of heparins. Int J Cell Biol **2012**: 676731.

Bennett, J. S. (2005). Structure and function of the platelet integrin alphaIIbbeta3. <u>J Clin Invest</u> **115**(12): 3363-3369.

Bergmeier, W. and Hynes, R. O. (2012). Extracellular matrix proteins in hemostasis and thrombosis. <u>Cold Spring Harb Perspect Biol</u> **4**(2).

Berinstein, A.; Roivainen, M.; Hovi, T.; Mason, P. W. and Baxt, B. (1995). Antibodies to the vitronectin receptor (integrin alpha V beta 3) inhibit binding and infection of foot-and-mouth disease virus to cultured cells. <u>J Virol</u> **69**(4): 2664-2666.

Bernfield, M.; Gotte, M.; Park, P. W.; Reizes, O.; Fitzgerald, M. L.; Lincecum, J. and Zako, M. (1999). Functions of cell surface heparan sulfate proteoglycans. <u>Annu Rev Biochem</u> **68**: 729-777.

Berting, A.; Farcet, M. R. and Kreil, T. R. (2010). Virus susceptibility of Chinese hamster ovary (CHO) cells and detection of viral contaminations by adventitious agent testing. <u>Biotechnol Bioeng</u> **106**(4): 598-607.

Besnard, M.; Lastere, S.; Teissier, A.; Cao-Lormeau, V. and Musso, D. (2014). Evidence of perinatal transmission of Zika virus, French Polynesia, December 2013 and February 2014. <u>Euro Surveill</u> **19**(13).

Bessaud, M.; Pastorino, B. A.; Peyrefitte, C. N.; Rolland, D.; Grandadam, M. and Tolou, H. J. (2006). Functional characterization of the NS2B/NS3 protease complex from seven viruses belonging to different groups inside the genus Flavivirus. <u>Virus Res</u> **120**(1-2): 79-90.

Bhella, D. (2015). The role of cellular adhesion molecules in virus attachment and entry. <u>Philos Trans R Soc Lond B Biol Sci</u> **370**(1661): 20140035.

Blitvich, B. J. and Firth, A. E. (2015). Insect-specific flaviviruses: a systematic review of their discovery, host range, mode of transmission, superinfection exclusion potential and genomic organization. <u>Viruses</u> **7**(4): 1927-1959.

Blitvich, B. J. and Firth, A. E. (2017). A Review of Flaviviruses that Have No Known Arthropod Vector. <u>Viruses</u> **9**(6).

Boettcher, M. and McManus, M. T. (2015). Choosing the Right Tool for the Job: RNAi, TALEN, or CRISPR. <u>Mol Cell</u> **58**(4): 575-585.

Bogovic, P. and Strle, F. (2015). Tick-borne encephalitis: A review of epidemiology, clinical characteristics, and management. <u>World J Clin Cases</u> **3**(5): 430-441.

Bokel, C. and Brown, N. H. (2002). Integrins in development: moving on, responding to, and sticking to the extracellular matrix. <u>Dev Cell</u> **3**(3): 311-321.

Bollati, M.; Alvarez, K.; Assenberg, R.; Baronti, C.; Canard, B.; Cook, S.; Coutard, B.; Decroly, E.; de Lamballerie, X.; Gould, E. A.; Grard, G.; Grimes, J. M.; Hilgenfeld, R.; Jansson, A. M.; Malet, H.; Mancini, E. J.; Mastrangelo, E.; Mattevi, A.; Milani, M.; Moureau, G.; Neyts, J.; Owens, R. J.; Ren, J.; Selisko, B.; Speroni, S.; Steuber, H.; Stuart, D. I.; Unge, T. and Bolognesi, M. (2010). Structure and functionality in flavivirus NS-proteins: perspectives for drug design. <u>Antiviral Res</u> **87**(2): 125-148.

Brabant, M.; Baux, L.; Casimir, R.; Briand, J. P.; Chaloin, O.; Porceddu, M.; Buron, N.; Chauvier, D.; Lassalle, M.; Lecoeur, H.; Langonne, A.; Dupont, S.; Deas, O.; Brenner, C.; Rebouillat, D.; Muller, S.; Borgne-Sanchez, A. and Jacotot, E. (2009). A flavivirus protein M-derived peptide directly permeabilizes

mitochondrial membranes, triggers cell death and reduces human tumor growth in nude mice. <u>Apoptosis</u> **14**(10): 1190-1203.

Brault, J. B.; Kudelko, M.; Vidalain, P. O.; Tangy, F.; Despres, P. and Pardigon, N. (2011). The interaction of flavivirus M protein with light chain Tctex-1 of human dynein plays a role in late stages of virus replication. <u>Virology</u> **417**(2): 369-378.

Brazillian Ministry of Health - MS (2016a, 06.01.17). "MONITORAMENTO DOS CASOS DE MICROCEFALIA NO BRASIL." Retrieved 15.05.17, 2017, from http://combateaedes.saude.gov.br/images/pdf/Informe-Epidemiologico-n57-SE-52_2016-09jan2017.pdf.

Brazillian Ministry of Health - MS (2016b, 12.12.16). "Situação Epidemiológica de Zika, Brasil, Semana Epidemiológica 1 a 49/2016." Retrieved 15.05.2017, 2017, from http://portalsaude.saude.gov.br/index.php/situacao-epidemiologica-dados-zika.

Briesewitz, R.; Kern, A. and Marcantonio, E. E. (1995). Assembly and function of integrin receptors is dependent on opposing alpha and beta cytoplasmic domains. <u>Mol Biol Cell</u> **6**(8): 997-1010.

Brinton, M. A. (2013). Replication cycle and molecular biology of the West Nile virus. <u>Viruses</u> **6**(1): 13-53.

Brower, D. L.; Brower, S. M.; Hayward, D. C. and Ball, E. E. (1997). Molecular evolution of integrins: genes encoding integrin beta subunits from a coral and a sponge. <u>Proc Natl Acad Sci U S A</u> **94**(17): 9182-9187.

Burke, R. D. (1999). Invertebrate integrins: structure, function, and evolution. <u>Int Rev Cytol</u> **191**: 257-284.

Busch, M. P.; Kleinman, S. H.; Tobler, L. H.; Kamel, H. T.; Norris, P. J.; Walsh, I.; Matud, J. L.; Prince, H. E.; Lanciotti, R. S.; Wright, D. J.; Linnen, J. M. and Caglioti, S. (2008). Virus and antibody dynamics in acute west nile virus infection. <u>J Infect Dis</u> **198**(7): 984-993.

Bustos-Arriaga, J.; Garcia-Machorro, J.; Leon-Juarez, M.; Garcia-Cordero, J.; Santos-Argumedo, L.; Flores-Romo, L.; Mendez-Cruz, A. R.; Juarez-Delgado, F. J. and Cedillo-Barron, L. (2011). Activation of the innate immune response against DENV in normal non-transformed human fibroblasts. <u>PLoS Negl Trop Dis</u> **5**(12): e1420.

Calderwood, D. A.; Shattil, S. J. and Ginsberg, M. H. (2000). Integrins and actin filaments: reciprocal regulation of cell adhesion and signaling. <u>J Biol Chem</u> **275**(30): 22607-22610.

Calisher, C. H.; Karabatsos, N.; Dalrymple, J. M.; Shope, R. E.; Porterfield, J. S.; Westaway, E. G. and Brandt, W. E. (1989). Antigenic relationships between flaviviruses as determined by cross-neutralization tests with polyclonal antisera. <u>J Gen Virol</u> **70 (Pt 1)**: 37-43.

Campbell, G. L.; Hills, S. L.; Fischer, M.; Jacobson, J. A.; Hoke, C. H.; Hombach, J. M.; Marfin, A. A.; Solomon, T.; Tsai, T. F.; Tsu, V. D. and Ginsburg, A. S. (2011a). Estimated global incidence of Japanese encephalitis: a systematic review. <u>Bull World Health Organ</u> **89**(10): 766-774, 774A-774E.

Campbell, G. L.; Marfin, A. A.; Lanciotti, R. S. and Gubler, D. J. (2002). West Nile virus. <u>Lancet Infect Dis</u> **2**(9): 519-529.

Campbell, I. D. and Humphries, M. J. (2011b). Integrin structure, activation, and interactions. <u>Cold Spring Harb Perspect Biol</u> **3**(3).

Campos, R. K.; Wong, B.; Xie, X.; Lu, Y. F.; Shi, P. Y.; Pompon, J.; Garcia-Blanco, M. A. and Bradrick, S. S. (2017). RPLP1 and RPLP2 Are Essential Flavivirus Host Factors That Promote Early Viral Protein Accumulation. J Virol **91**(4).

Cao-Lormeau, V. M.; Blake, A.; Mons, S.; Lastere, S.; Roche, C.; Vanhomwegen, J.; Dub, T.; Baudouin, L.; Teissier, A.; Larre, P.; Vial, A. L.; Decam, C.; Choumet, V.; Halstead, S. K.; Willison, H. J.; Musset, L.; Manuguerra, J. C.; Despres, P.; Fournier, E.; Mallet, H. P.; Musso, D.; Fontanet, A.; Neil, J. and Ghawche, F. (2016). Guillain-Barre Syndrome outbreak associated with Zika virus infection in French Polynesia: a case-control study. Lancet **387**(10027): 1531-1539.

Carracedo, S.; Lu, N.; Popova, S. N.; Jonsson, R.; Eckes, B. and Gullberg, D. (2010). The fibroblast integrin alpha11beta1 is induced in a mechanosensitive manner involving activin A and regulates myofibroblast differentiation. J Biol Chem **285**(14): 10434-10445.

Castillo-Olivares, J. and Wood, J. (2004). West Nile virus infection of horses. Vet Res **35**(4): 467-483.

Catteau, A.; Kalinina, O.; Wagner, M. C.; Deubel, V.; Courageot, M. P. and Despres, P. (2003). Dengue virus M protein contains a proapoptotic sequence referred to as ApoptoM. J Gen Virol **84**(Pt 10): 2781-2793.

Chambers, T. J.; Hahn, C. S.; Galler, R. and Rice, C. M. (1990). Flavivirus genome organization, expression, and replication. Annu Rev Microbiol **44**: 649-688.

Chan, J. F.; Yip, C. C.; Tsang, J. O.; Tee, K. M.; Cai, J. P.; Chik, K. K.; Zhu, Z.; Chan, C. C.; Choi, G. K.; Sridhar, S.; Zhang, A. J.; Lu, G.; Chiu, K.; Lo, A. C.; Tsao, S. W.; Kok, K. H.; Jin, D. Y.; Chan, K. H. and Yuen, K. Y. (2016). Differential cell line susceptibility to the emerging Zika virus: implications for disease pathogenesis, non-vector-borne human transmission and animal reservoirs. Emerg Microbes Infect **5**: e93.

Charo, I. F.; Nannizzi, L.; Smith, J. W. and Cheresh, D. A. (1990). The vitronectin receptor alpha v beta 3 binds fibronectin and acts in concert with alpha 5 beta 1 in promoting cellular attachment and spreading on fibronectin. J Cell Biol **111**(6 Pt 1): 2795-2800.

Chavez, J. H.; Silva, J. R.; Amarilla, A. A. and Moraes Figueiredo, L. T. (2010). Domain III peptides from flavivirus envelope protein are useful antigens for serologic diagnosis and targets for immunization. Biologicals **38**(6): 613-618.

Chen, J. M.; Fan, Y. C.; Lin, J. W.; Chen, Y. Y.; Hsu, W. L. and Chiou, S. S. (2017). Bovine Lactoferrin Inhibits Dengue Virus Infectivity by Interacting with Heparan Sulfate, Low-Density Lipoprotein Receptor, and DC-SIGN. Int J Mol Sci **18**(9).

Chen, L. H. and Wilson, M. E. (2016). Update on non-vector transmission of dengue: relevant studies with Zika and other flaviviruses. Tropical Diseases, Travel Medicine and Vaccines **2**(1): 15.

Chen, Y.; Maguire, T.; Hileman, R. E.; Fromm, J. R.; Esko, J. D.; Linhardt, R. J. and Marks, R. M. (1997). Dengue virus infectivity depends on envelope protein binding to target cell heparan sulfate. Nat Med **3**(8): 866-871.

Chien, Y. J.; Chen, W. J.; Hsu, W. L. and Chiou, S. S. (2008). Bovine lactoferrin inhibits Japanese encephalitis virus by binding to heparan sulfate and receptor for low density lipoprotein. Virology **379**(1): 143-151.

112

Chin, R. and Torresi, J. (2013). Japanese B Encephalitis: An Overview of the Disease and Use of Chimerivax-JE as a Preventative Vaccine. Infect Dis Ther **2**(2): 145-158.

Choquet, D.; Felsenfeld, D. P. and Sheetz, M. P. (1997). Extracellular matrix rigidity causes strengthening of integrin-cytoskeleton linkages. Cell **88**(1): 39-48.

Chothia, C. and Jones, E. Y. (1997). The molecular structure of cell adhesion molecules. Annu Rev Biochem **66**: 823-862.

Chu, J. J.; Leong, P. W. and Ng, M. L. (2006). Analysis of the endocytic pathway mediating the infectious entry of mosquito-borne flavivirus West Nile into Aedes albopictus mosquito (C6/36) cells. Virology **349**(2): 463-475.

Chu, J. J. and Ng, M. L. (2003). Characterization of a 105-kDa plasma membrane associated glycoprotein that is involved in West Nile virus binding and infection. Virology **312**(2): 458-469.

Chu, J. J. and Ng, M. L. (2004a). Infectious entry of West Nile virus occurs through a clathrin-mediated endocytic pathway. J Virol **78**(19): 10543-10555.

Chu, J. J. and Ng, M. L. (2004b). Interaction of West Nile virus with alpha v beta 3 integrin mediates virus entry into cells. J Biol Chem **279**(52): 54533-54541.

Chung, K. M.; Liszewski, M. K.; Nybakken, G.; Davis, A. E.; Townsend, R. R.; Fremont, D. H.; Atkinson, J. P. and Diamond, M. S. (2006). West Nile virus nonstructural protein NS1 inhibits complement activation by binding the regulatory protein factor H. Proc Natl Acad Sci U S A **103**(50): 19111-19116.

Cobo, F. (2016). Viruses Causing Hemorrhagic Fever. Safety Laboratory Procedures. Open Virol J **10**: 1-9.

Colpitts, T. M.; Rodenhuis-Zybert, I.; Moesker, B.; Wang, P.; Fikrig, E. and Smit, J. M. (2011). prM-antibody renders immature West Nile virus infectious in vivo. J Gen Virol **92**(Pt 10): 2281-2285.

Conway, M. J.; Colpitts, T. M. and Fikrig, E. (2014). Role of the Vector in Arbovirus Transmission. Annu Rev Virol **1**(1): 71-88.

Cruet-Hennequart, S.; Maubant, S.; Luis, J.; Gauduchon, P.; Staedel, C. and Dedhar, S. (2003). alpha(v) integrins regulate cell proliferation through integrin-linked kinase (ILK) in ovarian cancer cells. Oncogene **22**(11): 1688-1702.

Cuellar, K.; Chuong, H.; Hubbell, S. M. and Hinsdale, M. E. (2007). Biosynthesis of chondroitin and heparan sulfate in chinese hamster ovary cells depends on xylosyltransferase II. J Biol Chem **282**(8): 5195-5200.

Darribere, T.; Skalski, M.; Cousin, H. L.; Gaultier, A.; Montmory, C. and Alfandari, D. (2000). Integrins: regulators of embryogenesis. Biol Cell **92**(1): 5-25.

Davis, C. W.; Nguyen, H. Y.; Hanna, S. L.; Sanchez, M. D.; Doms, R. W. and Pierson, T. C. (2006). West Nile virus discriminates between DC-SIGN and DC-SIGNR for cellular attachment and infection. J Virol **80**(3): 1290-1301.

Davis, L. E.; Beckham, J. D. and Tyler, K. L. (2008). North American encephalitic arboviruses. Neurol Clin **26**(3): 727-757, ix.

Dick, G. W.; Kitchen, S. F. and Haddow, A. J. (1952). Zika virus. I. Isolations and serological specificity. Trans R Soc Trop Med Hyg **46**(5): 509-520.

Dobler, G. (2010). Zoonotic tick-borne flaviviruses. Vet Microbiol **140**(3-4): 221-228.

Dong, H.; Fink, K.; Zust, R.; Lim, S. P.; Qin, C. F. and Shi, P. Y. (2014). Flavivirus RNA methylation. J Gen Virol **95**(Pt 4): 763-778.

Drexler, J. F.; Corman, V. M.; Muller, M. A.; Lukashev, A. N.; Gmyl, A.; Coutard, B.; Adam, A.; Ritz, D.; Leijten, L. M.; van Riel, D.; Kallies, R.; Klose, S. M.; Gloza-Rausch, F.; Binger, T.; Annan, A.; Adu-Sarkodie, Y.; Oppong, S.; Bourgarel, M.; Rupp, D.; Hoffmann, B.; Schlegel, M.; Kummerer, B. M.; Kruger, D. H.; Schmidt-Chanasit, J.; Setien, A. A.; Cottontail, V. M.; Hemachudha, T.; Wacharapluesadee, S.; Osterrieder, K.; Bartenschlager, R.; Matthee, S.; Beer, M.; Kuiken, T.; Reusken, C.; Leroy, E. M.; Ulrich, R. G. and Drosten, C. (2013). Evidence for novel hepaciviruses in rodents. PLoS Pathog **9**(6): e1003438.

Duffy, M. R.; Chen, T. H.; Hancock, W. T.; Powers, A. M.; Kool, J. L.; Lanciotti, R. S.; Pretrick, M.; Marfel, M.; Holzbauer, S.; Dubray, C.; Guillaumot, L.; Griggs, A.; Bel, M.; Lambert, A. J.; Laven, J.; Kosoy, O.; Panella, A.; Biggerstaff, B. J.; Fischer, M. and Hayes, E. B. (2009). Zika virus outbreak on Yap Island, Federated States of Micronesia. N Engl J Med **360**(24): 2536-2543.

Dulbecco, R. and Vogt, M. (1953). Some problems of animal virology as studied by the plaque technique. Cold Spring Harb Symp Quant Biol **18**: 273-279.

Duong, V.; Lambrechts, L.; Paul, R. E.; Ly, S.; Lay, R. S.; Long, K. C.; Huy, R.; Tarantola, A.; Scott, T. W.; Sakuntabhai, A. and Buchy, P. (2015). Asymptomatic humans transmit dengue virus to mosquitoes. Proc Natl Acad Sci U S A **112**(47): 14688-14693.

ECDC, E. C. F. D. C.-. (2016, 11.07.2017). "Epidemiological update: West Nile virus transmission season in Europe, 2016 - " Retrieved 17.02.2018, 2018, from https://ecdc.europa.eu/en/news-events/epidemiological-update-west-nile-virus-transmission-season-europe-2016.

Engel, D.; Jost, H.; Wink, M.; Borstler, J.; Bosch, S.; Garigliany, M. M.; Jost, A.; Czajka, C.; Luhken, R.; Ziegler, U.; Groschup, M. H.; Pfeffer, M.; Becker, N.; Cadar, D. and Schmidt-Chanasit, J. (2016). Reconstruction of the Evolutionary History and Dispersal of Usutu Virus, a Neglected Emerging Arbovirus in Europe and Africa. MBio **7**(1): e01938-01915.

Evans, R.; Patzak, I.; Svensson, L.; De Filippo, K.; Jones, K.; McDowall, A. and Hogg, N. (2009). Integrins in immunity. J Cell Sci **122**(Pt 2): 215-225.

Fan, W.; Qian, P.; Wang, D.; Zhi, X.; Wei, Y.; Chen, H. and Li, X. (2017). Integrin alphavbeta3 promotes infection by Japanese encephalitis virus. Res Vet Sci **111**: 67-74.

Farias, K. J.; Machado, P. R. and da Fonseca, B. A. (2013). Chloroquine inhibits dengue virus type 2 replication in Vero cells but not in C6/36 cells. ScientificWorldJournal **2013**: 282734.

Farias, K. J.; Machado, P. R.; de Almeida Junior, R. F.; de Aquino, A. A. and da Fonseca, B. A. (2014). Chloroquine interferes with dengue-2 virus replication in U937 cells. Microbiol Immunol **58**(6): 318-326.

Farias, K. J.; Machado, P. R.; Muniz, J. A.; Imbeloni, A. A. and da Fonseca, B. A. (2015). Antiviral activity of chloroquine against dengue virus type 2 replication in Aotus monkeys. Viral Immunol **28**(3): 161-169.

Fassler, R. and Meyer, M. (1995a). Consequences of lack of beta 1 integrin gene expression in mice. Genes Dev **9**(15): 1896-1908.

Fassler, R.; Pfaff, M.; Murphy, J.; Noegel, A. A.; Johansson, S.; Timpl, R. and Albrecht, R. (1995b). Lack of beta 1 integrin gene in embryonic stem cells affects morphology, adhesion, and migration but not integration into the inner cell mass of blastocysts. J Cell Biol **128**(5): 979-988.

Feire, A. L.; Koss, H. and Compton, T. (2004). Cellular integrins function as entry receptors for human cytomegalovirus via a highly conserved disintegrin-like domain. Proc Natl Acad Sci U S A **101**(43): 15470-15475.

Feire, A. L.; Roy, R. M.; Manley, K. and Compton, T. (2010). The glycoprotein B disintegrin-like domain binds beta 1 integrin to mediate cytomegalovirus entry. J Virol **84**(19): 10026-10037.

Felding-Habermann, B.; Silletti, S.; Mei, F.; Siu, C. H.; Yip, P. M.; Brooks, P. C.; Cheresh, D. A.; O'Toole, T. E.; Ginsberg, M. H. and Montgomery, A. M. (1997). A single immunoglobulin-like domain of the human neural cell adhesion molecule L1 supports adhesion by multiple vascular and platelet integrins. J Cell Biol **139**(6): 1567-1581.

Fernandez-Garcia, M. D.; Mazzon, M.; Jacobs, M. and Amara, A. (2009). Pathogenesis of flavivirus infections: using and abusing the host cell. Cell Host Microbe **5**(4): 318-328.

Figueiredo, L. T. (2000). The Brazilian flaviviruses. Microbes Infect **2**(13): 1643-1649.

Foo, K. Y. and Chee, H. Y. (2015). Interaction between Flavivirus and Cytoskeleton during Virus Replication. Biomed Res Int **2015**: 427814.

Foy, B. D.; Kobylinski, K. C.; Chilson Foy, J. L.; Blitvich, B. J.; Travassos da Rosa, A.; Haddow, A. D.; Lanciotti, R. S. and Tesh, R. B. (2011). Probable non-vector-borne transmission of Zika virus, Colorado, USA. Emerg Infect Dis **17**(5): 880-882.

Friedrich, S.; Engelmann, S.; Schmidt, T.; Szczepankiewicz, G.; Bergs, S.; Liebert, U. G.; Kummerer, B. M.; Golbik, R. P. and Behrens, S. E. (2017). The Host Factor AUF1 p45 Supports Flavivirus Propagation by Triggering the RNA Switch Required for Viral Genome Cyclization. J Virol.

Froger, A. and Hall, J. E. (2007). Transformation of plasmid DNA into E. coli using the heat shock method. J Vis Exp(6): 253.

Gaibani, P.; Pierro, A.; Alicino, R.; Rossini, G.; Cavrini, F.; Landini, M. P. and Sambri, V. (2012). Detection of Usutu-virus-specific IgG in blood donors from northern Italy. Vector Borne Zoonotic Dis **12**(5): 431-433.

Gamino, V. and Hofle, U. (2013). Pathology and tissue tropism of natural West Nile virus infection in birds: a review. Vet Res **44**: 39.

Gao, F.; Duan, X.; Lu, X.; Liu, Y.; Zheng, L.; Ding, Z. and Li, J. (2010). Novel binding between pre-membrane protein and claudin-1 is required for efficient dengue virus entry. Biochem Biophys Res Commun **391**(1): 952-957.

Garrigues, H. J.; DeMaster, L. K.; Rubinchikova, Y. E. and Rose, T. M. (2014). KSHV attachment and entry are dependent on alphaVbeta3 integrin localized to specific cell surface microdomains and do not correlate with the presence of heparan sulfate. Virology **464-465**: 118-133.

Garrigues, H. J.; Rubinchikova, Y. E.; Dipersio, C. M. and Rose, T. M. (2008). Integrin alphaVbeta3 Binds to the RGD motif of glycoprotein B of Kaposi's sarcoma-associated herpesvirus and functions as an RGD-dependent entry receptor. J Virol **82**(3): 1570-1580.

Gaunt, M. W.; Sall, A. A.; de Lamballerie, X.; Falconar, A. K.; Dzhivanian, T. I. and Gould, E. A. (2001). Phylogenetic relationships of flaviviruses correlate with their epidemiology, disease association and biogeography. J Gen Virol **82**(Pt 8): 1867-1876.

Gavrilovskaya, I. N.; Brown, E. J.; Ginsberg, M. H. and Mackow, E. R. (1999). Cellular entry of hantaviruses which cause hemorrhagic fever with renal syndrome is mediated by beta3 integrins. J Virol **73**(5): 3951-3959.

Gavrilovskaya, I. N.; Shepley, M.; Shaw, R.; Ginsberg, M. H. and Mackow, E. R. (1998). beta3 Integrins mediate the cellular entry of hantaviruses that cause respiratory failure. Proc Natl Acad Sci U S A **95**(12): 7074-7079.

Gebhard, L. G.; Filomatori, C. V. and Gamarnik, A. V. (2011). Functional RNA elements in the dengue virus genome. Viruses **3**(9): 1739-1756.

Geiger, B. and Yamada, K. M. (2011). Molecular architecture and function of matrix adhesions. Cold Spring Harb Perspect Biol **3**(5).

Georgiadou, M.; Lilja, J.; Jacquemet, G.; Guzman, C.; Rafaeva, M.; Alibert, C.; Yan, Y.; Sahgal, P.; Lerche, M.; Manneville, J. B.; Makela, T. P. and Ivaska, J. (2017). AMPK negatively regulates tensin-dependent integrin activity. J Cell Biol **216**(4): 1107-1121.

Germi, R.; Crance, J. M.; Garin, D.; Guimet, J.; Lortat-Jacob, H.; Ruigrok, R. W.; Zarski, J. P. and Drouet, E. (2002). Heparan sulfate-mediated binding of infectious dengue virus type 2 and yellow fever virus. Virology **292**(1): 162-168.

Gianni, T.; Cerretani, A.; Dubois, R.; Salvioli, S.; Blystone, S. S.; Rey, F. and Campadelli-Fiume, G. (2010a). Herpes simplex virus glycoproteins H/L bind to cells independently of {alpha}V{beta}3 integrin and inhibit virus entry, and their constitutive expression restricts infection. J Virol **84**(8): 4013-4025.

Gianni, T.; Gatta, V. and Campadelli-Fiume, G. (2010b). {alpha}V{beta}3-integrin routes herpes simplex virus to an entry pathway dependent on cholesterol-rich lipid rafts and dynamin2. Proc Natl Acad Sci U S A **107**(51): 22260-22265.

Gianni, T.; Salvioli, S.; Chesnokova, L. S.; Hutt-Fletcher, L. M. and Campadelli-Fiume, G. (2013). alphavbeta6- and alphavbeta8-integrins serve as interchangeable receptors for HSV gH/gL to promote endocytosis and activation of membrane fusion. PLoS Pathog **9**(12): e1003806.

Gilmore, A. P. (2005). Anoikis. Cell Death Differ **12 Suppl 2**: 1473-1477.

Gould, E. A. and Solomon, T. (2008). Pathogenic flaviviruses. Lancet **371**(9611): 500-509.

Grard, G.; Moureau, G.; Charrel, R. N.; Lemasson, J. J.; Gonzalez, J. P.; Gallian, P.; Gritsun, T. S.; Holmes, E. C.; Gould, E. A. and de Lamballerie, X. (2007). Genetic characterization of tick-borne flaviviruses: new insights into evolution, pathogenetic determinants and taxonomy. Virology **361**(1): 80-92.

Grischott, F.; Puhan, M.; Hatz, C. and Schlagenhauf, P. (2016). Non-vector-borne transmission of Zika virus: A systematic review. Travel Med Infect Dis **14**(4): 313-330.

Grove, J. and Marsh, M. (2011). The cell biology of receptor-mediated virus entry. J Cell Biol **195**(7): 1071-1082.

Gubler, D. J. (2001). Human arbovirus infections worldwide. Ann N Y Acad Sci **951**: 13-24.

Gulati, S. and Maheshwari, A. (2007). Atypical manifestations of dengue. Trop Med Int Health **12**(9): 1087-1095.

Gumbiner, B. M. (1996). Cell adhesion: the molecular basis of tissue architecture and morphogenesis. Cell **84**(3): 345-357.

Guo, H. B.; Lee, I.; Bryan, B. T. and Pierce, M. (2005). Deletion of mouse embryo fibroblast N-acetylglucosaminyltransferase V stimulates alpha5beta1 integrin expression mediated by the protein kinase C signaling pathway. J Biol Chem **280**(9): 8332-8342.

Guy, B.; Briand, O.; Lang, J.; Saville, M. and Jackson, N. (2015). Development of the Sanofi Pasteur tetravalent dengue vaccine: One more step forward. Vaccine **33**(50): 7100-7111.

Halstead, S. B. (1979). In vivo enhancement of dengue virus infection in rhesus monkeys by passively transferred antibody. J Infect Dis **140**(4): 527-533.

Hamel, R.; Dejarnac, O.; Wichit, S.; Ekchariyawat, P.; Neyret, A.; Luplertlop, N.; Perera-Lecoin, M.; Surasombatpattana, P.; Talignani, L.; Thomas, F.; Cao-Lormeau, V. M.; Choumet, V.; Briant, L.; Despres, P.; Amara, A.; Yssel, H. and Misse, D. (2015). Biology of Zika Virus Infection in Human Skin Cells. J Virol **89**(17): 8880-8896.

Han, N. R.; Lee, H.; Baek, S.; Yun, J. I.; Park, K. H. and Lee, S. T. (2015). Delivery of episomal vectors into primary cells by means of commercial transfection reagents. Biochem Biophys Res Commun **461**(2): 348-353.

Hanahan, D.; Jessee, J. and Bloom, F. R. (1991). Plasmid transformation of Escherichia coli and other bacteria. Methods Enzymol **204**: 63-113.

Harburger, D. S. and Calderwood, D. A. (2009). Integrin signalling at a glance. J Cell Sci **122**(Pt 2): 159-163.

Harris, E. S.; McIntyre, T. M.; Prescott, S. M. and Zimmerman, G. A. (2000). The leukocyte integrins. J Biol Chem **275**(31): 23409-23412.

Hastings, A. K.; Yockey, L. J.; Jagger, B. W.; Hwang, J.; Uraki, R.; Gaitsch, H. F.; Parnell, L. A.; Cao, B.; Mysorekar, I. U.; Rothlin, C. V.; Fikrig, E.; Diamond, M. S. and Iwasaki, A. (2017). TAM Receptors Are Not Required for Zika Virus Infection in Mice. Cell Rep **19**(3): 558-568.

Hayes, E. B.; Sejvar, J. J.; Zaki, S. R.; Lanciotti, R. S.; Bode, A. V. and Campbell, G. L. (2005). Virology, pathology, and clinical manifestations of West Nile virus disease. Emerg Infect Dis **11**(8): 1174-1179.

Heinz, F. X.; Stiasny, K.; Puschner-Auer, G.; Holzmann, H.; Allison, S. L.; Mandl, C. W. and Kunz, C. (1994). Structural changes and functional control of the tick-borne encephalitis virus glycoprotein E by the heterodimeric association with protein prM. Virology **198**(1): 109-117.

Hermann, L. L.; Thaisomboonsuk, B.; Poolpanichupatam, Y.; Jarman, R. G.; Kalayanarooj, S.; Nisalak, A.; Yoon, I. K. and Fernandez, S. (2014). Evaluation of a dengue NS1 antigen detection assay sensitivity and specificity for the diagnosis of acute dengue virus infection. PLoS Negl Trop Dis **8**(10): e3193.

Hertle, M. D.; Adams, J. C. and Watt, F. M. (1991). Integrin expression during human epidermal development in vivo and in vitro. Development **112**(1): 193-206.

Hilgard, P. and Stockert, R. (2000). Heparan sulfate proteoglycans initiate dengue virus infection of hepatocytes. Hepatology **32**(5): 1069-1077.

Hodivala-Dilke, K. M.; McHugh, K. P.; Tsakiris, D. A.; Rayburn, H.; Crowley, D.; Ullman-Cullere, M.; Ross, F. P.; Coller, B. S.; Teitelbaum, S. and Hynes, R. O. (1999). Beta3-integrin-deficient mice are a model for Glanzmann thrombasthenia showing placental defects and reduced survival. J Clin Invest **103**(2): 229-238.

Hoffmann, B.; Beer, M.; Schelp, C.; Schirrmeier, H. and Depner, K. (2005). Validation of a real-time RT-PCR assay for sensitive and specific detection of classical swine fever. J Virol Methods **130**(1-2): 36-44.

Holbrook, M. R. (2012). Kyasanur forest disease. Antiviral Res **96**(3): 353-362.

Horton, E. R.; Humphries, J. D.; James, J.; Jones, M. C.; Askari, J. A. and Humphries, M. J. (2016). The integrin adhesome network at a glance. J Cell Sci **129**(22): 4159-4163.

Hou, S.; Isaji, T.; Hang, Q.; Im, S.; Fukuda, T. and Gu, J. (2016). Distinct effects of beta1 integrin on cell proliferation and cellular signaling in MDA-MB-231 breast cancer cells. Sci Rep **6**: 18430.

Huang, Y. J.; Higgs, S.; Horne, K. M. and Vanlandingham, D. L. (2014). Flavivirus-mosquito interactions. Viruses **6**(11): 4703-4730.

Hughes, A. L. (2001). Evolution of the integrin alpha and beta protein families. J Mol Evol **52**(1): 63-72.

Humphries, J. D.; Byron, A. and Humphries, M. J. (2006). Integrin ligands at a glance. J Cell Sci **119**(Pt 19): 3901-3903.

Hung, S. L.; Lee, P. L.; Chen, H. W.; Chen, L. K.; Kao, C. L. and King, C. C. (1999). Analysis of the steps involved in Dengue virus entry into host cells. Virology **257**(1): 156-167.

Hussein, H. A.; Walker, L. R.; Abdel-Raouf, U. M.; Desouky, S. A.; Montasser, A. K. and Akula, S. M. (2015). Beyond RGD: virus interactions with integrins. Arch Virol **160**(11): 2669-2681.

Hwang, J.; Kim, Y. Y.; Huh, S.; Shim, J.; Park, C.; Kimm, K.; Choi, D. K.; Park, T. K. and Kim, S. (2005). The time-dependent serial gene response to Zeocin treatment involves caspase-dependent apoptosis in HeLa cells. Microbiol Immunol **49**(4): 331-342.

Hynes, R. O. (1987). Integrins: a family of cell surface receptors. Cell **48**(4): 549-554.

Hynes, R. O. (1992). Integrins: versatility, modulation, and signaling in cell adhesion. Cell **69**(1): 11-25.

Hynes, R. O. (2002). Integrins: bidirectional, allosteric signaling machines. Cell **110**(6): 673-687.

Hynes, R. O. (2004). The emergence of integrins: a personal and historical perspective. Matrix Biol **23**(6): 333-340.

Hyun, Y. M.; Lefort, C. T. and Kim, M. (2009). Leukocyte integrins and their ligand interactions. Immunol Res **45**(2-3): 195-208.

Jackson, A. L. and Linsley, P. S. (2010). Recognizing and avoiding siRNA off-target effects for target identification and therapeutic application. Nat Rev Drug Discov **9**(1): 57-67.

Jackson, T.; Clark, S.; Berryman, S.; Burman, A.; Cambier, S.; Mu, D.; Nishimura, S. and King, A. M. (2004). Integrin alphavbeta8 functions as a receptor for foot-and-mouth disease virus: role of the beta-chain cytodomain in integrin-mediated infection. J Virol **78**(9): 4533-4540.

Jackson, T.; Mould, A. P.; Sheppard, D. and King, A. M. (2002). Integrin alphavbeta1 is a receptor for foot-and-mouth disease virus. J Virol **76**(3): 935-941.

Jan, J. T.; Byrnes, A. P. and Griffin, D. E. (1999). Characterization of a Chinese hamster ovary cell line developed by retroviral insertional mutagenesis that is resistant to Sindbis virus infection. J Virol **73**(6): 4919-4924.

Jemielity, S.; Wang, J. J.; Chan, Y. K.; Ahmed, A. A.; Li, W.; Monahan, S.; Bu, X.; Farzan, M.; Freeman, G. J.; Umetsu, D. T.; Dekruyff, R. H. and Choe, H. (2013). TIM-family proteins promote infection of multiple enveloped viruses through virion-associated phosphatidylserine. PLoS Pathog **9**(3): e1003232.

Jordens, I.; Marsman, M.; Kuijl, C. and Neefjes, J. (2005). Rab proteins, connecting transport and vesicle fusion. Traffic **6**(12): 1070-1077.

Josekutty, J.; Yeh, R.; Mathew, S.; Ene, A.; Ramessar, N. and Trinidad, J. (2013). Atypical presentation of West Nile virus in a newly diagnosed human immunodeficiency virus patient in New York City. J Clin Microbiol **51**(4): 1307-1309.

Jöst, H.; Bialonski, A.; Maus, D.; Sambri, V.; Eiden, M.; Groschup, M. H.; Gunther, S.; Becker, N. and Schmidt-Chanasit, J. (2011). Isolation of usutu virus in Germany. Am J Trop Med Hyg **85**(3): 551-553.

Kalia, M.; Khasa, R.; Sharma, M.; Nain, M. and Vrati, S. (2013). Japanese encephalitis virus infects neuronal cells through a clathrin-independent endocytic mechanism. J Virol **87**(1): 148-162.

Kärber, G. (1931). Beitrag zur kollektiven Behandlung pharmakologischer Reihenversuche. Archiv f experiment Pathol u Pharmakol(162): 480–483.

Kaufmann, B. and Rossmann, M. G. (2011). Molecular mechanisms involved in the early steps of flavivirus cell entry. Microbes Infect **13**(1): 1-9.

Kielian, M. (2014). Mechanisms of Virus Membrane Fusion Proteins. Annu Rev Virol **1**(1): 171-189.

Kim, C.; Ye, F. and Ginsberg, M. H. (2011). Regulation of integrin activation. Annu Rev Cell Dev Biol **27**: 321-345.

Kim, S. Y.; Zhao, J.; Liu, X.; Fraser, K.; Lin, L.; Zhang, X.; Zhang, F.; Dordick, J. S. and Linhardt, R. J. (2017). Interaction of Zika Virus Envelope Protein with Glycosaminoglycans. Biochemistry **56**(8): 1151-1162.

Kindhauser, M. K.; Allen, T.; Frank, V.; Santhana, R. S. and Dye, C. (2016). Zika: the origin and spread of a mosquito-borne virus. Bull World Health Organ **94**(9): 675-686C.

Klema, V. J.; Padmanabhan, R. and Choi, K. H. (2015). Flaviviral Replication Complex: Coordination between RNA Synthesis and 5'-RNA Capping. Viruses **7**(8): 4640-4656.

Koistinen, P.; Ahonen, M.; Kahari, V. M. and Heino, J. (2004). alphaV integrin promotes in vitro and in vivo survival of cells in metastatic melanoma. Int J Cancer **112**(1): 61-70.

Koivisto, L.; Heino, J.; Hakkinen, L. and Larjava, H. (2014). Integrins in Wound Healing. Adv Wound Care (New Rochelle) **3**(12): 762-783.

Kraemer, M. U.; Sinka, M. E.; Duda, K. A.; Mylne, A. Q.; Shearer, F. M.; Barker, C. M.; Moore, C. G.; Carvalho, R. G.; Coelho, G. E.; Van Bortel, W.; Hendrickx, G.; Schaffner, F.; Elyazar, I. R.; Teng, H. J.; Brady, O. J.; Messina, J. P.; Pigott, D. M.; Scott, T. W.; Smith, D. L.; Wint, G. R.; Golding, N. and Hay, S. I. (2015). The global distribution of the arbovirus vectors Aedes aegypti and Ae. albopictus. Elife **4**: e08347.

Kraushaar, D. C.; Dalton, S. and Wang, L. (2013). Heparan sulfate: a key regulator of embryonic stem cell fate. Biol Chem **394**(6): 741-751.

Krishnan, M. N.; Sukumaran, B.; Pal, U.; Agaisse, H.; Murray, J. L.; Hodge, T. W. and Fikrig, E. (2007). Rab 5 is required for the cellular entry of dengue and West Nile viruses. J Virol **81**(9): 4881-4885.

Kroschewski, H.; Allison, S. L.; Heinz, F. X. and Mandl, C. W. (2003). Role of heparan sulfate for attachment and entry of tick-borne encephalitis virus. Virology **308**(1): 92-100.

Kuno, G. and Chang, G. J. (2005). Biological transmission of arboviruses: reexamination of and new insights into components, mechanisms, and unique traits as well as their evolutionary trends. Clin Microbiol Rev **18**(4): 608-637.

Kuno, G.; Chang, G. J.; Tsuchiya, K. R.; Karabatsos, N. and Cropp, C. B. (1998). Phylogeny of the genus Flavivirus. J Virol **72**(1): 73-83.

Kuno, G.; Mackenzie, J. S.; Junglen, S.; Hubalek, Z.; Plyusnin, A. and Gubler, D. J. (2017). Vertebrate Reservoirs of Arboviruses: Myth, Synonym of Amplifier, or Reality? Viruses **9**(7).

La Linn, M.; Eble, J. A.; Lubken, C.; Slade, R. W.; Heino, J.; Davies, J. and Suhrbier, A. (2005). An arthritogenic alphavirus uses the alpha1beta1 integrin collagen receptor. Virology **336**(2): 229-239.

Lai, C. Y.; Tsai, W. Y.; Lin, S. R.; Kao, C. L.; Hu, H. P.; King, C. C.; Wu, H. C.; Chang, G. J. and Wang, W. K. (2008). Antibodies to envelope glycoprotein of dengue virus during the natural course of infection are predominantly cross-reactive and recognize epitopes containing highly conserved residues at the fusion loop of domain II. J Virol **82**(13): 6631-6643.

Lammermann, T.; Bader, B. L.; Monkley, S. J.; Worbs, T.; Wedlich-Soldner, R.; Hirsch, K.; Keller, M.; Forster, R.; Critchley, D. R.; Fassler, R. and Sixt, M. (2008). Rapid leukocyte migration by integrin-independent flowing and squeezing. Nature **453**(7191): 51-55.

Lanciotti, R. S.; Kerst, A. J.; Nasci, R. S.; Godsey, M. S.; Mitchell, C. J.; Savage, H. M.; Komar, N.; Panella, N. A.; Allen, B. C.; Volpe, K. E.; Davis, B. S. and Roehrig, J. T. (2000). Rapid detection of west nile virus from human clinical specimens, field-collected mosquitoes, and avian samples by a TaqMan reverse transcriptase-PCR assay. J Clin Microbiol **38**(11): 4066-4071.

Lanciotti, R. S.; Kosoy, O. L.; Laven, J. J.; Velez, J. O.; Lambert, A. J.; Johnson, A. J.; Stanfield, S. M. and Duffy, M. R. (2008). Genetic and serologic properties of Zika virus associated with an epidemic, Yap State, Micronesia, 2007. Emerg Infect Dis **14**(8): 1232-1239.

Lanza, A. M.; Kim, D. S. and Alper, H. S. (2013). Evaluating the influence of selection markers on obtaining selected pools and stable cell lines in human cells. Biotechnol J **8**(7): 811-821.

Lasala, P. R. and Holbrook, M. (2010). Tick-borne flaviviruses. Clin Lab Med **30**(1): 221-235.

Laukaitis, C. M.; Webb, D. J.; Donais, K. and Horwitz, A. F. (2001). Differential dynamics of alpha 5 integrin, paxillin, and alpha-actinin during formation and disassembly of adhesions in migrating cells. J Cell Biol **153**(7): 1427-1440.

Lee, E.; Hall, R. A. and Lobigs, M. (2004). Common E protein determinants for attenuation of glycosaminoglycan-binding variants of Japanese encephalitis and West Nile viruses. J Virol **78**(15): 8271-8280.

Lee, E. and Lobigs, M. (2002). Mechanism of virulence attenuation of glycosaminoglycan-binding variants of Japanese encephalitis virus and Murray Valley encephalitis virus. J Virol **76**(10): 4901-4911.

Lee, E.; Wright, P. J.; Davidson, A. and Lobigs, M. (2006a). Virulence attenuation of Dengue virus due to augmented glycosaminoglycan-binding affinity and restriction in extraneural dissemination. J Gen Virol **87**(Pt 10): 2791-2801.

Lee, J. W.; Chu, J. J. and Ng, M. L. (2006b). Quantifying the specific binding between West Nile virus envelope domain III protein and the cellular receptor alphaVbeta3 integrin. J Biol Chem **281**(3): 1352-1360.

Lee, M.; Chea, K.; Pyda, R.; Chua, M. and Dominguez, I. (2017). Comparative Analysis of Non-viral Transfection Methods in Mouse Embryonic Fibroblast Cells. J Biomol Tech **28**(2): 67-74.

Leis, A. A. and Stokic, D. S. (2012). Neuromuscular manifestations of west nile virus infection. Front Neurol **3**: 37.

Leitinger, B.; McDowall, A.; Stanley, P. and Hogg, N. (2000). The regulation of integrin function by Ca(2+). Biochim Biophys Acta **1498**(2-3): 91-98.

Lequime, S.; Paul, R. E. and Lambrechts, L. (2016). Determinants of Arbovirus Vertical Transmission in Mosquitoes. PLoS Pathog **12**(5): e1005548.

Leung, J. Y.; Pijlman, G. P.; Kondratieva, N.; Hyde, J.; Mackenzie, J. M. and Khromykh, A. A. (2008). Role of nonstructural protein NS2A in flavivirus assembly. J Virol **82**(10): 4731-4741.

Li, E.; Stupack, D.; Klemke, R.; Cheresh, D. A. and Nemerow, G. R. (1998). Adenovirus endocytosis via alpha(v) integrins requires phosphoinositide-3-OH kinase. J Virol **72**(3): 2055-2061.

Li, L.; Lok, S. M.; Yu, I. M.; Zhang, Y.; Kuhn, R. J.; Chen, J. and Rossmann, M. G. (2008). The flavivirus precursor membrane-envelope protein complex: structure and maturation. Science **319**(5871): 1830-1834.

Li, W.; Wang, G.; Liang, W.; Kang, K.; Guo, K. and Zhang, Y. (2014). Integrin beta3 is required in infection and proliferation of classical swine fever virus. PLoS One **9**(10): e110911.

Liang, G.; Gao, X. and Gould, E. A. (2015). Factors responsible for the emergence of arboviruses; strategies, challenges and limitations for their control. Emerg Microbes Infect **4**(3): e18.

Liang, J. J.; Yu, C. Y.; Liao, C. L. and Lin, Y. L. (2011). Vimentin binding is critical for infection by the virulent strain of Japanese encephalitis virus. Cell Microbiol **13**(9): 1358-1370.

Lima-Camara, T. N. (2016). Emerging arboviruses and public health challenges in Brazil. Rev Saude Publica **50**.

Lin, Y. L.; Lei, H. Y.; Lin, Y. S.; Yeh, T. M.; Chen, S. H. and Liu, H. S. (2002). Heparin inhibits dengue-2 virus infection of five human liver cell lines. Antiviral Res **56**(1): 93-96.

Lindenbach, B. M., CL; Thiel, HJ; Rice, CM (2013). Flaviviridae. . Fields Virology. D. M. K. a. P. Howley. **1:** 2664.

Lindquist, L. (2014). Tick-borne encephalitis. Handb Clin Neurol **123**: 531-559.

Lindquist, L. and Vapalahti, O. (2008). Tick-borne encephalitis. Lancet **371**(9627): 1861-1871.

Lindsey, N. P.; Lehman, J. A.; Staples, J. E.; Fischer, M.; Division of Vector-Borne Diseases, N. C. f. E. and Zoonotic Infectious Diseases, C. D. C. (2014). West nile virus and other arboviral diseases - United States, 2013. MMWR Morb Mortal Wkly Rep **63**(24): 521-526.

Liu, W. J.; Wang, X. J.; Mokhonov, V. V.; Shi, P. Y.; Randall, R. and Khromykh, A. A. (2005). Inhibition of interferon signaling by the New York 99 strain and Kunjin subtype of West Nile virus involves blockage of STAT1 and STAT2 activation by nonstructural proteins. J Virol **79**(3): 1934-1942.

Llorente-Cortes, V.; Otero-Vinas, M. and Badimon, L. (2002). Differential role of heparan sulfate proteoglycans on aggregated LDL uptake in human vascular smooth muscle cells and mouse embryonic fibroblasts. Arterioscler Thromb Vasc Biol **22**(11): 1905-1911.

Lodish H, B. A., Zipursky SL, et al. (2000). Cell-Cell Adhesion and Communication. Molecular Cell Biology. New York, W. H. Freeman.

Longmate, W. M. and Dipersio, C. M. (2014). Integrin Regulation of Epidermal Functions in Wounds. Adv Wound Care (New Rochelle) **3**(3): 229-246.

Lu, N.; Karlsen, T. V.; Reed, R. K.; Kusche-Gullberg, M. and Gullberg, D. (2014). Fibroblast alpha11beta1 integrin regulates tensional homeostasis in fibroblast/A549 carcinoma heterospheroids. PLoS One **9**(7): e103173.

Ma, L.; Jones, C. T.; Groesch, T. D.; Kuhn, R. J. and Post, C. B. (2004). Solution structure of dengue virus capsid protein reveals another fold. Proc Natl Acad Sci U S A **101**(10): 3414-3419.

Mackenzie, J. M.; Khromykh, A. A.; Jones, M. K. and Westaway, E. G. (1998). Subcellular localization and some biochemical properties of the flavivirus Kunjin nonstructural proteins NS2A and NS4A. Virology **245**(2): 203-215.

Mackenzie, J. S. and Williams, D. T. (2009). The zoonotic flaviviruses of southern, south-eastern and eastern Asia, and Australasia: the potential for emergent viruses. Zoonoses Public Health **56**(6-7): 338-356.

Mandl, C. W.; Kroschewski, H.; Allison, S. L.; Kofler, R.; Holzmann, H.; Meixner, T. and Heinz, F. X. (2001). Adaptation of tick-borne encephalitis virus to BHK-21 cells results in the formation of multiple heparan sulfate binding sites in the envelope protein and attenuation in vivo. J Virol **75**(12): 5627-5637.

Mandl, C. W.; Kunz, C. and Heinz, F. X. (1991). Presence of poly(A) in a flavivirus: significant differences between the 3' noncoding regions of the genomic RNAs of tick-borne encephalitis virus strains. J Virol **65**(8): 4070-4077.

Mansfield, K. L.; Johnson, N.; Phipps, L. P.; Stephenson, J. R.; Fooks, A. R. and Solomon, T. (2009). Tick-borne encephalitis virus - a review of an emerging zoonosis. J Gen Virol **90**(Pt 8): 1781-1794.

Marceau, C. D.; Puschnik, A. S.; Majzoub, K.; Ooi, Y. S.; Brewer, S. M.; Fuchs, G.; Swaminathan, K.; Mata, M. A.; Elias, J. E.; Sarnow, P. and Carette, J. E. (2016). Genetic dissection of Flaviviridae host factors through genome-scale CRISPR screens. Nature **535**(7610): 159-163.

Martina, B. E.; Koraka, P. and Osterhaus, A. D. (2009). Dengue virus pathogenesis: an integrated view. Clin Microbiol Rev **22**(4): 564-581.

Martines, R. B.; Bhatnagar, J.; de Oliveira Ramos, A. M.; Davi, H. P.; Iglezias, S. D.; Kanamura, C. T.; Keating, M. K.; Hale, G.; Silva-Flannery, L.; Muehlenbachs, A.; Ritter, J.; Gary, J.; Rollin, D.; Goldsmith, C. S.; Reagan-Steiner, S.; Ermias, Y.; Suzuki, T.; Luz, K. G.; de Oliveira, W. K.; Lanciotti, R.; Lambert, A.; Shieh, W. J. and Zaki, S. R. (2016). Pathology of congenital Zika syndrome in Brazil: a case series. Lancet **388**(10047): 898-904.

Medigeshi, G. R.; Hirsch, A. J.; Streblow, D. N.; Nikolich-Zugich, J. and Nelson, J. A. (2008). West Nile virus entry requires cholesterol-rich membrane microdomains and is independent of alphavbeta3 integrin. J Virol **82**(11): 5212-5219.

Meertens, L.; Carnec, X.; Lecoin, M. P.; Ramdasi, R.; Guivel-Benhassine, F.; Lew, E.; Lemke, G.; Schwartz, O. and Amara, A. (2012). The TIM and TAM families of phosphatidylserine receptors mediate dengue virus entry. Cell Host Microbe **12**(4): 544-557.

Merviel, P.; Challier, J. C.; Carbillon, L.; Foidart, J. M. and Uzan, S. (2001). The role of integrins in human embryo implantation. Fetal Diagn Ther **16**(6): 364-371.

Miao, H.; Burnett, E.; Kinch, M.; Simon, E. and Wang, B. (2000). Activation of EphA2 kinase suppresses integrin function and causes focal-adhesion-kinase dephosphorylation. Nat Cell Biol **2**(2): 62-69.

Miller, S.; Kastner, S.; Krijnse-Locker, J.; Buhler, S. and Bartenschlager, R. (2007). The non-structural protein 4A of dengue virus is an integral membrane protein inducing membrane alterations in a 2K-regulated manner. J Biol Chem **282**(12): 8873-8882.

Miranti, C. K. and Brugge, J. S. (2002). Sensing the environment: a historical perspective on integrin signal transduction. Nat Cell Biol **4**(4): E83-90.

Mitra, S. K.; Hanson, D. A. and Schlaepfer, D. D. (2005). Focal adhesion kinase: in command and control of cell motility. Nat Rev Mol Cell Biol **6**(1): 56-68.

Mitroulis, I.; Alexaki, V. I.; Kourtzelis, I.; Ziogas, A.; Hajishengallis, G. and Chavakis, T. (2015). Leukocyte integrins: role in leukocyte recruitment and as therapeutic targets in inflammatory disease. Pharmacol Ther **147**: 123-135.

Modis, Y.; Ogata, S.; Clements, D. and Harrison, S. C. (2004). Structure of the dengue virus envelope protein after membrane fusion. Nature **427**(6972): 313-319.

Monath, T. P.; McCarthy, K.; Bedford, P.; Johnson, C. T.; Nichols, R.; Yoksan, S.; Marchesani, R.; Knauber, M.; Wells, K. H.; Arroyo, J. and Guirakhoo, F. (2002). Clinical proof of principle for ChimeriVax: recombinant live, attenuated vaccines against flavivirus infections. Vaccine **20**(7-8): 1004-1018.

Montgomery, A. M.; Reisfeld, R. A. and Cheresh, D. A. (1994). Integrin alpha v beta 3 rescues melanoma cells from apoptosis in three-dimensional dermal collagen. Proc Natl Acad Sci U S A **91**(19): 8856-8860.

Mori, Y.; Okabayashi, T.; Yamashita, T.; Zhao, Z.; Wakita, T.; Yasui, K.; Hasebe, F.; Tadano, M.; Konishi, E.; Moriishi, K. and Matsuura, Y. (2005). Nuclear localization of Japanese encephalitis virus core protein enhances viral replication. J Virol **79**(6): 3448-3458.

Mukhopadhyay, S.; Kuhn, R. J. and Rossmann, M. G. (2005). A structural perspective of the flavivirus life cycle. Nat Rev Microbiol **3**(1): 13-22.

Muller, D. A. and Young, P. R. (2013). The flavivirus NS1 protein: molecular and structural biology, immunology, role in pathogenesis and application as a diagnostic biomarker. Antiviral Res **98**(2): 192-208.

Muller, J. A.; Harms, M.; Schubert, A.; Jansen, S.; Michel, D.; Mertens, T.; Schmidt-Chanasit, J. and Munch, J. (2016). Inactivation and Environmental Stability of Zika Virus. Emerg Infect Dis **22**(9): 1685-1687.

Murray, C. L.; Jones, C. T. and Rice, C. M. (2008). Architects of assembly: roles of Flaviviridae non-structural proteins in virion morphogenesis. Nat Rev Microbiol **6**(9): 699-708.

Murray, N. E.; Quam, M. B. and Wilder-Smith, A. (2013). Epidemiology of dengue: past, present and future prospects. Clin Epidemiol **5**: 299-309.

Natarajan, S. (2010). NS3 protease from flavivirus as a target for designing antiviral inhibitors against dengue virus. Genet Mol Biol **33**(2): 214-219.

Navarro-Sanchez, E.; Altmeyer, R.; Amara, A.; Schwartz, O.; Fieschi, F.; Virelizier, J. L.; Arenzana-Seisdedos, F. and Despres, P. (2003). Dendritic-cell-specific ICAM3-grabbing non-integrin is essential for the productive infection of human dendritic cells by mosquito-cell-derived dengue viruses. EMBO Rep **4**(7): 723-728.

Nemerow, G. R. and Stewart, P. L. (2016). Insights into Adenovirus Uncoating from Interactions with Integrins and Mediators of Host Immunity. Viruses **8**(12).

Nemesio, H.; Palomares-Jerez, F. and Villalain, J. (2012). NS4A and NS4B proteins from dengue virus: membranotropic regions. Biochim Biophys Acta **1818**(11): 2818-2830.

Nimmagadda, S. S.; Mahabala, C.; Boloor, A.; Raghuram, P. M. and Nayak, U. A. (2014). Atypical Manifestations of Dengue Fever (DF) - Where Do We Stand Today? J Clin Diagn Res **8**(1): 71-73.

Niven, D. J.; Afra, K.; Iftinca, M.; Tellier, R.; Fonseca, K.; Kramer, A.; Safronetz, D.; Holloway, K.; Drebot, M. and Johnson, A. S. (2017). Fatal Infection with Murray Valley Encephalitis Virus Imported from Australia to Canada, 2011. Emerg Infect Dis **23**(2): 280-283.

Oliveira, E. R.; Mohana-Borges, R.; de Alencastro, R. B. and Horta, B. A. (2017). The flavivirus capsid protein: Structure, function and perspectives towards drug design. Virus Res **227**: 115-123.

Osada, N.; Kohara, A.; Yamaji, T.; Hirayama, N.; Kasai, F.; Sekizuka, T.; Kuroda, M. and Hanada, K. (2014). The genome landscape of the african green monkey kidney-derived vero cell line. DNA Res **21**(6): 673-683.

Paixao, E. S.; Barreto, F.; Teixeira Mda, G.; Costa Mda, C. and Rodrigues, L. C. (2016). History, Epidemiology, and Clinical Manifestations of Zika: A Systematic Review. Am J Public Health **106**(4): 606-612.

Papa, A. (2017). Emerging arboviral human diseases in Southern Europe. J Med Virol **89**(8): 1315-1322.

Paranavitane, S. A.; Gomes, L.; Kamaladasa, A.; Adikari, T. N.; Wickramasinghe, N.; Jeewandara, C.; Shyamali, N. L.; Ogg, G. S. and Malavige, G. N. (2014). Dengue NS1 antigen as a marker of severe clinical disease. BMC Infect Dis **14**: 570.

Parry, C.; Bell, S.; Minson, T. and Browne, H. (2005). Herpes simplex virus type 1 glycoprotein H binds to alphavbeta3 integrins. J Gen Virol **86**(Pt 1): 7-10.

Pastorino, B.; Nougairede, A.; Wurtz, N.; Gould, E. and de Lamballerie, X. (2010). Role of host cell factors in flavivirus infection: Implications for pathogenesis and development of antiviral drugs. Antiviral Res **87**(3): 281-294.

Patkar, C. G. and Kuhn, R. J. (2008). Yellow Fever virus NS3 plays an essential role in virus assembly independent of its known enzymatic functions. J Virol **82**(7): 3342-3352.

Perera-Lecoin, M.; Meertens, L.; Carnec, X. and Amara, A. (2013). Flavivirus entry receptors: an update. Viruses **6**(1): 69-88.

Perera, R.; Khaliq, M. and Kuhn, R. J. (2008). Closing the door on flaviviruses: entry as a target for antiviral drug design. Antiviral Res **80**(1): 11-22.

Pettersson, J. H.; Golovljova, I.; Vene, S. and Jaenson, T. G. (2014). Prevalence of tick-borne encephalitis virus in Ixodes ricinus ticks in northern Europe with particular reference to Southern Sweden. Parasit Vectors **7**: 102.

Pfaffl, M. W. (2001). A new mathematical model for relative quantification in real-time RT-PCR. Nucleic Acids Res **29**(9): e45.

Pierson, T. C. and Diamond, M. S. (2012). Degrees of maturity: the complex structure and biology of flaviviruses. Curr Opin Virol **2**(2): 168-175.

Plow, E. F.; Haas, T. A.; Zhang, L.; Loftus, J. and Smith, J. W. (2000). Ligand binding to integrins. J Biol Chem **275**(29): 21785-21788.

Popov, C.; Radic, T.; Haasters, F.; Prall, W. C.; Aszodi, A.; Gullberg, D.; Schieker, M. and Docheva, D. (2011). Integrins alpha2beta1 and alpha11beta1 regulate the survival of mesenchymal stem cells on collagen I. Cell Death Dis **2**: e186.

Popova, S. N.; Rodriguez-Sanchez, B.; Liden, A.; Betsholtz, C.; Van Den Bos, T. and Gullberg, D. (2004). The mesenchymal alpha11beta1 integrin attenuates PDGF-BB-stimulated chemotaxis of embryonic fibroblasts on collagens. <u>Dev Biol</u> **270**(2): 427-442.

Posen, H. J.; Keystone, J. S.; Gubbay, J. B. and Morris, S. K. (2016). Epidemiology of Zika virus, 1947-2007. <u>BMJ Glob Health</u> **1**(2): e000087.

Protopopova, E. V.; Konavalova, S. N. and Loktev, V. B. (1997). [Isolation of a cellular receptor for tick-borne encephalitis virus using anti-idiotypic antibodies]. <u>Vopr Virusol</u> **42**(6): 264-268.

Prow, N. A. (2013). The changing epidemiology of Kunjin virus in Australia. <u>Int J Environ Res Public Health</u> **10**(12): 6255-6272.

Puck, T. T.; Cieciura, S. J. and Robinson, A. (1958). Genetics of somatic mammalian cells. III. Long-term cultivation of euploid cells from human and animal subjects. <u>J Exp Med</u> **108**(6): 945-956.

Ramos-Castaneda, J.; Barreto Dos Santos, F.; Martinez-Vega, R.; Galvao de Araujo, J. M.; Joint, G. and Sarti, E. (2017). Dengue in Latin America: Systematic Review of Molecular Epidemiological Trends. <u>PLoS Negl Trop Dis</u> **11**(1): e0005224.

Rastogi, M.; Sharma, N. and Singh, S. K. (2016). Flavivirus NS1: a multifaceted enigmatic viral protein. <u>Virol J</u> **13**: 131.

Ray, D.; Shah, A.; Tilgner, M.; Guo, Y.; Zhao, Y.; Dong, H.; Deas, T. S.; Zhou, Y.; Li, H. and Shi, P. Y. (2006). West Nile virus 5'-cap structure is formed by sequential guanine N-7 and ribose 2'-O methylations by nonstructural protein 5. <u>J Virol</u> **80**(17): 8362-8370.

Raymond, T.; Gorbunova, E.; Gavrilovskaya, I. N. and Mackow, E. R. (2005). Pathogenic hantaviruses bind plexin-semaphorin-integrin domains present at the apex of inactive, bent alphavbeta3 integrin conformers. <u>Proc Natl Acad Sci U S A</u> **102**(4): 1163-1168.

Reed, L. J. M., H. (1938). A SIMPLE METHOD OF ESTIMATING FIFTY PER CENT ENDPOINTS <u>American Journal of Epidemiology</u> **27**: 493-497.

Reisen, W. K.; Fang, Y. and Martinez, V. (2007). Is nonviremic transmission of West Nile virus by Culex mosquitoes (Diptera: Culicidae) nonviremic? <u>J Med Entomol</u> **44**(2): 299-302.

Reiter, P. (2010). Yellow fever and dengue: a threat to Europe? <u>Euro Surveill</u> **15**(10): 19509.

Rodenhuis-Zybert, I. A.; da Silva Voorham, J. M.; Torres, S.; van de Pol, D. and Smit, J. M. (2015). Antibodies against immature virions are not a discriminating factor for dengue disease severity. <u>PLoS Negl Trop Dis</u> **9**(3): e0003564.

Rodenhuis-Zybert, I. A.; Moesker, B.; da Silva Voorham, J. M.; van der Ende-Metselaar, H.; Diamond, M. S.; Wilschut, J. and Smit, J. M. (2011a). A fusion-loop antibody enhances the infectious properties of immature flavivirus particles. <u>J Virol</u> **85**(22): 11800-11808.

Rodenhuis-Zybert, I. A.; van der Schaar, H. M.; da Silva Voorham, J. M.; van der Ende-Metselaar, H.; Lei, H. Y.; Wilschut, J. and Smit, J. M. (2010a). Immature dengue virus: a veiled pathogen? <u>PLoS Pathog</u> **6**(1): e1000718.

Rodenhuis-Zybert, I. A.; Wilschut, J. and Smit, J. M. (2010b). Dengue virus life cycle: viral and host factors modulating infectivity. Cell Mol Life Sci **67**(16): 2773-2786.

Rodenhuis-Zybert, I. A.; Wilschut, J. and Smit, J. M. (2011b). Partial maturation: an immune-evasion strategy of dengue virus? Trends Microbiol **19**(5): 248-254.

Romero-Brey, I. and Bartenschlager, R. (2014). Membranous replication factories induced by plus-strand RNA viruses. Viruses **6**(7): 2826-2857.

Rossi, S. L.; Tesh, R. B.; Azar, S. R.; Muruato, A. E.; Hanley, K. A.; Auguste, A. J.; Langsjoen, R. M.; Paessler, S.; Vasilakis, N. and Weaver, S. C. (2016). Characterization of a Novel Murine Model to Study Zika Virus. Am J Trop Med Hyg **94**(6): 1362-1369.

Ruiz-Ojeda, F. J.; Ruperez, A. I.; Gomez-Llorente, C.; Gil, A. and Aguilera, C. M. (2016). Cell Models and Their Application for Studying Adipogenic Differentiation in Relation to Obesity: A Review. Int J Mol Sci **17**(7).

Russell, R. C. and Dwyer, D. E. (2000). Arboviruses associated with human disease in Australia. Microbes Infect **2**(14): 1693-1704.

Saeedi, B. J. and Geiss, B. J. (2013). Regulation of flavivirus RNA synthesis and capping. Wiley Interdiscip Rev RNA **4**(6): 723-735.

Sakoonwatanyoo, P.; Boonsanay, V. and Smith, D. R. (2006). Growth and production of the dengue virus in C6/36 cells and identification of a laminin-binding protein as a candidate serotype 3 and 4 receptor protein. Intervirology **49**(3): 161-172.

Salmela, M.; Jokinen, J.; Tiitta, S.; Rappu, P.; Cheng, R. H. and Heino, J. (2017). Integrin alpha2beta1 in nonactivated conformation can induce focal adhesion kinase signaling. Sci Rep **7**(1): 3414.

Samsa, M. M.; Mondotte, J. A.; Iglesias, N. G.; Assuncao-Miranda, I.; Barbosa-Lima, G.; Da Poian, A. T.; Bozza, P. T. and Gamarnik, A. V. (2009). Dengue virus capsid protein usurps lipid droplets for viral particle formation. PLoS Pathog **5**(10): e1000632.

Samuel, M. A. and Diamond, M. S. (2006). Pathogenesis of West Nile Virus infection: a balance between virulence, innate and adaptive immunity, and viral evasion. J Virol **80**(19): 9349-9360.

Samy, A. M.; Elaagip, A. H.; Kenawy, M. A.; Ayres, C. F.; Peterson, A. T. and Soliman, D. E. (2016). Climate Change Influences on the Global Potential Distribution of the Mosquito Culex quinquefasciatus, Vector of West Nile Virus and Lymphatic Filariasis. PLoS One **11**(10): e0163863.

Sanger, F.; Nicklen, S. and Coulson, A. R. (1977). DNA sequencing with chain-terminating inhibitors. Proc Natl Acad Sci U S A **74**(12): 5463-5467.

Sarrazy, V.; Koehler, A.; Chow, M. L.; Zimina, E.; Li, C. X.; Kato, H.; Caldarone, C. A. and Hinz, B. (2014). Integrins alphavbeta5 and alphavbeta3 promote latent TGF-beta1 activation by human cardiac fibroblast contraction. Cardiovasc Res **102**(3): 407-417.

Schmid, R. S. and Anton, E. S. (2003). Role of integrins in the development of the cerebral cortex. Cereb Cortex **13**(3): 219-224.

Schmidt, K. (2012). Cellular factors modulating the entry efficiency of West Nile virus – Involvement of integrins. Dr. med vet Electronic, Tierärztliche Hochschule Hannover / Bibliothek – School of Veterinary Medicine Hannover.

Schmidt, K.; Keller, M.; Bader, B. L.; Korytar, T.; Finke, S.; Ziegler, U. and Groschup, M. H. (2013a). Integrins modulate the infection efficiency of West Nile virus into cells. J Gen Virol **94**(Pt 8): 1723-1733.

Schmidt, S.; Moser, M. and Sperandio, M. (2013b). The molecular basis of leukocyte recruitment and its deficiencies. Mol Immunol **55**(1): 49-58.

Schornberg, K. L.; Shoemaker, C. J.; Dube, D.; Abshire, M. Y.; Delos, S. E.; Bouton, A. H. and White, J. M. (2009). Alpha5beta1-integrin controls ebolavirus entry by regulating endosomal cathepsins. Proc Natl Acad Sci U S A **106**(19): 8003-8008.

Schweitzer, B. K.; Chapman, N. M. and Iwen, P. C. (2009). Overview of the Flaviviridae With an Emphasis on the Japanese Encephalitis Group Viruses. Laboratory Medicine **40**(8): 493-499.

Sejvar, J. J.; Leis, A. A.; Stokic, D. S.; Van Gerpen, J. A.; Marfin, A. A.; Webb, R.; Haddad, M. B.; Tierney, B. C.; Slavinski, S. A.; Polk, J. L.; Dostrow, V.; Winkelmann, M. and Petersen, L. R. (2003). Acute flaccid paralysis and West Nile virus infection. Emerg Infect Dis **9**(7): 788-793.

Shapiro, L. and Weis, W. I. (2009). Structure and biochemistry of cadherins and catenins. Cold Spring Harb Perspect Biol **1**(3): a003053.

Shen, B.; Delaney, M. K. and Du, X. (2012). Inside-out, outside-in, and inside-outside-in: G protein signaling in integrin-mediated cell adhesion, spreading, and retraction. Curr Opin Cell Biol **24**(5): 600-606.

Shiryaev, S. A.; Chernov, A. V.; Aleshin, A. E.; Shiryaeva, T. N. and Strongin, A. Y. (2009). NS4A regulates the ATPase activity of the NS3 helicase: a novel cofactor role of the non-structural protein NS4A from West Nile virus. J Gen Virol **90**(Pt 9): 2081-2085.

Simirskii, V. N.; Wang, Y. and Duncan, M. K. (2007). Conditional deletion of beta1-integrin from the developing lens leads to loss of the lens epithelial phenotype. Dev Biol **306**(2): 658-668.

Simmonds, P.; Becher, P.; Bukh, J.; Gould, E. A.; Meyers, G.; Monath, T.; Muerhoff, S.; Pletnev, A.; Rico-Hesse, R.; Smith, D. B.; Stapleton, J. T. and Ictv Report, C. (2017). ICTV Virus Taxonomy Profile: Flaviviridae. J Gen Virol **98**(1): 2-3.

Singh, M. P.; Majumdar, M.; Singh, G.; Goyal, K.; Preet, K.; Sarwal, A.; Mishra, B. and Ratho, R. K. (2010). NS1 antigen as an early diagnostic marker in dengue: report from India. Diagn Microbiol Infect Dis **68**(1): 50-54.

Sips, G. J.; Wilschut, J. and Smit, J. M. (2012). Neuroinvasive flavivirus infections. Rev Med Virol **22**(2): 69-87.

Smit, J. M.; Moesker, B.; Rodenhuis-Zybert, I. and Wilschut, J. (2011). Flavivirus cell entry and membrane fusion. Viruses **3**(2): 160-171.

Smith, C. E. (1956). A virus resembling Russian spring-summer encephalitis virus from an ixodid tick in Malaya. Nature **178**(4533): 581-582.

Smith, D. W.; Speers, D. J. and Mackenzie, J. S. (2011). The viruses of Australia and the risk to tourists. Travel Med Infect Dis **9**(3): 113-125.

Somnuke, P.; Hauhart, R. E.; Atkinson, J. P.; Diamond, M. S. and Avirutnan, P. (2011). N-linked glycosylation of dengue virus NS1 protein modulates secretion, cell-surface expression, hexamer stability, and interactions with human complement. Virology **413**(2): 253-264.

Spearman, C. (1908). The Method of "Right and Wrong Cases" (Constant Stimuli) without Gauss's Formula. Br J Psychol.(2): 227-242.

Srichai, M. B. Z., R. (2010). Integrin Structure and Function. Cell-Extracellular Matrix Interactions in Cancer. R. Z. a. A. Pozzi, Springer-Verlag New York**:** 19-41.

Stadler, K.; Allison, S. L.; Schalich, J. and Heinz, F. X. (1997). Proteolytic activation of tick-borne encephalitis virus by furin. J Virol **71**(11): 8475-8481.

Stiasny, K.; Kossl, C.; Lepault, J.; Rey, F. A. and Heinz, F. X. (2007). Characterization of a structural intermediate of flavivirus membrane fusion. PLoS Pathog **3**(2): e20.

Streuli, C. H. (2009). Integrins and cell-fate determination. J Cell Sci **122**(Pt 2): 171-177.

Strober, W. (2015). Trypan Blue Exclusion Test of Cell Viability. Curr Protoc Immunol **111**: A3 B 1-3.

Suen, W. W.; Prow, N. A.; Hall, R. A. and Bielefeldt-Ohmann, H. (2014). Mechanism of West Nile virus neuroinvasion: a critical appraisal. Viruses **6**(7): 2796-2825.

Suksanpaisan, L.; Susantad, T. and Smith, D. R. (2009). Characterization of dengue virus entry into HepG2 cells. J Biomed Sci **16**: 17.

Sutherland, A. E.; Calarco, P. G. and Damsky, C. H. (1993). Developmental regulation of integrin expression at the time of implantation in the mouse embryo. Development **119**(4): 1175-1186.

Symington, B. E.; Takada, Y. and Carter, W. G. (1993). Interaction of integrins alpha 3 beta 1 and alpha 2 beta 1: potential role in keratinocyte intercellular adhesion. J Cell Biol **120**(2): 523-535.

Takagi, J.; Kamata, T.; Meredith, J.; Puzon-McLaughlin, W. and Takada, Y. (1997). Changing ligand specificities of alphavbeta1 and alphavbeta3 integrins by swapping a short diverse sequence of the beta subunit. J Biol Chem **272**(32): 19794-19800.

Tamkun, J. W.; DeSimone, D. W.; Fonda, D.; Patel, R. S.; Buck, C.; Horwitz, A. F. and Hynes, R. O. (1986). Structure of integrin, a glycoprotein involved in the transmembrane linkage between fibronectin and actin. Cell **46**(2): 271-282.

Tan, C. W.; Sam, I. C.; Chong, W. L.; Lee, V. S. and Chan, Y. F. (2017). Polysulfonate suramin inhibits Zika virus infection. Antiviral Res **143**: 186-194.

Tang, Q. H.; Zhang, Y. M.; Xu, Y. Z.; He, L.; Dai, C. and Sun, P. (2010). Up-regulation of integrin beta3 expression in porcine vascular endothelial cells cultured in vitro by classical swine fever virus. Vet Immunol Immunopathol **133**(2-4): 237-242.

Tassaneetrithep, B.; Burgess, T. H.; Granelli-Piperno, A.; Trumpfheller, C.; Finke, J.; Sun, W.; Eller, M. A.; Pattanapanyasat, K.; Sarasombath, S.; Birx, D. L.; Steinman, R. M.; Schlesinger, S. and Marovich, M. A.

(2003). DC-SIGN (CD209) mediates dengue virus infection of human dendritic cells. J Exp Med **197**(7): 823-829.

Tesh, R. B.; Siirin, M.; Guzman, H.; Travassos da Rosa, A. P.; Wu, X.; Duan, T.; Lei, H.; Nunes, M. R. and Xiao, S. Y. (2005). Persistent West Nile virus infection in the golden hamster: studies on its mechanism and possible implications for other flavivirus infections. J Infect Dis **192**(2): 287-295.

Theiler, M. and Smith, H. H. (1937). The Effect of Prolonged Cultivation in Vitro Upon the Pathogenicity of Yellow Fever Virus. J Exp Med **65**(6): 767-786.

Thepparit, C.; Phoolcharoen, W.; Suksanpaisan, L. and Smith, D. R. (2004a). Internalization and propagation of the dengue virus in human hepatoma (HepG2) cells. Intervirology **47**(2): 78-86.

Thepparit, C. and Smith, D. R. (2004b). Serotype-specific entry of dengue virus into liver cells: identification of the 37-kilodalton/67-kilodalton high-affinity laminin receptor as a dengue virus serotype 1 receptor. J Virol **78**(22): 12647-12656.

Thongtan, T.; Wikan, N.; Wintachai, P.; Rattanarungsan, C.; Srisomsap, C.; Cheepsunthorn, P. and Smith, D. R. (2012). Characterization of putative Japanese encephalitis virus receptor molecules on microglial cells. J Med Virol **84**(4): 615-623.

Tio, P. H.; Jong, W. W. and Cardosa, M. J. (2005). Two dimensional VOPBA reveals laminin receptor (LAMR1) interaction with dengue virus serotypes 1, 2 and 3. Virol J **2**: 25.

Tomori, O. (2004). Yellow fever: the recurring plague. Crit Rev Clin Lab Sci **41**(4): 391-427.

Tompkins, D.; Johansen, C.; Jakob-Hoff, R.; Pulford, D.; Castro, I. and Mackereth, G. (2013). Surveillance for arboviral zoonoses in New Zealand birds. Western Pac Surveill Response J **4**(4): 16-23.

Triantafilou, K.; Takada, Y. and Triantafilou, M. (2001). Mechanisms of integrin-mediated virus attachment and internalization process. Crit Rev Immunol **21**(4): 311-322.

Tsuda, Y.; Mori, Y.; Abe, T.; Yamashita, T.; Okamoto, T.; Ichimura, T.; Moriishi, K. and Matsuura, Y. (2006). Nucleolar protein B23 interacts with Japanese encephalitis virus core protein and participates in viral replication. Microbiol Immunol **50**(3): 225-234.

Turtle, L.; Griffiths, M. J. and Solomon, T. (2012). Encephalitis caused by flaviviruses. QJM **105**(3): 219-223.

Ulmer, T. S. (2010). Structural basis of transmembrane domain interactions in integrin signaling. Cell Adh Migr **4**(2): 243-248.

van den Hurk, A. F.; Ritchie, S. A. and Mackenzie, J. S. (2009). Ecology and geographical expansion of Japanese encephalitis virus. Annu Rev Entomol **54**: 17-35.

van der Most, R. G.; Corver, J. and Strauss, J. H. (1999). Mutagenesis of the RGD motif in the yellow fever virus 17D envelope protein. Virology **265**(1): 83-95.

van der Schaar, H. M.; Rust, M. J.; Chen, C.; van der Ende-Metselaar, H.; Wilschut, J.; Zhuang, X. and Smit, J. M. (2008). Dissecting the cell entry pathway of dengue virus by single-particle tracking in living cells. PLoS Pathog **4**(12): e1000244.

Vasilakis, N.; Cardosa, J.; Hanley, K. A.; Holmes, E. C. and Weaver, S. C. (2011). Fever from the forest: prospects for the continued emergence of sylvatic dengue virus and its impact on public health. Nat Rev Microbiol **9**(7): 532-541.

Vasilakis, N. and Weaver, S. C. (2017). Flavivirus transmission focusing on Zika. Curr Opin Virol **22**: 30-35.

Vaughn, D. W.; Green, S.; Kalayanarooj, S.; Innis, B. L.; Nimmannitya, S.; Suntayakorn, S.; Endy, T. P.; Raengsakulrach, B.; Rothman, A. L.; Ennis, F. A. and Nisalak, A. (2000). Dengue viremia titer, antibody response pattern, and virus serotype correlate with disease severity. J Infect Dis **181**(1): 2-9.

Vina-Rodriguez, A.; Sachse, K.; Ziegler, U.; Chaintoutis, S. C.; Keller, M.; Groschup, M. H. and Eiden, M. (2017). A Novel Pan-Flavivirus Detection and Identification Assay Based on RT-qPCR and Microarray. Biomed Res Int **2017**: 4248756.

Wai Wong, C.; Dye, D. E. and Coombe, D. R. (2012). The role of immunoglobulin superfamily cell adhesion molecules in cancer metastasis. Int J Cell Biol **2012**: 340296.

Waldenstrom, J.; Lundkvist, A.; Falk, K. I.; Garpmo, U.; Bergstrom, S.; Lindegren, G.; Sjostedt, A.; Mejlon, H.; Fransson, T.; Haemig, P. D. and Olsen, B. (2007). Migrating birds and tickborne encephalitis virus. Emerg Infect Dis **13**(8): 1215-1218.

Wang, G.; Wang, Y.; Shang, Y.; Zhang, Z. and Liu, X. (2015a). How foot-and-mouth disease virus receptor mediates foot-and-mouth disease virus infection. Virol J **12**: 9.

Wang, H. and Liang, G. (2015b). Epidemiology of Japanese encephalitis: past, present, and future prospects. Ther Clin Risk Manag **11**: 435-448.

Wang, K. and Deubel, V. (2011). Mice with different susceptibility to Japanese encephalitis virus infection show selective neutralizing antibody response and myeloid cell infectivity. PLoS One **6**(9): e24744.

Wang, X.; Huang, D. Y.; Huong, S. M. and Huang, E. S. (2005). Integrin alphavbeta3 is a coreceptor for human cytomegalovirus. Nat Med **11**(5): 515-521.

Wang, Y. and Zhang, P. (2017). Recent advances in the identification of the host factors involved in dengue virus replication. Virol Sin **32**(1): 23-31.

Ward, A. M.; Calvert, M. E.; Read, L. R.; Kang, S.; Levitt, B. E.; Dimopoulos, G.; Bradrick, S. S.; Gunaratne, J. and Garcia-Blanco, M. A. (2016). The Golgi associated ERI3 is a Flavivirus host factor. Sci Rep **6**: 34379.

Weaver, S. C. and Barrett, A. D. (2004). Transmission cycles, host range, evolution and emergence of arboviral disease. Nat Rev Microbiol **2**(10): 789-801.

Weaver, S. C. and Reisen, W. K. (2010). Present and future arboviral threats. Antiviral Res **85**(2): 328-345.

Wehrle-Haller, B. and Imhof, B. (2002). The inner lives of focal adhesions. Trends Cell Biol **12**(8): 382-389.

Weissenbock, H.; Bakonyi, T.; Rossi, G.; Mani, P. and Nowotny, N. (2013). Usutu virus, Italy, 1996. Emerg Infect Dis **19**(2): 274-277.

WHO (1985). Arthropod-borne and rodent-borne viral diseases. Report of a WHO Scientific Group. World Health Organ Tech Rep Ser **719**: 1-116.

Wickham, T. J.; Mathias, P.; Cheresh, D. A. and Nemerow, G. R. (1993). Integrins alpha v beta 3 and alpha v beta 5 promote adenovirus internalization but not virus attachment. Cell **73**(2): 309-319.

Wiwanitkit, V. (2016). The current status of Zika virus in Southeast Asia. Epidemiol Health **38**: e2016026.

Wong, S. S.; Haqshenas, G.; Gowans, E. J. and Mackenzie, J. (2012). The dengue virus M protein localises to the endoplasmic reticulum and forms oligomers. FEBS Lett **586**(7): 1032-1037.

Wozniak, M. A.; Modzelewska, K.; Kwong, L. and Keely, P. J. (2004). Focal adhesion regulation of cell behavior. Biochim Biophys Acta **1692**(2-3): 103-119.

Wu, J.; Bera, A. K.; Kuhn, R. J. and Smith, J. L. (2005). Structure of the Flavivirus helicase: implications for catalytic activity, protein interactions, and proteolytic processing. J Virol **79**(16): 10268-10277.

Xu, X.; Nagarajan, H.; Lewis, N. E.; Pan, S.; Cai, Z.; Liu, X.; Chen, W.; Xie, M.; Wang, W.; Hammond, S.; Andersen, M. R.; Neff, N.; Passarelli, B.; Koh, W.; Fan, H. C.; Wang, J.; Gui, Y.; Lee, K. H.; Betenbaugh, M. J.; Quake, S. R.; Famili, I.; Palsson, B. O. and Wang, J. (2011). The genomic sequence of the Chinese hamster ovary (CHO)-K1 cell line. Nat Biotechnol **29**(8): 735-741.

Yamauchi, Y. and Helenius, A. (2013). Virus entry at a glance. J Cell Sci **126**(Pt 6): 1289-1295.

Yang, J. S.; Ramanathan, M. P.; Muthumani, K.; Choo, A. Y.; Jin, S. H.; Yu, Q. C.; Hwang, D. S.; Choo, D. K.; Lee, M. D.; Dang, K.; Tang, W.; Kim, J. J. and Weiner, D. B. (2002). Induction of inflammation by West Nile virus capsid through the caspase-9 apoptotic pathway. Emerg Infect Dis **8**(12): 1379-1384.

Yasunaga, A.; Hanna, S. L.; Li, J.; Cho, H.; Rose, P. P.; Spiridigliozzi, A.; Gold, B.; Diamond, M. S. and Cherry, S. (2014). Genome-wide RNAi screen identifies broadly-acting host factors that inhibit arbovirus infection. PLoS Pathog **10**(2): e1003914.

Yu, C.; Achazi, K.; Moller, L.; Schulzke, J. D.; Niedrig, M. and Bucker, R. (2014). Tick-borne encephalitis virus replication, intracellular trafficking, and pathogenicity in human intestinal Caco-2 cell monolayers. PLoS One **9**(5): e96957.

Yu, I. M.; Zhang, W.; Holdaway, H. A.; Li, L.; Kostyuchenko, V. A.; Chipman, P. R.; Kuhn, R. J.; Rossmann, M. G. and Chen, J. (2008). Structure of the immature dengue virus at low pH primes proteolytic maturation. Science **319**(5871): 1834-1837.

Zaidel-Bar, R.; Itzkovitz, S.; Ma'ayan, A.; Iyengar, R. and Geiger, B. (2007). Functional atlas of the integrin adhesome. Nat Cell Biol **9**(8): 858-867.

Zanluca, C.; Melo, V. C.; Mosimann, A. L.; Santos, G. I.; Santos, C. N. and Luz, K. (2015). First report of autochthonous transmission of Zika virus in Brazil. Mem Inst Oswaldo Cruz **110**(4): 569-572.

Zhang, K. and Chen, J. (2012). The regulation of integrin function by divalent cations. Cell Adh Migr **6**(1): 20-29.

Zhang, Y.; Corver, J.; Chipman, P. R.; Zhang, W.; Pletnev, S. V.; Sedlak, D.; Baker, T. S.; Strauss, J. H.; Kuhn, R. J. and Rossmann, M. G. (2003). Structures of immature flavivirus particles. EMBO J **22**(11): 2604-2613.

Zhang, Y.; Zhang, W.; Ogata, S.; Clements, D.; Strauss, J. H.; Baker, T. S.; Kuhn, R. J. and Rossmann, M. G. (2004). Conformational changes of the flavivirus E glycoprotein. Structure **12**(9): 1607-1618.

Zhang, Z.; Morla, A. O.; Vuori, K.; Bauer, J. S.; Juliano, R. L. and Ruoslahti, E. (1993). The alpha v beta 1 integrin functions as a fibronectin receptor but does not support fibronectin matrix assembly and cell migration on fibronectin. J Cell Biol **122**(1): 235-242.

Zhang, Z.; Vuori, K.; Reed, J. C. and Ruoslahti, E. (1995). The alpha 5 beta 1 integrin supports survival of cells on fibronectin and up-regulates Bcl-2 expression. Proc Natl Acad Sci U S A **92**(13): 6161-6165.

Zhang, Z. G.; Bothe, I.; Hirche, F.; Zweers, M.; Gullberg, D.; Pfitzer, G.; Krieg, T.; Eckes, B. and Aumailley, M. (2006). Interactions of primary fibroblasts and keratinocytes with extracellular matrix proteins: contribution of alpha2beta1 integrin. J Cell Sci **119**(Pt 9): 1886-1895.

Zhao, X. and Guan, J. L. (2011). Focal adhesion kinase and its signaling pathways in cell migration and angiogenesis. Adv Drug Deliv Rev **63**(8): 610-615.

Zhu, C. Q.; Popova, S. N.; Brown, E. R.; Barsyte-Lovejoy, D.; Navab, R.; Shih, W.; Li, M.; Lu, M.; Jurisica, I.; Penn, L. Z.; Gullberg, D. and Tsao, M. S. (2007). Integrin alpha 11 regulates IGF2 expression in fibroblasts to enhance tumorigenicity of human non-small-cell lung cancer cells. Proc Natl Acad Sci U S A **104**(28): 11754-11759.

7) Appendix

Appendix I: Chemicals

1) Chemicals

Name	Manufacturer
Acetic acid, 100 %, p.a.	Carl Roth GmbH & Co, Karlsruhe, Germany
Acetone, Rotipuran®, ≥ 99.8 %, p.a.	Carl Roth GmbH & Co, Karlsruhe, Germany
Agar, Bacteriological Grade	MP Biomedicals Inc., Solon, OH, USA
Agarose, Ultra Pure	Invitrogen GmbH, Darmstadt, Germany
Ammonium chloride, ≥ 99.5 %	Carl Roth GmbH & Co, Karlsruhe, Germany
Ampicillin sodium salt	Carl Roth GmbH & Co, Karlsruhe, Germany
Bovine Serum Albumin fraction V, Chemical grade	Merck KGAA, Darmstadt, Germany
Bromphenol blue, powder	Sigma-Aldrich Chemie GmbH, Munich, Germany
Calcium chloride dihydrate, ≥ 99 %, p.a.	Carl Roth GmbH & Co, Karlsruhe, Germany
Citric acid, ≥99.5 %, p.a., anhydrous	Carl Roth GmbH & Co, Karlsruhe, Germany
Crystal Violet, powder (Dye content ≥90 %)	Sigma-Aldrich Chemie GmbH, Munich, Germany
4',6-Diamidino-2-phenylindoldihydrochloride (DAPI)	Sigma-Aldrich Chemie GmbH, Munich, Germany
Dimethyl sulfoxide (DMSO), ≥ 99.5, for microbiology	Carl Roth GmbH & Co, Karlsruhe, Germany
Disodium hydrogen phosphate (Na_2HPO_4), ≥ 99 %, p.a.	Carl Roth GmbH & Co, Karlsruhe, Germany
Ethanol, ≥ 96 %, denatured with 1 % MEK ethyl alcohol	Carl Roth GmbH & Co, Karlsruhe, Germany
Ethanol, >99.8%, p.a.	Carl Roth GmbH & Co, Karlsruhe, Germany
Ethidium bromide, solution in water, for electrophoresis (10g/l)	Merck KGAA, Darmstadt, Germany

Name	Manufacturer
Ethylenediamine tetraacetatic acid (EDTA), pure, powder	Serva Feinbiochemica GmbH & Co, Heidelberg, Germany
Formaldehyde, 37 % (Formalin), p.a.	Carl Roth GmbH & Co, Karlsruhe, Germany
Glycerine, ≥ 99 %, p.a.	Carl Roth GmbH & Co, Karlsruhe, Germany
Glycine, ≥ 99 %, p.a.	Carl Roth GmbH & Co, Karlsruhe, Germany
Hydrochloric Acid, reagent grade, 37%	Sigma-Aldrich Chemie GmbH, Munich, Germany
Kanamycin disulfate salt	Carl Roth GmbH & Co, Karlsruhe, Germany
Magnesium chloride ($MgCl_2$) hexahydrate, ≥ 99 %, p.a.	Carl Roth GmbH & Co, Karlsruhe, Germany
Mangan (II) chloride monohydrate	Carl Roth GmbH & Co, Karlsruhe, Germany
2-Mercaptoethanol, 99 %, p.a.	Carl Roth GmbH & Co, Karlsruhe, Germany
Methanol, , ≥ 99.9 %, p.a.	Carl Roth GmbH & Co, Karlsruhe, Germany
Paraformaldehyde, ≥ 95 %, pure,powder	Carl Roth GmbH & Co, Karlsruhe, Germany
Polyethylene glycol 6000	Carl Roth GmbH & Co, Karlsruhe, Germany
Potassium chloride (KCl), ≥ 99.5 %, p.a.	Carl Roth GmbH & Co, Karlsruhe, Germany
Potassium dihydrogen phosphate (KH_2PO_4), ≥ 99.5 %, p.a.	Carl Roth GmbH & Co, Karlsruhe, Germany
2-Propanol, ≥ 99.8 %	Carl Roth GmbH & Co, Karlsruhe, Germany
Skim milk powder, MAMIPU	Hobbybäcker-Versand, Bellenberg, Germany
BD-Difco Skim Milk	BD-Becton-Dickinson,New Jersey, USA
Sodium azide, ≥ 99 %, p.a.	Carl Roth GmbH & Co, Karlsruhe, Germany
Sodium carbonate (Na_2CO_3), p.a.	Carl Roth GmbH & Co, Karlsruhe, Germany
Sodium chloride (NaCl), ≥ 99.5 %, p.a.	Carl Roth GmbH & Co, Karlsruhe, Germany

Name	Manufacturer
Sodium dihydrogen phosphate (NaH_2PO_4) dihydrate, ≥ 99 %, p.a.	Carl Roth GmbH & Co, Karlsruhe, Germany
Sodium hydrogen carbonate ($NaHCO_3$), ≥ 99.5 %, p.a.	Carl Roth GmbH & Co, Karlsruhe, Germany
Sucrose	Carl Roth GmbH & Co, Karlsruhe, Germany
Tris(hydroxymethyl)-aminomethane (TRIS), Ultra Pure	Invitrogen GmbH, Darmstadt, Germany
Triton® X-100	Sigma-Aldrich Chemie GmbH, Munich, Germany
Trypton, Casein Hydrolysate	Oxoid Deutschland GmbH, Wesel, Germany
Tween®20, Polyoxyethylene sorbitan monolaureate	Sigma-Aldrich Chemie GmbH, Munich, Germany
Yeast extract	Carl Roth GmbH & Co, Karlsruhe, Germany

Appendix II: Buffers, solutions, media and antibiotics

1) Buffers and Solutions

Buffer	Composition	Storage
10X Phosphate Buffered Saline (PBS) pH 7.2	80 g NaCl 2.0 g KCl 14.4 g Na_2HPO4 2.4 g KH_2PO4 add 1 liter distilled water	RT
1M Calcium Buffer (stock solution)	1.1 g $CaCl_2$ add 100 ml distilled water	RT
1M Magnesium Buffer (stock Solution)	508.26 mg $MgCl_2$ add 100 ml distilled water	RT
Calcium-Magnesium Buffer	7.5 ml $CaCl_2$ (1M stock solution) 2.5 ml $MgCl_2$ (1M stock solution) add 100 ml distilled water	RT
Tris-Acetate- EDTA buffer 50X (pH 8.3)	242 g Tris-base 18.61 g Disodiumn EDTA 57.1 ml Glacial Acetic Acid add 1 liter distilled water	RT
6X loading Dye buffer	1 mg/ml Bromphenol blue 2 mg/ml Xylene cyanol blue 2 mg/ml Orange G 10 g Sucrose 20 mM EDTA add 20 ml distilled water	+4°C
Trypsin solution (pH 7.2)	8.5 g NaCl 0.4 g KCl 1.0 g Dextrose 0.58 g NaHCO3 0.5 g Trypsin 1:250 0.2 g EDTA add 1 liter distilled water	+4°C
DAPI stock solution	2 g 4´, 6-diamidino-2´-phenylindole, dihydrochloride (DAPI) add 1 liter distilled water	-20°C

Buffer	Composition	Storage
3 % Paraformaldehyde (pH 7.3)	3 g Paraformadehyde, powder add 100 ml distilled water	-20°C
Tris-Natrium-EDTA buffer (pH 7.4) (TNE)	50 mM Tris–HCl (pH 7.4) 100 mM NaCl 0.1 mM EDTA add 1 liter distilled water	+4°C
30% sucrose buffer	30 g Sucrose add 100 ml TNE buffer	+4°C
60% sucrose buffer	60 g Sucrose add 100 ml TNE buffer	+4°C
Luria Bertani medium (LB medium)	10 g Tryptone 10 g NaCl 5 g Yeast extract add distilled water to 1 liter	+4°C
Luria Bertani agar (LB agar)	10 g Tryptone 10 g NaCl 5 g Yeast extract add distilled water to 1 liter	+4°C
1M EDTA stock solution (pH 8.0)	372.2 g EDTA (ethylenediamenetetraacetic acid) add 1 liter distilled water	RT/+4°C
50 mM EDTA solution (pH 7.4)	5 ml 1M EDTA stock solution 95 ml 1X PBS	+4°C
10 % buffered formalin	100 ml formalin 900 ml 1X PBS	RT
1% crystal violet fixative/staining solution solution	1 g crystal violet powder 100 ml 10% buffered formalin	RT
1 M ammonium chloride stock solution	53.5 g ammonium chloride (NH_4Cl) 1 liter distilled water	RT
1% crystal violet staining solution	1 g crystal violet powder 20 ml Methanol 80 ml 1X PBS	RT
50 mM NH_4Cl quenching solution (for immunofluorescence)	5 ml 1 M Ammonium Chloride solution 95 ml 1X PBS	RT

Buffer	Composition	Storage
100 mM acid glycine solution (pH 2.5)	7.5 g Glycine 1X PBS to 100 ml	+4°C
1M sodium citrate buffer (pH 4.5)	214.10 g Sodium Citrate 1 liter distilled water	+4°C
Dye removal solution (pH 4.5)	50 ml Ethanol (absolute) 10ml 1M sodium citrate buffer 40 ml 1X PBS	RT
Tris-EDTA (TE) buffer (pH 8.0)	10 ml 1M tTris-HCl 1 ml 1 M EDTA 1 liter distilled water	RT
RNA Safe Buffer (RSB) – Provide by Dr. Bernard Hoffmann (IVD – FLI)	50 µM Carrier RNA (poly A) 0.2 µM Tween 20 0.2 µM sodium acid 1 liter RNAse free water	-20°C

2) Cell culture media

Name	Manufacturer	Cat n°
Dulbecco's Modified Eagle Medium (DMEM), powder, high glucose, pyruvate	ThermoFisher, Whaltham, MA, USA	12800017
Eagle's Minimun Essential Medium (E-MEM), with Non-essential Amino acids (NEAA), powder	ThermoFisher, Whaltham, MA, USA	41500-018

3) Antibiotics

Name	Manufacturer	Cat n°
Penicillin-Streptomycin (10,000 units penicillin and 10 mg streptomycin/mL)	Sigma-Aldrich Chemie GmbH, Munich, Germany	P4333-100ML
Zeocin™	Invivogen, San Diego, CA, USA	ant-zn-5p
Hygromycin B	Invitrogen, Carlsbad,CA, USA	10687010
Ampicillin	Carl Roth GmbH & Co, Karlsruhe, Germany	HP62.2
Kanamycin	Carl Roth GmbH & Co, Karlsruhe, Germany	T832.3

Appendix III: Antibodies and cell sorting system

1) Antibodies used for indirect immunofluorescence (IF)

Antibody	Host	Target	Dilution/Concentration	Manufacturer
LEAF™ Purified anti-mouse Anti-CD51 (αV integrin)	Rat	Mouse	1:50	Biolegends, San Diego, CA, USA
LEAF™ Purified anti-mouse Anti-CD61 (β3 integrin)	Hamster	Mouse	1:10	Biolegends, San Diego, CA, USA
LEAF™ Purified anti-mouse Anti-CD29 (β1 integrin)	Hamster	Mouse	1:25	Biolegends, San Diego, CA, USA
AffiniPure Goat Anti-Rat IgG Cyanine Cy3	Goat	Rat	1:100	Jackson ImmunoResearch, West Grove, PA, USA
AffiniPure Goat Anti-Armenian Hamster IgG Alexa-488	Goat	Hamster	1:400	Jackson ImmunoResearch, West Grove, PA, USA

2) Antibodies used for flow cytometry analysis (FCA)

Antibody	Host	Target	Dilution/Concentration	Manufacturer
LEAF™ Purified anti-mouse Anti-CD51 (αV integrin)	Rat	Mouse	0,5 µl per 10^6 cells	Biolegends, San Diego, CA, USA
LEAF™ Purified anti-mouse Anti-CD61 (β3 integrin)	Hamster	Mouse	1 µl per 10^6 cells	Biolegends, San Diego, CA, USA
LEAF™ Purified anti-mouse Anti-CD29 (β1 integrin)	Hamster	Mouse	1 µl per 10^6 cells	Biolegends, San Diego, CA, USA
AffiniPure Goat Anti-Rat IgG Alexa-647	Goat	Rat	1:400	Jackson ImmunoResearch, West Grove, PA, USA
AffiniPure Goat Anti-Armenian Hamster IgG Alexa-488	Goat	Hamster	1:400	Jackson ImmunoResearch, West Grove, PA, USA

3) Antibodies used for cell sorting

Antibody	Host	Target	Dilution/Concentration	Manufacturer
Biotin anti-mouse CD51 (αV integrin)	Rat	Mouse	1 µg/10^7 cells	Biolegends, San Diego, CA, USA
Biotin anti-mouse/rat CD61 Antibody (β3 integrin)	Hamster	Mouse	1 µg/10^7 cells	Biolegends, San Diego, CA, USA
Anti-Biotin MicroBeads	Mouse	Biotin	50 µl/ sorting	Miltenyi Biotec,Teterow, Germany

4) Cell sorting system and related reagents

Name	Manufacturer	Cat n°
MS Columns	Miltenyi Biotec,Teterow, Germany	130-042-201
OctoMACS Separator	Miltenyi Biotec,Teterow, Germany	130-042-109
Anti-Biotin MicroBeads	Miltenyi Biotec,Teterow, Germany	130-090-485
autoMACS Pro Washing Solution	Miltenyi Biotec,Teterow, Germany	130-092-987
autoMACS Running Buffer – MACS Separation Buffer	Miltenyi Biotec,Teterow, Germany	130-091-221

Appendix IV: Kits

1) Kits

Name	Manufacturer	Cat n°
Rapid DNA Ligation Kit	ThermoFisher Whaltham, MA, USA	K1422
QuantiTect Probe RT-PCR Kit	Qiagen, Hilden Germany	204443
SuperScript® III One-Step RT-PCR System with Platinum® Taq DNA Polymerase	ThermoFisher, Whaltham, MA, USA	12574026
DreamTaq™ Hot Start DNA Polymerase (5 U/µl)	ThermoFisher, Whaltham, MA, USA	EP0701
Maxima Reverse Transcriptase (200 U/µL)	ThermoFisher, Whaltham, MA, USA	EP0742
Phusion High-Fidelity PCR Master Mix with GC Buffer	ThermoFisher Whaltham, MA, USA	F532S
QIAamp Viral RNA Mini Kit	Qiagen, Hilden Germany	52904
RNeasy Mini Kit	Qiagen, Hilden Germany	74104
QIAquick Gel Extraction Kit	Qiagen, Hilden Germany	28704
QIAquick PCR Purification Kit	Qiagen, Hilden Germany	28104
QIAprep Spin Miniprep Kit	Qiagen, Hilden Germany	27106
QIAprep Plasmid Midi Kit	Qiagen, Hilden Germany	12145
QIAquick Nucleotide Removal Kit	Qiagen, Hilden Germany	28304
GeneJET Gel Extraction Kit	ThermoFisher, Whaltham, MA, USA	K0692

**Appendix V**: Vector systems and restriction endonucleases.

1) Vector systems

Name	Company	Cat n°
pcDNA 3.1 (+) Hygromycin	ThermoFisher, Whaltham, MA, USA	V87020
pcDNA 3.1 (+) Zeocin	ThermoFisher, Whaltham, MA, USA	V86020

2) Restriction Endonucleases and Buffers

Name	Company	Cat n°
BamHI-High Fidelity® (20,000 units/ml)	New England Biolabs, Ipswich, MA,USA	R3136S
NotI-High Fidelity® (20,000 units/ml)	New England Biolabs, Ipswich, MA,USA	R3189S
CutSmart® Buffer	New England Biolabs, Ipswich, MA,USA	B7204S

3) Vector: pcDNA 3.1 (+) Hygro

Source: ThermoFisher, Whaltham, MA, USA

Catalog Number: V87020

Plasmid Type: Mammalian Expression

Promotor: Cytomegalovirus (CMV)

Size: 5597 base pairs

Bacterial Resistance: Ampicillin

Selectable Marker: Hygromycin

Notes: Constitutive system, suitable for transient and stable expression
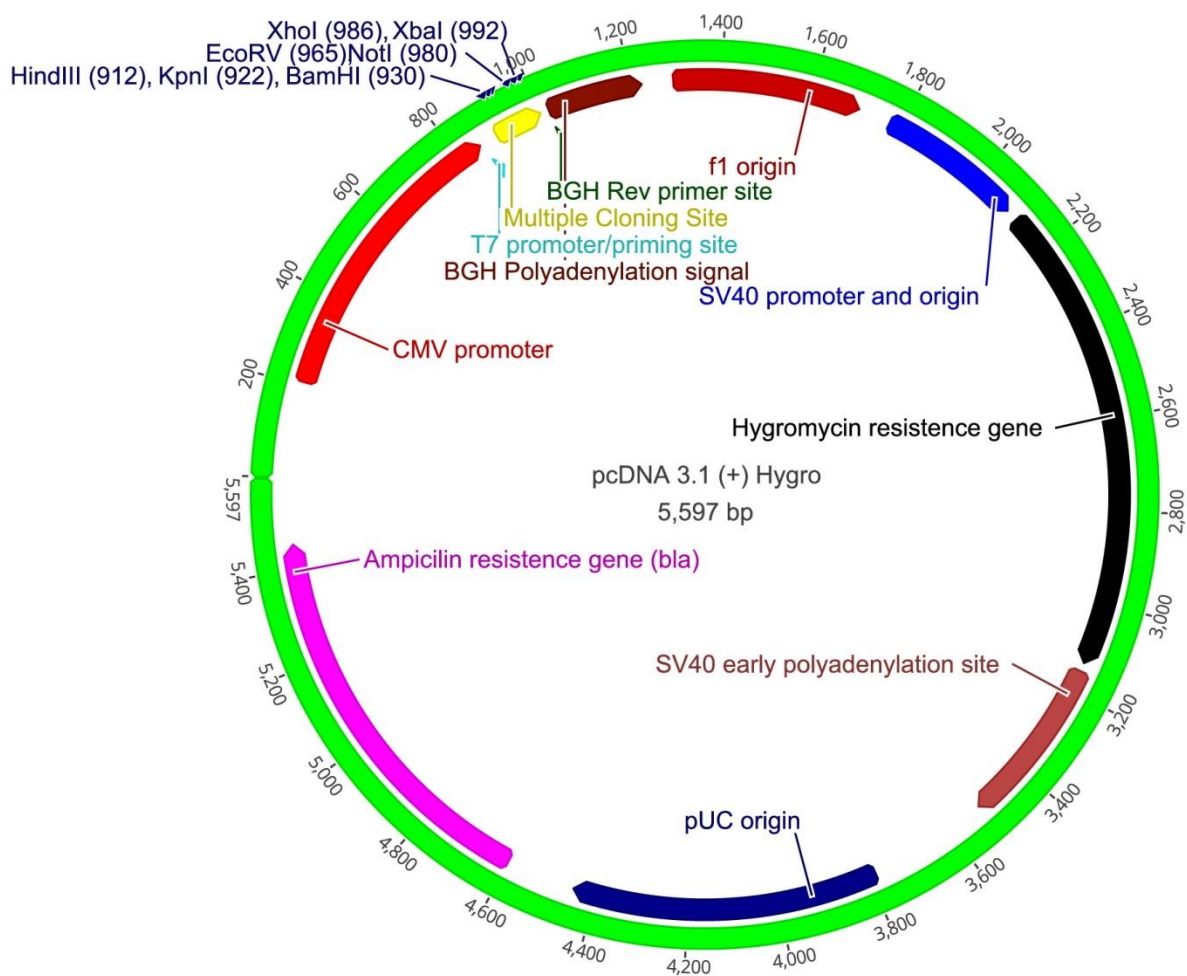
Informations about the vector were taken from the manufacturer's website (http://www.thermofisher.com/order/catalog/product/V87020).
Vector map was designed based on the original sequence available in the above mentioned website using the Geneious software.

4) Vector: pcDNA 3.1 (+) Zeo

Source: ThermoFisher, Whaltham, MA, USA

Catalog Number: V86020

Plasmid Type: Mammalian Expression

Promotor: Cytomegalovirus (CMV)

Size: 5015 base pairs

Bacterial Resistance: Ampicillin

Selectable Marker: Zeocin

Notes: Constitutive system, suitable for transient and stable expression
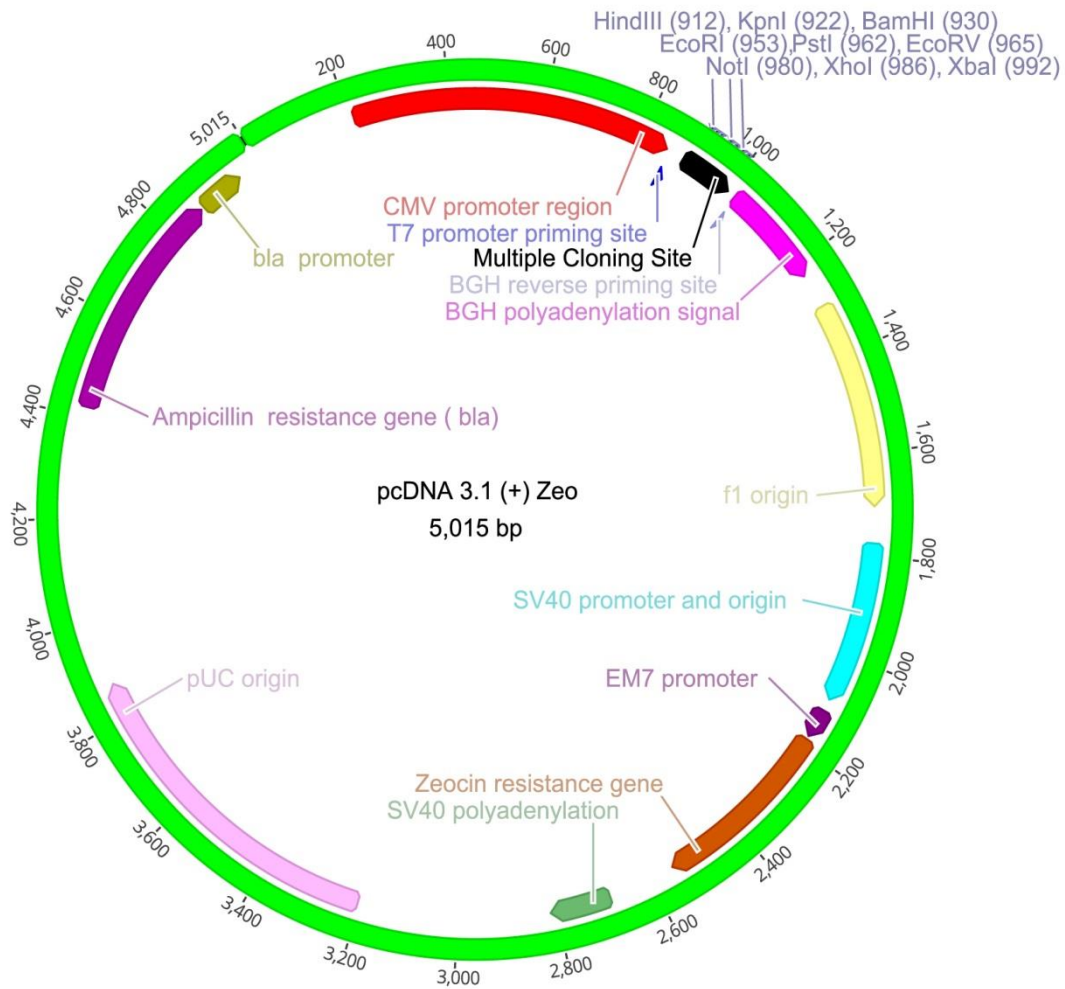
Informations about the vector were taken from the manufacturer's website (http://www.thermofisher.com/order/catalog/product/V86020).
Vector map was designed based on the original sequence available in the above mentioned website using the Geneious software.

Appendix VI: Primers and probes

1) Primers, probe used for WNV RT-qPCR.

Orientation	Sequence (5'-3')	Target region	Reference
FWR	TCAGCGATCTCTCCACCAAAG	1160-1180	
REV	GGGTCAGCACGTTTGTCATTG	1229-1209	Lanciotti et al., 2000
Oligonucleotide Probe			
	FAM-TGCCCGACCATGGGAGAAGCTC-TAMRA	1186-1207	

FWR: forward; REV: reverse; FAM: 6-carboxyfluorescein; TAMRA: tetramethylrhodamine

2) Primers and probe used for USUV RT-qPCR

Orientation	Sequence (5'-3')	Target region	Reference
FWR	CGTTCTCGACTTTGACTA	3294-3311	
REV	GCTAGTAGTAGTTCTTATGGA	3384-3364	Jöst et al., 2011
Oligonucleotide Probe			
	HEX-ACCGTCACAATCACTGAAGCAT-BHQ1	3325-3346	

FWR: forward; REV: reverse; HEX: hexachloro-fluorescein; BHQ1: black hole quencher 1

3) Primers and probe used for YFV RT-qPCR

Orientation	Sequence (5'-3')	Target region	Reference
FWR	TACAACATGATGGGAAAGAGAGAGAARAA	8968-8996**	
REV	GTGTCCCAKCCRGCTGTGTCATC	9223-9211**	Vina-Rodriguez et al., 2017*
Oligonucleotide Probe			
	FAM-TCAGAGACCTGGCTGCAATGGATGGT-TAMRA	9170-1195*	

FWR: forward; REV: reverse; FAM: 6-carboxyfluorescein; TAMRA: tetramethylrhodamine
*Probes were designed separately; ** target regions according to YFV virus strain 17D (Genbank: JX949181.1)

4) Primers and probe used for LGTV RT-qPCR

Orientation	Sequence (5'-3')	Target region	Reference
FWR	TACAACATGATGGGAAAGAGAGAGAARAA	9020-9048**	
REV	GTGTCCCAKCCRGCTGTGTCATC	9263-9285**	Vina-Rodriguez et al., 2017*
Oligonucleotide Probe			
	FAM-TGAAAAAACTGGCTTCCTTGAGTGGT-BHQ1	9222-9247*	

FWR: forward; REV: reverse; FAM: 6-carboxyfluorescein; BHQ1: black hole quencher 1
*Probes were designed separately; ** target regions according to Langat virus strain TP21 (Genbank: NC_003690.1)

5) Primers and probe used for ZIKV RT-qPCR

Orientation	Sequence (5'-3')	Target region	Reference
FWR	CCGCTGCCCAACACAAG	1086-1102	
REV	CCACTAACGTTCTTTTGCAGACAT	1062-1039	Lanciotti et al., 2008
Oligonucleotide Probe			
FAM- AGCCTACCTTGACAAGCAGTCAGACACTCAA-TAMRA		1107-1137	

FWR: forward; REV: reverse; FAM: 6-carboxyfluorescein; TAMRA: tetramethylrhodamine

6) Primers and probe used for Beta actin RT-qPCR

Orientation	Sequence (5'-3')	Target region	Reference
FWR	CAGCACAATGAAGATCAAGATCATC	1005-1029	
REV	CGGACTCATCGTACTCCTGCTT	1135-1114	Toussaint et al., 2007
Oligonucleotide Probe			
VIC-TCGCTGTCCACCTTCCAGCAGATGT-TAMRA		1081-1105	

FWR: forward; REV: reverse; VIC: VIC fluorescent dye (ABI) TAMRA: tetramethylrhodamine

7) Primers and PCR cycle used for detection of mouse αV integrin
*According to the sequence NM_008402.3

Orientation	Sequence (5'-3')	Target region	Amplicon Size
FWR	CTCCGGCCAACGTCAGTCGG	2173-2192*	300 bp
REV	CGCACACCACCTGCCGAGTTT	2472-2453*	

8) Primers and PCR cycle used for detection of mouse β3 integrin
*According to the sequence NM_016780.2

Orientation	Sequence (5'-3')	Target region	Amplicon Size
FWR	GGCTGCCCCCAGGAGAAGGAGCC	1377-1396*	200 bp
REV	CACATGGACCCCAGCCAGCC	1576-1557*	

9) Primers and PCR cycle used for detection of mouse β1 integrin
*According to the sequence NM_010578.2

Orientation	Sequence (5'-3')	Target region	Amplicon Size
FWR	GCCAGTCCCAAGTGCCATGAGG	1723-1724*	500 bp
REV	ACGCCAAGGCAGGTCTGACAGCC	2222-2203*	

Appendix VII: Equipments

1) Centrifuges

Instrument/Equipment	Manufacturer
Centrifuge 5415D	Eppendorf AG, Hamburg, Germany
Centrifuge 5460	Eppendorf AG, Hamburg, Germany
Centrifuge Rotina 380	Hettich, Ebersberg, Germany
Micro-Centrifuge 0.2 ml tube	Neo-Lab Migge GmbH, Heidelberg, Germany
Micro-Centrifuge 1.5 ml tube	Neo-Lab Migge GmbH, Heidelberg, Germany
96-well plates centrifuge MPS-1000	Labnet International, Edison, New Jersey, USA
Ultracentrifuge Optima L-100 XP	Beckman Coulter GmbH, Krefeld, Germany
Ultracentrifuge TL-100	Beckman Coulter GmbH, Krefeld, Germany

2) Electrophoresis system

Instrument/Equipment	Manufacturer
Agarose gel chamber system	Bio-Rad Laboratories GmbH, Munich, Germany
PowerPac 300 Basic Power Supply	Bio-Rad Laboratories GmbH, Munich, Germany

3) **Counting Chamber**

Instrument/Equipment	Manufacturer
Improved Neubauer chamber	Neo-Lab Migge GmbH, Heidelberg, Germany

4) **ELISA/microplate reader**

Instrument/Equipment	Manufacturer
Tecan Infinite 200 PRO	Tecan, Männedorf, Switzerland

5) Flow Cytometer

Instrument/Equipment	Manufacturer
BD FACS CAnto II	Becton-Dickinson,Franklin lakes, NJ, USA

6) Incubator

Instrument/Equipment	Manufacturer
Incucell (Bacteria)	MMM Medcenter Einrichtungen GmbH, Planegg, Germany
Thermo Forma 3851 CO_2 incubator	ThermoFisher Scientific Inc., Waltham, MA, USA

7) Refrigerator, freezer, ultra low temperature tanks and storage equipment

Instrument/Equipment	Manufacturer
Liebherr Premium	Liebherr-Hausgeräte Lienz GmbH,Lienz, Austria
Liebherr Profi Line	Liebherr-Hausgeräte Lienz GmbH,Lienz, Austria
High Efficiency Ultra Low temperature freezer (-80°C)	New Brunswick Scientific-Eppendorf GmbH,Wesseling-Berzdorf, Germany
Mr Frosty™, freezing container for cell culture	ThermoFisher Scientific Inc., Waltham, MA, USA
Dewar flasks for liquid nitrogen	KGW Isotherm, Karlsruhe, Germany
Cryotherm-BIOSAFE, liquid nitrogen tank	Cryotherm, Kirchen/Sieg, Germany

8) Magnetic stander

Instrument/Equipment	Manufacturer
MACS Magnetic MultiStand	Miltenyi Biotec GmbH, Bergisch Gladbach, Germany

9) Microscopes

Instrument/Equipment	Manufacturer
Light microscope, Zeiss, Axiovert 25, inverted	Carl Zeiss GmbH, Jena, Germany
Fluorescence microscope Axiovert 200, inverted	Carl Zeiss GmbH, Jena, Germany
CLSM Leica TCS SP5 setup with inverted microscope Leica DMI600 CS	Leica Camera Microsystems, Mannheim, Germany

10) Pipette, automatic pipette and multi-dispenser

Instrument/Equipment	Manufacturer
Pipetboy® comfort	IBS Integra Biosciences, Fernwald, Germany
Pipette 0.5-10µl	Eppendorf AG, Hamburg, Germany
Pipette 2-20µl	Eppendorf AG, Hamburg, Germany
Pipette 10-100µl	Eppendorf AG, Hamburg, Germany
Pipette 20-200µl	Eppendorf AG, Hamburg, Germany
Pipette 100-1000 µl	Eppendorf AG, Hamburg, Germany
Pipette multi-channel 20-200µl	Brand, Wertheim, Germany
Pipette multi-channel 0.5-10µl	Brand, Wertheim, Germany

11) Scales, pH meter and spectrophotometer

Instrument/Equipment	Manufacturer
Sartorius M-Power Analytical Scale	Sartorius AG, Göttingen, Germany
pH Meter HI221	Hanna Instruments GmbH, Kehl a. Rhein, Germany
NanoDrop® 2000c	ThermoFisher Scientific Inc., Waltham, MA, USA
Bio-Photometer 8,5 mm	Eppendorf AG, Hamburg, Germany

12) Shakers, rocker, mixers and magnetic stirrer

Instrument/Equipment	Manufacturer
Incubated/Refrigerated Stackable Shaker MaxQ 8000	ThermoFisher Scientific Inc., Waltham, MA, USA
HulaMixer® Sample Mixer	ThermoFisher Scientific Inc., Waltham, MA, USA
Shaker, horizontal GFL 3006	GFL, Burgwedel, Germany
Minishaker MS2	IKA, Staufen im Breisgau, Germany
Stuart Vortex Mixer	Cole Parmer, Staffordshire, ST15 OSA, UK,
Thermomixer/Thermoblock comfort	Eppendorf AG, Hamburg, Germany
Thermomixer/Thermoblock 5436	Eppendorf AG, Hamburg, Germany
Magnetic Stirrer VWR	VWR/IKA Radnor,PA, USA
Magnetic Stirrer hot plate	IKA Staufen im Breisgau, Germany

13) Thermocyclers

Instrument/Equipment	Manufacturer
CFX96-Real-Time PCR Detection System	Bio-Rad Laboratories GmbH, Munich, Germany
Thermal cycler C1000TM	Bio-Rad Laboratories GmbH, Munich, Germany
Biometra T3 Thermal Cycler	Biometra GmhH, Göttingen, Germany

14) Transilluminator system and documentation apparatus

Instrument/Equipment	Manufacturer
Transilluminator UV light pulse	AGS, Heidelberg, Germany
Coupled Camera device (CCD) - UV light documentation system	Hama, Monheim, Germany
Thermal Printer DPU-414	Seiko Instruments GmbH, Neu-Isenburg, Germany
Mitsubishi P93DW Printer	Mitsubishi Electronics, Cypress, CA, USA

15) Waterbath

Instrument/Equipment	Manufacturer
Waterbath 0-100°C	GFL GmbH, Burgwendel, Germany

16) Workstations, laminar flow and safety cabinets

Instrument/Equipment	Manufacturer
Thermo Herasafe KS12 Sterile Hood (Laminar flow)	ThermoFisher Scientific Inc., Waltham, MA, USA
UV-CLEANER UVC/T-M-AR	Biosan Medical Technologies, Riga, Latvia

Appendix VIII: Cell lines and bacteria strains

1) Mammalian cell lines

Name	Organism	Tissue	Background	Source	ATCC n°
Vero 76	*Chlorocebus aethiops*	Kidney	A clone derivative from the original Vero cells	FLI-Cell Bank	CRL-1587
Vero	*Chlorocebus aethiops*	Kidney	-	FLI-Cell Bank	CCL-81
Vero E6	*Chlorocebus aethiops*	Kidney	A clone derivatived from the original Vero 76 cells	FLI Cell Bank	CRL-1586
Vero-B4	*Chlorocebus sabaeus*	Kidney	-	FLI-Cell Bank	Unknown
Chinese Hamster Ovary Cell (CHO) clone K1	*Cricetulus griseus*	Ovary	-	FLI-Cell Bank	CCL-61
MEF Wild-type	*Mus musculus*	Embryonal	C57/BL6	FLI-Dr. Markus Keller	n.a.
MEF 24.3 αVβ3$^{-/-}$	*Mus musculus*	Embryonal	C57/BL6	FLI-Dr. Markus Keller	n.a.
MEF 8.1 β3$^{-/-}$	*Mus musculus*	Embryonal	C57/BL6	Dr. Kairbaan Hodivala-Dilke - Barts Cancer Institute, London, UK	n.a.
MKF β1^{flox}	*Mus musculus*	Kidney	C57BL6X 129SV	Dr. Reinhard Faessler, Institute of Biochemistry, Max Planck Society,Munich, Germany	n.a.
MKF β1$^{-/-}$	*Mus musculus*	Kidney	C57BL6X 129SV	Dr. Reinhard Faessler, Institute of Biochemistry, Max Planck Society, Munich, Germany	n.a.

MEF: mouse embryonic fibroblast; MKF: mouse kidney fibroblast; n.a.: not available

2) Bacterial strain

Bacteria	Strain	Genetic Background	Source	Cat n°
Escherichia coli	DH5α	F⁻ endA1 glnV44 thi-1 recA1 relA1 gyrA96 deoR nupG purB20 φ80dlacZΔM15 Δ(lacZYA-argF)U169, hsdR17(rK⁻mK⁺), λ⁻	Clontech-Takara, Laboratories, USA	9057

Appendix IX: Softwares and databases

1) Softwares

Name	Application	Version	Developer
Graphpad Prism	Graphing	6.0	GraphPad Software, La Jolla, CA, USA
Graphpad Prism	Statistics	6.0	GraphPad Software, La Jolla, CA, USA
Geneious	Molecular Biology/ Bioinformatic Tool	10	Biomatters Limited, Auckland, New Zealand
Axiovision AC Release	Microscopy	4.5	Carl Zeiss, Micro-Imaging GmbH, Göttingen, Germany
LAS AF, Leica Application Suite	Confocal Microscopy	2.4	Leica Microsystems CMS GmbH, Mannheim, Germany
Flowing Software	Flow Cytometry Analysis	2.5.1	University of Turku, Cell Imaging Core, Turku Centre for Biotechnology, Turku, Finland
Bio-Rad CFX Manager® Software	Real Time PCR	3.1	Bio-Rad Labaratories GmbH, Munich, Germany
ImageJ	Picture edition/Image processing	1.49u	Wayne Rasband, National Institute of Health – NIH, Bethesda, MD, USA

2) Database

Name	Developer	URL
PubMed	United States National Library of Medicine (NLM), Bethesda, USA	www.pubmed.com
GenBank, NCBI Data base	National Center for Biotechnology Information, Bethesda,MD, USA	https://www.ncbi.nlm.nih.gov/genbank/
Nucleotide	National Center for Biotechnology Information, Bethesda,MD, USA	https://www.ncbi.nlm.nih.gov/nucleotide/
CHO genome.org	Consortium, several partners	http://www.chogenome.org/
BLAST	National Center for Biotechnology Information, Bethesda, USA	https://blast.ncbi.nlm.nih.gov/Blast.cgi

Appendix X: Sequences

1) YFV-17D synthetic RNA synthesis

Accession number: JX949181.1

1	10	20	30	40	50

ATTTAGGTGACACTATAGAAGGTGTGTCCATACAACATGATGGGGAAAAG
AGAGAAGAAGCTGTCAGAGTTTGGGAAAGCAAAGGGAAGCCGTGCCATAT
GGTATATGTGGCTGGGAGCGCGGTATCTTGAGTTTGAGGCCCTGGGATTC
GTCAATCACCAGGATTGGGCTTCCAGGGAAAACTCAGGAGGAGGAGTGGA
AGGCATTGGCTTACAATACCTAGGATATGTGATCAGAGACCTGGCTGCAA
TGGATGGTGGTGGATTCTACGCGGATGACACCGCTGGATGGGACAC

2) WNV synthetic RNA synthesis

Accession number: AF260967.1

1	10	20	30	40	50

ATTTAGGTGACACTATAGAAGGTGTGTCCATCAGCGATCTCTCCACCAAA
GCTGCGTGCCCGACCATGGGAGAAGCTCACAATGACAAACGTGCTGACCC
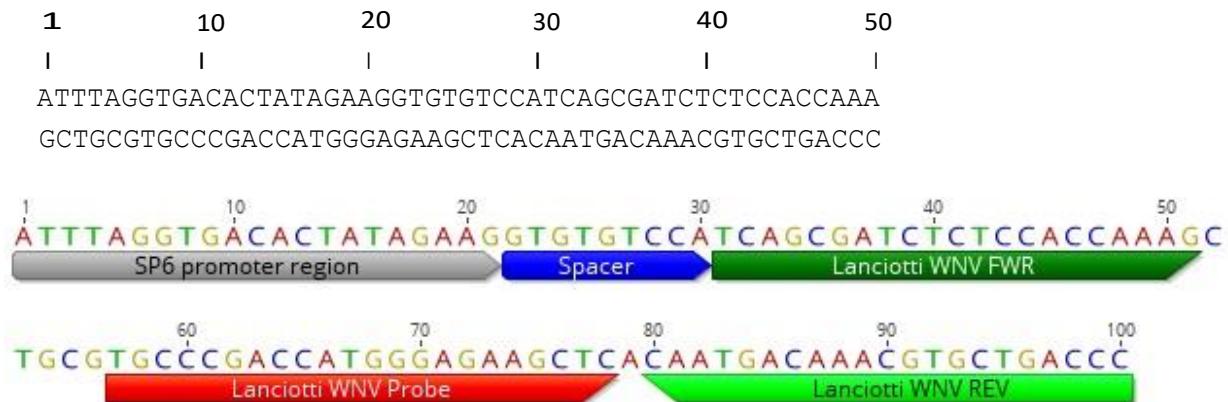
3) USUV synthetic RNA synthesis

Accession number: KM659877.1

```
1          10         20         30         40         50
|          |          |          |          |          |
ATTTAGGTGACACTATAGAAGGTGTGTCCACGTTCTTGACTTTGACTATT
GCCCAGGCACCACCGTCACAATCACTGAAGCATGTGGGAAGAGAGGACCC
TCCATAAGAACCACTACTAGC
```
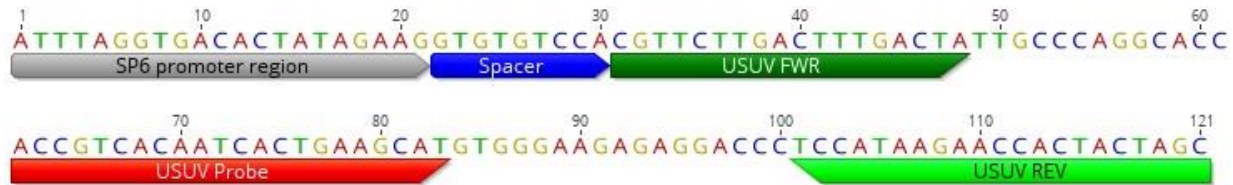

4) LGTV synthetic RNA synthesis

Accession number: NC_003690.1

```
1          10         20         30         40         50
|          |          |          |          |          |
ATTTAGGTGACACTATAGAAGGTGTGTCCATACAACATGATGGGGAAAAG
AGAGAAAAAGCTTGGTGAATTTGGAGTAGCCAAGGGCAGCAGGGCCATCT
GGTACATGTGGCTGGGCAGTCGGTTCCTGGAGTTTGAGGCCCTCGGTTTG
GTGAATCACCATGAGTGGGCGTCCAGGGCTTCTAGTGGAGCTGGAGTGGA
AGGAATCAGCCTCAACTACCTGGGGTGGCATTTGAAAAAACTGGCTTCCT
TGAGTGGTGGTCTGTTTTATGCCGACGACACTGCTGGCTGGGACAC
```
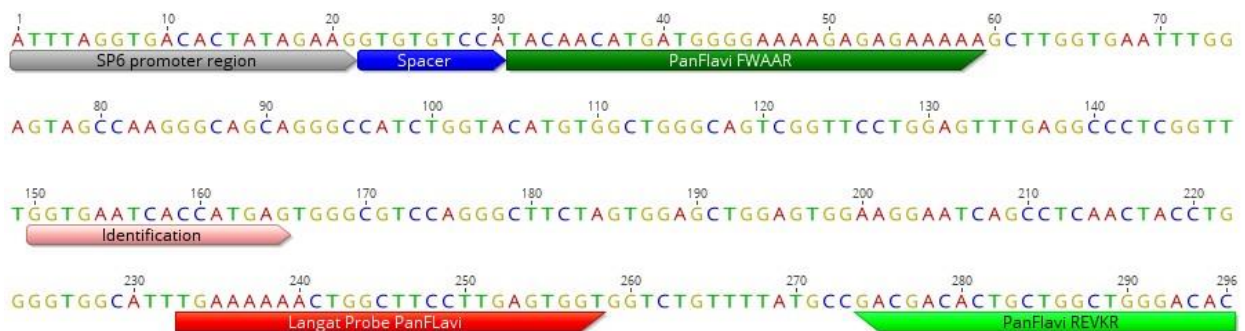
5) ZIKV and MVEV synthetic RNA synthesis

Accession number: AY632535

```
1            10          20          30          40          50
|            |           |           |           |           |
ATTTAGGTGACACTATAGAAGGTGTGTCCACCGCTGCCCAACACAAGGTG
AAGCCTACCTTGACAAGCAATCAGACACTCAATATGTCTGCAAAAGAACG
TTAGTGG
```

8) Curriculum Vitae

Publications

Chávez JH, **Reis VP**, Silva JR, Laure HJ, Rosa JC, Fonseca BA, Figueiredo LT. Production and diagnostic application of recombinant domain III of West Nile envelope protein in Brazil. *Rev Soc Bras Med Trop*. 2013 Jan-Feb;46(1):97-9. PubMed PMID: 23563834.

Silva JR, Medeiros LC, **Reis VP**, Chavez JH, Munhoz TD, Borges GP, Soares OA, Campos CH, Machado RZ, Baldani CD, Silva ML, Faria JL, Silva EE, Figueiredo LT. Serologic survey of West Nile virus in horses from Central-West, Northeast and Southeast Brazil. *Mem Inst Oswaldo Cruz*. 2013 Nov;108(7):921-3. PubMed PMID: 24037110.

Fischer K, **dos Reis VP**, Finke S, Sauerhering L, Stroh E, Karger A, Maisner A, Groschup MH, Diederich S, Balkema-Buschmann A. Expression, characterisation and antigenicity of a truncated Hendra virus attachment protein expressed in the protozoan host Leishmania tarentolae. *J Virol Methods*. 2016 Feb;228:48-54. PubMed PMID: 26585033.

Fischer K, **dos Reis VP**, Balkema-Buschmann A. Bat Astroviruses: Towards Understanding the Transmission Dynamics of a Neglected Virus Family. *Viruses*. 2017 Feb 21;9(2). pii: E34. Review. PubMed PMID: 28230787.

Fischer K, Diedrich S, Smith G, Reiche S, **Reis, VP,** Stroh E, Groschup MH, Weingartl H, Balkema-Buschmann A. Indirect ELISA based on Hendra and Nipah virus proteins for the detection of henipavirus specific antibodies in pigs. Accepted: Plos One (PONE-D-17-27278R2: [EMID:87468442ea78234e)

Poster presentations in congresses and other scientific meetings

Reis, Vinicius; Keller, Markus; Schmidt, K; Groschup MH. Flaviviruses and integrin αVβ3: viral entry receptors or modulators of virus infectivity? Junior Scientist Meeting: 2nd - 4th June 2014, Hannover Germany.

Fischer, K; **Reis, VP**; Finke, S; Groschup, MH; Karger, A; Diederich, S; Balkema-Buschmann, A. The expression of a truncated Hendra virus attachment protein in *Leishmania tarentolae*. 10th International Congress for Veterinary Virology: August 31st to September 3rd, 2015 Montpellier, France.

Fischer, K; **Reis, VP**; Finke, S; Groschup, MH; Karger, A; Diederich, S; Balkema-Buschmann, A. Hendra virus attachment protein expressed in the protozoan host *Leishmania tarentolae* displays interaction with ephrin-B2 receptor. National Symposium on Zoonoses Research: 15th - 16th of October 2015, Berlin, Germany.

Fischer, K; **Reis, VP**; Finke, S; Sauerhering, L; Stroh, E; Karger, A; Maisner, A; Weingartl, H; Groschup, MH; Diederich, S; Balkema-Buschmann, A. Hendra virus attachment protein expression in a novel eukaryotic expression system based on *Leishmania tarentolae*. 26th Annual Meeting of the Society for Virology: 4th - 9th of April 2016, Münster, Germany.

Reis, Vinicius; Keller, Markus; Schmidt, K; Groschup MH. Cell adhesion molecules (integrins) modulate flavivirus infection in mouse cell lines. 1st Summer School "Infection Biology": 28th - 30th September 2016, Alfried-Krupp Kolleg, Greifswald, Germany.

Reis, Vinicius; Keller, Markus; Ulrich, Rainer; Groschup MH. Integrin αVβ3 influences flavivirus replication in mouse cell lines. National Symposium on Zoonoses Research: 12th - 13th October 2016, Berlin, Germany.

Reis, Vinicius; Keller, Markus; Ulrich, Rainer; Groschup MH. Integrin αvβ3 is necessary for efficient flavivirus replication in mouse cell lines. 6th European Congress of Virology: October 19th – 22nd October 2016, Hamburg Germany.

Reis, Vinicius; Keller, Markus; Ulrich, Rainer; Groschup MH. Modulation of flavivirus replication: integrin αVβ3 as a new flavivirus host cell factor. Junior Scientist Meeting: 7th - 9th June, 2017 Langen, Germany.

Reis, Vinicius; Keller, Markus; Ulrich, Rainer; Groschup MH. Integrin αvβ3 ablation impairs Zika virus replication. National Symposium on Zoonoses Research: 12th - 13th October 2017, Berlin, Germany.

Congress and scientific meetings

Junior Scientist Meeting: 2nd - 4th June 2014, Hannover Germany.

10th International Congress for Veterinary Virology: August 31st - September 3rd, 2015 Montpellier, France.

National Symposium on Zoonoses Research: 15th - 16th of October 2015, Berlin, Germany.

26th Annual Meeting of the Society for Virology: 4th - 9th of April 2016, Münster, Germany.

1st Summer School "Infection Biology": 28th - 30th September 2016, Alfried-Krupp Kolleg, Greifswald, Germany.

National Symposium on Zoonoses Research: 12th - 13th October 2016, Berlin, Germany.

6th European Congress of Virology: October 19th – 22nd October 2016, Hamburg Germany.

27th Annual Meeting of the Society for Virology: 22nd - 25th March 2017, Marburg, Germany.

Junior Scientist Meeting: 7th - 9th June 2017, Langen, Germany.

National Symposium on Zoonoses Research: 12th - 13th October 2017, Berlin, Germany.

9) Eigenständigkeitserklärung

Eigenständigkeitserklärung

Hiermit erkläre ich, dass diese Arbeit bisher von mir weder an der Mathematisch-Naturwissenschaftlichen Fakultät der Ernst-Moritz-Arndt-Universität Greifswald noch einer anderen wissenschaftlichen Einrichtung zum Zwecke der Promotion eingereicht wurde.

Ferner erkläre ich, dass ich diese Arbeit selbstständig verfasst und keine anderen als die darin angegebenen Hilfsmittel und Hilfen benutzt und keine Textabschnitte eines Dritten ohne Kennzeichnung übernommen habe.

Unterschrift des Promovenden

Erklärung zur Abgabe einer elektronischen Kopie der Dissertation

Mathematisch-Naturwissenschaftliche Fakultät

Einverständniserklärung nach § 4 Abs. 1 Nr. c Promotionsordnung

Hiermit erkläre ich, dass von der Arbeit eine elektronische Kopie gefertigt und gespeichert werden darf, um unter Beachtung der datenschutzrechtlichen Vorschriften eine elektronische Überprüfung der Einhaltung der wissenschaftlichen Standards zu ermöglichen.

Datum:

Unterschrift:

10) Acknowledgements